HYDRAULIC CHARACTERISTICS AND PLANT-MICROORGANISM MICRO-ECOSYSTEM OF SAND-SLUDGE SOIL (ECO-SOIL) FOR ANTI-DESERTIFICATION

LIU YAOHUI

Ph.D

The Hong Kong Polytechnic University

2016

The Hong Kong Polytechnic University

Department of Civil and Environmental Engineering

Hydraulic Characteristics and Plant-Microorganism Micro-Ecosystem of Sand-Sludge Soil (Eco-Soil) for Anti-Desertification

LIU Yaohui

A thesis submitted in partial fulfillment of the requirements for the degree of Doctor of Philosophy

Mar 2016

Certification of Originality

I hereby declare that this thesis is my own work and that, to the best of my knowledge and belief, it reproduces no material previously published or written, nor material that has been accepted for the award of any other degree or diploma, except where due acknowledgement has been made in the text.

_______________________________ (Signed)

__________LIU Yaohui_________(Name of student)

Abstract

Desertification has been one of the severe worldwide environmental problems due to the loss of land productivity, including water retention capacity and nutrients. However, nutrients are rich in activated sludge from wastewater treatment processes. As a win-win strategy, this study aims to develop and investigate a novel growing medium, which is the mixture of arid sand and thickened activated sludge, namely the Eco-Soil, to rebuild the land productivity from the margin of the arid area. This study carried out comprehensive investigations of the hydraulic properties and plant growing capabilities of the Eco-Soils with different Sand-Sludge Volumetric Ratios (SSVR), 100:0, 80:20, 60:40, 40:60 and 80:20. The results were compared with the properties of commercial potting soil. The Soil Water Characteristic Curve (SWCC) of the Eco-Soils were determined by experiments and numerical simulations using the van Genuchten model in the RETC software. The seed germination index experiment was carried out to study the phyto-toxicity of Eco-Soils. The growth of *Abelmoschus esculentus* (Okra) in Eco-Soil was also investigated to reveal the productivity improvement. In addition, the runoff patterns of the soil under rainfall intensities from 10 to 100 mm/hr were investigated to elucidate the maximum rainfall retention capacity.

The results reveal the relation between SSVR and Sand Sludge Weight Ratio (SSWR) and indicate the hydraulic properties, which include bulking density, particle density, porosity, particle size distribution, field capacity and hydraulic conductivity, affected by activated sludge. Seed germination percentage, root length ratio and seed germination index further illustrate the plant affinity for Eco-Soil leachates. The

optimal SSVR of Eco-Soil for anti-desertification purposes is suggested to be 60:40 based on the performance of hydraulic properties and phyto-toxicity results.

The SWCC of Eco-Soils changes when sludge content increases indicating that the water retention abilities of Eco-Soils can be greatly improved by sludge introduction and the performance is comparable to potting soil. The numerical simulation results show that the van Genuchten model fits well to the Eco-Soil in the suction head range of 0~-1.19×10^6 cmH_2O. The regression relation between the sludge weight content and the two essential fitting factors, α and n, offers a way to introduce the sludge weight ratio into the van Genuchten model to develop numerical SWCC equation for Eco-Soil.

Observations and findings of the plant vertical development, the dried weights of organs, the root shoot ratio (RSR), the pod and seed productions show that the plant growing in Eco-Soils of SSVR 60:40 and 40:60 perform comparably and stably. From the consideration of maximizing the utilization of activated sludge and achieving sustainable development of vegetations, the SSVR 60:40 of Eco-Soil is recommended.

The rainfall runoff results show that the maximum rainfall retention under one hour rainfall on arid sand is improved from 3.62 to 16.08 L and is linearly related to the sludge weight ratio.

Finally, based on the present comprehensive analysis, Eco-Soil of SSVR 60:40 has suitable physical properties and plant affinity for anti-desertification.

Keywords: *Eco-Soil, Desertification, Sand-Sludge Volumetric Ratio (SSVR), Activated Sludge, Hydraulic Properties, Abelmoschus esculentus*

List of Publication

Y.H., LIU, W.H.O., WAI, H. CHUA, Hydraulic Properties and Plant Growing Capacity of Eco-Soil for Anti-Desertification, submitted

Y.H., LIU, W.H.O., WAI, H. CHUA, Study of Soil Water Characteristics Curve for Eco-Soils, submitted

Y.H., LIU, W.H.O., WAI, H. CHUA, Study of Growth of Abelmoschus esculentus (Okra) in Eco-Soils, submitted

Y.H., LIU, W.H.O., WAI, H. CHUA, Investigation of Rainwater Retention for Eco-Soils, pending submitted

Acknowledgement

I would also like to express my sincere gratitude towards my chief supervisor, Professor WAI Wing Hong, Onyx, for his enthusiastic guidance, suggestions and supports throughout the whole period of this research.

Special thanks are given to Mr. LEUNG Kwok Hing, Mr. LAM Kit Wa, Mr. YAN Xufeng for their kind supports in laboratory works.

Last but not least, I would also want to devote my deepest appreciation towards my family and friends in the Polytechnic University for their continuous encouragement and moral support. Without their love, patience and supports, successful completion of this work would have been impossible.

Table of Contents

List of Tables

List of Figures

Abbreviations

[θ]	Moisture Content
[Ψ]	Water Potential
4WD	4 Wheel Drive
BD	Bulk Density
BS	British Standard
C:N	Carbon To Nitrogen
CBS	Chlorobenzenes
CIV	Cyclic Irrigation Vehicle
DAS	Dewatered Activated Sludge
DCD	Dicyandiamide
DPDT	Double Pole Double Throw
DSD	Drainage Services Department
EDTA	Ethylene Di-Amine Tetraacetic Acid
EPS	Extracellular Polysaccharides
ES	Effective Saturation
FPA	Five-Phase Analysis
GI	Germination Index
HK	Hong Kong
MIP	Mercury Intrusion Porosimetry
MTB	Measuring Tipping Bucket
NAD	Nitrogen Adsorption/Desorption
NT	Non-Tillage

NTA	Nitrilotriacetic Acid
OM	Organic Matter
PAHs	Polycyclic Aromatic Hydrocarbons
PAS	Primary Activated Sludge
PCBs	Polychlorinated Biphenyls
PCDD/Fs	Polychlorinated Dibenzo-P-Dioxins And Furans
PCDD/Fs	Polychlorinated Dibenzo-Pdioxins And Furans
PD	Particle Density
PEP	Polysaccharidase Enzyme Preparation
PoSD	Pore Size Distribution
PSD	Particle Size Distribution
PRSS	Precipitation Runoff Simulation System
RAS	Return Activated Sludge
RETC	
RH	Relative Humidity
RLR	Root Length Ratio
RSR	Root/Shoot Ratio
SAS	Secondary Activated Sludge
SAS	Secondary Activated Sludge
SDBOD	Slowly Degradable Biochemical Oxygen Demand
SSVR	Sand-Sludge Volumetric Ratio
StAS	Stablized Activated Sludge
SWCC	Soil Water Characteristic Curve
SWRC	Soil Water Retention Curve

TAS	Thicken Activated Sludge
TPSTW	Tai Po Sewage Treatment Works
TSS	Total Suspended Solids
UNCED	United Nation Conference On Environment And Development
UNSODA	Unsaturated Soil Hydraulic Database
VWC	Olumetric Water Content
WAS	Wasted Activated Sludge
μ CT	X-Ray Micro-Computed Tomography

1. Introduction

1.1 Background

Our routine life has been changed tremendously because of the fast development of human society. The high-speed urbanization and industrialization bring us brand-new and convenient lifestyle, but the pollution problems arising from the unsustainable development also deteriorate our living quality. The water, ambient air, noise and solid waste pollutions are the four major disturbing problems which upset our living environment. One of the significant environment problems is desertification because of over assart of forest and global warming. It has brought us lots of environmental impacts including sand storm to cities, destroy of water balance, lost of farmland and debris flow in rainy seasons.

The United Nation (UN) had addressed the desertification as a worldwide problem for the first time (Uwe, 2008). China is one of the most severe countries suffering from desertification. According to the desertification and sandy land monitoring carried out in 2004, the total area of desertification land was added up to be 26,361.68 hectares while the sandy land area was 17,396.63 hectares, which occupied 27.46% and 18.12% of national land area respectively (State Forestry Administration, China, 2005).

The major reason for desertification is the lost of moisture content in the soil.

However, in wastewater treatment area, removal of moisture content in the activated sludge is always an annoying issue because the treatment requires complicate process and increases the operation cost. In addition, the amount of sludge production is huge in a 1.3 billion-people country. It was reported the sludge production in China reach up to 22 million tons per year (Sun, 2011). Disposal of secondary sludge is costly due to its poor dewaterability (Mahmood and Elliot, 2006). The wasted activated sludge (WAS) is not only high in moisture content but also in the quantity amount. In most of the time, the final destination for WAS is the landfill sites. However, the methane generation and the offensive odour make it unfavorable.

In fact, the activated sludge is a treasure when applied in a good way because of its rich nutrient and organic content. In recent years, researchers become interested in the reuse of waste activated sludge, such as composting, recovering the biodegradable-plastic and transforming to activated carbon and so forth.

To the author’s opinion, desertification is because of the degradation of land while the wasted activated sludge is rich in moisture and nutrient content. Why not trying to kill two birds with one stone? Therefore, it would be very valuable to carried out the study of combining the activated sludge and the arid sand to form a soil-mix (herein Eco-Soil) for anti-desertification. Turning a waste into a treasure.

1.2 Objectives

1.2.1 General Objective

In order to find out environmental friendly means for anti-desertification, this research aims to carry out a detailed study of the hydraulic characteristics, plants growing patterns and soil water retention characteristics for a novel growing medium which is a sand-sludge mixture, namely Eco-Soil.

1.2.2 Specific Objectives

1) To study the hydraulic characteristics of the Eco-Soils, which include the mixture fraction, bulk density, particle density, porosity, particle size distribution and the performance in evaporation experiment.

2) To study growing characteristics of different plants in Eco-Soil, which include the water, nutrient and mineral uptake, and to suggest which kinds of plants would be suitable for anti-desertification.

3) To study the water retention characteristics, which include the soil water characteristics curve by both experimental methods and numerical simulation methods.

4) To investigate the rainfall runoff patterns under various rainfall scenarios to determine rain water retention capability of the Eco-Soil.

1.3 Organization of the Thesis

This thesis elucidates a comprehensive study of a type of novel growing substrate of sand-sludge mixture, namely Eco-Soil, through the hydraulic properties, water retention characteristics, stormwater retention capabilities and vegetation growing performances.

Chapter 1 introduces the background of the study and the concept of anti-desertification by Eco-Soil. The desertification is a worldwide environmental issue due to loss of water retention capabilities as fundamental reason while the activated sludge contains rich moisture and nutrient contents, and large in amount. The concept of Eco-Soil is able to solve two environmental issues together in a sustainable way.

Chapter 2 reviews the previous studies about desertification, activated sludge, sludge amended soil and vegetation to find the way to carry out the current study. The previous study mainly focused on the causes and developments of desertification. Main methods for desertification control are by growing vegetation and applying policies. The review of studies about activated sludge reveals the complexity and high cost for its treatment. The heavy metal limits the application of activated sludge in modifying the soil. However, no existing studies provide the finding by using activated sludge to combat desertification. Therefore, the current study is necessary.

Chapter 3 describes the methods for carrying out this study. The selection, collection, and treatment of materials including the thickened activated sludge, arid sand and potting soil, are clearly described. The hydraulics properties such as bulk density, particle density, particle size distribution, porosity and soil water characteristics curve were done according to standards or literatures. Seed germination index and vegetation growing experiments were designed and carried out to investigate the performance of Eco-Soil. The rainfall runoff study was fulfilled by automatic precipitation runoff simulation system. The methodology of study provides the indication for carrying out similar study for anti-desertification purposes.

Chapter 4 illustrates the studies of hydraulic properties of Eco-Soil, soil water retention curve, growing capabilities and the rainwater retentions. The properties and performances of Eco-Soils were compared with arid sand, commercial potting soil and other related literature data to reveal the enhancement of anti-desertification abilities brought by Eco-Soils. The discussion provides valuable findings for optimal mixing ratio of sand and sludge for achieving highest performance in anti-desertification purposes.

Chapter 5 summarizes the discussion in the previous chapter and come to the conclusions of the outcomes and optimal mixing ratio of Eco-Soil. In addition, topics for further study are suggested to develop the findings from this thesis.

2. Literature Review

2.1 Desertification

The earliest definition of desertification was described by the United Nation Conference on Environment and Development (UNCED, 1992), i.e., land degradation in arid, semi-arid and dry sub-humid areas resulting from various factors, including climatic variations and human activities. Land sandification is one of the terms defined by Chinese researchers and describes the narrow sense of desertification. The land sandification is the appearance of sandy land in the non-desert area due to the breakdown of the ecosystem balance by the undue human activities (Shen *et al*., 2001). In China, desertification has usually occurred in arid and semi-arid regions, with annual precipitation less than 450 mm and spring precipitation less than 90mm (Wang *et al*., 2008). The sandification is considered as the extreme status of desertification. For carrying out anti-desertification study, it is important to review the hazard, affected area and the causes of desertification.

2.1.1 Hazard of Desertification

The desertification could cause degradation of the land (terrestrial bio-productive system including soil, water, plant growth, other biota and the ecological processes (Kassas, 1995)). The degradation of land could be defined as the lost of land productivity, including the economic loss and ecologic deterioration. The symptoms of desertification are different in various land-use forms (Kassas *et al*., 1991). Deterioration in irrigated farmlands often results from the rise of water table mainly because of imbalance between inefficient drainage and excessive Irrigation. Precipitation and other forms of chemical damage of the soil often result in water-clogging. Degradation of rain-fed crops often resulted in soil erosion, loss of nutrients and organic matter (OM), crust formation and compaction, and extensive invasion of weeds. Degradation of rangelands includes loss of bio-productivity, invasion of non-palatable species such as thorn-bushes and succulents, poorer livestock, soil erosion, etc. Degradation of land could result in the loss of the vegetation. Therefore, without the fixation effect by plant root, the land would become unstable. The surface layer of the land would be easily brought away by the strong wind which leads to the formation of dust storms. In the rainy season, the unstable land would also have high potential to be washed away that leads to the formation of debris flow. It is reported that 1442 times of debris flow happened in China in the year 2009 and Hu Nan, Si Chuan and Tibet were the three provinces which suffered the most debris flow (Ministry of Land and Resources, 2009).

2.1.2 Affected Area of Desertification

Drylands occupy 41 % of Earth's land area and are home to more than 2 billion people (Uwe, 2008). Table 2.01 indicates that the Africa and Asia suffer the most from the desertification (Dregne *et al*., 1991). It has been estimated that some 10~20 % of drylands are already degraded, the total area being affected by desertification is between 6 and 12 million square kilometers and cover about 1~6 % of the inhabitants of drylands living in desertified areas, and about a billion people are under threat from further desertification (Adeel *et al*., 2005). In China, the third desertification and sandy land surveying was carried out in 2004, which stated that the total desertification land area was 26,361.68 hectares while the sandy land area was 17396.63 hectares, which occupied 27.46% and 18.12% of total land area respectively (State Forestry Administration, China, 2005). From the data above, the area be affected by desertification is very large and action should be taken to combat the desertification.

Table 2. 1 World drylands in millions of hectares (Adapted from Dregne *et al.*, 1991)

	Africa	Asia	Australia	Europe	North America	South America	World total	%
Hyper-arid	672	277	0	0	3	26	978	16
Arid	504	626	303	11	82	45	1571	26
Semi-arid	514	693	309	105	419	265	2305	37
Dry sub-humid	269	353	51	184	232	207	1296	21
Total	1959	1949	663	300	736	543	6150	100
% world total	32	32	11	5	12	8	100	
% total global land area	13·1	13·0	4·4	2·0	4·9	3·6	41·0	
% continent area	66	46	75	32	34	31	41	

Figure 2. 1 Vegetation boundary of the arid area in Shanxi province

2.1.3 Causes of Desertification

Desertification is found to be caused by a combination of factors that change over time and vary by location. The indirect factors include population pressure, socioeconomic and policy factors, and international trade while the direct factors for climate-change and land use patterns and practices (Adeel *et al*., 2005).

The desertification in arid- and semi-arid areas in China has been shown to rehabilitate for several phases in the past thousands of years and was proven by historical data. Wang *et al.* (2008) indicated that periods of desertification are related to specific trends in drought, temperature and wind regime. In other words, desertification always occurs during periods with drought, low temperature and strong winds conditions. In addition, desertification in China in the past thousands of years always accompanied with changes in extent grazing. The border areas grazed by nomadic nations historically moved southward due to moist and warm climate, population growth and agricultural cultivation development (Wang *et al.*, 2008).

Modern forms and causes of desertification are different from those observed in history, due to increasing impacts from human. Based on remote-sensing data of China, the rate of modern desertification from the late 1950s to the mid-1970s was found to be 1560 km^2/yr, compared to 2100km^2/yr from the mid-1970s to the late 1980s (Zhu and Chen, 1994).

The causes of desertification in China are debatable. Some of the studies stated that the desertification was triggered by human activities including inadequate reclamation, grazing, cutting of trees, and (in some regions) unsustainable use of water resources (Zhu *et al*., 1980, 1981; Zhu and Liu, 1982; Zhu, 1994; Wang *et al*., 2003, 2004b, 2006; Liu, 1988; Yang *et al*., 1994). Others indicated that the desertification in arid and semiarid China is mainly due to climatic change, and especially increases in potential sand transport, decreases in spring precipitation (Wang *et al*., 2004, 2005a, 2006a, 2007). Rehabilitation occurred since the 1990s has instead resulted in decreasing potential sand transport, increasing temperature, and increasing spring precipitation.

2.1.3.1 Wind Erosion

One of the key factors affecting dust transportation and deposition, aeolian geomorphological processes and desertification is wind activities in arid- and semi-arid China. Compared with other regions such as Southern Africa and North America, low-energy wind regime dominated geomorphological processes in China (Wang *et al*., 2005b, 2007). Many regions were highly vulnerable to desertification due to surface materials, which resulted in severe wind erosion. Therefore, significant variations in wind activity have played major roles in the cycles of desertification and rehabilitation in the region (Wang *et al.*, 2008).

Studies found that the trends of potential sand transport are highly consistent with the developments of rehabilitation and desertification. For the highly rehabilitation decades (1960s to 1970s), the potential sand transport was two to three times the values as that of 1980s and the present. The desertification was most rapid and severe in this period and indicated that the magnitude of the wind erosion (determined by the wind erosivity) from the 1980s to the present was only 20 to 50% of that before the 1980s. In addition, the erosivity was lower than that during the 1970s from the 1990s compared with the early 2000s. As a result, wind activity was found to be a major factor in determining the trends in desertification and rehabilitation. Previous studies shown wind activities significantly affect the development of extensive aeolian geomorphological types arid- and semi-arid area China (Dong *et al*., 1988; Liu *et al*., 2002; Yang, 1985; Wang *et al*., 2008).

2.1.3.2 Variations of Rainfall

Climate change constitutes growing pressures that could endanger or even change ecosystems. The two major reasons for climate change are burning of fossil fuels and changing land cover (Sivakumar, 2007). These activities modify the concentration of atmospheric constituents or properties of gaseous substances on the Earth's surface therefore affect the absorption and reflection of radiant energy. In particular, the increases of amount of greenhouse gases (GHGs) and aerosols are considered to be major contributors to climatic changes (Sivakumar, 2007). Emanuel (1987) predicted a 17% increase in the world area of desert land during the climate changes expected with a doubling of atmospheric CO_2 content.

Climate change results in the variation of spring rainfall and melting of glaciers. Change of climates in the form of spring precipitation reduction is considered to be affecting factor for vegetation growth in arid and semi arid area. In the past decades (1950s to 2000s), the variation of total annual rainfall was significant in the arid- and semi-arid China (Ding *et al*., 2006). However, previous studies indicated that the total annual rainfall data is not enough to reveal the causes of desertification (Si, 1994; Qiu *et al*., 2001). Spring rainfall is a more important indicator because most of vegetations have high growing trend in spring due to warm temperature. The growth of vegetation is beneficial to reduce sand transport, which results in significant rehabilitation. The spring rainfall depth increased significantly in Northwest China since the 1990s (Shi *et al*., 2003) and in other regions of arid- and semi-arid China, for which precipitation generally increased by 20 to 50% compared with the recorded before the 1980s. This mainly activated the rehabilitation of land in the region. In addition, the melting of glaciers due to global warming also improves the rehabilitation in Northwest China. The continuous melting of glaciers in Northwest China would result in decrease in moisture and lead to more severe desertification (Wang *et al.*, 2008).

2.1.3.3 Mobilization of Dunes

The dune mobility has been found to be related to vegetation cover and soil moisture and wind activity (Thomas *et al*., 2005; Thomas and Leason, 2005). Significant variations in rainfall and aeolian sand transport are able to affect vegetation cover strongly then evolves the mobility of dunes among the mobile, semi-anchored, and anchored forms (Zhu, 1998). Strong aeolian dune activity is found in 80% arid- and semi-arid China and is classified as sandy desertification (Wang *et al*., 2003, 2004a). The dune activities, as measured by dune mobility index, are found to be consistent with the development desertification (Wang *et al.*, 2008).

Inactive and partly inactive dunes and sand sheets are majorly located at the margins of the Badain Jaran, Taklimakan and Tengger deserts after 2000. In regions which occurred rehabilitation, such as most parts of the Gurbantunggut, Horqin, Hulunbuir Mu Us and Otindag deserts, the dunes experience high mobility after the 1980s. The fully active dunes are mainly located in the eastern and central Taklimakan desert, the southern part of the Badain Jaran Desert, parts of the Ulan Buh and Hobq deserts, some parts of the Tibet Plateau, and the whole Tengger Desert, (SFAC, 2005).

The vegetation cover has been found to have great changed on the surfaces of semi-anchored dunes. During the 1970s, most of the crests of linear dunes were active and the vegetation cover ranged from 15 ~ 25% in the Gurbantunggut Desert (Zhu *et al*., 1980). However, field investigations in the early 2000s revealed that few of these dune crests were still active due to the vegetation cover reached 40 ~ 50% (Fang *et al*., 2003). During the 1960s and 1970s, the Otindag and Hobq deserts were comprised by trees and shrubs and experienced highly movable variable duns, resulting in occurrence of some nebkha dunes. However, after growing herbaceous vegetation on the dune surfaces in early 2000s, the dunes mobility has been further limited (Wang *et al.*, 2008).

2.1.3.5 Human Impacts

The causes of desertification could be divided into two major categories, which are human activities and climate change. Studies found that the major reasons of land degradation in Ethiopia relate to rapid population increases, severe soil loss, deforestation, low vegetative cover and unbalanced crop and livestock production (Girma, 2001). Other studies found that the population pressure is the most important cause of the desertification (Darkoh, 1998; Ayoub, 1998; Liu and Ci, 2000). The climate change is considered to be another reason for desertification. However, the climate change is also caused majorly by the human activities. Hence, the major cause of desertification should be due to the results of human activities.

Many of the research studies indicated that human activities are the major contributors to desertification in arid and semiarid China (Zhu *et al.*, 1980, 1981; Zhu and Liu, 1982). However, the trends human impacts are not significantly coherent with the desertification development Northwestern China (Wang *et al.*, 2008). Most of the documents provided descriptive evidences for studying the relation of human impacts and their significance to the development of desertification. However, these explanations are not able to elucidate reason for the increasing three proxies for human impacts, including human population, livestock populations and the area devoted to agriculture, but on-going rehabilitation occurrence since the 1990s (Wang *et al.*, 2008).

2.2 Activated Sludge

2.2.1 Typical Wastewater Treatment Process

The biological wastewater is widely used in water pollutant removal in the world. The common wastewater treatment consisted of four major treatment parts, which are pretreatment, primary treatment, secondary treatment and tertiary treatment (Figure 2.2).

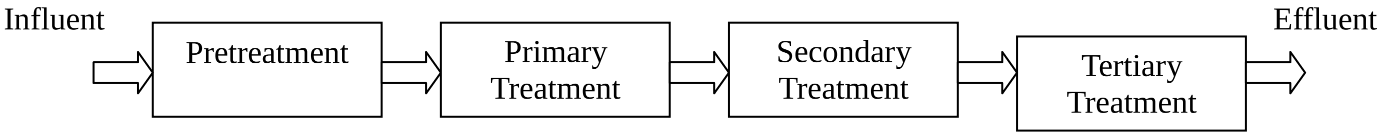

Figure 2. 2 General wastewater treatment process

The pretreatment aims to eliminate the large particles in order not to conflict the following treating units. Coarse screen, fine screen and degritting operation are mainly used for the particle removal. The pH adjustment is usually carried out in the pre-treatment step. The solid generated from the pretreatment is classified as primary sludge and commonly contained coarse solids, grit and scum.

Primary treatment, also named as physical treatment or primary sedimentation, aims to settle the remaining suspended solids and colloidal particles left in the sewage after the screening and degritting operations. Tsang *et al*. (2008) stated that around 80% suspended solid was removed in the primary treatment unit in Hong Kong. A typical sedimentation tank, including the circular and rectangular types, removes 70-80% of total suspended solids (TSS) on average (Gao and Gu, 2004). The solid removal in the primary treatment is called the primary activated sludge (PAS). The majority of the PAS contains woods, plastics, grease, grits and other large particles which can be removed by physical treatments. Most of the PAS contains Slowly Degradable BOD (SDBOD) or even undegradable matters, therefore, the reuse of PAS is limited.

After primary treatment, the suspended solid is significantly removed while the soluble organic compound is untreated. Secondary treatment aims to removal this kind of matter. Biological treatment is commonly used in treating biodegradable wastewater since it is microbial driven. The carbonaceous organic matters of the wastewater provide energy sources for the production of new microbial cells for a mixed population of microorganisms in an aquatic aerobic environment (Francis *et al*., 2002; Tsang *et al*., 2008). The pollutants in the wastewater are utilized by the microorganisms to produce new cells or become gaseous compound that leave the system. The activated sludge is mainly generated from the secondary treatment, called the Secondary Activated Sludge (SAS). Secondary sludge consists of microbial biomass, cell-decay products and non-biodegradable lignin precipitates (Puhakka *et al*., 1992). It is reported that average 8~10 tons excessive sludge is generated from every 10,000 tons wastewater in sewage treatment plants in China (Yi, 2010). The production of activated sludge from domestic wastewater treatment plants reached up to 22 million tons per year (Sun, 2011). Approximately 1 and 7 million tonnes of sewage sludge solids are produced each year in the UK and USA, respectively (Bruce and Davis, 1989). Pathak *et al*., 2009 had summarized the amount of activated sludge generation in some countries and regions as listed in Table 2.2. From the table, the amount of sludge generation in Hong Kong is large as compared to the small land area.

Table 2. 2 Sludge generation in various countries and regions (Adapted from Pathak *et al*., 2009)

Country	Sludge produced (ton of dry solid)	Year	Reference
China	4,000,000	2000	Lee et al. (2002)
Denmark	140,000	2002	Jensen and Jepson (2005)
Finland	160	2005	Magoarou (2000)
France	1172	2005	Magoarou (2000)
Germany	99	2005	Magoarou (2000)
Hong-Kong	170,000	2006	Honk Kong SAR (1999)
Ireland	113	2005	Magoarou (2000)
Israel	113	2005	Magoarou (2000)
Luxembourg	166	2005	Magoarou (2000)
New Zealand	401	2005	Magoarou (2000)
Spain	160	2005	Magoarou (2000)
Thailand	63,000	2010 (Projected)	Stoll (1995)
UK	2,180,000	2006	Wilson (1998)
USA	8,000,000	2000	Lee et al. (2002)

In pulp and paper mills, secondary sludge is typically mixed with primary sludge, thickened and dewatered and then disposed by landfilling or incineration. If the EAS is sent to landfill site, the value of these raw materials is wasted and may result in gaseous emissions and water pollution. On the other hand, incineration may be energetically unfavorable due to the high water content of the secondary sludge (Bayr *et al*., 2013).

For fulfilling some discharge standards in particular area, tertiary treatment should be conducted to eliminate some pollutant in the treatment effluent from the secondary treatment. The tertiary usually contain the disinfection, nitrogen and phosphorus removal. In the tertiary treatment units, less solid would be generated.

2.2.2 Sludge Treatment

The sludge is combination of pure water, soluble substances such as minerals and salts (Eckenfelder and Santhanam, 1981). Sludge is the largest in volume and usually consists of four major constituents, including grease, grit, scum and biosolid (Tchobanoglous *et al*., 2004). Processing and disposal of activated sludge are the most complex and expensive. The handling of excessive activated sludge represents 30%–40% of the capital cost and about 50% of the operating cost of many wastewater treatment facilities (Vlyssides and Karlis, 2004; Appels *et al.*, 2008). Some activated sludge contain heavy metals, virus, pathogens, nutrients and high moisture content (Table 2.3 and Table 2.4), therefore it should be treated prior to disposing to landfill.

Table 2. 3 Typical chemical composition of untreated sludge and digested biosolids (Adapted from Environment Protection Agency, USA, 1979)

	Untreated primary sludge		Digested primary sludge		Untreated activated sludge
	Range	Typical	Range	Typical	Range
Total dry solids (TS), %	5~9	6	2~5	4	0.8~1.2
Volatile solid (% of TS)	60~80	65	30~60	40	59~88
Grease and fats (% of TS)					
Ether soluble	6~30	-	5~20	18	-
Ether extract	7~35	-	-	-	5~12
Protein (% of TS)	20~30	25	15~20	18	32~41
Nitrogen (N, % of TS	1.5~4	2.5	1.6~3.0	3.0	2.4~5.0
Phosphorus (P_2O_5, % of TS)	0.8~2.8	1.6	1.5~4.0	2.5	2.8~11
Potash (K_2O, % of TS)	0~1	0.4	0~3.0	1.0	0.5~0.7
Cellulose (% of TS)	8~15	10	8~15	10	-
Iron (not as sulfide)	2.0~4.0	2.5	3.0~8.0	4.0	-
Silica (SiO_2, % of TS)	15~20	-	10~20	-	-
pH	5.0~8.0	6.0	6.5~7.5	7.0	6.5~8.0
Alkalinity (mg/L as $CaCO_3$)	500~1500	600	2500~3500	3000	580~1100
Organic acids (mg/L as HAc)	200~2000	500	100~600	200	1100~1700
Energy content, kj/kg TSS	23,000~29,000	25,000	9,000~14,000	12,000	19,000~23,000

Table 2. 4 Typical metal content in wastewater solids (Adapted from Environment Protection Agency, USA, 1984)

	Dry Solid, mg/kg	
Metal	Range	Median
Arsenic	1.1~230	10
Cadmium	1~3410	10
Chromium	10~99,000	500
Cobalt	11.3~2490	30
Copper	84~17,000	800
Iron	1000~154,000	17,000
lead	13~26,000	500
Manganese	32~9870	260
Mercury	0.6~56	6
Molybdenum	0.1~214	4
Nickel	2~5300	80
Selenium	1.7~17.2	5
Tin	2.6~329	14
Zinc	101~49,000	1700

In the United States, regulations were promulgated in 1993 by the U.S. Environmental Protection Agency that established pollutant numerical limits and management practices for the reuse and disposal of solids generated from the processing of municipal wastewater and septage (Federal Register, 1993). The sludge treatment should be carried out to reduce the risk of activated sludge disposal. The sludge treatment process consists of seven major components, which are preliminary operations, thickening, stabilization, conditioning, dewatering, heat drying and other processing and thermal reduction (Figure 2.3).

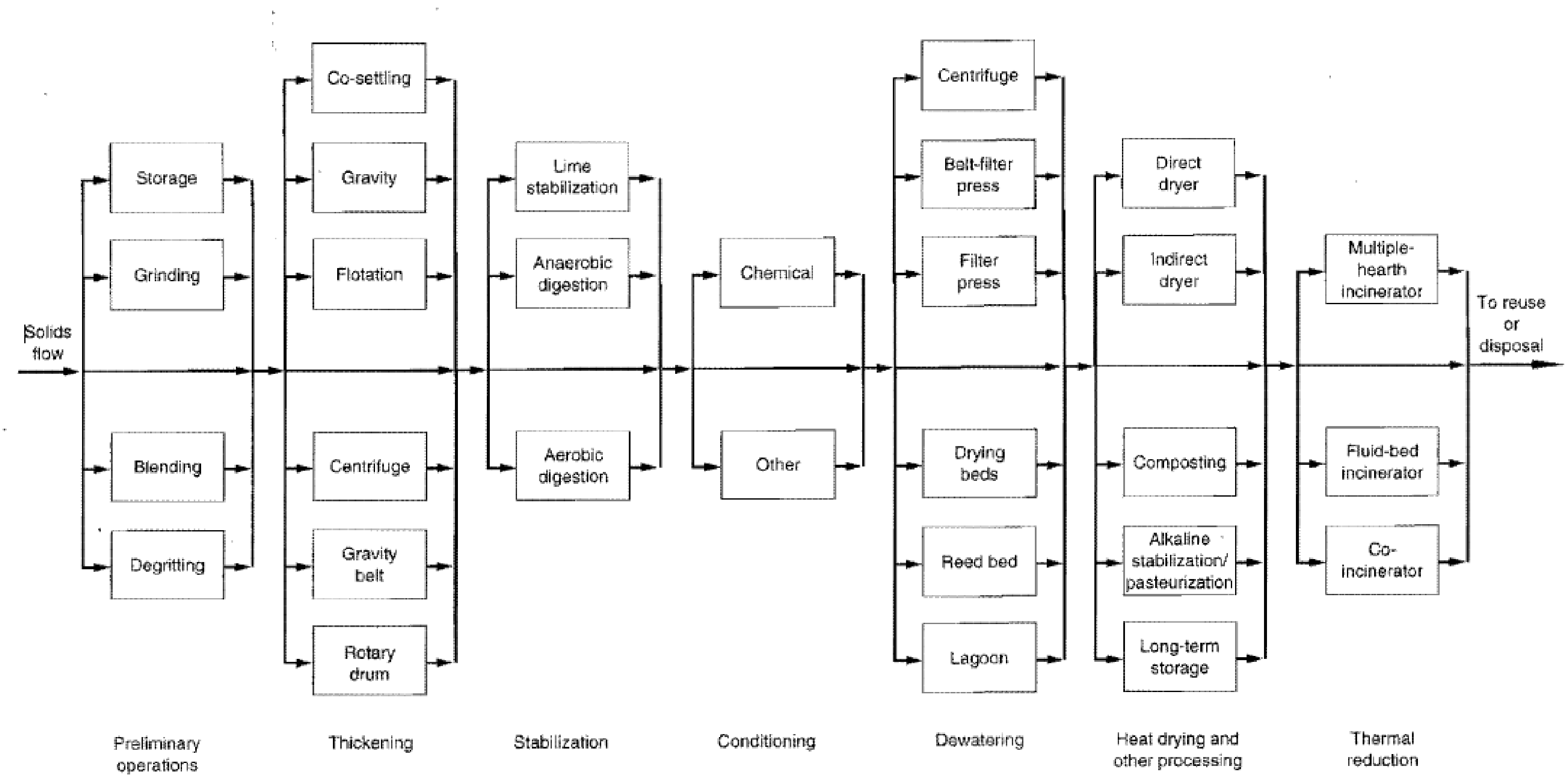

Figure 2. 3 Generalized sludge-processing flow diagram (Adapted from Tchobanoglous *et al*., 2004).

2.2.2.1 Preliminary Operations

The preliminary operations of sludge treatment, which include grinding, degritting, blending and storage, aims to provide a relatively constant, homogeneous feed to subsequence processing facilities (Tchobanoglous *et al*., 2004). Carlsson *et al*.(2012) stated that pretreatment technologies viz., physical, mechanical, thermal, chemical, biological and physico-chemical have been studied and applied to increase anaerobic biodegradability and methane yields of various biomasses including wastewater treatment plant sludges. Sludge grinding is a process to cut or shear the sludge from large particles to small ones. The degritting should be conduct before further treatment of the sludge since some plants do not use primary sedimentation tank or the grit removal facilities are not adequate to handle peak flows and peak grit loads. Cyclone degritting is one of the widely used methods for removing grits for subsequent processes. Blending is to produce a uniform flow for the following treatment processes. Storage of the sludge provides a smooth feeding rate for the subsequent treatment process (Tchobanoglous *et al.*, 2004).

2.2.2.2 Thickening

Thickening of sludge can have a significant impact of the size and cost equipment required to perform downstream operations. It also makes the plant operation more stable, as well as more economical (Eckenfelder and Santhanam, 1981). Thickening is achieved by physical operations such as gravity settling, flotation, and centrifugation.

2.2.2.3 Stabilization

Two major obstacles for sludge disposal are the pathogens and offensive odours. The stabilization process in the sludge treatment aims to reduce the pathogens, eliminate offensive odours and mitigate the potential for putrefaction. The sludge should be both stable and mature for the application as a fertilizer for agricultural (Iannotti *et al*., 1993; Wu *et al*., 2000). Stability refers to the decomposition capability for organic matter by the microbial activity, which is usually reflected by the CO_2 generation or the oxygen consumption (Iannotti *et al*., 1993). In addtion, maturity is directly related to the effect of an organic material on plant growth or on seed germination (Wu *et al*., 2000). To achieve stabilized sludge, alkaline stabilization, heat treatment, anaerobic digestion, aerobic digestion and composting are the five common stabilization methods (Table 2.5). Table 2.6 shows the relative degree of attenuation achieved with various sludge stabilization processes.

Table 2. 5 Five processes for stabilization (Adapted from Tchobanoglous *et al*., 2004)

Process	Description	Comments
Alkaline stabilization	Addition of an alkaline material, usually lime, to maintain a high pH level to effect the destruction of pathogenic organisms	An advantage of alkaline stabilization is that a rich soil-like product results with substantially reduced pathogens. A disadvantage is that the product moss is increased by the addition of the alkaline material. Some alkaline stabilization processes are capable of producing a Class A sludge
Anaerobic digestion	The biological conversion of organic matter by fermentation in a heated reactor to produce methane gas and carbon dioxide. Fermentation occurs in the absence of oxygen	Methane gas can be used beneficially for the generation of heat or electricity. The resulting biosolids may be suitable for land application. The process requires skilled operation as it may be susceptible to upsets and recovery is slow
Aerobic digestion	the biological conversion of organic matter in the presence of air (or oxygen) usually in an open-top tank	Process is much simpler to operate than an anaerobic digester, but no usable gas is produced. The process is energy-intensive because of the power requirements necessary for mixing and oxygen transfer
Autothermal thermophilic digestion (Heat treatment)	Process is similar to aerobic digestion except higher amounts of oxygen are added to accelerate the conversion of organic matter. Process operates at temperatures of 40 to 80°C, autothermally in an insulated tank	Process is capable of producing a Class A sludge. Skilled operators are required and the process is a high-energy user (to produce air or oxygen)
Composting	The biological conversion of solid organic matter in an enclosed reactor or in windrows or piles	A variety of solids or biosolids can be composted. Composting requires the addition of a bulking agent to provide an environment suitable for biological activity. Volume of compast produced is usually greater than the volume of wastewater solids being composted. Class A or Class B sludge can be produced. Odor control is very important, as process is odorous

Table 2. 6 Relative degree of attenuation achieved with various sludge stabilization process (Adapted from Water Environment Federation, 1998)

	Degree of attenuation		
Process	Pathogens	Putrefaction	Odour potential
Alkaline stabilization	Good	Fair	Fair
Anaerobic digestion	Fair	Good	Good
Aerobic digestion	Fair	Good	Good
Autothermal thermophilic digestion (ATAD) (Heat treatment)	Excellent	Good	Good
Composting	Fair	Good	Poor to fair
Composting (thermophilic)	Excellent	Good	Poor to fair

Alkaline stabilization

The alkaline stabilization includes the lime pretreatment and posttreatment. The pretreatment has been used for either the direct application of liquid sludge to land or combining benefits of sludge conditioning and stabilization prior to dewatering while the posttreatment utilized the hydrated lime or quicklime to raise the pH even the temperature of dewatered sludge to inactivated worm eggs (Tchobanoglous *et al*., 2004). Table 2.7 showed the dosage requirement for the lime pretreatment for maintain pH at 12 for 30 min.

Table 2. 7 Typical lime dosage for pretreatment sludge stabilization (Adapted from Water Environment Federation, 1995)

Anaerobic digestion

	Soli conc. %		Lime dosage g $Ca(OH)_2$ / kg dry solids	
Type of sludge	Range	Average	Range	Average
Primary	3~6	4.3	60~170	120
Waste activated	1~1.5	1.3	210~430	300
Anaerobically digested mixed	6~7	5.5	140~250	190
Septage	1~4.5	2.7	90~510	200

Anaerobic digestion is traditionally used to stabilize mixed sludge in municipal wastewater treatment plants and also increasingly to produce biogas, renewable energy, from biowastes and manure and from energy crops (Bayr and Rintala, 2012). Anaerobic digestion is an energy efficient stabilization method which involves the decomposition of organic matter and inorganic matter (principally sulfate) in the absence of molecular oxygen (Tchobanoglous *et al*., 2004). Decomposition proceeds in three stages, hydrolysis, acidogenesis and methanogenesis. The end products of the anaerobic digestion are carbon dioxide, methane, nitrogen, hydrogen sulfide and hydrogen phosphide. The volatile solids reductions for the digestion system are reported to be on the order of 63% (Schafer and Farrel, 2000).

Organic substance (C, H, N, O, P, S) + Nutrients (N, P) + 2 [O] $\rightarrow$ $CO_2 + CH_4 + N_2 + PH_3 + H_2S + C_{60}H_{87}O_{23}N_{12}P$ (new cells) + Energy + Exocellular by-products

The anaerobic digestion holds the advantages of energy efficient, low bacterial growth, low nutrient requirement and methane production.

Aerobic digestion

Compared to the anaerobic digestion, the aerobic digestion has advantages of (1) equal volatile solids reduction in a well-operated aerobic digester; (2) lower BOD in the supernatant; (3) production of odourless, humuslike, biologically stable end products; (4) recovery of more of the basic fertilizer values in the sludge; (5) relatively easy operation; (6) lower capital cost; and (7) suitability for digesting nutrient-rich biosolids.

Organic substance (C, H, N, O, P, S) + Nutrients (N, P) + $O_2 \rightarrow CO_2 + H_2O + NO_3^- + PO_4^{3-} + SO_4^{2-} + C_{60}H_{87}O_{23}N_{12}P$ (new cells) + Energy + Exocellular by-products

In the aerobic digestion, the oxygen needs to be maintained in an adequate level. The oxygen requirement for the complete oxidation of the BOD contained in primary sludge varies from about 1.6 to 1.9 kg/kg destroyed (Tchobanoglous *et al.*, 2004).

Composting

Composting is a cost-effective and environmentally sound alternate for the stabilization of activated sludge. Approximately 20 to 30 % of VSS would be degraded to be carbon dioxide and water. The sludge after composting could be utilized as fertilizer for the agriculture purposes.

2.2.2.4 Conditioning

Conditioning is a process, in which chemical is added to improve the dewaterability of the sludge. Factors affecting the conditioning are the properties of the solids and the type of mixing and dewatering devices to be used (Tchobanoglous *et al*., 2004). For the chemical dosage, there are inorganic and organic conditioning agents. Divalent and trivalent metal salts, such as ferrous and aluminium salts, would be commonly used as inorganic conditioner (Gao and Gu, 2004). Heat treatment is also an alternative method for conditioning.

2.2.2.5 Dewatering

The dewatering is to remove the moisture content of the treated sludge in order to save the trucking fee, increase calorific value prior to incineration, reduce bulking agent dosage for composting and reduce leachate production for landfill (Tchobanoglous *et al*., 2004). The dewatering is a physical process using the methods such as solid-bowl centrifuge, belt-filter press, recessed-plate filter press, sludge drying beds and sludge lagoons (Eckenfelder and Santhanam, 1981). Odour control is an important design consideration as the level of odour release varies based on the type of sludge and the mechanical equipment selected. The treatment methods of sludge drying beds and sludge lagoons would have high potential of odour release than mechanical treatment. However, high shear dewatering and conveyance equipment can increase odour release, especially from anaerobically digested sludge.

From the introduction above, the sludge treatment process is a complicated and costly process. To reduce the cost for sludge treatment but also reuse valuable organic matter and nutrients in activated sludge, a environmentally way should be developed.

2.3 Sludge Amended Soil

The sludge after the process of preliminary operations, thickening, stabilization, conditioning and dewatering is commonly sent to further treatment, such as heat drying, incineration and final disposal, or reuse, such as composting. From the former section, the moisture, nutrients, organic matters and heavy metals content are the major obstacles for the disposal and reuse of the activated sludge.

Studies investigated the reused of the sludge mixing with the normal soil, named as sludge-amended soil. The sludge-amended soil is widely studied and used in agricultural area. In the USA, 13% of the sludge produced is applied to agricultural land and a further 10% is used in the composting industry (Anon, 1989) while in The Netherlands, France, Denmark and Switzerland over 30% is applied to agricultural land (Sauerbeck, 1987).

The application of sludge-amended soil aims to utilize the valuable nutrient, including N, P and K, to enhance the growth of plants (Frink and Hullar, 1985; Planquart *et al*., 1999). Chu and Poon (1998) studied the mixture of natural soil and lime/pulverized fuel ash (PFA) stabilized sewage sludge by growing the wheat grass (*Apropyron elongatum*) and found it is feasible to plant grass on the sludge-amended soil. However, the heavy metal and recalcitrant organics affect the utilization of the sludge-amended soil.

2.3.1 Heavy Metal

Recently, legislation in different countries limit the use of sewage sludge in agriculture, due to the total amounts of heavy metals in these wastes and in soils, and recommend that soil pH to be maintained at 6 or higher (Planquart *et al*., 1999). As described in Table 2.4, the activated sludge usually contained kinds of heavy metals. It was reported that in most of the anaerobic digested sewage sludge samples, more than 40% Cr and 90% Cu were in the oxidizable fraction. The oxidizable fraction shows that Cr and Cu were associated with organic matter of the sludge (Wang *et al*. 2005). This information is useful to understand the low solubilization of these metals in the various bioleaching studies. On the other hand, Ni and Zn were found mainly in the exchangeable and reducible fractions of the sludge, indicating the presence of Ni and Zn in more mobile forms. Table 2.8 summarized the typical heavy metal concentration in activated sludge in some countries.

Table 2. 8 Heavy metals content of various sludges (mg/kg of dry sludge solids)(Adapted from Pathak *et al*., 2009)

Country	Cu	Ni	Zn	Cr	Cd	Pb
Canada	180–2300	37–179	354–640	66–2021	2.3–10	26–465
China	131.2–394.5	49.3–95.5	783.4–3096	45.8–78.4	5.9–13	57.5–109.3
Germany	275	23.3	834	50	1.5	67.7
Hong Kong	112–255	44.5–622	1009–2823	663	–	52.5–57
India	280–543	192–293	870–1510	102–8110	41–54	91–129
Italy	370	19	1500		2.1	72
Spain	204–337	23.2–36.5	871–1626	54.4–3809	2.37–18.3	167–223
UK	562	58.5	778	159.5	3.5	221.5
USA	616	71	1285	178	25	170

The heavy metals in the sludge-amended soil bring them into the food chain, ultimately causing metabolic disorder and chronic diseases in humans. Studies were carried out to decontamination of the heavy metal in the sludge prior it application in the land. Use of various chemicals such as $Fe_2(SO_4)_3$ and $FeCl_3$ (Strasser *et al*., 1995; Ito *et al*., 2000), chelating agents such as ethylene di-amine tetraacetic acid (EDTA) and nitrilotriacetic acid (NTA) (Lo and Chen, 1990) and organic and inorganic acids

(Marchioretto, 2003) have been reported for extraction of metals from sludge. The methods by addition of chemicals have disadvantages including high operation cost and secondary pollution. Compared to chemical method, bioleaching is a low cost environment friendly technique. The Bioleaching process uses the catalytic effect produced by the metabolic activities of iron-oxidizing and sulfur-oxidizing microorganisms resulting in an acceleration of the chemical degradation of the sulfides (Morin *et al*., 2005).

However, studies still need to be carried out to find out the adequate methods for heavy metal extraction from the activated sludge used for anti-desertification purpose.

2.3.2 Recalcitrant and Persistent Organics

The (Beck *et al*., 1996). Typical United Kingdom soil concentrations of polychlorinated dibenzo-p-dioxins and furans (PCDD/Fs) in soils have been reported to range from 0.01 ng/kg 1,2,3,7,8,9-HexaCDF to 27 ng/kg 1,2,3,4,6,7,8-HeptaCDD (Wild *et al*., 1994). The recalcitrant and persistent organics, such as polychlorinated biphenyls (PCBs), polycyclic aromatic hydrocarbons (PAHs), chlorobenzenes (CBS) and (PCDD/Fs), have a wide range of physicochemical properties so that some are volatile or leachable whilst others are strongly sorbed and persist in soils over prolonged periods (Beck *et al*., 1996). Wang *et al*., (2011) studied the degradation of hexazinone, an effective herbicide for general weed control in agricultural and forestry area, in the forest soils amended with sewage sludge and found that the degradation rate of hexazinone is increased up to 51.6% as comparing with the non-amended forest soil. Studies found that the recalcitrant and persistent organics would be degraded in the sludge-amended soil, however, the time period was long and the efficiency was low. More studies should be carried out for adequate methods to enhance the degradation of the recalcitrant and persistent organics.

2.4 Physical Properties of Soil

As the Eco-Soil is a novel type of growing medium, the physical properties including bulk density, particle density, hydraulic conductivity, porosity, field capacity and saturation moisture should be studied to analyze the water retention capabilities. The physical properties are important also for numerical simulation of the soil water retention curve and water flow under various boundary conditions.

2.4.1 Bulk Density

Soil bulk density (BD) is one of the important properties for hydraulic conductivity, water retention, vegetation water uptake, growth of root and rainfall infiltration (Dam *et al*., 2005). In addition, it has indirect effects on growth of root and yield of crop (Reichert *et al*., 2009). Soil bulk density is defined as the clastic weight and other solid materials per unit volume of soil and ranges from 1.0 to 2.65 g/cm^3, while compacted soil is able to achieve as high as 2.3 g/cm^3 (Schaetzl and Anderson, 2005). Depend on some factors affecting soil bulk density, most mineral soil value ranged between 1.1 and 1.6 g/cm^3 (Manrique and Jones, 1991). A study in greenhouse examined the effects of uniform conditions of bulk density on the growth of *Quercus ilex L.*(holm oak) shown that the conditions of a bulk density of 1.62 Mg/m^3 had negative local effects on the development of root density and rooting depth, respectively (Cubera *et al*., 2009).

Many methods can be used for determining bulk density via both conventional and modern procedures (Timm *et al*., 2005; Rossi *et al*., 2008). One of the conventional standard methods namely the volumetric ring method is still in used by many laboratory works (Grossman and Reinsch, 2002). However, Standard dimension and material of volumetric ring used by some research vary on the location of sampling. A research in large and small column showed that the dispersivity of small column with 30 cm of length and 5.1 cm of internal diameter is 1 cm while large column with 0.945 m of internal diameter and 6 m of length is 5 cm (Wierenga and Van Genuchten, 1989). In addition, dispersivity is the function of pore water velocity and mechanical dispersion coefficient (Van Genuchte and Wierenga, 1986). Because pore water velocity is determined by the ratio of volumetric water content and Darcian fluid flux density, the value of dispersivity is approximately linear with flux density. Hence, the different dimension in soil column result in different values in water movement in the same type of soil (Suuster *et al*., 2011; Lestariningsih *et al*., 2013).

Despite the importance of BD, it is not usually determined in soil surveys. Direct measurement of BD is considered to be time-consuming, labour intensive, tedious and expensive. Therefore, several empirical functions has been developed to predict BD from more easily collected chemical and physical soil data (Heuscher *et al*., 2005; Tranter *et al*., 2007; Benites *et al*., 2007; Kaur *et al*., 2002). These predictive functions are usually termed pedotransfer functions (PTFs) in soil science and are used for certain soil properties from other routinely, inexpensively or easily measured parameters (McBratney *et al*., 2002). The systematic variation of BD is described mostly by SOC and texture (Bernoux *et al.*, 1998; Huntington *et al*., 1989; Heuscher *et al*., 2005; Kaur *et al*., 2002; Manrique and Jones, 1991; Tomasella and Hodnett, 1998). Benites *et al*., (2007) indicated that soil chemical properties were shown to be highly important for the determination of BD. Some studies have investigated the relevance of soil sample depth and the suborder of the soil profile to Db estimation (De Vos *et al*., 2005; Harrison and Bocock, 1981; Tranter *et al*., 2007).

2.4.2 Particle Density

To determine porosity and other hydraulic properties, the particle density (PD) of soil is one of the important factors. The PD represents one of the basic physical properties and is defined as mass per unit volume of solid soil components, excluding voids and water. The standard mean value of PD for most mineral soils is 2.65 g/cm^3 (Skopp, 2000), which is identical to the mean PD for quartz. However, typical values for mineral soils range from 2.4–2.9 g/cm^3. The PD depends on the constitutions of the mineral and the organic soil substances. The particle density varies from 2.2 to 2.9 g/cm^3 and 2.9 to 4.0 g/cm^3 for clay and heavy minerals, respectively (Schachtschabel *et al*., 1992). These results are directly influenced by the type of mineral, such as biotite hematite and gypsum, with values of 2.80–3.20, 4.80–5.30 and 2.32 g/cm^{-3}, respectively (Skopp, 2000). Therefore, the particle density of mineral soil components averaged the portion of the soil minerals. For soil containing high fraction of organic matters, the particle density depended on the degree of composition and ranged from 1.0 to 1.5 g/cm^3 (Ellies *et al*., 2003; Hassink, 1995; Leuschner *et al*., 1981; Ladd *et al*., 1995; Golchin *et al*., 1994, 1995; Skopp, 2000; Young and Spycher, 1979;).

The variability is important for the properties estimated by the function using particle density (Ball *et al*., 2000), especially before pedotransfer functions became a 'white-hot' topic for environmental research and soil science (McBratney *et al*., 2002). In addtion, because the organic soil particles and specific heat of mineral vary a lot, it is necessary to obtain the mixture fraction in order to describe the heat dynamics of soils accurately (Kuntze *et al*., 1994). Furthermore, the values of PD were able to be used for calculating other useful soil properties such as the porosity, which can be calculated from the quotient of PD and BD (Danielson and Sutherland, 1986; Riek *et al*., 1995). This was able to be used in combing with the pore size distribution (PSD) to determine transport processes in soil (Rühlmanna *et al*., 2006).

2.4.3 Particle Size Distribution

Particle size distribution (PSD) is one of the essential properties for substrates. The results of PSD decide the classification of the group of textures and affect the hydraulic conductivity, moisture retention. The PSD was usually used as inputting parameter for OM, SWCC, DB models.

In arid and semi-arid area soil studies, PSD is frequently used for organic matter analysis (Breulmann *et al*., 2014; Nicolás *et al*., 2012). Semi-arid soils in some Mediterranean regions are often characterized by organic matter (OM) content lower than 2% (Van-Camp *et al*., 2004). Nicolás *et al*. (2012) reported that the environmental conditions in arid area, such as scarce and intense rainfalls, are caused by the degradation and loss of soil OM. To increase the OM of semiarid soils and to improve their properties, the organic amendments were widely used (Bastida *et al*., 2007; Fernández *et al*., 2009). However, this amendment has not taken activated sludge into account. Soil physical fractionation has been used for investigating the distribution of the organic matter associated with various soil particle fractions (Kandeler *et al*., 1999; Stemmer *et al*., 1998). Some studies assessed the quality and biological activities of the OM due to the differences of soil particle-size fractions after introducing external organic substrates (Christensen, 1987; Gerzabek *et al*., 2002).

Study found that silt and clay-sized particles showed low microorganism degradation of the OM associated (Christensen, 1987; Hassink, 1997; Marschner *et al*., 2008; Sollins *et al*., 2006). Therefore, the association of OM with fine particles is considered to be stable and important in the retention of soil OM.

For the soil in semi-arid area, Caravaca *et al*. (2001) found that the silt fraction accumulates the most organic carbon after the application of urban refuse. The silt fraction also accumulates the largest amount of organic carbon when Caravaca *et al*. (2004) studied the fine fractions of agricultural and forest soils under semi-arid climate.

Some studies investigated the physical protection of the organic matter in semi-arid soils through aggregates (Noellemeyer *et al*., 2009; García-Orenes *et al*., 2005; Sarah, 2006) or the biochemical stabilization of it through chemical transformation of the organic compounds (Fernández *et al*., 2009). However, for degraded soils after organic amendment, information about the degradation, distribution and protection of the OM associated in various particle-size fractions is still not enough.

Soil erosion is one of serious environmental issues affecting the further development of agriculture and also induces desertification by washing out of organic matters. The adverse effects of widespread soil erosion on agricultural production, soil health, ecosystem well-beings and water quality exert severe adverse influence on sustainability of ecosystem (Lal, 1998). The PSD is also used for predicting the soil erosion behavior in semi-arid and arid area. Raei *et al*. (2015) indicated that threshold stream power and critical shear stress are two main soil characteristics controlling the detachment of soil particles by surface runoff. Critical shear stress is dependent on the weight and angle of repose of particles, which relate to the particles size distribution (Julien, 2010). In addition, it also strongly relates to the forces of adhesion strongly (Oliveira, 1997). The threshold stress is usually calculated shear stress and transport rate (James *et al*., 1990).

In most of soil erosion models, the critical shear stress/threshold stream power is depended on the bulk characteristic of the soil. However, some studies stated larger particles show less resistance to movement than the relatively smaller ones and are transported at a higher rate for specimen of various particle size distribution (Asadi *et al*., 2007, 2011; Shi *et al*., 2012; Wang *et al*., 2014; Wiberg and Smith, 1985). This phenomenon is due to the possible reasons of different size classifications and greater resistance to movement for smaller particles. In addition, discrepancies are still found in the publications for the measurements of critical shear stress (Araujo *et al*., 2008;

Bohling, 2009; Moody *et al*., 2005; Salehi and Strom, 2012; Wilcock, 1988; Petit, 1990).

Studies found that particles transport as aggregates under flow dominant condition and rainfall of various kinetic energies for well aggregated soils (Asadi *et al*., 2007, 2011; Shi *et al*., 2012; Wang *et al*., 2014). On the other hand, the study of the initial motion of soil aggregates is very rare, and most of the studies have focus on sand particle and/or cohesive soils.

In view of the previous study, the PSD closely relates to the organic matter and the wind erosion activities. However, there was no study carried out on the PSD of Eco-Soils and the associated behavior under surface runoff conditions.

2.4.4 Hydraulic Conductivity

Hydraulic conductivity (also referred to as coefficient of permeability) is the property related to the conduit function of an aquifer. It is a function of both the porous medium and the fluid properties with dimensions of (L/T). The hydraulic conductivity is the rate of flow of water through a cross section of unit area of the aquifer under a unit hydraulic gradient (Mays, 2011). It is related to intrinsic permeability of material, degree of saturation, density and viscosity of fluid.

The hydraulic conductivity for soil related to the water infiltration, evaportranspiration and water management. For the tillage in semi arid and arid area, hydraulic conductivity is an important factor to determine the water retention and infiltration (Lampurlanés and Cantero-Martínez, 2006). In rainfed agriculture in arid- and semi-arid area, the capability of retention of water in soil is important for the crops. Soil water storage is determined by infiltration and evaporation processes, which were closely related to land surface conditions. The surface conditions are usually modified by tillage activities. Soil water storage is able to be optimized by specific soil management system, which is dependent on soil and environment conditions (Godwin, 1990). Soil characteristics that define surface conditions are able to exert significant effects on soil processes involved in water infiltration, evaporation and redistribution. One of the typical examples could be the high porosity and pore continuity in the soil. These conditions offer good characteristics for high soil water storage capacity and infiltration, but also favour evaporation from lower subsoil layers. If the soil surface is modified by residue cover, infiltration is able to be improved but evaporation was reduced under extended dry conditions (Godwin, 1990).

Studies found that disruption of macro-pore continuity through tillage activities is able to control infiltration and hydraulic conductivity (Godwin, 1990; Ehlers and van der Ploeg, 1976; Logsdon *et al*., 1990). However, some other studies found that, in non-tillage (NT), infiltration and hydraulic conductivity are smaller than that with inversion tillage (Ferreras *et al*., 2000; Pelegrin *et al*., 1988). The reasons are indicated to be due to high bulk density (low porosity) in non-tillage soils and high porosity by affecting large pores from tillage activities (Hubbard *et al*., 1994; Pelegrin *et al*., 1990; Pelegrin and Moreno, 1994; Tebrügge and Düring, 1999).

Studies found that hydraulic conductivity decreases in tilled soils within the growing season (Logsdon *et al*., 1993; Messing and Jarvis, 1993; Mwendera and Feyen, 1993).

It is because of soil breakdown of structure, surface sealing and root growth which gradually blocks pores (Ankeny *et al*., 1990; Suwardji and Eberbach, 1998). Under this condition, at the beginning of growing season, saturated hydraulic conductivity can be higher for tillage than non-tillage conditions due to increased porosity produced by tillage activities (Hill, 1990; Radcliffe *et al*., 1988; Suwardji and Eberbach, 1998). It could be lower for tilled soil than untilled soil at the end of the season (Suwardji and Eberbach, 1998; López and Arrúe, 1997).

Some studies reported hydraulic conductivity affects land application of treated wastewater on soil for nutrient leaching, especially nitrate leaching (Magesan *et al*., 1998, 1999) and soil microfauna, including nematodes (Yeates, 1995; Gupta *et al*., 1998). The hydraulic conductivity is a unique parameter to control these processes (Magesan *et al*., 2000). In some large rural area, land treatment systems are popular for treating wastewaters (Cameron *et al*., 1997). Some studies reported that soil hydraulic conductivity decreases after wastewater application (Balks *et al*., 1997; Cook *et al*., 1994). Sustainable hydraulic conductivity is important for the quality of the receiving environment and site performance, because decreases of soil hydraulic conductivity result in surface runoff and ponding. Increased runoff would lead to soil erosion and contamination of surface waters while ponding increased dominates flow of contaminants into soil (Vinten *et al*., 1983).

Physical or biological cloggings are able to reduce soil hydraulic conductivity (Ragusa *et al*., 1994). Biological (microbial) clogging is contributed by the accumulation of biomass and metabolic products in the pores, such as the production of extracellular polymers (EPS) (Baveye *et al*., 1998). Physical clogging is because of the trapping of colloidal and suspended materials in the pores (Bouwer and Chaney, 1974). Microbial clogging, which results from production of insoluble organic and inorganic compounds by microbes (Chou *et al*., 2011; Stocks-Fischer *et al*., 1999), and occurs via many pathways, such as photosynthesis, urea hydrolysis, and sulfate reduction (Okwadha *et al*., 2010), is considered as one such maintenance method used for hazardous waste confinement. When the soil is irrigated by wastewater with a high C:N ratio (50:1), the deposition of extracellular carbon and soil microbial biomass reduce the hydraulic conductivity of soil (Magesan *et al*., 1999). Soil pore clogging is found after irrigation by meatworks wastewater due to increases of EPS, which are able to be biodegraded about 23 days after stopping irrigation. Therefore, the return time is important to control the biodegradation of the EPS to maintain suitable hydraulic conductivity for land wastewater treatment (Balks *et al*., 1997).

Various mechanical and chemical treatments have been investigated to reduce biological cloggings to recover hydraulic conductivity. Treatment with 5% sodium hypochlorite is able to kill the bacteria, remove the EPS biofilm and recover permeability to the plugged cores (Shaw *et al*., 1985). Some bacteria are able to reduce hydraulic conductivity but provide valuable nutrients for vegetation growth. Bacterial and enzymatic $CaCO_3$ precipitation has been found to be able to reduce the permeability of porous media (Nemati *et al*., 2003; Yasuhara *et al*., 2012; Chu *et al*., 2012). *Sporosarcina pasteurii* (formerly named as *Bacillus pasteurii*) is used by researchers to investigate the $CaCO_3$ precipitation (Ivanov and Chu, 2008; Mitchell *et al*., 2006; Tobler *et al*., 2011) and found that *S. pasteurii* produces urease, which is the enzyme for hydrolyzing urea to ammonia and carbon dioxide. *S. pasteurii* is non-pathogenic, high urease production (Whiffin, 2010). In addition, it is tolerant to ammonium, salt (high electrical conductivity) and high pH conditions. The production of ammonia increases the pH then the $CaCO_3$ precipitation in calcium-rich environments.

Some hydraulic conductivity prediction models are developed to provide estimation of soil properties for some types of soil. Ebina *et al.* (2004) used the soil clay content to correlate the hydraulic content for sand-clay specimen. Some other study used Na-type bentonites for hydraulic conductivity determination (Keijzer *et al*., 1999). Therefore, to correlate the hydraulic conductivity with clay properties is important for better prediction. However, A few theoretical and empirical approaches have been done (Ogata *et al*., 1994; Benson and Trast, 1995). The essential material of clay liners, which is bentonite, has been investigated to reduce the hydraulic conductivity of landfills (Benson *et al*., 1999; Benson *et al*., 2007; Gleason *et al*., 1997). However, the long-term durability of landfill liners is still arguable. Landfill waste degradation is a long-term process and it took 20-30 years after the landfill completion to stabilize the waste to inert state continues (Wall and Zeiss, 1995). Some studies found that the introduction of inorganic salt solutions (Egloffstein *et al*., 2001; Kolstad *et al*., 2004; Petrov *et al*., 1997) and seasonal drying, which reduce the volume of clay and developed cracks (Daniel *et al*., 1993), are able to increase in hydraulic conductivity of clay liners.

However, the hydraulic conductivity of Eco-Soils was not yet studied. For anti-desertification, this physical property is important to control the evaporation and infiltration for soil water storage.

2.4.5 Porosity

Porosity is the pore volume divided by the total volume, expressed as a percent. Porosity represents the potential storage of an aquifer but does not indicate the amount of water a porous material will yield (Mays, 2011). Porosity is used in pharmaceutics, ceramics, metallurgy, materials, manufacturing, earth sciences, soil mechanics and engineering. There are many ways to test porosity in a substance or part, such as industrial CT scanning. (Wikipedia, 2016).

Lu *et al.* (2004) stated that soil pore characteristics are important soil property indicators. The total volume, shape of soil pore spaces and size distribution are related to many soil functions and processes, including water storage, transmission, microbial activity, gas diffusion and soil mechanical resistance to root penetration (Munkholm *et al*., 2012; Cameron and Buchan, 2006; Strong *et al*., 2004). Studies indicated that soil pore size distribution (PoSD) are useful for explaining lots of soil processes, including water and solute movement, structural stability, and organic carbon sequestration (Lipiec *et al*., 2012; Six *et al*., 2004; Strong *et al*., 2004; Pagliai *et al*., 2004). Hence, studies on soil pore characteristics are significantly important to evaluate soil quality and soil structure.

Soil pore structure is mainly dependent on environment and soil management practices. Studies indicated that land use, fertilization, tillage and compaction is able to affect the size distribution, total porosity and functionality of soil pores. As a result, the activities influence the physical, chemical and biological processes in the soils (Cameira *et al*., 2003; Bhattacharyya *et al*., 2006; da Costa *et al*., 2014; Cassaro *et al*., 2011; Lipiec *et al*., 2012). Therefore, changes in pore volume, pore shape pattern and pore size distribution have been used to compare the effects of tillage and non-tillage condition, organic matter waste, and land use on soil structure and quality (Cassaro *et al*., 2011; Deurer *et al*., 2009; Zhou *et al*., 2012, 2013; Wairiu and Lal, 2006). The soil pore size distribution and macroporosity significantly change during soil tillage and compaction (Cassaro *et al*., 2011; da Costa *et al*., 2014; Lipiec *et al*., 2012; Deurer *et al*., 2009). This preferential loss of larger pores is able to change many important soil ecological functions. The quantification of shape, size and continuity of pores can be used to find out the effects of environmental changes and management practices in soil quality.

In soil science, many methods including mercury intrusion porosimetry (MIP), X-ray micro-computed tomography (μ CT), nitrogen adsorption/desorption (NAD) and soil water retention curve (SWRC) are widely used to characterize soil pore structure (Echeverria *et al*., 1999; Pires *et al*., 2008; Hajnos *et al*., 2006; Sasanian and Newson, 2013). However, no study investigated the pore properties for the sand sludge mixture for anti-desertification purposes.

2.4.6 Soil Water Characteristics Curve

The Soil Water Characteristics Curve (SWCC) describes the relation between the soil water potential and soil water content. It is a significant and unique relation for every texture and also named Soil Water Retention Curve (SWRC). Soil moisture content and water potential are the two major parameters to describe the water content within the soil and appears an intrinsic relation. SWCC usually plots the soil water potential in the form of suction head as the x-axis. In the y-axis, soil Volumetric Water Content

(VWC) or Effective Saturation (ES) are plotted according to the simulation models. The measurement of SWCC can be done by hanging water, tention plate, tempe cell, pressure cell, sand funnel, sand column, dew point potential, freezing point reduction, filter paper, centrifuge and chemical solution methods (Li *et al*, 2007; Yi, 2009; Chen *et al*., 2010). However, these methods have its measuring ranges, advantages and limitations.

The measurement of soil parameters for unsaturated soils is time consuming and requires complicated laboratory tests. The soil water characteristic curve (SWCC), also named as soil water retention curve (SWRC) is often used to evaluate the unsaturated soil property functions, including permeability, shear strength and thermal property functions. Many methods or soil property indexes have been investigated to evaluate the SWCC and its correlations between suction head or soil water potential (Gupta and Larson, 1979; Saxton *et al*., 1986).

Studies investigated empirical relations between soil properties and fitting factors of the SWCC models (Chin *et al*., 2010; Ahuja *et al*., 1985). Some other studies used a physics-based conceptual model to simulate SWCC (Arya and Paris, 1981; Fredlund *et al*., 1997). Conversion of the PSD into the PoSD of a soil is required for using the aforementioned models. In addition, Fredlund and Xing (1994) developed an SWCC equation by assuming that the SWCC is dependent on the shape of PoSD of a soil. Leong and Rahardjo (1997) reviewed and evaluated five widely used SWCC models and found that the Fredlund and Xing (1994) model offers best fit than the others. Zhang and Chen (2005) applied the Fredlund and Xing (1994) and the van Genuchten (1980) models to predict bimodal and multimodal SWCCs.

The SWCC is affected by many factors, including initial water content, BD and pressure state (Zhou and Yu, 2005). Yang *et al*. (2004) indicated that the shape of SWCC is similar as the PSD and affected by the BD of the soil. Gallipoli *et al*. (2003) developed a modified form of the van Genuchten (1980) model with the consideration of the influence of porosity. Tarantino (2009) developed a SWCC model for deformable soils associated with an empirical power function of the water ratio. Rajkai *et al*. (1996) investigated the prediction of water retention characteristic based on various BD and PSD parameters. Gallage and Uchimura (2010) evaluated the effects of BD and PSD on SWCC by using sandy soils. Vanapalli *et al*. (1999) investigated the effects of porosity and initial water content. It was found their effects on SWCC are reduced at high suction state. Sheng and Zhou (2011) investigated the effects of deformation on the soil water retention and revealed the influences on initial porosity on the air-entry value and the slope of SWCC.

To correlate the measured SWCC data with the numerical models, data is required to obtain the optimal curve-fitting parameters. However, the complicated unmodeled influencing factors usually led to high level of uncertainty for fitting the measured data for SWCC. Because of geotechnical uncertainties, three primary sources for uncertainty were found to be measurement error, transformation uncertainty and inherent variability (Phoon and Kulhawy, 1999a, 1999b). The uncertainty of empirical models is able to be treated as a random vector by regarding the curve-fitting parameters (Chiu *et al*., 2012; Phoon *et al*., 2010; Wang *et al*., 2011). Some probabilistic methods were adopted to determine the uncertainties of empirical models in civil or geotechnical engineering problems (Ching *et al*., 2009, 2012; Juang *et al*., 2012; Phoon and Kulhawy, 2003; Phoon *et al*., 2003; Wang *et al*., 2010; an *et al*., 2009; Yuen, 2010b; Yuen and Kuok, 2011; Yuen and Mu, 2011; Zhang *et al*., 2004; Y Zhou *et al*., 2013). Equations for the confidence limits of the bestfit SWCC were developed by Zhai and Rahardjo (2013) to quantify the uncertainties for the associated fitting parameters.

2.4.6.1 Experimental Methods for SWCC

Hanging water method is able to perform for both wetting and drying media. Sample is saturated and placed on the ceramic plate which is linked to a water tank. Water potentials are observed by the elevation differences between the samples and the free water surface. VWCs of the sample are determined by oven method to correlate with the water potential. This method is directly derived from the concept of water potential and fits for 0 to -20 cm H_2O (equivalent to 0~0.976 kPa) (Steinberg and Poritz, 2005, Steinberg *et al*., 2005).

Tension plate allows the moisture come out from the sample under a positive air pressure. The sample is placed on a ceramic plate which is installed in a closed container. The air pressure is added into the container on top of the sample and the moisture comes out from the sample and passes the ceramic plate which is linked by a water column. The readings from the water column reflect the VWCs corresponding to the air pressures added, which are translated as soil water potential. The range of this method covers up to -1,500 kPa (Agus *et al*, 2001; Li *et al*, 2007).

Tempe cell, also named as pressure cell, method is similar to tension plate. However, the water came out from tempe cell is not collected. The moisture is measured by oven drying method by taking small parts of sample. It can be used for analyzing particles with larger size and covers the range of suction pressure up to 100 kPa (Steinberg *et al.*, 2005; Li *et al*, 2007)

Sand funnel method can be used to measure three or more samples at the same time. In other words, duplicate or triplicate study is able to be carried in one measurement. The saturated sample is placed on a G5 (average pore size: 1.5~2.5μ m) sand funnel which is supported by a conical flask. The flask is connected to a suction pump and pressure meter. When the suction pump turns on, the water comes out from the sample through the sand plate under a certain suction pressure and retains at the bottom of the conical flask. VWC of the sample is measured and corresponding to the suction pressure. This is a quick and efficient method to determine the SWCC but the range only covers 0 ~ -85 kPa (Yi, 2009).

Sand column method applies for substrate with high hydraulic conductivity such as sandy soil. Sample is filled into a glass column and the bottom is connected to a empty gradually cylinder. The sample is saturated by filling water from the gradually cylinder. The free water surface is lowered down by draining a certain amount of water. When the deference of potential head is measure corresponding to the change of water volume, the relation between VWC and soil potential is obtained. The method has been shown to be valid for the potential head range 0~80 cm H2O (equiverlant to 0~3.906 kPa) (Chen *et al*., 2010)

Total suction is able to be obtained by Dew-Point potential measurement. Sample is placed in a closed chamber and let the steam saturate at a certain temperature. The humidity for the saturated status is measured and used to calculate the corresponding soil suction potential. Dew-Point potential measurement is an indirect method and takes very short time (from a couple of minutes to about18 min) (Leong *et al*., 2003; Li *et al*, 2007).

The freezing point of soil is affected by the soil potential. The amount of freezing point reduced is measured by Beckmann thermometer to determine the potential of the soil at a certain moisture. This is also a quick and indirect method to determine the SWCC (Yi, 2009). However, this method apply effectively for frozen soil and the volume of soil expends under freezing process then affects the VWC.

Filter pater method is also an indrect method and able to determine wide range of suction potential. The sample is placed in a closed container and contact to three filter paper in the bottom. Other two filter on top of the soil is not contact. When the moisture reaches the equilibrium status, the moisture in the contact and non-contact filter paper are fitted into calibration curve to obtain the potential of soil(Li *et al*, 2007; Fredlund *et al*., 1997).

Centrifuge method uses centrifugal force to offer a pressure on the soil sample in the special designed centrifugal tube. In tempe cell and tension plate methods, the pressure is added on the soil sample by the air pressure. These two mehods take long time to get to equilibrium status. Under a certain rotaiton speed, the centrifugal force forms pressure on the soil sample and force the moisture passing through the ceramic plate to store in the bottom of the tube. The moisure can be obtained by weight measurement of extracted water amount to work out the SWCC with respect to the centrifugal pressure, which is equivalent to suction pressure (Chen *et al.,* 2010; Khanzode, 2002). This method is able to obtain SWCC in short period and covers the rainge up to -1000 kPa. In addition, the centrifugal facility is easy to prepare and the expreiment can be done in small lab. However, special design of centrifugal tube and ceramic plate are required.

When the suction pressure is lower than -300 kPa to -3000 kPa, the common physical methods are unable to obtain the SWCC for this range. The chemical solution method allows soil sample reach a equilibrium moisture status under various relative humiditiy conditions in a sealed container. The saturated salt solution is placed in the sealed with sample and a certain relative humidity is form. After 7 days, the moisture in the soil reaches equilibrium status, the moisture is measured and plot with the suction potential form by the chemical solution to obtain the SWCC (Li *et al*, 2007; Yi, 2009; Chen *et al*, 2010). This method takes long time to obtain one point. However, several parallel samples can be tested at a same container and it is an only mehtod for obtaining SWCC for the range lower than 1000 kPa.

2.4.6.2 SWCC Models

SWCC can be predicted by the numeric models. The earliest model was raised by Gardner (1922) and based on homogeneous pore size.

$$\theta = \frac{A}{\Psi - B} \qquad \text{(Eq 2. 1)}$$

where θ is VWC, Ψ is soil suction potential, A and B is fitting factors (Li *et al*, 2007).

Obviously, this model didn't consider most of the real situation for heterogeneous pore size.

The soil water characteristic curve model proposed by Brooks and Corey (1964) is expressed using exponential function.

$$S_e = \frac{\theta - \theta_r}{\theta_s - \theta_r} = (\alpha h)^{-\lambda} \qquad \text{(Eq 2. 2)}$$

where θ is VWC, θ_s is saturated VWC, θ_r is residual VWC, h soil water potential head. α is air entry value and inversively proportional to the mean pore size and λ describes the pore size distribution index (Fu *et al.*, 2011; Li *et al*, 2007).

Another exponential function form of SWCC model was derived by Mckee and Bumb(1984).

$$\theta = e^{-\frac{\Psi - a_2}{b_2}} \qquad \text{(Eq 2. 3)}$$

$$\theta = \left[1 + e^{\frac{\Psi - a_3}{b_3}}\right]^{-1} \qquad \text{(Eq 2. 4)}$$

Where θ and Ψ are VWC and soil suction potential, respectively. a_2, a_3, b_2 and b_3 are fitting factors. When the α (Eq 2.2) is bigger than the suction head, the equation 2.3 and 2.4 can be used. However, when α is lower than suction head, Eq 2.5 is suitable (Li *et al*, 2007).

A better fitted numerical model had been proposed by van Genuchten (1980):

$$S_e = \frac{\theta - \theta_r}{\theta_s - \theta_r} = \left[\frac{1}{1 + (\alpha h)^n}\right]^m \qquad \text{(Eq 2. 5)}$$

where S_e, θ, θ_s, θ_r and α have the same meaning as equation 2.2. m and n are fitting factors and m is equal to 1-1/n. This model had been shown to fit well in most of soil types and can combine with pore-size distribution function by Mualem (1976) in another way.

$$K\left(S_e\right) = K_s S_e^{\frac{1}{2}} \left[1 - \left(1 - S_e^{\frac{1}{m}} \right)^m \right]^2 \qquad \text{(Eq 2. 6)}$$

where the K and Ks is unsaturated and saturated hydraulic conductivity, respectively. m is fitting factor (Fu *et al.*, 2011).

Fredlund and Xing (1994) proposed a three-parameter equation by assuming the shape of SWCC is dependent on the soil pore-size distribution.

$$\theta = \frac{\theta_s}{\left\{ \ln\left[\exp(1) + (\Psi / \alpha)^k \right] \right\}^m} \left[1 - \frac{\ln(1 + \Psi / \Psi_r)}{\ln(1 + 10^6 / \Psi_r)} \right] \qquad \text{(Eq 2. 7)}$$

where α , k and m is the fitting factor related to air entry value, the maximum slope and the cuvature of the curve, respectively; Ψ_r stands for suction related to residual VWC status. Despite the soil types described by Sillers and Fredlund (2001), theΨ_r is suggested to be 3000 kPa . This model was reported to be suitable for wide range of soils (Fu *et al.*, 2011; Zhou *et al.*, 2014).

Among various models for plotting SWCC, the van Genuchten model is widely applied and showed better fitting. However, Eco-Soil is a novel growing medium. It is valuable to work out the SWCC for Eco-Soil by both experimental and simulation methods to see whether the conventional model can describe the novel growing medium.

2.5 Vegetations in Arid Area

Desertification had been affecting semi-arid and arid area for many of years. Especially in recently decades, as the urbanization and industrialization process, global warming excites the expanding of arid area due to the loss of soil productivities.

As a conventional method to mitigate desertification, the vegetation plays an important role in mitigating desertification. In arid- and semi-arid China, the dunes and sand sheets are usually anchored when the vegetation cover exceed 40%, but the dunes and sand sheets become semi-anchored between 15 and 40% cover, and they become mobile at cover levels under 15% (Zhu *et al.*, 1980; Zhong, 1998).

However, in most of the arid- and semi-arid area, the vegetations are not able to grow due to loss of land productivities. Eco-Soil is composed by activated sludge from wastewater treatment works and arid sand, and rebuilds the productivity of arid substrates to combat the desertification. Activated sludge contains rich macro nutrient, including nitrogen, phosphorus and potassium, and micro nutrient, such as zinc, ferrous, magnesium (Tchobanoglous, 2004). Therefore, studies had applied activated sludge as conditioner to supplement the lost nutrient in soil (Pathak *et al.*, 2009; Roca-Pérez *et al.*, 2009; Cuisinier *et al.*, 2011). However, those soils are able to maintain water and offer nutrient for plant growth. The substrates in arid area were found to have very low, even none, of nutrient and also perform low water retention abilities. By applying the novel concept of Eco-Soil, the rich nutrients in the activated sludge were utilized for vegetation growth to rebuild the eco-balance. In addition, great amount of wasted activated sludge from wastewater treatment works was able to be reused other than sending to landfill sites.

Studies found that the sludge amended soil performed well in growing vegetations and the outcomes were comparable to that grew in potting soils or natural soils (Fernández *et al*., 2009; Oleszczuk and Hollert, 2011; O'Connor, 1996). However, the growing abilities of Eco-Soils were yet to be investigated.

To study the growth of vegetation in the Eco-Soils, the plants with short growing period and completed cycle from seed to fruit were preferred. The okra is one of the suitable selections for this study. The okra (*Abelmoschus esculentus*) is one of popular vegetable around the world due to its succulent leaves and fresh pods (Akpan-Idiok *et al*., 2011). Annual production for okra was reported to be 6 million tonnes per year (Siemonsma and Kouame, 2004). The okra fruits could be cook for eating or making soup and sauces (Burkhill, 1997). The okra seeds contain 20% protein, which is similar to soyabean, and 20% oil, which is similar in fatty acid composition to cotton-seed oil (Siemonsma and Kouame, 2004). The roasted seeds could be used to make coffee (Akpan-Idiok *et al.*, 2011). Its mucilage was able to be use for medical and industrial applications (Burkhill, 1997; Alba *et al*., 2013). The okra was shown to be tolerant to various soil types but grows well in well-drained sandy loam under pH 6–7, and with high organic contents (Akpan-Idiok *et al*., 2011). Siemonsma and Kouame (2004) reported that the suggests total nutrient requirement for okra should be about 100 kg of nitrogen (N), 10 kg phosphorus (P), 60 kg potassium (K), 80 kg calcium (Ca) and 49 kg Magnesium (Mg) for every hectare of land to achieve a fruit yield of 10 t/ha. With such heavy nutrient demand, marginal soils must be amended with fertilizer for optimum yield. Many researchers have evaluated the response of the common okra to both organic and inorganic fertilizer treatments (Akpan-Idiok *et al.*, 2011; Akanbi *et al*., 2004; Asiegbu, 1987; Awodun and Olafusi, 2007; Olomilua *et al*., 2007; Uko *et al*., 2009). The literatures provided important information for the growth and nutrient requirements for okra growing in common soils or crops, however, as for anti-desertification, the growth of vegetation, in the form of okra, in Eco-Soils should be studied to evaluate the growing capabilities.

2.6 Summary for Literature Review

Application of activated sludge in arid sand offers a novel way to combat desertification and little literature investigated the same purposes. The literature review in this study summarizes the causes, hazard and affected area of desertification to indicate the severe circumstance brought by human activities and climate change. The review of activated sludge process indicates the nature of activated sludge generated in various stages to reveal the suitable applicable one. The sludge treatment processes indicate their complexities and high cost. Therefore, the combination of anti-desertification and sludge treatment is able to offer environmental friendly way to solve both issues.

Sludge amended soil is one of applications similar to Eco-Soil because it mainly utilizes the nutrients in growing vegetations to save the cost for fertilizer. However, the soil already has capability to grow vegetation and water retention. One of the major reasons for desertification is due to the loss of soil productivity in arid- and semi-arid area. The activated sludge is an important stuff for rebuilding the productivity for the growing medium.

To investigate the hydraulic properties and further the soil water retention of the Eco-Soil, the essential soil properties including bulk density, particle density, particle size distribution and hydraulic conductivities are reviewed to offer comparison with common soil properties. The SWCC is an important relation between soil suction head and moisture content and reveals the water retention capability. Different soil is characterized by its water retention capability via the shape of SWCC. However, no literature studied the aforementioned hydraulic related properties of Eco-Soil.

To mitigate desertification, the vegetation plays an important role. Its root system provides strong retention of soil and reduces the mobility of dunes. An appropriate substrate should be able to grow vegetation and provides sufficient nutrients for reproduction. Okra is one of popular economic crops in the world, especially welcome in some arid and semi-arid area in Africa. However, no study investigated the growth of Okra in Eco-Soil.

Consequently, the Eco-Soil offers a new way for anti-desertification. Its water retention and vegetation growing capabilities are two important aspects for evaluating the effectiveness of its application in anti-desertification purpose.

3. Methodology

The methodology section describes the material, experiment method, experimental site and processes for conducting the present study.

3.1 Experiment Site

The experiments took place on the roof on the P building in The Hong Kong Polytechnic University (PolyU) (Figure 3.1). Approximately 670 meters away from the experiment site, the HK Observatory records the weather of the closed area since 1883. The overall average monthly weather data including temperature, relative humidity, solar radiation and wind speed is retrieved from the observatory station of HK Observatory between 1981~2010 (HK Observatory Website, 2014). Because the distance between the experiment site and the observatory station is short, the weather data recorded is used as reference environment conditions for this study.

Figure 3. 1 Experiment site for study of hydraulic characteristics (red highlighted) (Adapted from PolyU Website, 2014)

Figure 3. 2 Geographical places between the experiment site in the HK Polytechnic University and the observatory station of the HK Observatory (Adapted from Google Map Website, 2014)

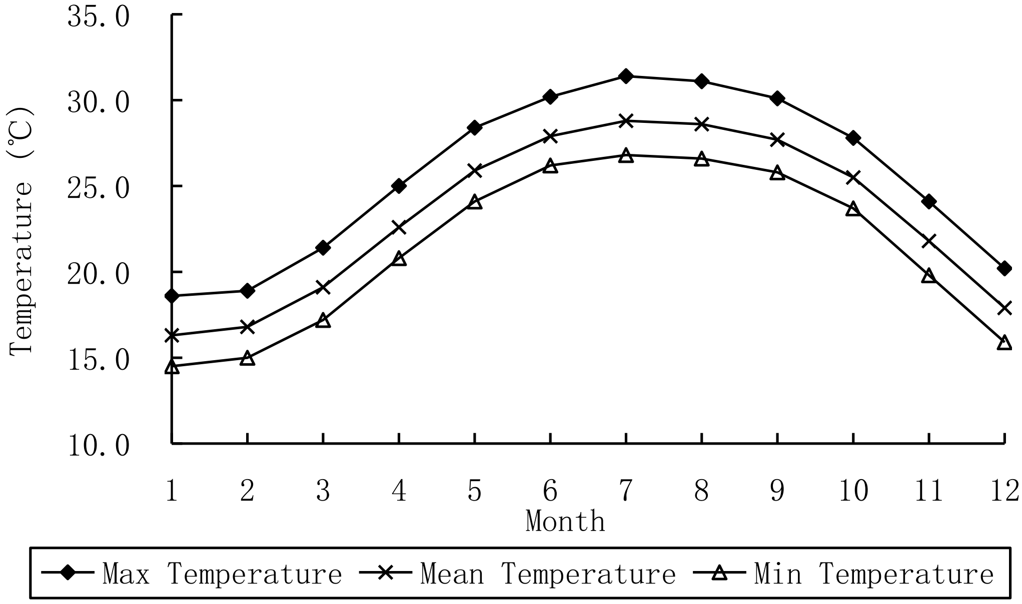

Figure 3. 3 Monthly means of daily maximum, mean and minimum temperature recorded at the Observatory between 1981-2010 (Adapted from HK Observatory Website, 2014)

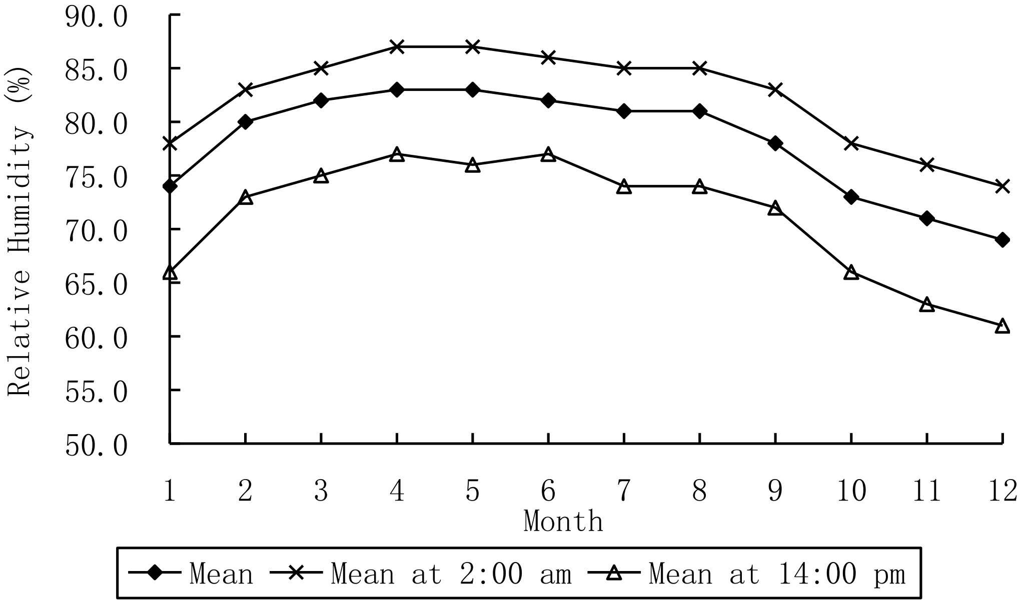

Figure 3. 4 Monthly means of relative humidity recorded at the Observatory between 1981-2010 (Adapted from HK Observatory Website, 2014)

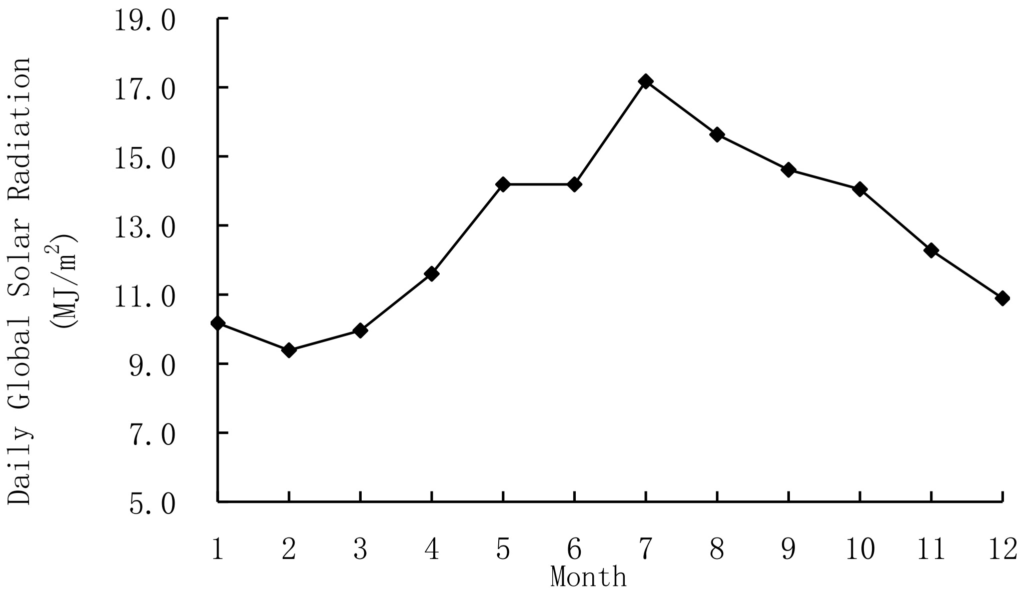

Figure 3. 5 Monthly mean of daily global solar radiation recorded at King's Park between 1981-2010 (Adapted from HK Observatory Website, 2014)

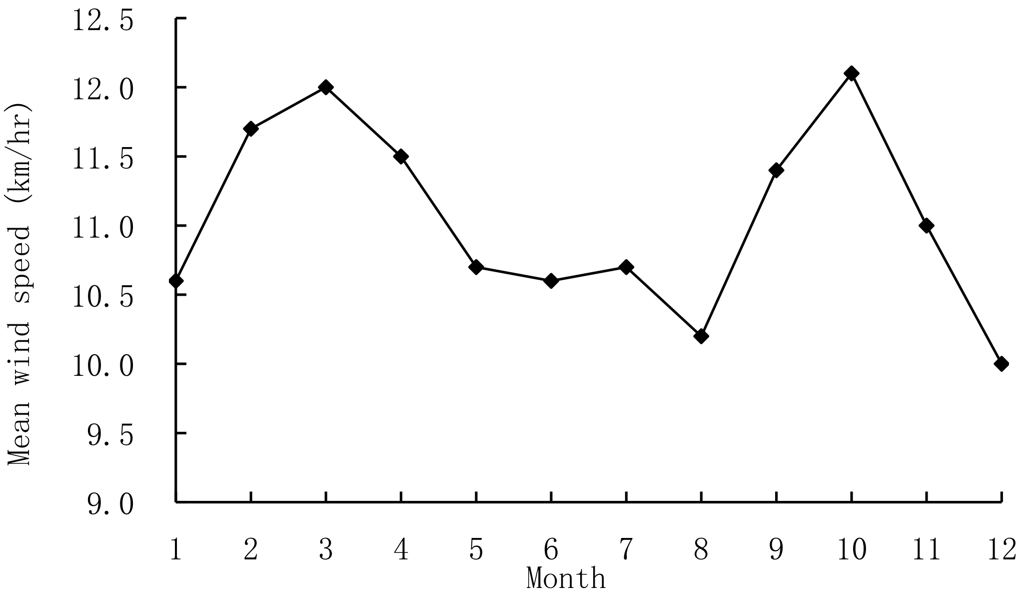

Figure 3. 6 Monthly mean wind speed recorded at the Observatory between 1981-2010 (Adapted from HK Observatory Website, 2014)

From the mean weather between 1981~2010, the year-average temperature of the experiment site reaches 25.6 ℃ and relative humidity of 78% (Figure 3.3, 3.4). The highest average temperature appeared between July and August and reaches up to 28.8℃. In addition, the year-average relative humidity keeps around 75% and its highest point appeared between April and May. The solar radiation was recorded from the King's Park station and appeared to be 12.85 MJ/m^2 in average (Figure 3.6). The reason for the appearance of highest temperature in July is the strongest solar radiation. The year-average wind speed in record is shown to be 11 km/hr (Figure 3.5). The wind speed appears to be low in July and August. The low wind speed will result in low heat dissipation and therefore the hot temperature. In addition, the wind speed also contributes to the evaporation behavior in the plant soil system.

3. 2 Materials

3.2.1 Activated Sludge

This study aims to find out a practical method for application of sludge in anti-desertification and, at the same time, to save the expense for sludge treatment. In a typical completed wastewater treatment process primary (PAS), secondary (SAS), return (RAS), excessive (EAS), thickened (TAS), stabilized (StAS) and dewatered activated sludge (DAS) can be obtained from preliminary settling tank, secondary settling tank, return activated sludge pipeline, excessive activated sludge pipeline sludge thickener, sludge digester and dewater facility, respectively. For saving the expense of the sludge, the sludge after secondary sedimentation tank is of interest for this study. The SAS will usually be separated into RAS and EAS, the former one is pumped back to the aeration tanks for reaction while the latter one is sent to the thicken facilities to reduce the volume prior going into digester. The water content sequence of the types of activated sludge should be SAS>PAS>RAS>EAS>TAS>StAS>DAS. Therefore, the last one is easier to be delivered to the experiment site. However, after anaerobic digestion of EAS, which is the preferred stabilization method for sludge treatment, its odour is usually offensive due to generation of metabolic products such as ammonia, hydrogen sulfide and volatile fatty acids. The application of StAS and DAS for this study is not considered because of the odour and the treatment expense. The sludge treatment occupied large portion of the caption and operation cost for the sewage treatment plant (Dodane *et al.*, 2012). Therefore, the TAS is a preference for this study because it is higher in concentration (compared to SAS, EAS and RAS) and lower in odour emission. In a well operated wastewater treatment process, the thickened sludge is produced after the thickening facilities, therefore, the sludge is not yet getting into endogenous respiration status. The odour emitted from the TAS comes from the same the products as aerobic reaction, i.e., oxides of the substances. The oxides, such as CO_2 and SO_2, usually appeared to have very little offensive smell. The low odour emission and high concentration make TAS to be a good choice for the study.

The sludge for this study was obtained from Tai Po Sewage Treatment Works (TPSTW) located at Tai Po, Kowloon, Hong Kong. Daily inflow and effluent information for year 2013 are obtained from the Drainage Services Department (DSD).

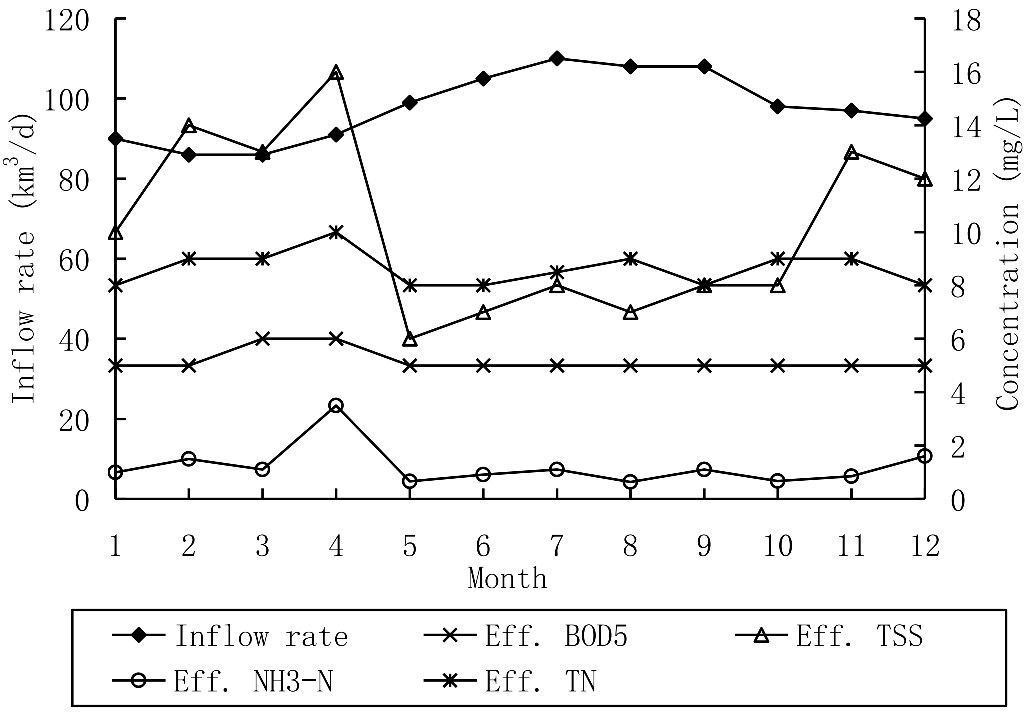

Figure 3. 7 Monthly averages of inflow rate and maximum effluent BOD5, TSS, NH3-N and TN concentration of Tai Po Sewage Treatment Works for the year 2013 (Adapted from HK DSD Website, 2014)

Unfortunately, the inflow sewage quality data is not available from the DSD website. Despite of this, the overall average inflow rate of the TPSTW in the year 2013 reached 97.75 km^3/d and effluent quality parameters, including BOD_5, TSS, NH_3-N and TN met the license standards (BOD_5 < 20 mg/L, TSS < 30 mg/L, NH_3-N < 5 mg/L and TN < 20 mg/L) (DSD Website, 2014).

Tai Po Sewage Treatment Works is classified as the Major Secondary type, which is the second highest level to date, in HK DSD sewage treatment facilities category. Completed general domestic sewage treatment and sludge treatment can be found in TPSTW. Before sample of thickened sludge, permission was obtained from HK DSD government. Because the official treatment process diagram for the TPSTW is unable, the brief treatment process was told from the technicians in TPSTW and shown in Figure

3.8.

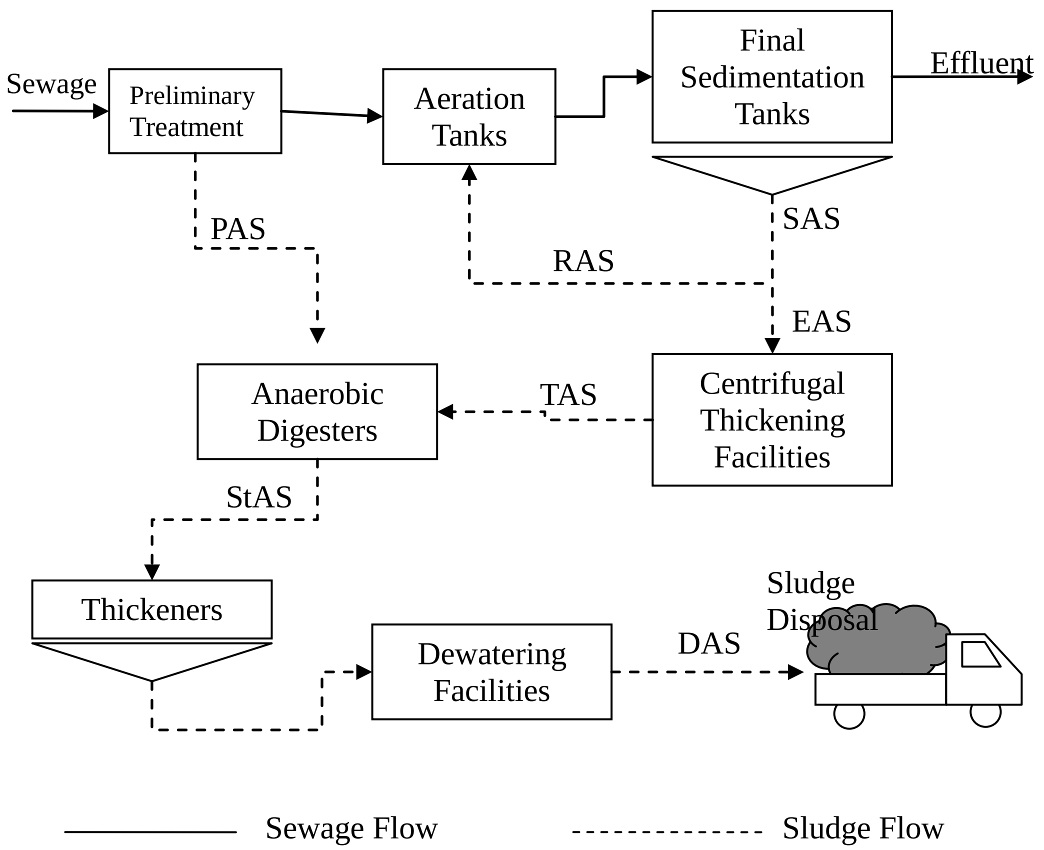

Figure 3. 8 Brief flow diagram for the treatment process for Tai Po Sewage Treatment Works

From the diagram, the excessive activated sludge is thickened by the centrifugal thickening facilities in the centrifugal facilities house prior to the anaerobic digesters together with the primary activated sludge. As told by technicians in TPSTW the thickeners are used to thicken the stabilized activated sludge after anaerobic stabilization. Because the activated sludge after anaerobic process emits offensive odour, which limited its application, the thickened excessive activated sludge after the centrifugal thickening facilities is preferred for the specific objectives of this study.

Figure 3. 9 The centrifugal facilities house in Tai Po Sewage Treatment Works

The TAS was collected from the sludge sampling port on each centrifugal facility (Figure 3.10) and stored in Poly-Propylene (PP) sampling bottles with 1 L effective volume.

Figure 3. 10 Sludge sampling port on a centrifugal thickening facility

Sludge samples were delivered to the PolyU laboratory immediately after collection and 1 hr is required for delivery. The samples were placed in the refrigeratory and kept at 5±1℃ to slow down the microorganism metabolism.

3.2.2 Sand

Another important material for this study is the sand from arid area. This type of sand is different from the one settled on the beach or river bed. Due to wind erosion, the sand particle size in arid or desert area is finer than others. The sand samples were collected from arid area in Yulin, Shanxi, Northwestern China, for this study. Because of the costly fee and complicated procedures for transference of a great amount of arid sand from the Shanxi Province to Hong Kong, purchasable river sand is considered to re-compose and simulate the arid one. River sand obtained from Dong Yin Sand and Rock Market located in Humen, Dongguan, Guangdong Province is selected for simulation. The river sand was filtered into different sizes through the sieves with pore diameters of 2.00, 1.20, 0.60, 0.30 and 0.15 mm (Figure 3.12~3.13).

The groups of sieved river sand were re-composed according to the particle size distribution (PSD) result of arid sand sample.

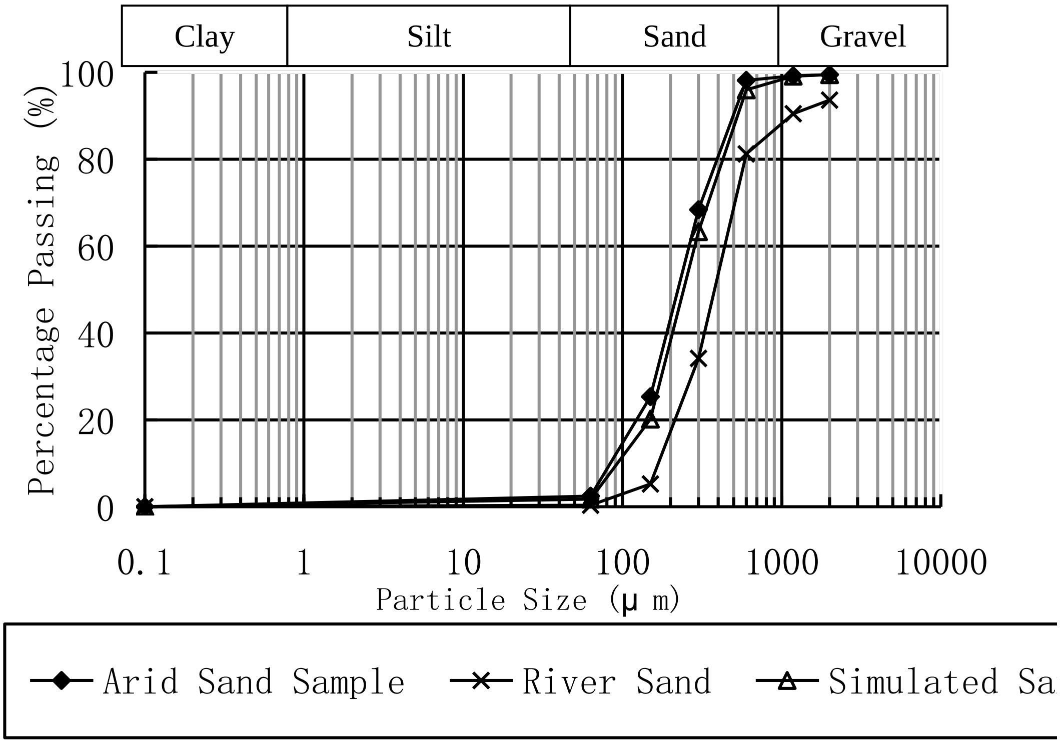

Figure 3. 11 Particle size distribution result of arid, river and simulated sand sample

The Dry Bulk Density (BD, ρ_d), Particle Density (PD, ρ_s), Particle Size Distribution (PSD) experiments were carried out according to British Standard (BS) 1377:1990 (BSI, 1990). The dry bulk density of the simulated sand is 11.99% lower than that of arid sample and 6.29% than river sand because the simulated sand contained lower fraction of the particles bigger than 2.00 mm in diameter. The BD of river sand is 6.09% lower than arid sand and fraction of the gravel, which retains on the 2mm sieve, contributes greatly on the overall density of river sand. Hence, the BD of simulated sand is lower than the river one and further more than the arid one. However, in this study, the density has little effects on the moisture retention and movement. This BD deference between simulated and arid sand is acceptable for the following study.

The particle size distribution (PSD) results shown in Figure 3.13 reveals the arid sand sample is composed by approximately 1.00% clay (<1 μ m), 1.00% silt (1~40μ m), 97.00% sand (40~900μ m) and 1.00% gravel (900~28,000μ m) according to British Standard. Compared to arid sand sample, the river one contains approximately 0.15% clay, 0.15% silt, 82.7% sand and 17.00% gravel. The major fraction of arid sand sample lays in between 150 and 300μ m (43.12% retained) while the river one is 300~600μ m (47.08% retained). Especially, the retained fraction of arid sand between 63 and 150μ m reaches 22.86 % and is about 3.63 times more than that of river one (4.94 %). In other words, 4~5 kg river sand is required to simulate 1 kg arid sand because of the large discrepancy of the composition in between 63 and 150μ m.

According to the PSD result of arid sand sample, river sand was sieved into 6 groups of different size ranges (<150, 150~300, 300~600, 600~1200, 1200~2000 and >2000 μ m) through five sieves. These sieves were made from stainless steel nets with the pore size of 150, 300, 600, 1200 and 2000μ m and were fixed to the Polyvinyl Chloride (PVC) pipe frames by strap tapes (Figure 3.12).

Figure 3. 12 Stainless steel sieves with pore size of 150, 300, 600, 1200 and 2000 μ m

The river sand was washed for three times and left air dried before sieving. The dry sand was sieved by hand and gone through the five sieves from coarse to fine. The sand which retained on the sieve was transferred to bag and stored, while the one passed through was collected and sieved by finer sieves (Figure 3.14).

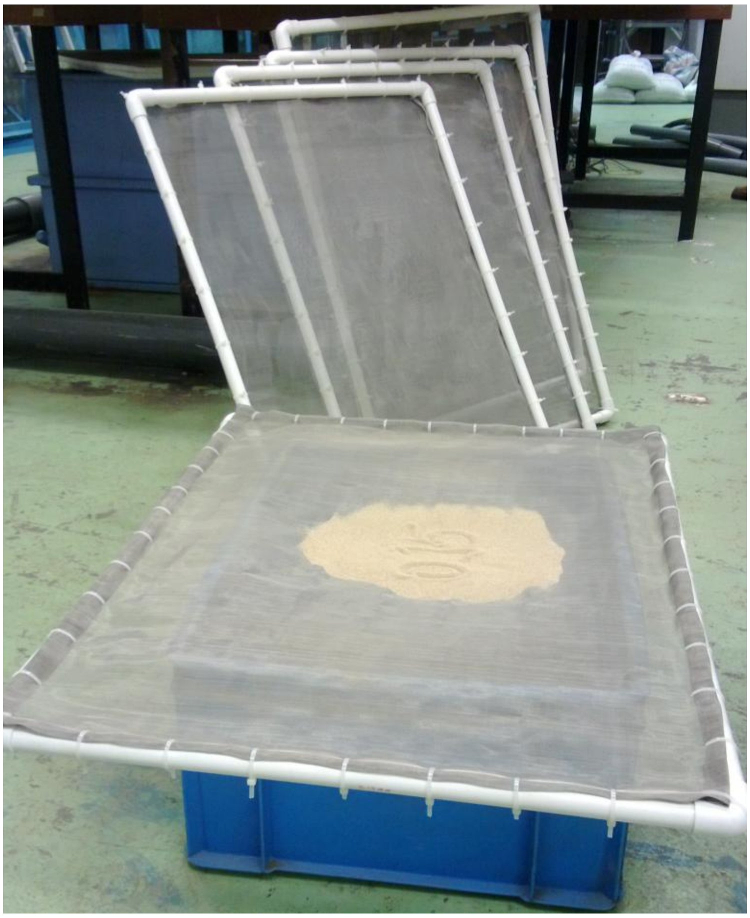

Figure 3. 13 Sieving of sand into different particle size groups

Figure 3. 14 Sorting of sand after sieving

The sorted river sand was remixed to compose the simulated sand according to weight fraction calculated from the PSD result of the arid sand. 50 kg of simulated sand was produced each time using a digital scale with a maximum weighing limit of 150 kg and detectability of 0.5 g. The systemic error was ± 0.5 g for each weighing so that the total error can be within ± 3.0 g for composing each simulated sample because the groups of sorted sand 6 should be added. In other words, the overall error for the simulated sand mixing is under 0.006%.

Table 3. 1 Weigh fraction of each sand group for mixing

Particle Size (μm)	<150	150~300	300~600	600~1200	1200~2000	>2000
Wt. Fraction for Mixing (%)	25.29	43.12	29.79	0.99	0.27	0.54

PSD test was carried out on simulated sand sample for checking. The comparison of simulated and arid sand was also shown on Figure 3.11. Because the pore size of purchasable stainless net from local supplier is 1200μm and the BS sieve is of 1180 μm, the fraction of 600~1200μm of simulated sand is 2.13 % larger than the arid one. However, the correlation coefficient (r) between these two PSD curves is calculated to be 99.87% and the t-test showed that $r \geqslant r_{0.01}$ (n=6), which implies significantly correlation. Therefore, the simulated was accepted for the following analysis.

3.2.3 Composing of Eco-Soils

Soil is defined as the mixture of minerals, organic matter, gases, liquids and a myriad of micro- and macro- organisms that can support plant life. It is a natural body that exists as part of the pedosphere and it performs four important functions: it is a medium for plant growth; it is a means of water storage, supply and purification; it is a modifier of the atmosphere; and it is a habitat for organisms that take part in decomposition and creation of a habitat for other organisms (Wikipedia, 2014).

Marshall *et al*. (2001) stated that soil is a porous material of widely varying properties and consists of the inorganic products of weathered rock or transported material together with the organic products of the flora and fauna that inhabit soil. The arid sand is lack of productivity due to low water storage that inhibits the growth of plants and organisms. Sand-Sludge Soil (Eco-Soils) is made from the sand simulated from desert and thickened sludge from municipal sewage plant. The Eco-Soils utilized the rich nutrient organic, and moist contents from the activated sludge to form suitable growing materials for re-claiming the productivity for growing vegetation from the deserted land.

Some literatures stated that the sludge destined for soil fertilization must be stabilized before its use in order to prevent an unacceptable accumulation of pollutants, bad odours and the risk of disease from microbes (Marttinen *et al.*, 2004; Spinosa and Vesilind, 2001). However, the sludge applied in the literature was based on the agriculture application while the Eco-Soils were used for re-claiming arid area where extreme living environment is dominant. This study utilized the unstablized thickened activated sludge as raw material for the Eco-Soils because 1) most micro-organisms in the thickened activated sludge, including pathogens, are unable to survive in dried conditions; 2) subsequently sludge treatment occupies the major operation cost in sewage treatment process; 3) sludge after anaerobic digestion, which is usually adopted by municipal sewage treatment plants due to higher efficiency and reusable biogas generation, emits offensive odour such as ammonia, volatile fatty acids and hydrogen sulfide.

3.2.3.1 Mixing of Sand-Sludge Soil

The mixing of Eco-Soils is based on the volumetric ratio of sand and sludge because 1) the volumetric measurement for mixing is more manageable and efficient in real application and 2) activated sludge is large in volume due to its high moisture content. The thickened activated sludge used in this study contains averagely 30.274 g MLSS/L. Eco-Soils were mixed in 50 mL beakers and on the Sand to Sludge Volumetric Ratio (SSVR) of 100:0, 90:10, 80:20, 70:30, 60:40, 50:50, 40:60, 30:70, 20:80 and 10:90. The SSVR is defined as the ratio when the simulated arid sand (Dry Bulking Density = 1272.83 kg/m^3) mixed with the fresh obtained sludge under the average concentration at 30,274 mg/L. The Sand to Sludge Weight Ratio (SSWR), which stands for the dried weight ratio for sand mixed with sludge, was normalized from the SSVR for reference. The Samples were mixed in triplication for each SSVR and transferred to 100 mL pre-weighed dried Gooch Crucibles. The crucibles contained mixed samples were weighed and placed in oven (LAB-LINE INSTUMENTS, Inc. Cat NO.3524, Figure 3.15) at temperature of 105±1℃ for 24 hr. After the dried mass of samples were weighed by electronic scale (SARTORIUS, BL2105, sensitivity 0.1 mg, Figure 3.16), they were ignited in furnace (CARBOLITE, CWF 12/5) at 440±1℃ for 3 hr and weighed the mass loss due to volatile organic contents (BS 1733: BSI).

Figure 3. 15 Oven for drying at 105±1℃, LAB-LINE INSTUMENTS, Inc. Cat NO.3524

Figure 3. 16 Electronic scale for weighing samples with sensitivity of 0.1 mg, SARTORIUS, BL2105

Figure 3. 17 Programmable furnace for ignition CARBOLITE, CWF 12/5

3.1.3 Commercial Potting Soil

At the same time, a type of commercial potting soil (FLORAGARD PRODUCT, Universal Potting Soil) was used in the experiment for comparing with Eco-Soils (Figure 3.22).

Figure 3. 18 FLORAGARD PRODUCT, Universal Potting Soil

3.2 Hydraulic Characteristics and Physics of Eco-Soils

The study of the hydraulic characteristics aims to find out the moisture retention ability, water infiltration, permeability, conductivity and mechanism for the moisture migration in the Eco-Soils. Based on the moisture retention, water retention characteristic curve and permeability, optimal mixture of Eco-Soils will be determined.

3.2.1 Constant Temperature Evaporation Test

This test aims to find out the comparison among the evaporation behavior for the Eco-Soils under various SSVR, arid sand and potting soil.

56~60 mL arid sand, potting soil and Eco-Soils samples with SSVR 80:20, 60:40, 40:60 and 20:80 (totally 6 types of samples) were placed in 18 Gooch crucibles (with an effective volume of 100 mL, Figure 3.22) for carrying out triple study. The Gooch crucibles were dried in oven (LAB-LINE INSTUMENTS, Inc. Cat NO.3524, Figure 3.33) at 105 ± 1 ℃ and weighted by electronic scale (SARTORIUS, BL2105, sensitivity 0.1 mg) before loading the samples. The crucibles contained samples were placed in a programmable incubator (CO_2 incubator, TC2323, Figure 3.23) under a constant temperature of 35.0 ± 1 ℃ and Relative Humidity (RH) of 40%. The crucibles were taken out from the incubator and placed in desicator for 30 min to cool down to room temperature and weighted by the same electronic scale aforementioned every 2 working days. After 90 days of observation, the samples were dried by the aforementioned oven and calculated the processing and residual moisture content.

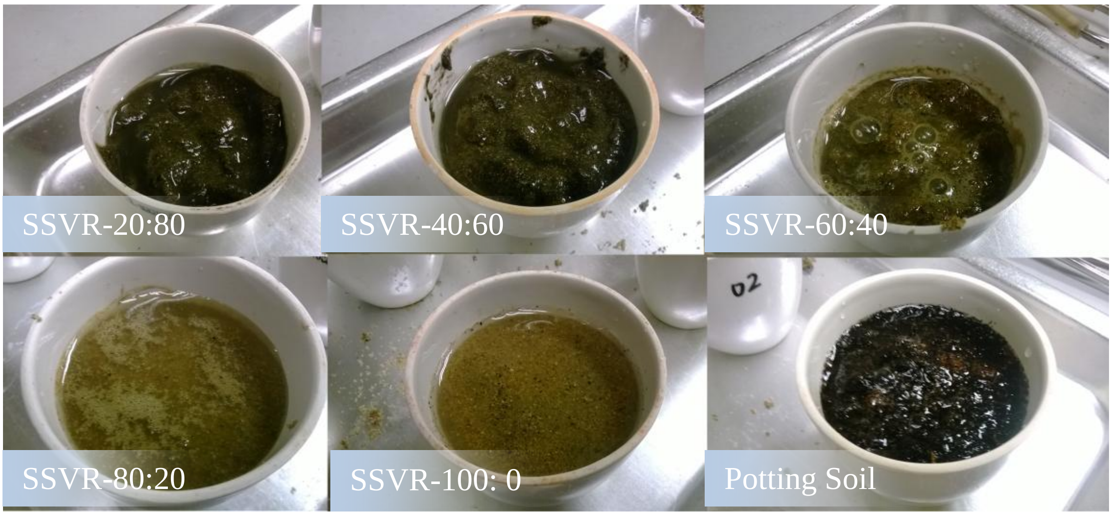

Figure 3. 19 Typical samples for Constant Temperature Evaporation Test

Figure 3. 20 Programmable incubator TC2323,

3.2.2 Field Capacity

After the excessive water drained by gravity, the residual water held in the soil itself by capillary retention is defined as the Field Capacity (FC) of the soil (Yi *et al*., 2009).

Compared to the saturate moisture content, the field capacity can be better describes the maximum moisture holding capacity after rainfall events. 10~15 g simulated arid sand, potting soil and Eco-Soils samples were placed in perforated Gooch crucibles (effective volume 25 ml), which were dried in oven (LAB-LINE INSTUMENTS, Inc. Cat NO.3524) at 105±1℃ for 24 hr and weighed by electronic scale (SARTORIUS, BL2105, sensitivity 0.1 mg) to get the [m_0]. A φ 20mm Whatman hardened ashleEco-Soils filter paper (Cat No. 1541 150, Figure 3.25), which was cut from aφ 150mm one, was place in the inner bottom of the crucibles to prevent washing out the particles from the perforated holes (Figure 3.26). Each sample was done in triplication.

Figure 3. 21 Whatman hardened ashleEco-Soils filter paper, Cat No. 1541 150

Figure 3. 22 Filter paper placed at the inner bottom of the 25 ml perforated Gooch crucible

The crucibles contained samples were soak in distilled water basin at a water level which was 10~20 mm higher than sample surface for 24 hr. Square plastic grids were placed below the crucibles to let the distilled water from into the crucibles through the perforated holes. 3 of crucibles contained nothing but a fitted filter paper as control crucibles.

Figure 3. 23 Perforated Gooch crucibles contained samples and soaked in over surface distilled water basin

The saturated samples were placed on test tube stands for 2 hr after 24 hr soaking to drain off the excessive water by gravity. Before weighing by the electronic scale aforementioned to get [m_{FC}], the water drops retained on the outer surface of the crucibles were carefully blotted up by ashless tissue. The crucibles were then placed in aforementioned oven and dried for 24 hr for obtaining the dried weight [m_{105}]. The field capacity were calculated by equation 3.1.

$$[FC_{wt.\%}] = \frac{([m_{FC}]-[m_{105}])-([m_{con.}]-[m_0])}{[m_{FC}]-[m_0]} \times 100\% \qquad \text{(Eq 3. 1)}$$

where [$FC_{wt.}$%] is field capacity of the samples, g water retained/ g sample;

[m_{FC}] is weight of the sample at its field capacity, g;

$[m_{105}]$ is weight of the sample dried at 105 ℃, g;

$[m_0]$ is the dried weight of the container, g;

$[m_{con.}]$ is the wet weight of the control sample, g.

3.2.3 Soil Water Retention Characteristics Curve

3.2.3.1 SWCC Plotted by Sand Funnel Method

Among various methods for plotting SWCC, the sand funnel method allows parallel samples perform the tests and one point can be obtained in one hour. Sand funnel method, which is showed in Figure 3.27, was applied for plotting the SWCC in this study.

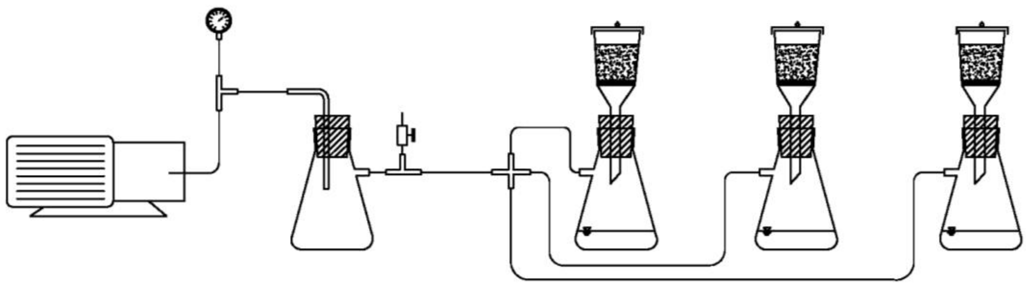

Figure 3. 24 Schematic diagram for sand funnel methods for plotting the soil water characteristics curve

Compared to other methods such as pressure chamber, tension plate, tensiometer, centrifuge tube and desicator, the sand filter method has its advantages: 1) the time for reaching a stable point is shorter (1 hr for each point); 2) the experiment setup requirement is lower; 3) triplication is able to be done by one measurement; but also disadvantages: 1) the measurable range is narrow (-85 ~ 0 kPa suction pressure) 2) only the drying path of SWCC is able to be measured. However, the range for this method occupies the major range for the SWCC in natural condition.

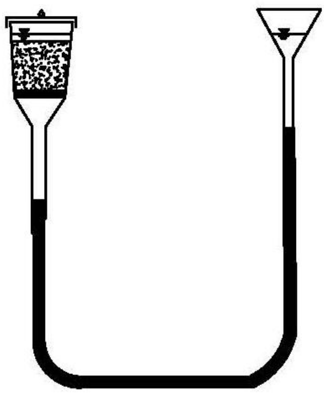

Figure 3. 25 Soaking the specimen 24 hr for saturation

Prior to placing 60~80 g samples into the filter cup, a φ 50mm filter paper (0.45 μm pore size) was place on the G5 sand plate (average pore size: 1.5~2.5μ m) to avoid the particle clogging in the sand plate. The filter outlet was connected to a funnel by silica tube. Distilled water was filled to form 1cm ponding above the specimen surface through the bottom of the sand filter via the connected funnel in order to avoid introducing the air bubbles. The specimen was soaked for 24 hr to reach saturate status before connected to the vacuum system. A cap was placed on the sand funnel to avoid moisture evaporation during experiment. The ball valve in Figure 3.29 was fully open initially and adjusted to reach the required pressure from 0 to -85 kpa via the reading of the pressure meter. The pressure of -1, -15, -30, -45, -60, -75 and -85 kpa were adjusted and kept for 1 hr to attain stable status. 3~5 g specimen was collected on a pre-weighed dried evaporation dish before adjusting to the next pressure. The moisture content of collected specimens under specific pressure was measured by the oven drying method. SWCC for the specimens were obtain by plotting the VWCs against the suction pressures.

3.2.3.2 SWCC Plotted by Chemical Solution Method

The SWCC for suction pressure range -300kPa~ -1500 kPa can not be obtained by phisical method but chemical solution method. In a closed container, certain relative humidity (P/P_0) were formed by saturated chemical solution. The water caputred in the substrate samples varied when exposed in different relative humidity situations. When the equilibrium stage of the Soil-Water exchange was reached, the VWCs of the substrate samples were measured to plot the SWCC for potentials, which were form by various RH conditions. The potential of substrate samples were calculated from the chemical potential of the solutions via equaiton 2.03.

$$\Psi = -\Psi_s = -\frac{RT}{M} \bullet \ln \frac{P}{P_0} \qquad \text{(Eq 3. 2)}$$

where, Ψ and Ψ_s stand for substrate potential and water potential for saturated solution, respectively; R, T and M are universal gas constant, absolute tempeture and molecular weight for water, respectively; P/P_0 stands for the relative humidity.

5g oven dried samples for SSVR 100:0, 80:20, 60:40, 40:60, 20:80 and commercial potting soil were placed in 18 pre-weighted 50 mL glass beakers for triplicate study purpose. Over saturated chemical solution were prepared and placed in the bottom of the vacumm desiccator. The beakers containing substrate samples were placed on the shelve inside the desiccator and above the over saturated solution. Vaseline was applied on edge of the desiccator before covering the cap. The glass valve on the top of desiccator was connected to a vacuum system and the vacuum pump was turned on for 20 min to pump away the air inside. The vacuumized desiccator was placed in room temperature (averagely 25 ℃) for 7 days. The samples were weighted after the moisture reached equilibrium status. The previous over saturated solution was replaced by the next, in the sequence of KNO_3, $ZnSO_4$, NaCl, NH_4NO_3, $Ca(NO_3)_2$, K_2CO_3, CH_2COOK and LiCl. The desiccator was vacuumized again and placed for another 7 days. After obtaining the final weight by using LiCl as over saturated solution, the dried weighted were esimated by overn dried methods. The moisture for the associated chemical solution were determined and plotted as y-axis against soil potential, which were calculated by equation Eq 3.2.

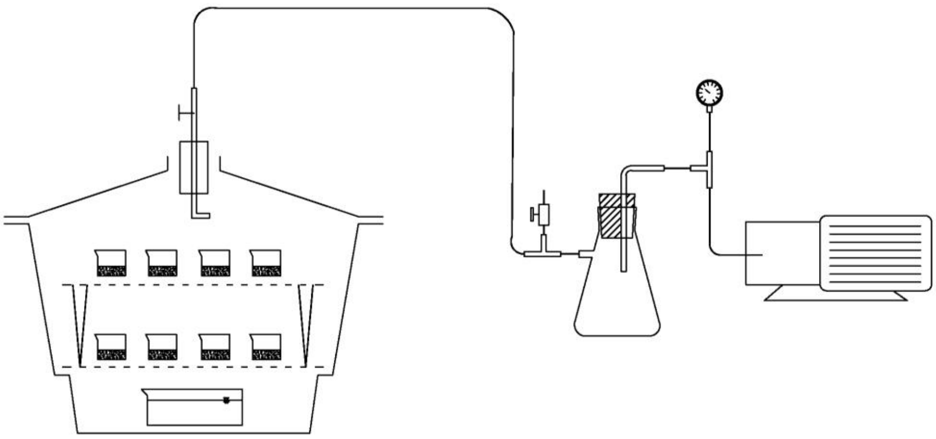

Figure 3. 26 Schematic diagram for chemical solution methods for plotting the soil water characteristics curve

3.2.4 Rainwater Retention and Detention

3.2.4.1 Experiment Model

Rainfall runoff experiment aims to study the moisture migration behavior in the Eco-Soils under saturate and unsaturated status. Six plastic tanks purchased from local supplier with a diameter of L-662 mm×W-501 mm×H-348 mm and total volume of 87 L were used for carrying out the pilot-scale study (Figure 3.30).

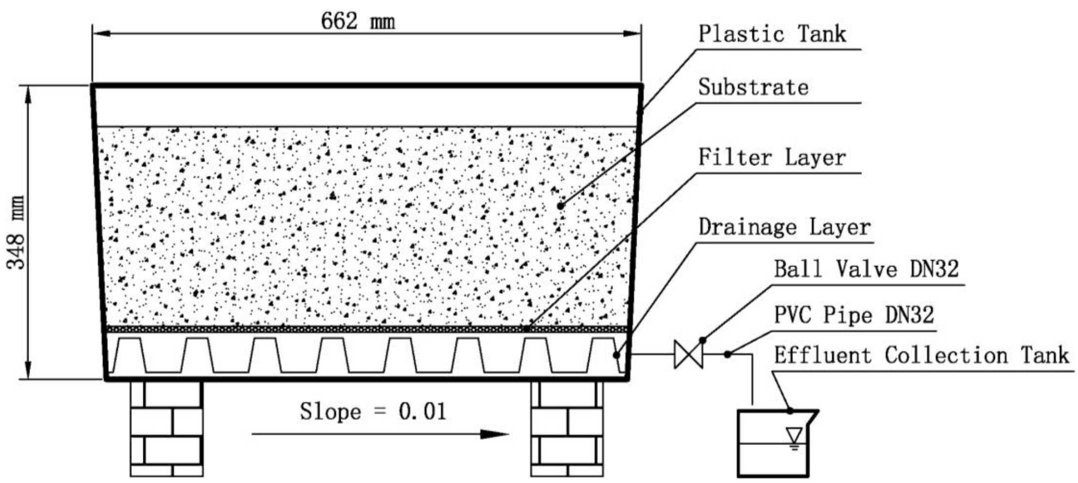

Figure 3. 27 Model setup for water retention, absorption and dispersion studies

Figure 3.30 shows the structure of the experiment model for this study. Drainage channel was place in the bottom of latitudinal side of the tank in order to collect the bottom runoff for analysis. The slope of tank was 0.01 towards the drainage side to allow bottom runoff be drawn out as much as possible.

From the top to the bottom, the setup consisted of 3 layers including: substrate, filter and drainage layer. In this study, the substrate layer was simulated arid sand, Eco-Soils or potting soil and held a substrate depth of 170 mm. 2.0 mm thick polypropylene non-woven cloth was applied as filter layer to avoid washing out of particles. A plane of square plastic grid was placed after the filter layer to give even supports. The grid was supported by 27 Lego-type plastic bricks and played as drainage layer offering a free space to drain the bottom runoff (Figure 3.31).

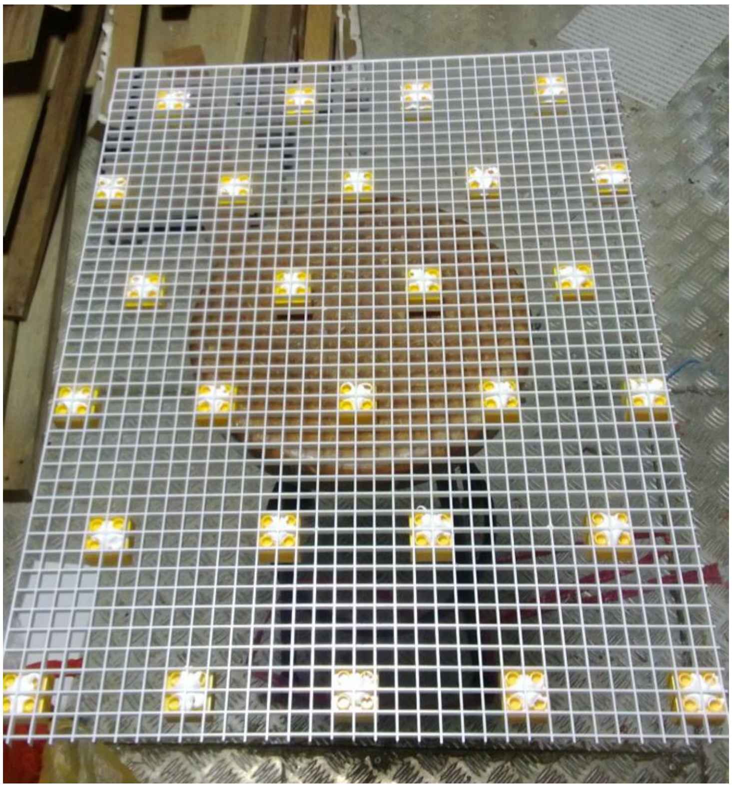

Figure 3. 28 Drainage layer in the bottom of the experiment tank

On the drainage side (latitudinal side) of the tank, 3×5 drainage holes were designed to observe the surface and sub-surface runoff for raining events. On the longitudinal side, a 3.00 mm thick transparent acrylic plastic was fixed to the perforated tanks by rubber sealing strips and stainless steel screws to offer three transparent windows for observation (Figure 3.32).

The drainage port was place at the bottom of the tank to drain out the leachate as much as possible. The upper cup of a polyvinyl chloride (PVC) male adapter was cut and a gap was made from the ring by filing (Figure 3.33) to form the drainage adapter for the experiment tank. Since the tank body is made from polyethylene (PE), common bonding agents, such as polyvinyl chloride (PVC) glue, glass cement, α-cyano-acrylate adhesive, epoxy resin adhesive and epoxy putty, are tested to be unable to join the drainage adapter firmly. Hence, the drainage adapter was fixed to the tank and sealed by special made rubber rings. Water sealing and drainage test was carried out on the experiment tank. The bottom drainage port was sealed by rubber stopple and water was filled in and left for 30 min to see whether leakage happened. Rubber stopple was removed to allow water drained from the bottom drainage port under the set slope. The test showed that the no water leaked from the seams and little water (3~5 ml) was left within the tank after drainage.

Figure 3. 29 Constitution of the experiment tank

Figure 3. 30 Design of drainage adapter for experiment tank

Figure 3. 31 Water sealing test on the experiment tank

Figure 3. 32 Sealing for the drainage adapter

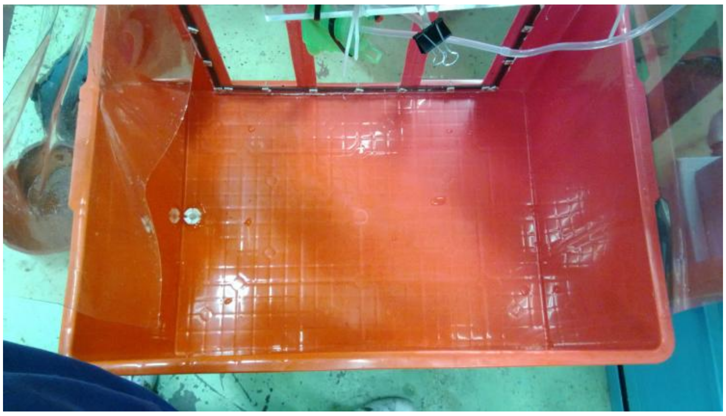

Figure 3. 33 Little water left in the tank after drainage

The experiment tanks were placed on the roof to utilize natural ultra violet and the ambient temperature, however, the rainfall is uncontrollable for studying the hydraulic characteristics. A fitted rainfall canopy was designed for each tank. The canopy showed in Figure 3.37 was made of PVC pipe frame and covered by transparent plastic film.

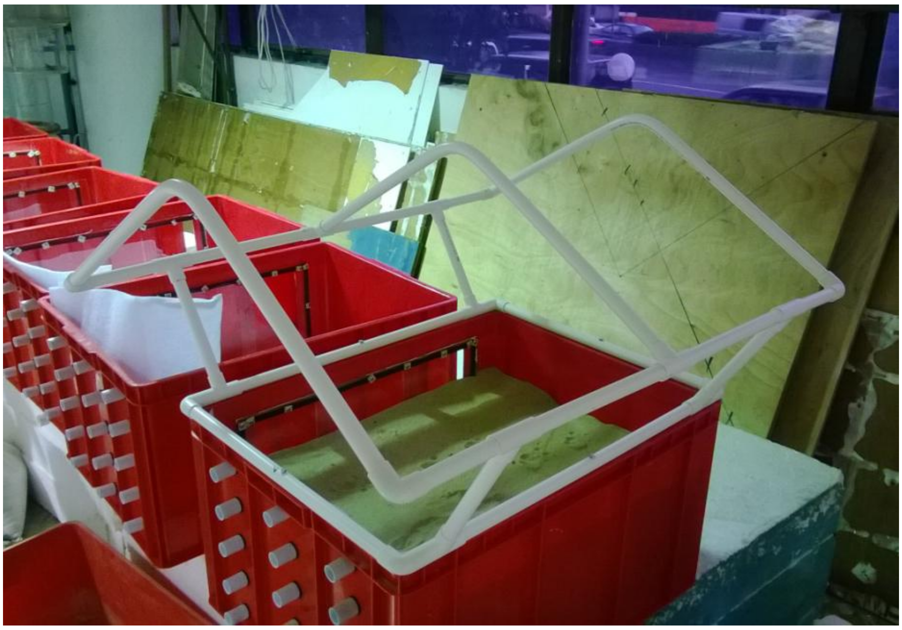

Figure 3. 34 Rainfall canopy for experiment tank

3.2.4.2 Hyrdograph analysis

In the study of the performance of Eco-Soil towards under various precipitation situations, hydrological model is usually applied to find out the relation between precipitation, infiltration, detention and retention. The hydrograph analysis aims to carry out the comparative investigation on the substrate under various rainfall conditions. The newly designed Precipitation Runoff Simulation Systems (PRSS), consisting of rotary flow rater meter for measuring the water input, sprayer for simulating precipitation for 10, 30, 50, 70 and 100 mm/hr, plastic film for regulating the precipitation area and measuring tipping bucket for measuring bottom and surface runoff, were used to carried out the precipitation-runoff experiments in parallel (Figure3.38).

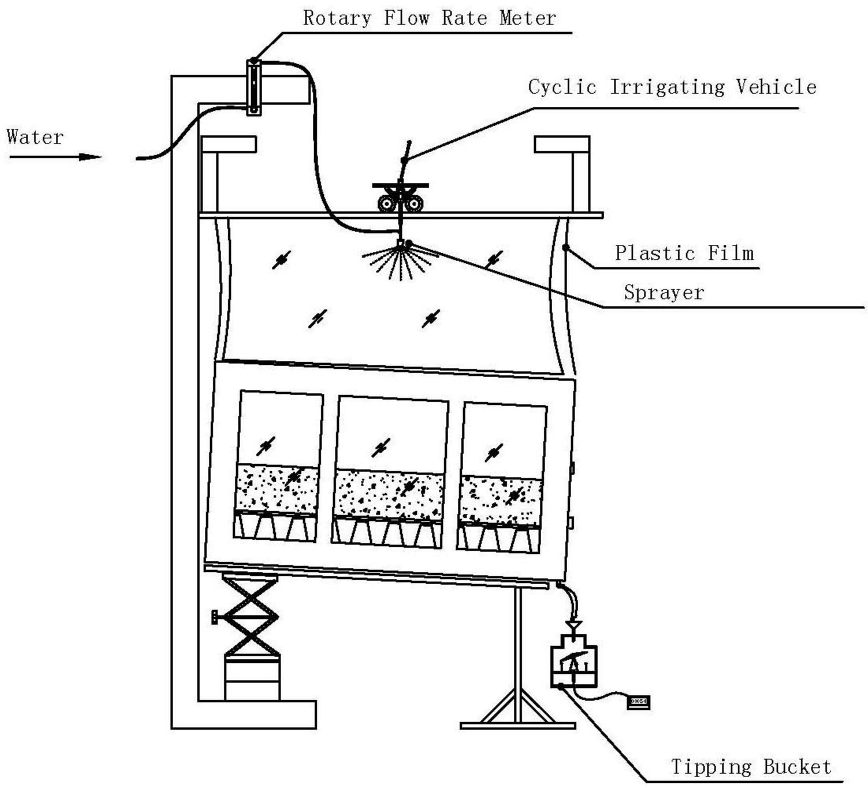

Figure 3. 35 Precipitation Runoff Simulation System (PRSS) for runoff experiment

3.2.4.3 Cyclic Irrigation Vehicle

The performance is essentially important for choosing suitable combination of Eco-Soil. To find out the numerical hydraulic relations between the design and performance, a comparable, parallel and controllable study should be carried out. The PRSS was referred to the green roof PRSS system according to our previous study for green roof retention and detention (Wai *et al*., 2014). Most of the rainfall-runoff studies were conducted in ambient environments (Spala *et al*., 2007; Gregoire and Clausen, 2011; Carter and Rasmussen, 2006). These studies were able to obtain valuable data of the green roof performance and vegetation growth under real situations. However, the hydraulic performance cannot be compared directly. Firstly, the precipitation event and amount were random and uncontrollable. In every event, the duration, intensity and pattern are different. Secondly, the vegetation growing stage and soil age varies with time, resulting in different transpiration rates. Thirdly, the time between events are also random, therefore the initial soil moistures are different. Consequently, it is difficult to make direct comparison of the green roof performance in the ambient studies. Lab-scale study is required to look for the quantitative relation of the hydraulic performances in well control situations.

In the lab-scale study, most of commercial gardening irrigation sprayers usually serve water with a large flow rate but a small coverage, resulting unevenly distributed precipitation and high rainfall intensity (larger than 30 mm/hr). After tens of times of selections and tests, the sprayer of a specific band watering pot is found to be able to simulate the rainfall intensity from lower than 10 mm/hr, which had high appearance probabilities in most of the semi-arid and arid area. In addition, the Eco-Soil shows high retention effects in low intensity events.

However, the coverage of the sprayer for simulating the precipitation of 10 mm/hr was not enough for the whole surface area. To solve this problem, a self designed Cyclic Irrigating Vehicle (CIV) was used to ensure the coverage and even distribution.

3.2.4.3.1 Compositions of the CIV

The cyclic irrigation vehicle was designed based on the non-AC, durable, sustainable, light-weight, simple-structure, adjustable and easy-handle ideas. Because the precipitation simulation concerns the water, it will be safer to use low-voltage direct current supply. Every precipitation for the runoff experiment lasts for 1 hr, therefore, the CIV should at least 1 hr. The power supply for the CIV should be durable enough and reusable. The CIV is a apparatus supplying the precipitation from the top of the green roof modules, so the weight of the CIV should be as light as possible to reduce the cost for construct the hanging track. For reducing the weight of the CIV and ensure long-term usage, the structure of the CIV is designed only with necessary components. In order to ensure the comparable experiment between experiments, the working speed of CIV is designed to be adjustable via the voltage control by the adjustable resistance. In addition, the runoff experiments may be conducted by different research personnel, therefore the operation of CIV should be convenient so that most of the researchers can reproduce the experiments or used for other purposes.

3.2.4.3.2 Structure of CIV

The main structure of CIV is constructed by a 100mm × 200 mm acrylic plate, 4 L-shape model plastic sticks (7mm × 7mm × 75 mm, L shape), 4 straight model plastic sticks (7mm × 7mm × 155 mm) and 6 small wheels (Figure 3.39).

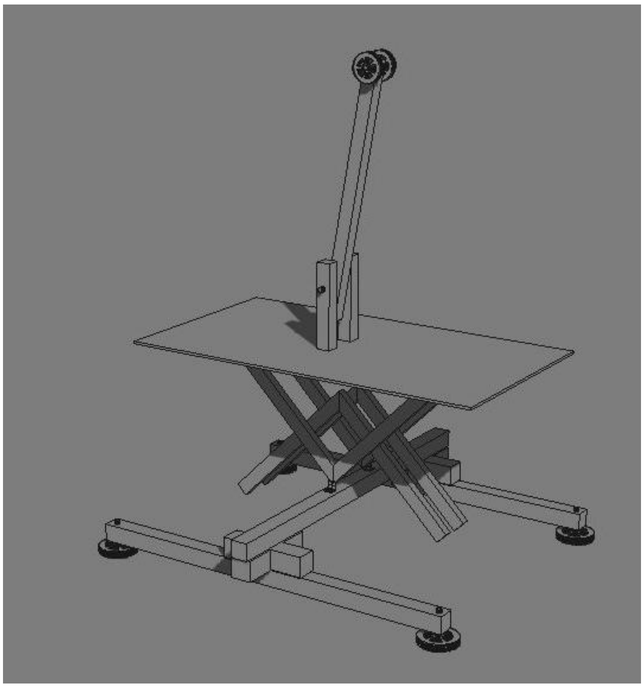

Figure 3. 36 Main structure of CIV

From the bottom to the top, plastic sticks were used to construct different sections of the CIV. The 3 straight sticks and 4 small wheels in the bottom showed in Figure 1 formed the restraining frame to ensure the CIV working along the hanging track (Figure 3.40). The 4 L-shape sticks constructed a fix and stable structure to hold the working sections of the CIV. On top of the working sections, an acrylic plate was connected to the L-shape sticks as a platform to place the rechargeable battery. The motor and the dual-way switch were attached to the bottom side of the plate. A mechanical lever was installed on the top of the CIV and this served as a self-reversing control method for cyclical running.

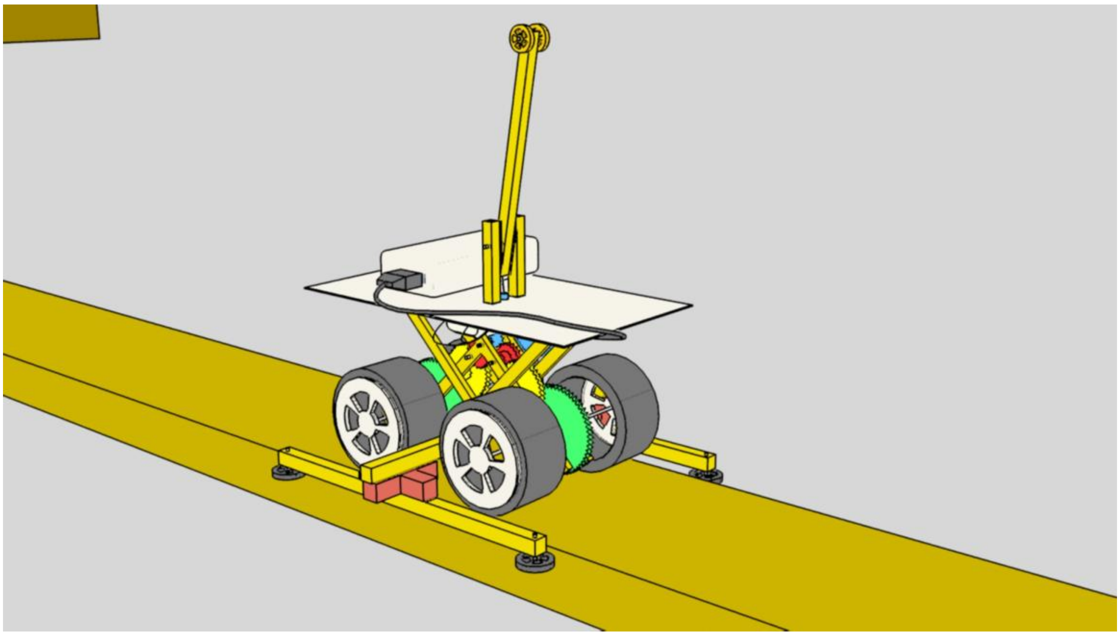

Figure 3. 37 CIV on the hanging track

3.2.4.3.3 Kinetic Section of CIV

The CIV was designed to fulfill the cyclic irrigation purpose and ran forth and back along the hanging track at an appropriate speed. Therefore, the 4 wheel drive (4WD) design was introduced into the kinetic section of CIV to ensure the output of kinetic energy to be even for running in both directions. If the CIV runs at a high speed, part of water from sprayer will fly outward of the irrigation due to the inertia of the water drop motion. And if the CIV runs at a very slow speed, the unevenness of the irrigation appears to be significant and affect the experiment results. After a series of test and observation, the appropriate time for one turn (from one end to the other) is 5~6 s for a 500 mm distance. The 4WD slow motion kinetic section of CIV was fulfilled by a model ship motor (Figure 3.41). The axle of the motor is 2.1mm and it operates under voltage 1.0~9.0 V. When the power supply is at 6V, the motor will output a resolution of 3833 RPM.

Figure 3. 38 Model ship motor (the axle is 2.1mm; operates within 1.0~9.0 V; 3833 RPM at 6V)

The primary speed of the CIV was control by the gears and adjustable electric resistance, which are shown in Figure 3.43.

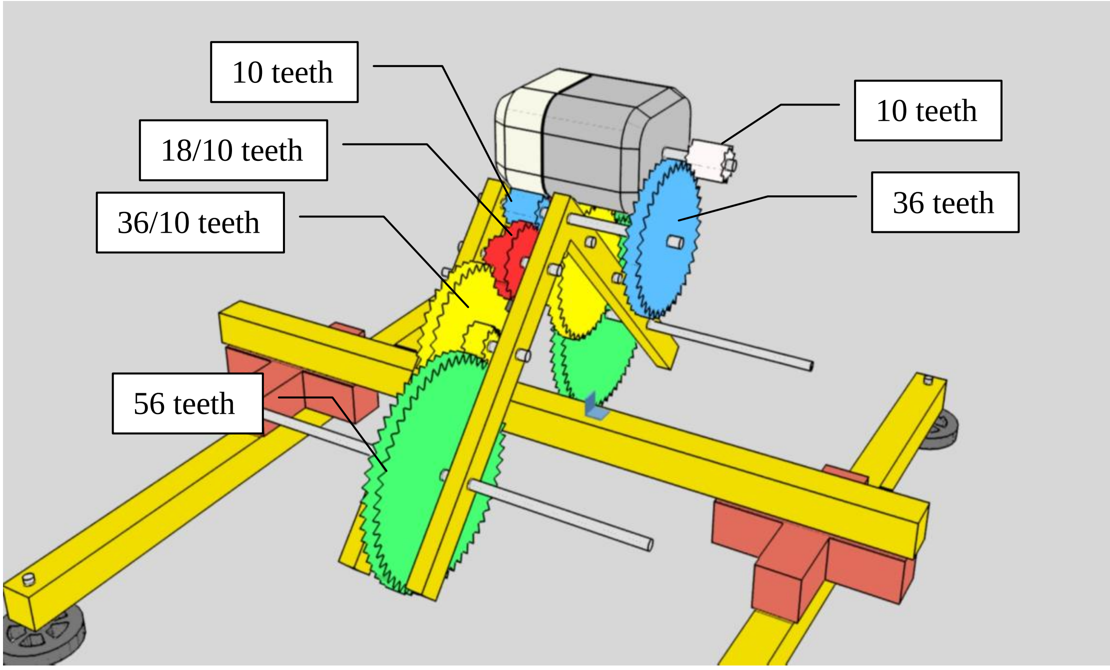

Figure 3. 39 The gear system of CIV kinetic section

The motor was connected to a 36-teeth gear which was linked to a 10-teeth gear within the central kinetic section. The 10-teeth gear (blue color in Figure 3.42) was in contact with two 18/10-teeth dual-layer gears in two directions to maintain a same rotating speed for the 4 wheels. The18/10-teeth gear was connected to a 36/10-teeth dual-layer gear and then a 56-teeth gear. This gear was fixed to the axle which connected every two wheels. The gear system formed a simple 4WD and slowed down the operation speed of the CIV.

3.2.4.3.4 Electric and Control Section of CIV

To ensure a durable, stable operation of CIV, a simple structure circuit diagram was designed for the CIV and shown in Figure 3.43.

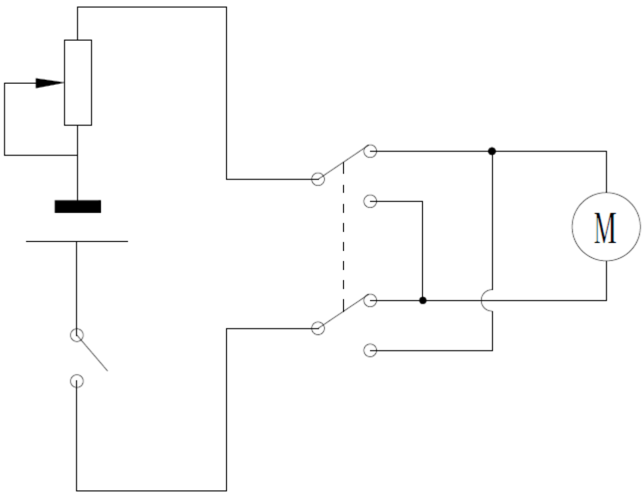

Figure 3. 40 Circuit diagram for CIV

A 5000 mA Li-ion rechargeable battery was used as power supply for the CIV. The rechargeable battery operates at 5V and 1A and it was tested to be able to supply the CIV enough electric energy for more than 3 hours running. The rheostat (adjustable resistance, 1~10 kΩ) was used to control the voltage that supply to the motor as a mean to adjust the operation speed of the CIV. A commercial Double Pole Double Throw (DPDT) switch was used to fulfill the reserves running purpose by hitting the switch. As described in Figure 3.43, when the DPDT switch was turned to other side, reversal current was supplied to the motor to reverse operation direction.

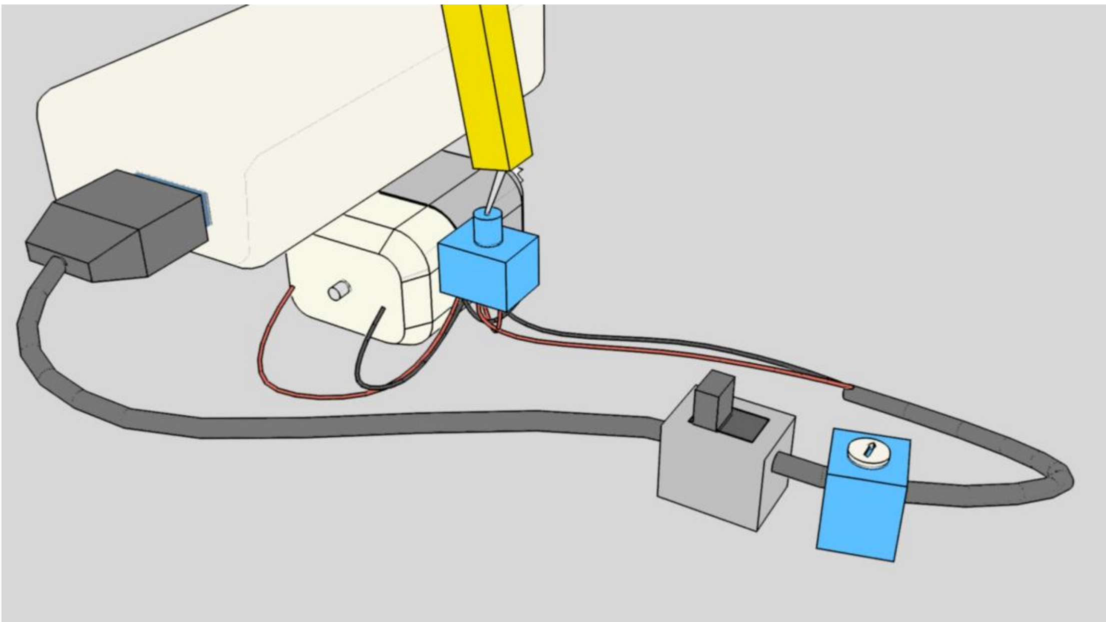

Figure 3. 41 Schematic setup of electric system

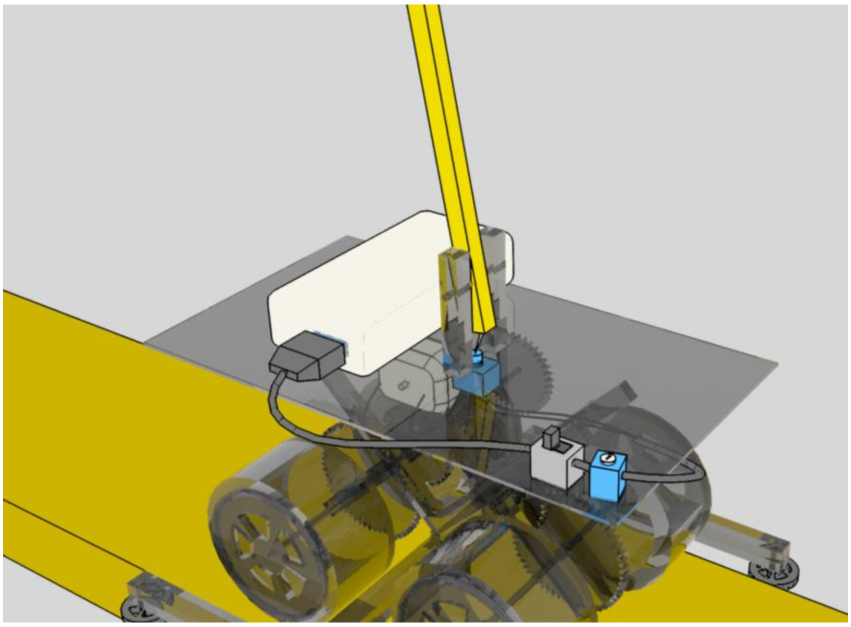

Figure 3. 42 The electric section installed in CIV

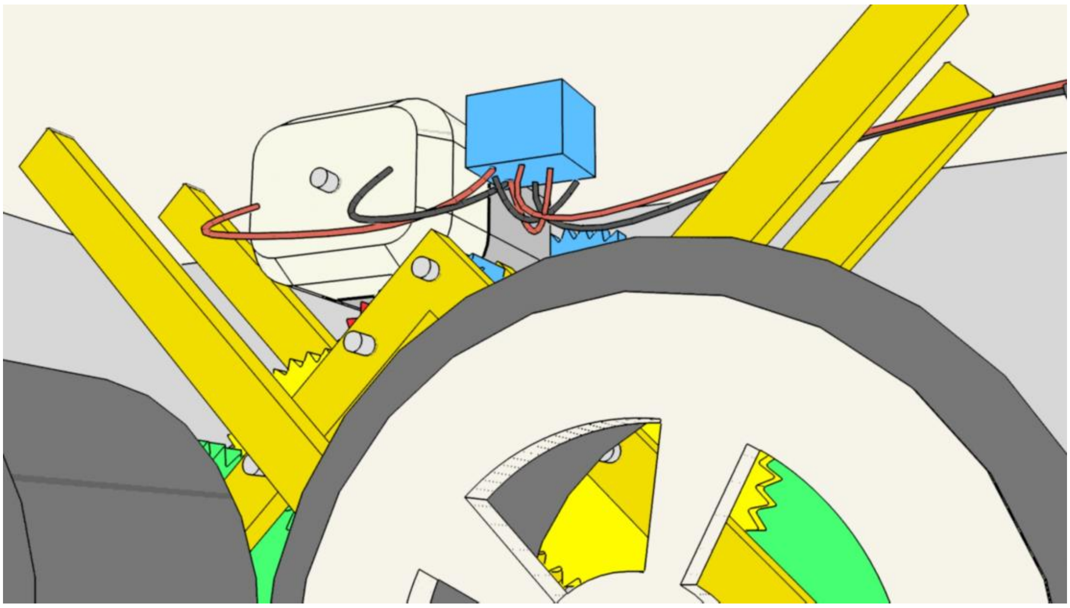

Figure 3. 43 The DPDT switch and motor installed in the CIV

The DPDT switch was connected to a lever as shown in Figure 6 and 7. When the other end of lever hit the stoppers, which were attached to the hanging track, the DPDT switch installed in the CIV (Figure 3.46) was turned to the other side by the inertia of CIV (Figure 3.47).

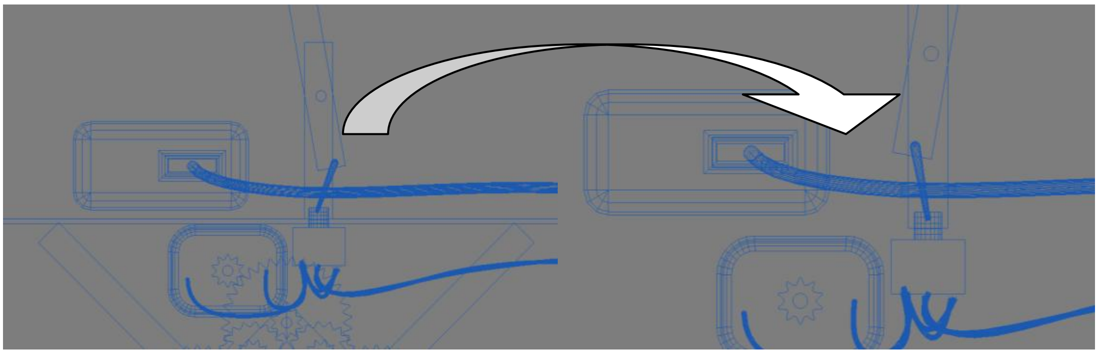

Figure 3. 44 Turning of DPDT switch by CIV inertia

If the DPDT switch directly hit to the stopper, the impulse may not be enough to turn the switch to the other side. By introducing the lever, the force in hitting was enlarged for switching. On the top of the lever stick, two small wheels were installed to reduce the resistance when hitting the stopper.

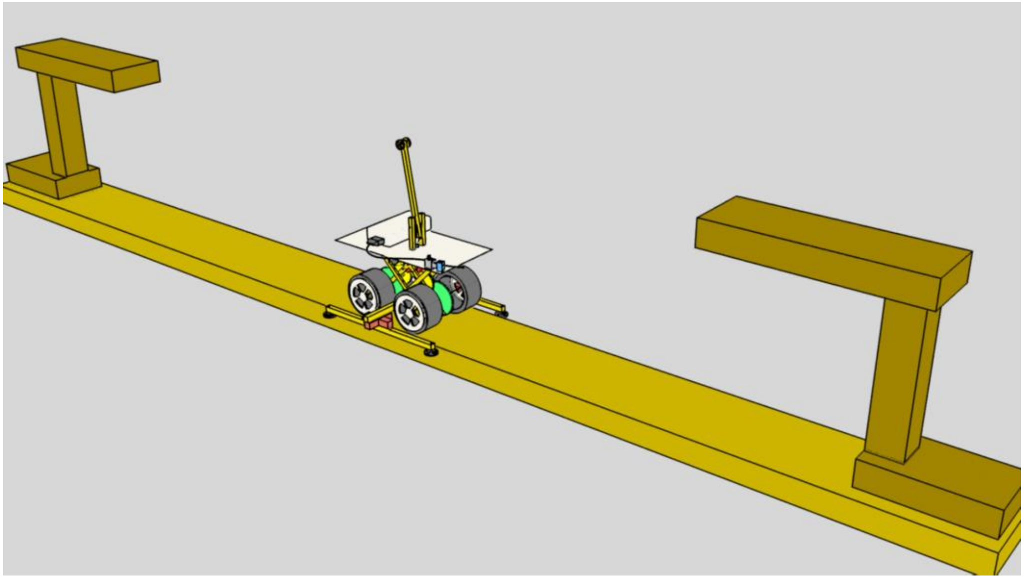

Figure 3. 45 Overall view of the CIV and hanging track

The overall view of the CIV and hanging track was shown in Figure 3.48. The two stoppers were attached to the track and the locations of the stoppers were adjustable to confine the operation range of the CIV.

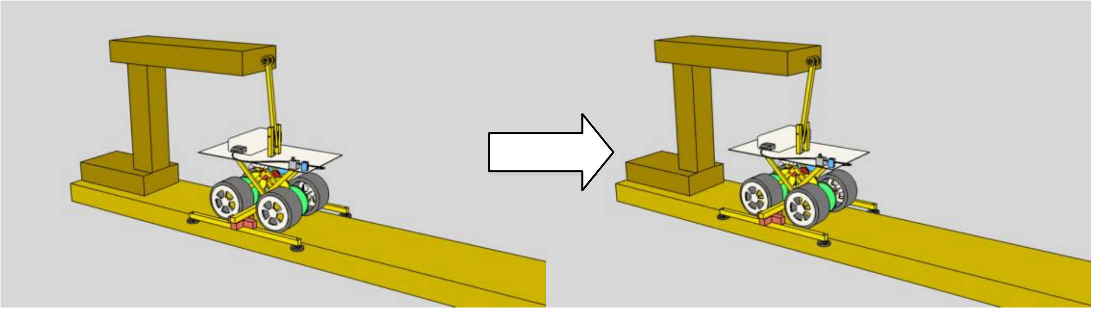

Figure 3. 46 Turning of the DPDT switch by hitting stopper

Figure 3.49 shows the figure when the lever stick of CIV hit the stopper. A moment is generated on the lever stick due to the momentum of the changed to zero. Because the moment arm of the force generate by the stopper is larger than the switch, the switch is turned to the other side.

This mean for turning the operation of CIV was found to be a reliable way to fulfill the cyclic running by in-complicated design.

The design of the CIV fulfills the cyclic and controllable irrigation for the runoff experiment, especially for low intensity rainfall event. The development of CIVs save human resources for conducting experiment and homogenize the irrigation activities. The in-complicated design makes the operation of CIV to be reliable and durable for tens of experiments. In addition, the CIV also can be applied to other experiments that using cyclic actions. The track for CIV can be curved or other shape if the radius of the curvature is appropriate.

3.2.4.4 Measurement of Runoff by Measuring Tipping Bucket

The measurement of the bottom runoff was achieved by the dedicated designed

Measuring Tipping Bucket (MTB), which was able to measure the lowest flow rate down to 2 mL/min.

3.2.4.4.1 Composition of Measuring Tipping Bucket

From top to bottom, the measuring tipping bucket consisted of a funnel, a tipping bucket, two balance adjusters, neodymium magnet, magnetic switch and digital counter (Figure 3.50). The funnel is for collecting and homogenizing the drainage. The drainage flow measuring was controlled to drop on the red point paint within the funnel bowl to dissipate the associated potential energy. The water collected filled the tipping buckets, which were consisted by two scoops made from a precisely cut 20 mm PVC-C pipe. When the bucket is filled up, the balance turned to the other side for a new collection. The neodymium magnet, which is packed by plastic for waterproofing, on the end of the central axis sweeps over the magnetic switch fixed at the bottom of the measuring tipping bucket. The magnetic switch closes accordingly and the signal is detected by the digital counter linked. The volume for one tipping was adjusted to be around 2.3 mL through the balance adjusters on the both sides under the tipping buckets. The flow rate coming is proportional to the tipping frequency.

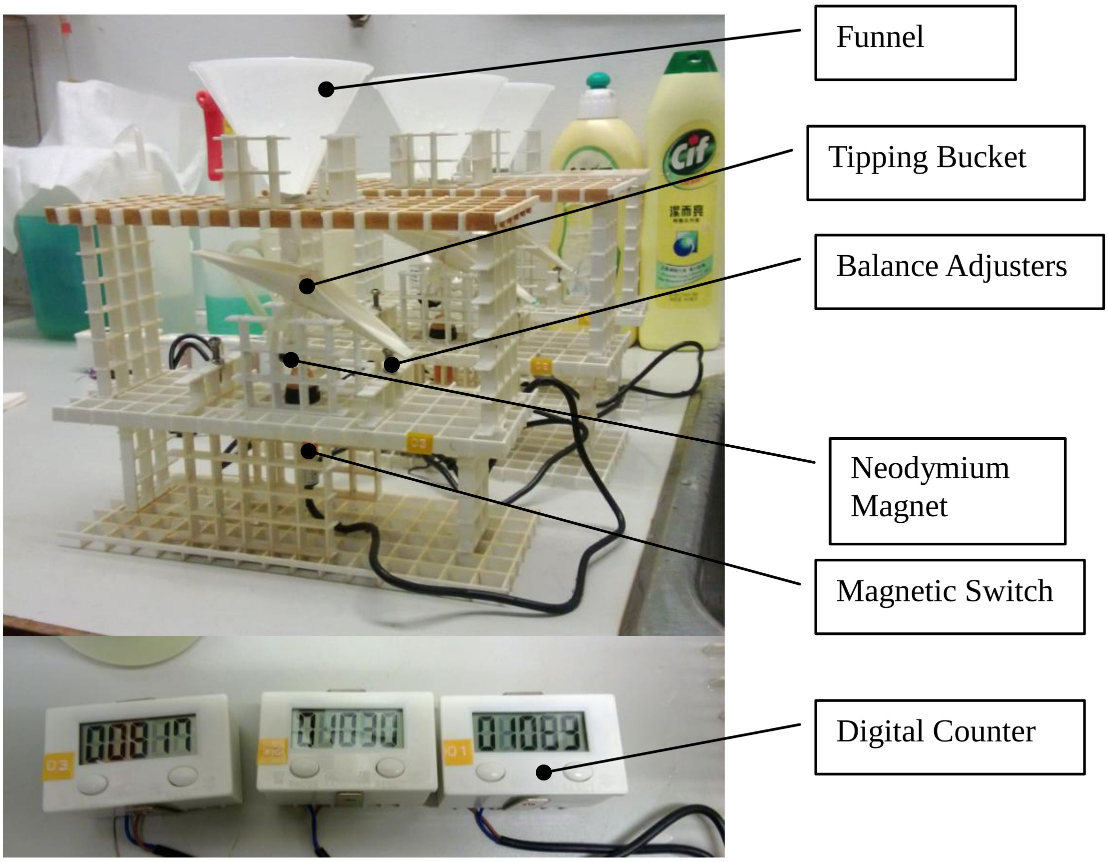

Figure 3. 47 Structure of the measuring tipping bucket

Calibration was carried out using tap water flow ranging from 3.05 to 580.00 mL/min. The flow rate was measured by the volume collected within 1 min counted by Citizen stopwatch.

The calibration flow start from 3.05 mL/min and increased to 580.00 mL/min gradually. When the flow rate was confirmed, the measuring tipping bucket (MTB) was placed under the flow to take measurement and calibrated separately. Tipping per minute was recorded for 3 times to calculate the average value. After calibrating all the MTB, the flow rate was measured again to check the variance of the inflow. The flow rate was found to be varied within 3.00 % and supposed to be reliable. When the calibration finished, a random flow rate 445.00 mL/min was set to check the reliability of the MTB result. Figure 3.51 shows the calibration curve for the 3 MTB.

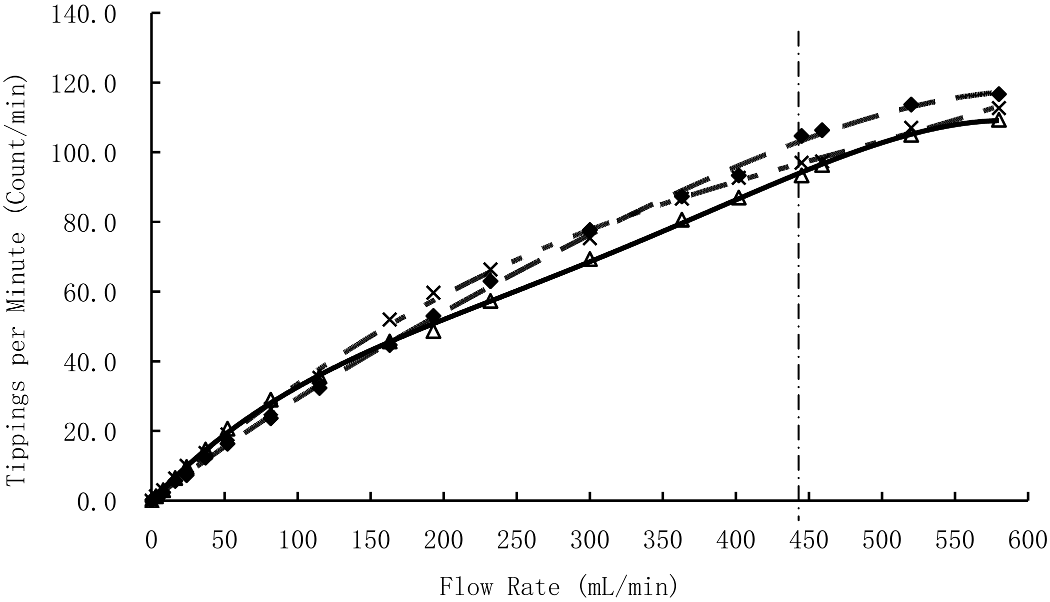

Figure 3. 48 Calibration curve for Measuring Tipping Buckets with the range for 3.05~580 mL/min

The calibration equations (3.3-3.4) for MTBs 1#, 2# and 3# were found to be highly correlated to the results and held associated correlation coefficients up to 0.998, 0.992 and 0.999, respectively.

MTB 1#: $$y = 4\times10^{-06}x^4 - 0.0007x^3 + 0.0514x^2 + 2.4169x + 1.4851 \quad \text{(Eq 3. 3)}$$

MTB 2#: $$y = 6\times10^{-06}x^4 - 0.0013x^3 + 0.116x^2 + 0.4315x + 4.8141 \quad \text{(Eq 3. 4)}$$

MTB 3#: $$y = -2\times10^{-06}x^4 + 0.0007x^3 - 0.0314x^2 + 3.4221x - 2.6721 \quad \text{(Eq 3. 5)}$$

The check point 445.00 mL/min was showed to be on the curve. The 3 sets of MTB were consequently considered to be reliable for flow measurement for the flow rate between 3.05 to 580.00 mL/min.

3.2.4.5 Procedure for Runoff Experiment

To obtain the runoff hydrograph based on the maximum retention and detention, the arid sand, Eco-Soil and commercial potting soil sample were air dried until residue moisture content were achieved. Each sample tank contained 200mm depth of sample. One of the tank containing only filter layer and drainage layer was used as control tests to determine the background rainfall retention and detention. The samples were placed in the PRSS and the slope was set to be 0.01 to allow runoff to discharge to the drainage port. 1 L of tap water was injected to the drainage layer of the experiment tank to saturate the drainage layer to mitigate the retention due to the surface tension of the surface of the structural materials. The simulated rainfall was supplied by submerge pump and the flow rate was indicated by a rotary meter. The flow rate was calibrated by Time-Volumetric method, i.e., the volume of water provided by the spray was collected for one minute to obtain the flow rate. Before the start of the experiment, the initial rainfall was adjusted to be within 3% error to the desired value.

$$[\mathrm{P_r}] = [I_r][A_s] \qquad \text{(Eq 3. 6)}$$

where $[P_r]$ is required rainfall rate, ml/min;

$[I_r]$ is required rainfall intensity, mm/hr;

$[A_s]$ is surface area of the sample, cm^2.

After one hour precipitation simulation, the final flow rate was measure by Time-Volumetric method to determine the mean rainfall by averaging the initial and final rainfall.

$$[\overline{P}] = \frac{[P_{\text{int.}}] + [P_f]}{2} \qquad \text{(Eq 3. 7)}$$

where [$\overline{P}$] is mean rainfall rate, ml/min;

[$P_{\text{int.}}$] is initial rainfall rate, ml/min;

[P_f] is final rainfall rate, ml/min.

Figure 3. 49 Procession of Rainfall-Runoff Experiment

The MTB counter was set zero and placed under the drainage port. The CIV was turned on to allow the simulated rain water sprayed across the whole surface of the samples. The tippings and time were recorded by a video camera and then transferred to be numerical data.

The tipping data was tabularized and transferred to be flow rate for every minute. The total rainfall was calculated by

$$[V_0] = [t_d][\overline{P}] \qquad \text{(Eq 3. 8)}$$

where $[V_0]$ is total rainfall volume, ml;

$[t_d]$ is duration of rainfall, min;

$[\overline{P}]$ is mean rainfall rate, ml/min.

The runoff volume was calculated by

$$[V_R] = \sum_{i=1}^{120} [R_i][t_i] \qquad \text{(Eq 3. 9)}$$

where $[V_R]$ is runoff volume, ml;

$[R_i]$ is runoff rate for specific duration, ml/min;

$[t_i]$ is time for specific duration, min.

Then, the retention for control tank was calculated by

$$[V_{RT,CTRL}] = [V_{0,CTRL}] - [V_{R,CTRL}] \qquad \text{(Eq 3. 10)}$$

where $[V_{RT,CTRL}]$ is retention volume for control tank, ml;

$[V_{0,CTRL}]$ is rainfall volume for control tank, ml;

$[V_{R,CTRL}]$ is runoff volume for control tank, ml.

The retention volume for sample tanks were calculated by

$$[\cancel{V}_{RT,SAMP}] = [\cancel{V}_{0,SAMP}] - [\cancel{V}_{R,SAMP}] - [\cancel{V}_{RT,CTRL}] \qquad \text{(Eq 3. 11)}$$

where [$\cancel{V}_{RT,SAMP}$] is retention volume for sample tank, ml;

[$\cancel{V}_{0,\ SAMP}$] is rainfall volume for sample tank, ml;

[$\cancel{V}_{R,\ SAMP}$] is runoff volume for sample tank, ml.

In addition, the percentage runoff for specific moment was calculated by

$$[R_i\%] = \frac{[R_i]}{[\overline{P}]} \times 100\% \qquad \text{(Eq 3. 12)}$$

where [R_i%] is percentage runoff for specific moment, %.

3.2.4.6 Five-Phase Analysis

With the help of the CIV, the simulated minimum precipitation intensity (PI) was able to reach 10 mm/hr. The PI of 10, 30, 50, 70 and 100 mm/hr were simulated for studying the rainfall runoff pattern. The bottom and surface runoff was recorded with respective with precipitation duration. The five-phase analysis (FPA) was introduced for analyzing the hydrograph. The hydrograph was divided into five phases, including detention, increasing, stationary, decreasing and prolonging phase.

The phase appearance was different due to different porosity, permeability, residue moisture content and precipitation intensity. The detention phase shows the runoff hysteresis effect due to the soil hydraulic properties in the precipitation events. The precipitation infiltrates into the substrate layer then penetrates horizontally and vertically. Within this migration, the water will be adsorb to and absorb by the soil matrix and root surface, intercepted by capillary effect and evaporated as vapor in the substrate pore. The precipitation finally becomes runoff after going through the filter and drainage layer. The duration between the start of the precipitation event and the appearance of first drop of runoff is defined as Start-Point Detention Time (SPDT). In this phase, the precipitation intensity, green coverage ratio, substrate depth, hydraulic conductivity and initial moisture govern the time of runoff formation.

The increasing phase represents the fast growing trend of runoff majorly due to the vertical transient water flow. Due to the adsorption, absorption, capillary retention and evaporation in the water migration process, the speed of runoff flowrate increasing is different under various precipitation intensities (PI), soil hydraulic conductivity, soil organic content and vegetation type. Under normal experiment conditions, the SPDT is hard to be observed accurately, since the water surface tension may affect the water coming out. The Half-Rate Detention Time (HRDT), which represents the time between the start of precipitation event and 50% of RPR, will be used for comparison among different scenarios. The pattern of increasing phase reflects the substrate layer property.

When the Runoff/Precipitation Ratio (RPR) increases to a certain percentage, the growth becomes lower and approaches 100 %. However, the RPR need a period of time to reach 100% since the absorption from soil matrix and root is still under process. Judged from the relative lower growth of RPR, this phase is defined as the stationary phase. In this phase, the PRSS starts to lose effects for precipitation retention. When the RPR reaches 95%~100%, the time spent is defined as Peak Runoff Detention Time (PRDT). Within this phase, if the soil hydraulic conductivity is lower than the PI, part of precipitation will become surface runoff. In that circumstance, the bottom RPR will not reach 100%. However, ponding was not observed in this study, even though under the PI of 100 mm/hr (100 yr return period in HK). In this phase, precipitation and Eco-Soils reaches an equilibrium status. The dominant affecting factors are the soil organic content, conductivity and PI.

The precipitation lasts for 1 hr in this study. Thereafter, the residue transient water keeps on coming out as runoff. This phase is described as decreasing phase. The decreasing phase reflects the water movement under the decreasing pressure head. The water comes out majorly due to gravity. Therefore, the pattern of deceasing phase is mainly affected by soil conductivity and PI.

The prolonging phase shows the extension of the runoff from the PRSS. The decreasing speed of the RPR becomes lower and non-linear when the pressure head of the soil water drops to a certain level. The speed of water coming out from the substrate layer is reduced because of the capillary effect from the substrate matrix. The prolonging phase can last for a long time. If the runoff flowrate is lower, the outflow rate from the bottom runoff hole will be affected by water surface tension. Therefore, the runoff experiment will be ended when the runoff flowrate is lower than 5 ml/min (approximately 0.12 mm/hr). The shape of the curve in the prolonging phase is affected by the PI and porosity.

This Five-Phase Analysis offers a way to investigate the soil performance under precipitation events which covered the routine and extreme cases. Through this Five-Phase Analysis, more accurate numerical simulation result could be obtained to predict the runoff pattern in specific precipitation events.

3.3 Plant-Soil Micro-Ecosystem

The study of microecosystem aims to find out the mechanisms behind the plant growth in each growing medium. The uptake and transformation of the three macro nutrient potassium, nitrogen and phosphorous were analyzed through the bottom runoff along the plant growing period.

3.3.1 Background Nutrient

According to the description of desertification, the soil lost its productivity and left mainly inorganic content. The addition of activated sludge aims to rebuild the soil productivity.

The arid sand, Eco-Soils and potting soil samples were mixed with distilled water at ratio of 1:10 (dried weight of sample: water volume). The mixtures were contained in 300 mL conical flasks and shaken via shaking incubator (TAI CANG, Model: THZ-D, rpm 30~280) at 120 rpm for 1 hr. The supernatant was diluted 10 times to analyze the nutrient content including reactive phosphorus, potassium, ammonia, nitrite and nitrate nitrogen for gaining the background nutrient of the growing medium. The analysis methods of the aforementioned nutrient contents were specified in Section-4.2. The nutrient content of each growing medium was compared with Hoagland nutrient solution (Lincoln *et al*, 2006) and the potting soil to suggest the optimal SSVR of the Eco-Soils for growing plants.

3.3.2 Nutrient Uptake in the Growing Period

The nitrogen, phosphorus and potassium play the major roles in okra growing period. The nutrient including reactive phosphorus, potassium, ammonia, nitrite and nitrate nitrogen in leachate after irrigation were analysis every 7 days. The leachate retained drainage layer (in the bottom of the growing cases) were poured out and the drainage layer was washed by distilled water for three times. The automatic watering system was turned on manually. The leachate was collected for analysis the extractable contents.

3.3.3 Materials and Models

3.3.3.1 Plants

Abelmoschus esculentus (Okra) was chosen for the study because it is angiosperm and has a complete growing pattern. The okra seeds (produced by High Mowing Organic Seeds Inc., Figure 3.50) were purchased from local garden supplier. Based on the specification printed on the package bag, the plant growing period (55 days), from seeding to harvesting, is suitable for carrying out the study. Compared to okra, the arid area plant species such as cactus, aloe and sedum usually have slow growing speed. Consequently, the time for carry out the study was longer. The okra also appeared a medium plant height (0.9~1.5 m) therefore a smaller growing space was enough for study.

Figure 3. 50 *Abelmoschus esculentus* seeds for carrying out plant growing experiment

The distilled water is the best choice to simplified the simulation for the real situation and reduce the interference for studying in the runoff properties. However, the quantity of distilled water required for irrigation was large for the whole experiment and more human activities should be required to transfer the large amount distilled water to the experiment site. Therefore, the other selection is the tap water. However, the chlorine content in the tap water from laboratory were tested to be 1.1~1.2 mg/L (by HACH Pocket Colorimeter) and is ineffectual towards plant growth or even harmful for the soil bacteria. To eliminate the chlorine, dechlorination agent containing 1000 mg/L sodium thiosulfate ($Na_2S_2O_3$) solution was added to the tap water prior to irrigation.

The okra seeds were seeding in the germination tray containing the corresponding Eco-Soil and potting soil samples. The tray were placed in the dark at room temperature (20.0~23.3℃) for 20 days for germination. The germinated plants were transferred to the growing cases from the 21st day.

Polypropylene (PP) cases with diameter of L-200 mm×W-150 mm×H-150 mm were used for growing the transplanted okra, which grew 4 leaves. The soil surface was 300 cm^2 and effective substrate volume 3000 cm^3 (3L). The growing cases contained 4 layers, including vegetation, substrate, filter and drainage layer (Figure 3.51). The filtrate was collect via the bottom drainage port.

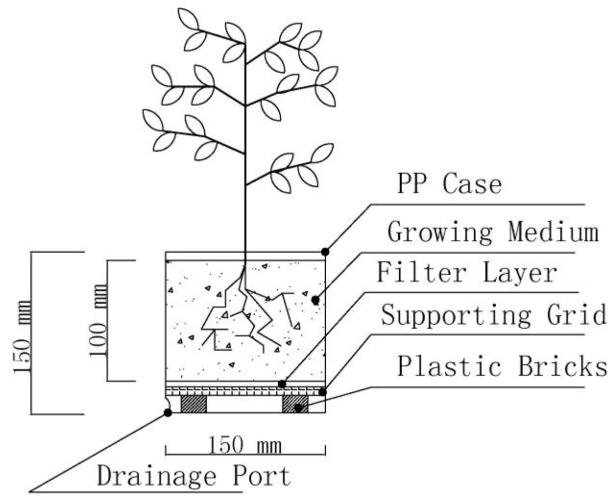

Figure 3. 51 Cases setup for the study of plant growing

18 cases were used for carrying out the triplication study for the 6 types of growing medium such as arid sand, Eco-Soils and plotting soil. Each series of cases (6 cases) were placed in the cabin constructed by PVC-C pipes and plastic film to control the environmental condition. The 3 cabin played as a small scale green house for growing the plants.

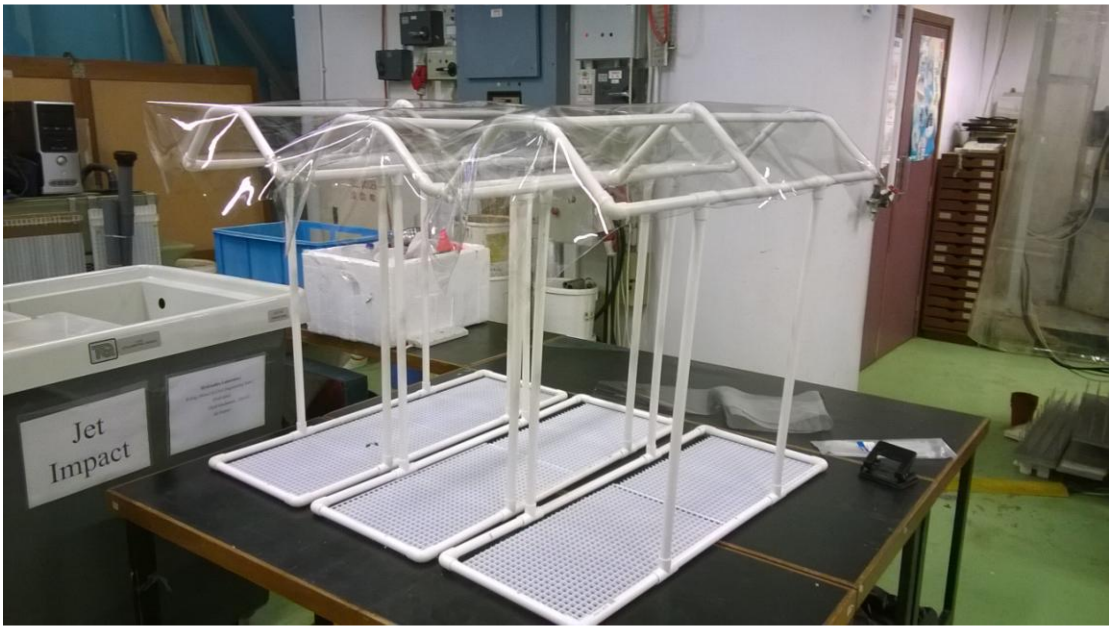

Figure 3. 52 Cabins for carrying out plant growing experiments

The mini green house helped to protect the plants from rainfall and strong wind, maintain suitable humidity and carbon dioxide level, and also separate the plants from birds and insects.

The automatic watering system (AWS) aims to have a fixed and even schedule for watering the plants. The AWS help to take care of the plants after office hour and save human power. The automatic watering system (Figure 3.53) consists of timer, aquatic type submerge pump, storage tank, valves and silica hose. The watering time was set to be 9:00 am and 17:00 pm to maintain suitable moisture content for the day and night time.

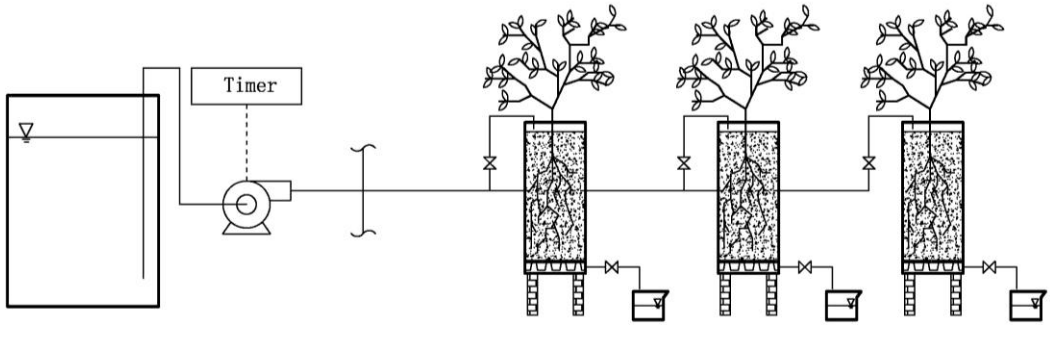

Figure 3. 53 Automatic watering system

The irrigation rate for every plant was set to be dripping style through adjusting the valve for each plant because every turn-on of the time switch was fixed to be 15 min due to the timer specification. The average irrigation rate was measured to be 17.5 ml/min.

The observing period started from 25th Apr 2013 to 6th Oct 2014, and the harvesting period started from 8th Aug 2013.

The plant height, shoot thickness and number of leaves were recorded every two or three days. The okra pods were harvest every 4 days and size, dried and wet weight were measured and recorded. The dried weight of shoot, leaves and root were determined after final harvesting. The dried weights were measured by drying the samples at 105℃ for 24 hour to reach constant values.

3.3.4 Phyto-toxicity Experiment

The plant growing characteristics study aims to find out the optimal Eco-Soils fraction for plant growth. The maturity of the Eco-Soils was firstly study via the seed germination index. Thereafter, the plant growing experiment were carried out in the controlled conditions. Based on analysis result for two experiments, an optimal SSVR of the Eco-Soils was concluded.

3.3.4.1 Seed Germination Index

In order to study the phytotoxicity of the Eco-Soils as reference for maturity, the seed germination assay was carried out and modified from Komilis and Tziouvaras (2009).

3.3.4.1.1 Separation of Seeds

Amish Paste Tomato (*Lycopersicon esculentum*) seeds were used for carrying out the analysis of seed germination assay.

Certain amount of amish paste tomato was purchased from local fruit supermarket. Each tomato contains 32~35 seeds at the diameter of 2~3 mm. The tomato was cut into 4 pieces and the seeds were taken out with the flesh and core. The seeds was picked out by spoon, placed in the sieve and washed by tap water. After most of the flesh was washed out, the seeds were transferred on coarse tissue and the mucous on the seeds was removed by friction. The clean seeds were transferred and store in cool dried conditions for following experiments.

3.3.4.1.2 Preparation for the Seed Germination Assay

20 g of undried samples (arid sand, Eco-Soils and plotting soil) were mixed with the distilled water separately in 300 ml conical flasks according to samples dried weight ratio 1:10 (dry mass of sample: water volume). Each sample was done for triplication. The conical flasks were placed in the shaking incubator (TAI CANG, Model: THZ-D, rpm 30~280) for mixing for 1 hr at 120 rpm (Figure 3.54).

Figure 3. 54 Mixing of the samples in the shaking incubator (TAI CANG, Model: THZ-D, rpm 30~280) at the rpm of 120 for 1 hr

Since the shaking incubator was capable for 6 conical flasks at one time, the mixing for the second and third series was done in sequence.

Spontaneous to the shaking, 2 pieces of φ 90 mm filter papers were placed in the φ 90 mm Petri dish. The 35 ([$Seed_{T,spl}$]= [$Seed_{T,ctrl}$]=35) tomato seeds were placed on the upper filter paper according to a centre radiation arrangement (Figure 3.55).

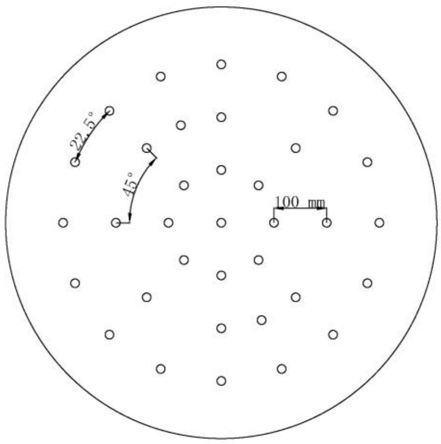

Figure 3. 55 Arrangement of the seeds on the filter paper

The mixed samples were placed in room temperature (23.5℃) for 30 min for sedimentation. 5 mL supernatant from each conical flask was introduced to the Petri dish contained arranged seeds along the wall at a low speed via pipet (Figure 3.56).

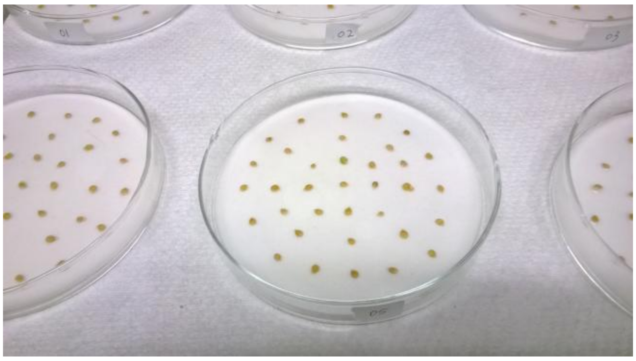

Figure 3. 56 Supernatant of sample mixtures were introduced to the Petri dishes

18 Petri dishes were used for carrying out triplication for the supernatant of 6 growth medium samples and additional 3 was for the distilled water as control (or blank) experiment. The 21 Petri dishes were wrapped by aluminium foil and placed in the incubator (THERMO SCIENTIFIC, Model: 3722) and stored for 7 days in the dark at the temperature of 20±1℃. The pH and electronic conductivity of the supernatant after injection to the Petri dishes was measured.

After 7-day incubation in the dark, the seeds were germinated and grew various root lengths. The arrangements of the seeds appeared to be have adequate growing space for each seed (Figure 3.57)

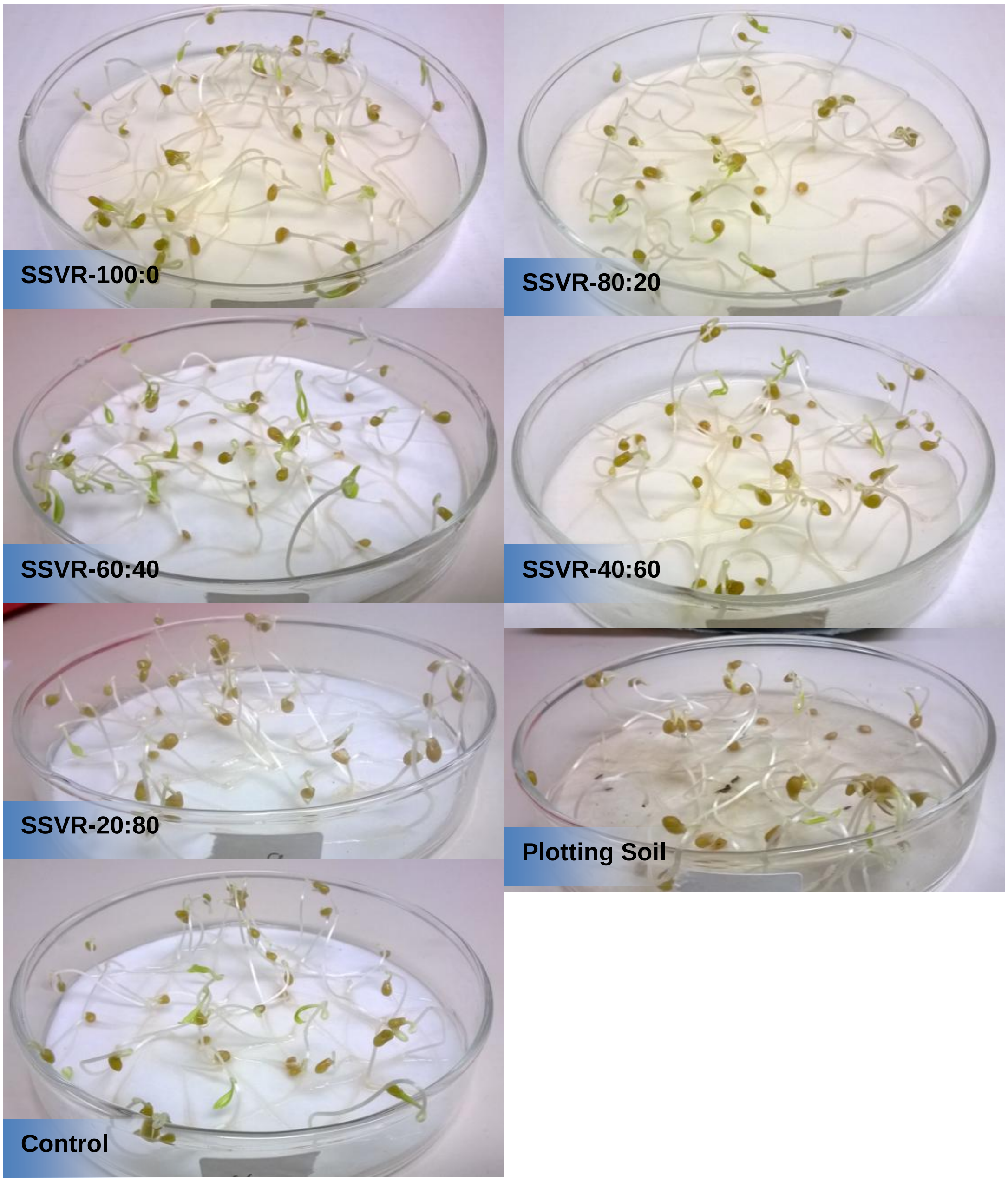

Figure 3. 57 Typical seed germination profiles for SSVR 100:0, 80:20, 60:40, 40:60, 20:80, plotting soil and control plates

The number of geminated seeds in sample ([$Seed_{Gd,spl}$]) and control plate ([$Seed_{Gd,ctrl}$]) were counted. The sum of root length of the germinated seeds in sample ([RL_{spl}]) and control ([RL_{spl}]) plate were measured precisely by ruler (Figure 3.58).

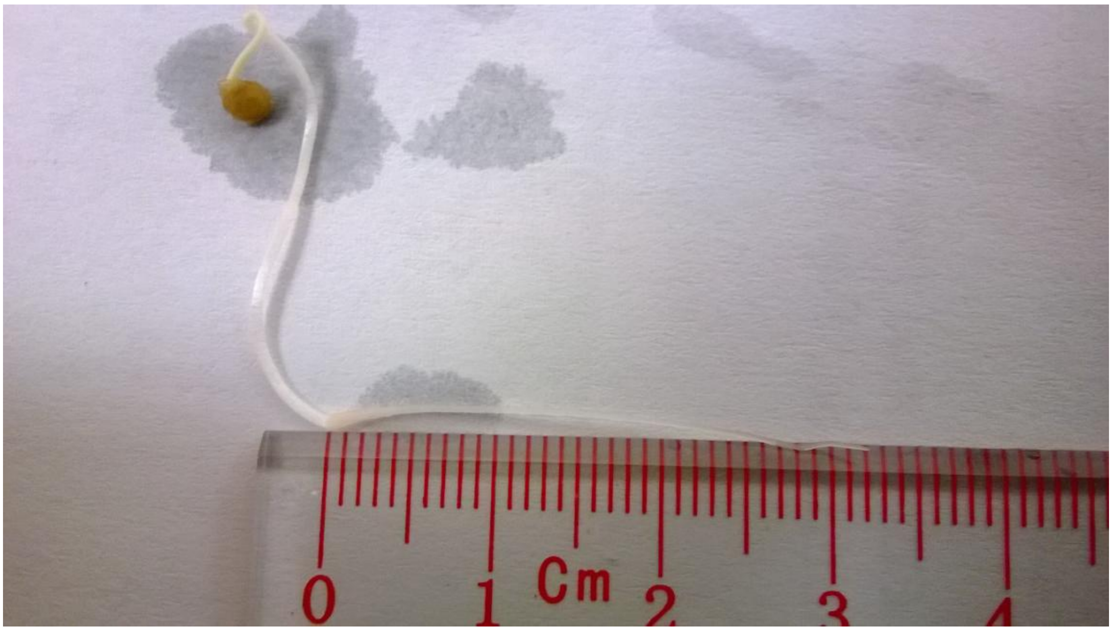

Figure 3. 58 Measurement of root length of a germinated seed by a ruler

The seeds with root length shorter than 2 mm were recorded [RL_{spl}]=0 and were considered to be un-germinated. Figure 3.59 shows a typical germination profile from SSVR 60:40

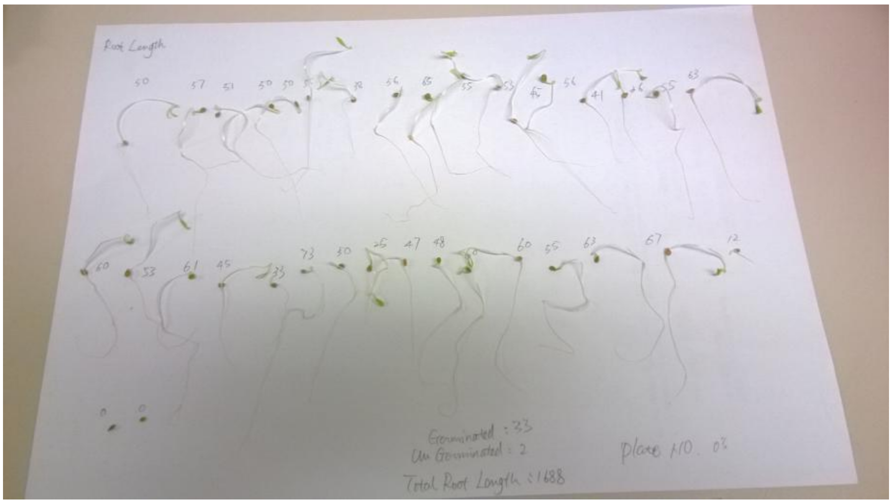

Figure 3. 59 Typical seed germination profile of the SSVR 60:40

The measured number of germinated seeds and root length of both sample and control plates were fitted into Equation-3.13 to work out the Germination Index (GI) in the form of percentage:

$$\mathrm{GI}=\frac{\dfrac{[Seed_{Gd,Spl}]}{[Seed_{T,Spl}]}}{\dfrac{[Seed_{Gd,Ctrl}]}{[Seed_{T,Ctrl}]}}\times\frac{\dfrac{[RL_{Spl}]}{[Seed_{Gd,Spl}]}}{\dfrac{[RL_{Ctrl}]}{[Seed_{Gd,Ctrl}]}}\times 100\% \qquad \text{(Eq 3. 13)}$$

The sample with GI lower than 100% is considered to be potentially phytotoxic and less mature for plant growth, while the medium appears to be phytoenhancing if its GI is higher than 100% (Komilis and Tziouvaras, 2009).

However, the results of this experiment only indicated the phytotoxicity of the leachate from the growing mediums. The real growing situation is also related to their hydraulic properties.

3.3.4.2 Plant Growing Experiment

The plant growing experiment aims to observe and analysis the physical properties the plants appeared reflecting the effects from the growing medium.

3.3.3.2.1 Germination of Seeds

The okra (as specified in previous section) was firstly germinated in the seeding tray then transferred to the growing cases. The seeds were soaked in distilled water for 24 hr to enhance the germination. The wetted seeds were planted in the seeding tray containing arid sand, Eco-Soils and plotting soil as growing medium (Figure 3.61). Each type of growing medium grew 3 seeds and additional one for spare. The automatic watering system offered plenty dechlorinated water to maintain the suitable moisture for seed germination.

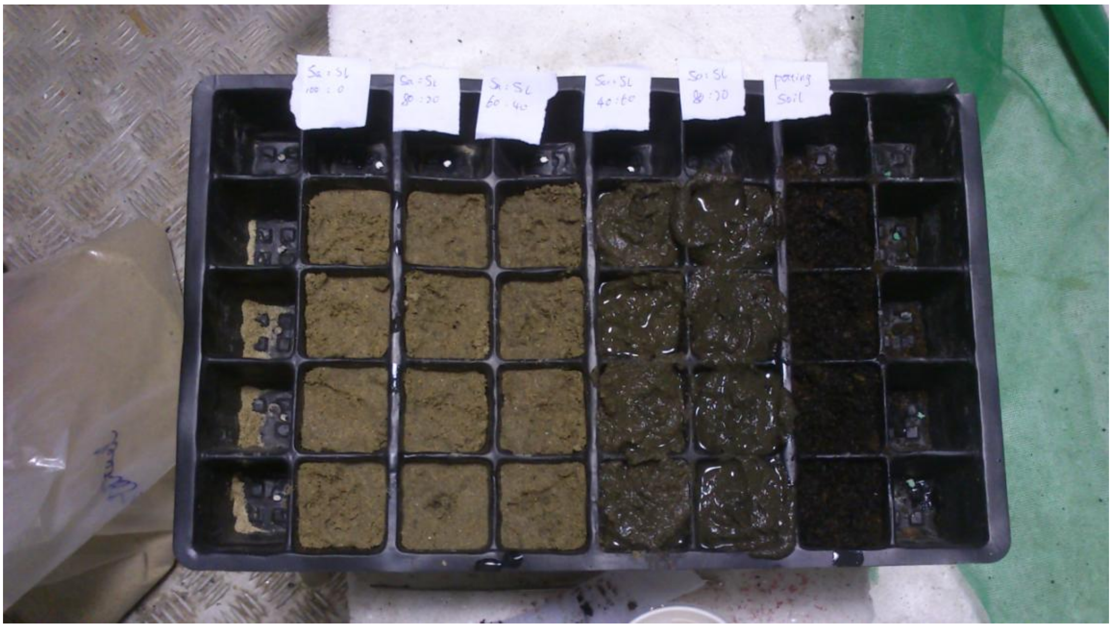

Figure 3. 60 Seeding of okra seeds in the seeding tray

The seeds germinated after 5 days from seeding and grew to 5~7 mm height. Along the growing period of the seedings, the shoot heights, leaves count and sized were recorded every two days.

After the seedings grew 4 leaves at the 7th week, the seedings were transplant to the growing cases within the mini green house (Figure 3.62). Within the growing periods, weeding and deinsectization was done manually. Pollination of was carried out at the flowing period.

Figure 3. 61 Transplanting of seedings after 4 leaves grown

The pots were water twice at 9:00 am and 17:00 pm accomplished by the automatic watering system specified at section 3.61. For better observing the growing of the okra, a graduated bamboo stick was inserted aside the plant in each pot.

Figure 3. 62 Graduated stick inserted in each growing case

Within the plant growing period, the plant height, internodes distance, leaves count and sized were recorded every two working days. The moisture differences between two irrigation periods were recorded to work out the evaporation-transpiration rate.

On the process to harvesting, the flowing, pod, seed counts were recorded for analysis. At the harvesting period, the root, shoot, leaf and seed samples were collect to conduct the dry weight, organic content, nutrient and heavy metal analysis.

3.5 Analysis Methods

This section specified the laboratory analysis methods conducted for the study. The methods were following standards or guidelines.

3.5.1 Physical Analysis

The physical analysis aims to carry out the evaluation of physical properties including particle size distribution (PSD), dry bulking density (BD, [ρ_b]), particle density (PD, [ρ_s]), permeability ([k]) and porosity (σ), which affect the substrate hydraulic performance.

3.5.1.1 Particle Size Distribution

The particle size distribution (PSD) describes the fraction of the particle in various ranges of diameter. The profile of PSD is unique for a specific substrate and affects the hydraulic properties including permeability, plant available water uptake. The particle size distribution experiment was done by dry sieving method according to British Standard (BS1377_1990, BSI, 1990).

The substrate specimen was dried in oven for 24 hr to reach constant weight. The dried samples were placed in the desiccators to have them cool down to room temperature. The cooled dried samples were crushed in the mortar because the some samples were bound to form big particles in the drying process. The crushed specimens were dried over night. 50.000 ± 0.100 g of sample was weighed via electronic scale (STARTORIUS, Model: 3200) and transferred to the brushed gradually BS sieves of from pore diameter of 2000 ~ 63 μm. The sieves were place in a top down manner with the sequence of 2000, 1180, 600, 300, 150, 63μm and the pan. The sieves cluster contained samples were fixed to the vibration generator and shaked for 10 min (Figure 3.64).

Figure 3. 63 Electronic scale for weighing the substrate specimen

Figure 3. 64 Dry sieving method for analysis the particle size distribution

The sample retained on each sieve were transferred to the evaporation dish and weighed by aforementioned electronic scale. The percentage of sample retained on each sieve was plotted against the sieve pore diameter on the log-scale particle size distribution graph. The dry sieving experiment was done for three times for each sample.

The results of the PSD profile were used for analysis the type of the substrate according to the soil texture diagram (USDA, 2014)

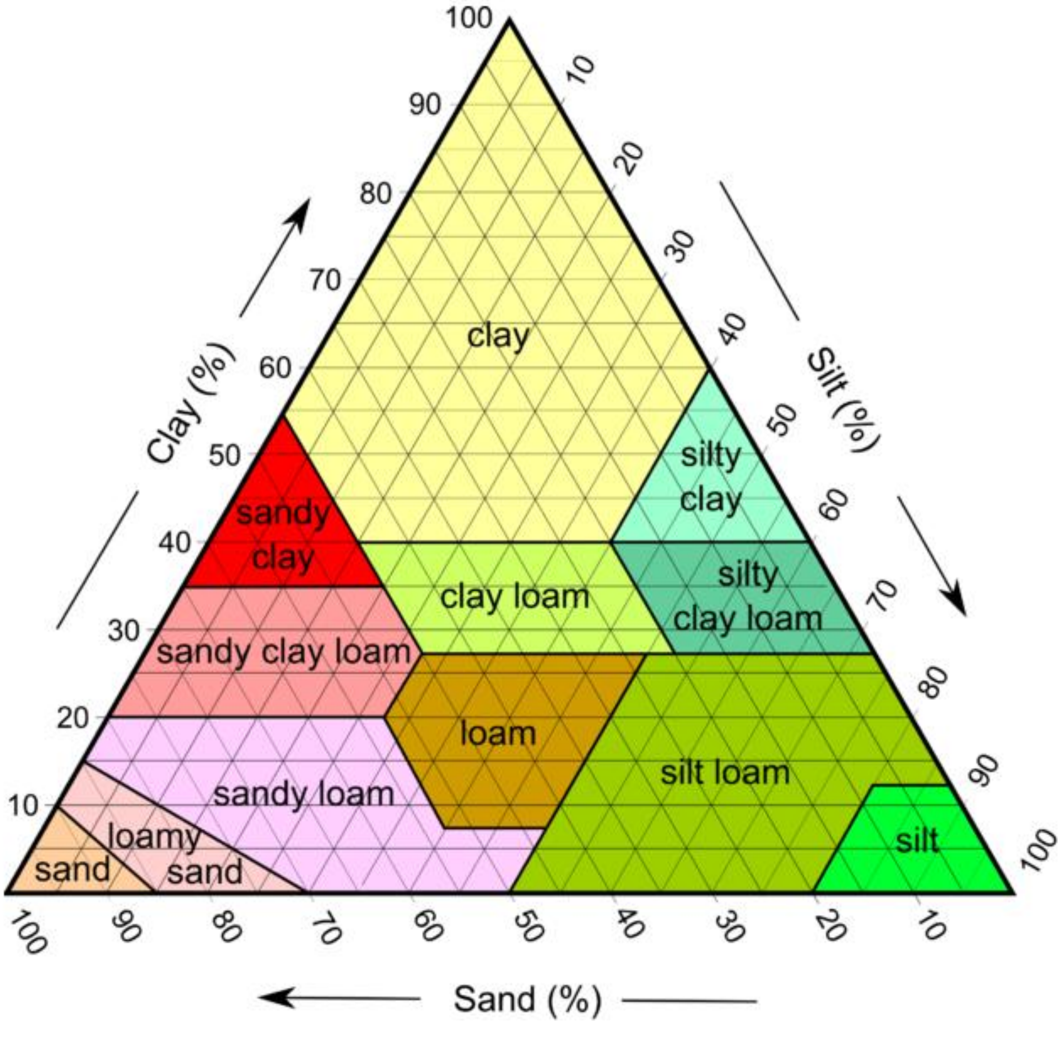

Figure 3. 65 Soil texture diagram (Adapted from USDA, 2014)

The PSD profile results were also used for the numerical modeling for the soil water characteristic curve (SWCC).

3.5.1.2 Dry Bulk Density

The dry bulk density aims to find out the substrate density under dry and natural stacking condition. The dry bulking density was determined according to the linear measurement method described in BS 1377-1:1990 (BSI, 1990).

The substrate specimens were dried at 105±1℃ for 24 hr in the oven (). After the specimens were cool down to room temperature, the bigger particles, which were together in the drying process, were crushed in the mortar. The crushed specimens were dried over night. Approximately 500g of prepared sample was weighed by the electronic scale (STARTORIUS, Model: 3200) and recorded as [$m_{specimen}$]. Because the dry bulking density of the potting soil was small, 150 g of potting soil sample, which occupied approximately 500 ml, was weighed for the experiment. The samples were transferred to a 1000 ml measuring cylinder. The opening of the cylinder was corked by rubber stopple. Then the cylinder was shaken thoroughly and turned to stand slowly to let the sample settle naturally to form an incline surface. The high and low volume graduations ([V_h], [V_l]) of the incline surface were recorded. The dry bulking density was calculated via Eq 3.14.

$$\rho_b = \frac{[m_{specimen}]}{0.5 \bullet ([V_h] + [V_l])} \qquad \text{(Eq 3. 14)}$$

The results of dry bulk density were used for the numeric modeling and porosity evaluation.

3.5.1.3 Particle Density

The analysis of particle density aims to further study the porosity, which is closely related to the available water for plant root uptake. The particle density (PD) was analysis fulfilled via the pyknometer (density bottle) method described in BS 1377-1:1990 (BSI, 1990).

The pyknometers were cleaned and dried at 105±1℃ for 3 hr in the oven. The prepared pyknometers were placed in the desiccator for cooling down to the room temperature. The empty pyknometers together with their stopper were weighed by the electronic scale (STARTORIUS, Model: 3200) and recorded as [m_{pykno}].

The substrate specimens were dried at 105±1℃ for 24 hr in the oven. After the specimens were cool down to room temperature, the bigger particles, which were together in the drying process, were crushed in the mortar. The crushed specimens were dried over night. Approximately 10 g of specimens, which had passed 2 mm sieves, were filled in the 50 mL pyknometers. Every substrate specimen was filled three pyknometers to carry out triplication tests. The pyknometers containing specimens were weighed by the aforementioned electronic scale and recorded as [m_1]. Distilled water was filled into the pyknometers along the inner surface till the water surface reached the half of the volume. The pyknometers were placed in the vacuum desiccator to allow small air bubbles, which entrapped within substrates, extracted under vacuum pressure (-60 kpa).

Figure 3. 66 Extraction of air bubbles in the substrates under vacuum pressure

After 60 min of air bubbles extraction, the pyknometers were filled up by air free distilled water and the stoppers were inserted. The neck of the stoppers was filled up with distilled water and the excessive water retained on the outside surface of the pyknometers was wiped carefully. The fully filled pyknometers were weighed again to obtain [m_{sw}].

Figure 3.67 Pyknometers saturated by distilled water

The pyknometers were emptied and were rinsed for three times using distilled water. The pyknometers were filled up with air-free distilled water and weighed again to obtain [m_w]. The particle densities of the substrates were calculated via the equation-3.69.

$$\rho_s = \frac{m_1 - m_{pykno}}{(m_w - m_{pykno}) - (m_{sw} - m_1)} \qquad \text{(Eq 3. 15)}$$

The results of particle density analysis were used for the calculation of porosities of the substrates together with the dry bulking densities.

3.5.1.4 Hydraulic Conductivity

The hydraulic conductivity experiment was conducted according to the ASTM-D5084-03. Sand and soil samples were taken by the soil sampler and vaseline was applied to the outer surface of the sampler to ensure water-tightness. The sampler then was placed in the Falling Head Permeability Cell (FHPC) and the excessive vaseline was erased. The upper and lower porous dishes were soaked in distilled water for 24 h and covered the sampling cylinders. The FHPC was assembled and connected to the stand pipe of diameter 5.0 mm. Water head not larger than 2.0 m above the specimen was applied as initial condition. The time for head drop for 50 cm was used to determine the hydraulic conductivity.

Figure 3. 67 Falling head permeability apparatus and the standpipes in the diameter of 1.5, 3.0 and 5.0 mm

3.5.2 Statistical Analysis for Particle Size Analysis

Statistical analysis for PSD was conducted according to a U.S. Geological Survey Marine Geology grain-size program (Folk, 1968; McHendrie 1988). The PSD data was transferred to phi units for applying the equations.

The phi unit (φ) transforms the millimeter to logarithm with the base of 2. The calculation is:

$$\phi = -\log_2 d \qquad \text{(Eq 3. 16)}$$

where d = grain diameter in mm.

"Median" - corresponds to the 50 percentile on a cumulative curve, where half the particles by weight are larger and half are smaller than the median. This parameter is measured in phi units.

Median size divides the particles into two half. 50% by weight is larger than the median size and the other 50% by weight are smaller. Median size is read from the cumulative PSD curve.

Mean size indicates the average particle size of a sample. The mean size is calculated by the following equation (Folk , 1968):

$$M_z = \frac{\phi 16 + \phi 50 + \phi 84}{3} \qquad \text{(Eq 3. 17)}$$

whereφ 16, φ 50, andφ 84 are the size at 16, 50, and 84 percent retention of the sample by weight. M_z is mean size in phi units.

Sorting is used to determine the variation of particle size of a sample by encompassing the most parts of size distribution from PSD curve. The inclusive graphic standard deviation is calculated by (Folk, 1968):

$$\sigma = \frac{\phi 84 - \phi 16}{4} + \frac{\phi 95 - \phi 5}{6.6} \qquad \text{(Eq 3. 18)}$$

where φ 84, φ 16, φ 95, and φ 5 are the phi values at 84, 16, 95, and 5 percentage retention, respectively.

Folk (1968) reported that the sorting value indicate the distribution of particle in various size of a sample. Table 3.2 shows the description for the sorting values.

Table 3. 2 Description for sorting values (Adapted from Folk, 1968)

Sorting Value	Indication
<0.350	Very well sorted
0.35-0.500	Well sorted
0.5-0.710	Moderately well sorted
0.71-1.00	Moderately sorted
1.00-2.00	Poorly sorted
2.00-4.00	Very poorly sorted
>4.00	Extremely poorly sorted

Skewness indicates the degree of a cumulative curve approaching to symmetry. Samples may exhibit the same mean size and sorting value. However, the PSD cumulative curve may show different degree of symmetry. The inclusive graphic skewness is calculated by (Folk, 1968):

$$sk = \frac{\phi 16 + \phi 84 - 2\phi 50}{2(\phi 84 - \phi 16)} + \frac{\phi 5 + \phi 95 - 2\phi 50}{2(\phi 95 - \phi 5)} \qquad \text{(Eq 3. 19)}$$

where the phi values have the same meaning as average size and sorting calculation.

Compared with the skewness calculation proposed by Inman (1952) and Trask (1950), the “tails” of the cumulative curve is included in the Eq 3.19 together with the central portion. The classification of the meaning of skewness is listed in Table 3.3.

Table 3. 3 Description for skewness values (Adapted from Folk, 1968)

Skewness Value	Indication
0.30 to 1.00	Strongly fine-skewed
0.10 to 0.30	Fine-skewed
0.00	Symmetrical
+0.10 to -0.10	Nearly symmetrical
-0.10 to -0.30	Coarse-skewed
-0.30 to -1.00	Strongly coarse-skewed

Kurtosis describes the peakedness of the cumulative curve. The calculation of kurtosis is (Folk, 1968):

$$k_g = \frac{\phi 95 - \phi 5}{2.44(\phi 75 - \phi 25)} \qquad \text{(Eq 3. 20)}$$

where the phi values represent the same meaning as those for sorting and skewness calculaiton.

The values and the indication of kurtosis are summarized in Table 3.4.

Table 3. 4 Description for kurtosis values (Adapted from Folk, 1968)

Kurtosis value	Indication
>1.00	Leptokurtic curves
<1.00	Platykurtic curves
1.00	Normal curves

A normal Gaussian distribution exhibits a kurtosis of 1.00. It indicates the sorting in the tails has same value as that in the central portion. If the PSD cumulative curve shows better sorting in the central part than the tails, the curve is classified as excessively peaked or leptokurtic. On the other hand, the curve is classified as flat peaked or platykurtic if the sample curve is better sorted in the tails than central portion.

3.5.3 Chemical Analysis

All the macro- and micro-nutrients examinations were according to the APHA standard methods.

The extracts from the arid sand, Eco-Soils and potting soils are used to determine NO_3^-, NO_2^-, NH_4^+, PO_4^{3-} and K^+ as macro-nutrient contents

The NO_3^- was determined by cadmium reduction method (4500-NO_3-E). The NO_2^- and N were determined by Colorimetric Method (4500-NO_2- B) and ammonia ion selective electrode method (4500-NH_3-D). The PO_4^{3-} was detected by ascorbic acid method (4500-P-E) and K^+ by potassium ion selective electrode method (3500-K-C).

1 g of dried substrate samples were digested by 20 ml concentrated nitric acid at 90℃ and then diluted to be 250 ml. The Zn^{2+}, Mn^{2+}, $Pb^{2+}$and Cr^{6+} in the extracts were analyzed by atomic absorption spectrum methods.

4. Results and Discussions

This section illustrates the studies of hydraulic properties of Eco-Soil, soil water retention curve, growing capabilities and the rainwater retentions. The properties and performances of Eco-Soils were compared with arid sand, commercial potting soil and other related literature data to reveal the enhancement of anti-desertification abilities brought by Eco-Soils.

4.1 Hydraulic Properties for Eco-Soils

Because Eco-Soil is a novel growing medium, the essential properties including the constitution, bulk density, particle density, porosity, hydraulic conductivity, particle size distribution and evaporation rate were investigate to obtain the physical data for further applications.

4.1.1 Composition of Eco-Soils and the Eco-Soil Mixing Model

To investigate the properties of Eco-Soils, the constitution is significantly important. The Eco-Soils are of various mixing ratios, therefore, a numerical way to express the constitution of Eco-Soil is necessary to find out the optimal selection for various purposes.

The arid sand is mixed with activated sludge based on the volumetric ratios from 100:0 to 10:90. The sludge volumetric ratios, weight ratios, sand sludge weight ratios

(SSWR), moisture contents and volatile solid contents under various sand sludge volumetric ratios (SSVR) are shown in Table 4.1.

Table 4. 1 Average properties of Eco-Soils under various SSVR

SSVR (Vol. Sand/ Vol. Sludge)	100:0	90:10	80:20	70:30	60:40	50:50	40:60	30:70	20:80	10:90
Sludge Volumetric Ratio (Vol. Sludge %)	0	10	20	30	40	50	60	70	80	90
SSWR (Wt. Sand/Wt. Sludge)	100:0	99.74: 0.26	99.44: 0.56	99.04: 0.96	98.52: 1.48	97.75: 2.25	96.80: 3.20	95.08: 4.92	92.04: 7.96	83.33: 16.67
Sludge Weight Ratio (Wt. Sludge %)	0	0.26	0.56	0.96	1.48	2.25	3.20	4.92	7.96	16.67
Moisture Cont. (Wt. %)	0.25	8.44	14.39	21.63	30.17	39.30	47.65	58.51	69.73	83.06
Volatile Solid (Wt. %)	0.24	0.46	0.89	1.01	1.46	2.00	2.27	3.99	6.21	13.32

The Sand Sludge Volumetric Ratio (SSVR) is defined as the volumetric ratio for arid and thickened activated sludge in mixing stage. As the SSVR drops from 100:0 to 10:90, the sludge weight ratio increases from 0 to 16.67 wt. %. Even though the volumetric ratio for the sludge under SSVR 10:90 is large, the dried weight percentage in the mixture is low due to high moisture contents of thickened sludge and high bulk density of arid sand (1277.47 kg/m^3). In addition, the moisture for the 10 mixtures increases from 0.25 to 83.06 wt.% and the volatile solid content (Organic Matter) also increases from 0.24 to 13.32 wt.%. The findings show that the moisture is mainly contributed by activated sludge.

4.1.1.1 Relation between SSVR and SSWR

The relation of SSVR and SSWR can be expressed by the relation of Sludge Volume Content ([$SLC_{vol.\%}$]) and Sludge Weight Content ([$SLC_{wt.\%}$]) in Eq 4.1.

$$\frac{1}{[SLC_{wt.\%}]}=\frac{[BD_{Sa}]}{[MLSS]}\bullet\frac{1}{[SLC_{vol.\%}]}+\left(1-\frac{[BD_{Sa}]}{[MLSS]}\right) \quad \text{(Eq 4. 1)}$$

or

$$[SLC_{wt.\%}]=\frac{1}{\frac{[BD_{Sa}]}{[MLSS]}\bullet\frac{1}{[SLC_{vol.\%}]}+\left(1-\frac{[BD_{Sa}]}{[MLSS]}\right)} \quad \text{(Eq 4. 2)}$$

where $[SLC_{wt.\%}]$ stands for the sludge weight ratio of the mixture, g sludge/g mixture;

$[SLC_{vol.\%}]$ stands for the sludge volume ratio of in the mixing, m^3 sludge/(m^3 sludge + m^3 sand);

[MLSS] stands for the mixed liquor suspended solid concentration of the sludge, kg/m^3;

$[BD_{Sa}]$ stands for the dry bulking density of the sand, kg/m^3.

In this study, the average [MLSS] of sludge and [BD] of sand are analyzed to be 30.274 g/L (30.274 kg/m^3) and 1272.83 kg/m^3, respectively. Eq 4.2 is written to be:

$$\frac{1}{[SLC_{wt.\%}]}=\frac{42.044}{[SLC_{vol.\%}]}-41.044 \quad \text{(Eq 4. 3)}$$

or

$$[SLC_{wt.\%}]=\frac{1}{\frac{42.044}{[SLC_{vol.\%}]}-41.044} \quad \text{(Eq 4. 4)}$$

The relation of $\frac{1}{[SLC_{wt.\%}]}$ and $\frac{1}{[SLC_{vol.\%}]}$ is plotted in Figure 4.1. The solid line represents the curve of the equation 4.3 while the solid diamond points represent the measured values of the $\frac{1}{[SLC_{wt.\%}]}$.

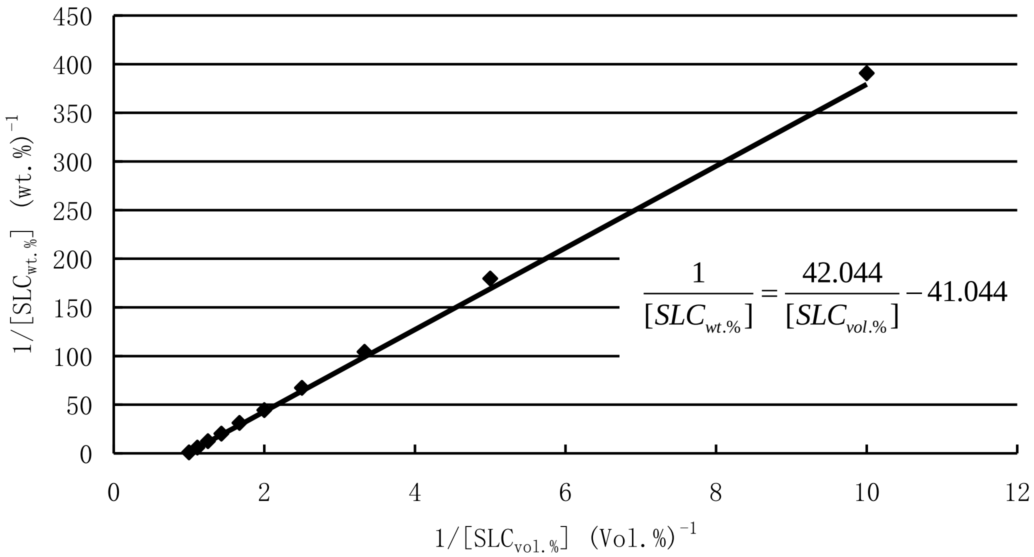

Figure 4. 1 Calibration curve between volume ratio and weight ratio of sludge in the mixtures.

Eq 4.1 is derived from the calculation of sludge weight ratio from the mixture and expressed in Eq 4.5.

$$[SLC_{wt.\%}] = \frac{[M_{Sl}]}{[M_{Sl}]+[M_{Sa}]} = \frac{[SLC_{vol.\%}]\bullet[MLSS]}{[SLC_{vol.\%}]\bullet[MLSS]+[SAC_{vol.\%}]\bullet[BD_{Sa}]} \qquad \text{(Eq 4. 5)}$$

Where $[M_{Sl}]$ and $[M_{Sa}]$ stand for the weight of sludge and sand in the mixture respectively, kg;

$[SAC_{vol.\%}]$ stands for the sand volume ratio in mixing, m^3 sand/(m^3 sludge + m^3 sand);

Because $\left[SAC_{vol.\%}\right]=1-\left[SLC_{vol.\%}\right]$

The equation 4.5 is written as

$$[SLC_{wt.\%}]=\frac{[SLC_{vol.\%}]\bullet[MLSS]}{[SLC_{vol.\%}]\bullet[MLSS]+(1-[SLC_{vol.\%}])\bullet[BD_{Sa}]} \qquad \text{(Eq 4. 6)}$$

If the equation 4.6 takes power (-1) on the both sides, the equation 4.7 is obtained as follow.

$$\left([SLC_{wt.\%}]\right)^{-1}=\left(\frac{[SLC_{vol.\%}]\bullet[MLSS]}{[SLC_{vol.\%}]\bullet[MLSS]+(1-[SLC_{vol.\%}])\bullet[BD_{Sa}]}\right)^{-1}$$

$$\frac{1}{[SLC_{wt.\%}]}=\frac{[SLC_{vol.\%}]\bullet[MLSS]+(1-[SLC_{vol.\%}])\bullet[BD_{Sa}]}{[SLC_{vol.\%}]\bullet[MLSS]}$$

$$\frac{1}{[SLC_{wt.\%}]}=\frac{[BD_{Sa}]}{[MLSS]}\bullet\frac{1}{[SLC_{vol.\%}]}+\left(1-\frac{[BD_{Sa}]}{[MLSS]}\right) \qquad \text{(Eq 4. 7)}$$

Eq 4.1 indicates strong correlation with the analyzed results and exhibits the R^2 up to 99.99% (Figure 4.1).

4.1.1.2 Relation between Organic Content and SSWR or SSVR

The sludge weight ratio appears to be linearly proportional to overall organic content of the mixtures. Figure 4.2 shows the relation between the organic content and sludge weight ratio.

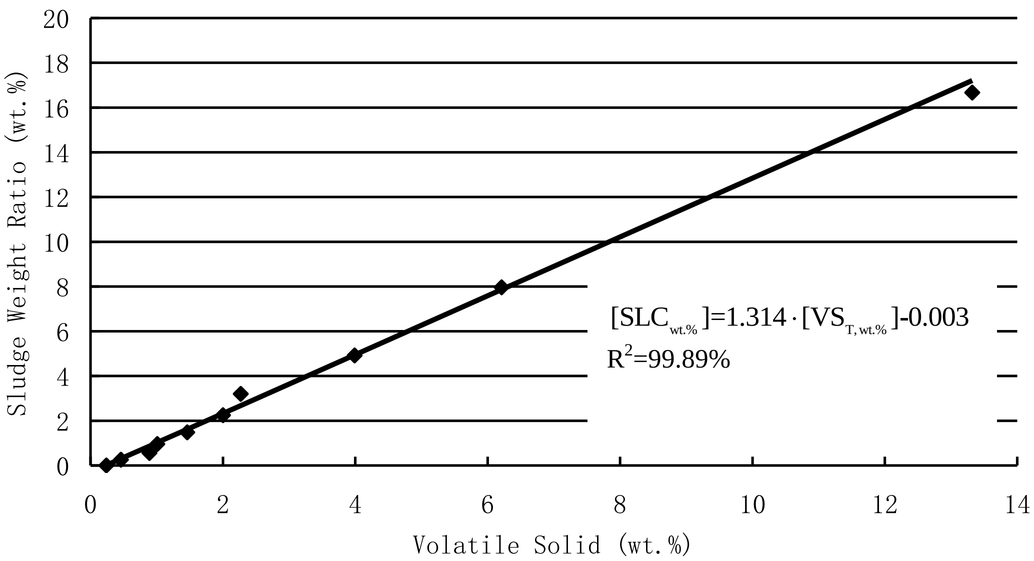

Figure 4. 2 Calibration curve between mixture total organic content and sludge weight ratio.

The linear relation between total organic content and sludge weight ratio is represented in Eq 4.8.

$$[SLC_{wt.\%}]=\frac{[VS_{T,wt.\%}]}{\Delta[VS]}-\frac{[VS_{Sa,wt.\%}]}{\Delta[VS]} \qquad \text{(Eq 4. 8)}$$

where $[SLC_{wt.\%}]$ stands for the sludge weight ratio of the mixture, g sludge/g mixture;

[$VS_{T,wt.\%}$] is the total volatile sold of the mixture, g organic content/ g mixture;

[$VS_{Sa,wt.\%}$] is the organic content of the sand sample, g organic content/ g mixture;

Δ [VS] is the organic content deference between sludge and sand, g volatile solid / g mixture. In normal circumstance, the former is larger.

Eq 4.8 is derived based on mass balance and is express by following equation:

$$[VS_{T,wt.\%}] = \frac{[VS_{Sa,wt.\%}]\cdot[M_{Sa}] + [VS_{Sl,wt.\%}]\cdot[M_{Sl}]}{[M_{Sa}] + [M_{Sl}]} \qquad \text{(Eq 4. 9)}$$

where [$VS_{Sl,wt.\%}$] is the volatile solid of the sludge sample, g volatile solid/ g mixture;

[M_{Sa}] and [M_{Sl}] are the absolute mass of sand and sludge in the mixture, respectively, g.

Let $[VS_{Sl,wt.\%}]=[VS_{Sa,wt.\%}]+\Delta[VS]$ (Eq 4. 10)

Eq 4.9 becomes,

$$[VS_{T,wt.\%}] = \frac{[VS_{Sa,wt.\%}]\cdot[M_{Sa}] + ([VS_{Sa,wt.\%}]+\Delta[VS])\cdot[M_{Sl}]}{[M_{Sa}]+[M_{Sl}]}$$
$$= \frac{[VS_{Sa,wt.\%}]\cdot([M_{Sa}]+[M_{Sl}])+\Delta[VS]\cdot[M_{Sl}]}{[M_{Sa}]+[M_{Sl}]}$$
$$= [VS_{Sa,wt.\%}]+\Delta[VS]\cdot\frac{[M_{Sl}]}{[M_{Sa}]+[M_{Sl}]} \qquad \text{(Eq 4. 11)}$$

Since $$\frac{[M_{Sl}]}{[M_{Sa}]+[M_{Sl}]} = [SLC_{wt.\%}] \qquad \text{(Eq 4. 12)}$$

Then $$[VS_{T,wt.\%}] = [VS_{Sa,wt.\%}]+\Delta[VS]\cdot[SLC_{wt.\%}] \qquad \text{(Eq 4. 13)}$$

After transforming Eq 4.11, Eq 4.13 is finally obtained.

The volatile solid (VS) of sand and sludge are able to be obtained by experiment, therefore, the sludge weight ratio of the mixed sample can be calculated from the total volatile solid content.

As the average VS for the sand and sludge in this experiment are 0.24% and 76.36% respectively, the sludge weight ratio (Eq 4.8) becomes:

$$[SLC_{wt.\%}]=1.314\cdot[VS_{T,wt.\%}]-0.003 \qquad \text{(Eq 4. 13a)}$$

The calibration curve in Figure 4.2 indicates strong linear with the actual value according to the correlation coefficient up to 99.89%.

If the Eq 4.13a is inserted in to Eq 4.3, the relation between the organic content of Eco-Soils and SSVR is obtained.

$$\frac{1}{\frac{42.044}{[SLC_{vol.\%}]}-41.044}=1.314\cdot[VS_{T,wt.\%}]-0.003$$

(Eq 4. 14)

Then it is written as

$$[SLC_{vol.\%}]=\frac{42.044\bullet\left(1.314\bullet[VS_{T,wt.\%}]-0.003\right)}{1+41.044\bullet\left(1.314\bullet[VS_{T,wt.\%}]-0.003\right)}$$
$$=\frac{55.246\bullet[VS_{T,wt.\%}]-0.126}{53.932\bullet[VS_{T,wt.\%}]+0.877}$$

(Eq 4. 15)

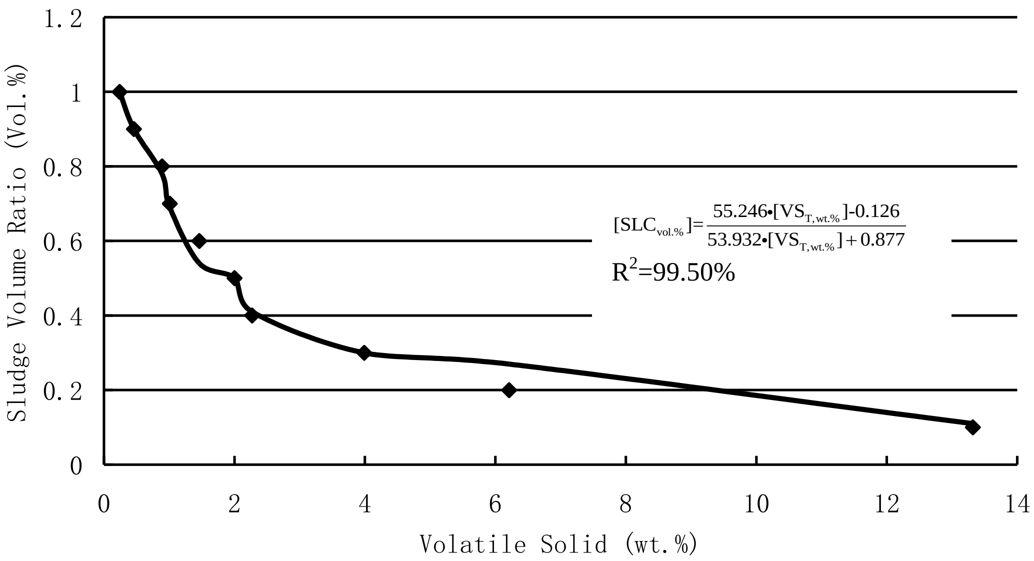

Figure 4. 3 Curve between mixture total organic content and sludge volumetric ratio

The sand and sludge mixture of the SSVR 100:0, 80:20, 60:40, 40:60 and 60:80 are chosen for carrying out the following study since the differences among them are suitable. Mixture under SSVR 0:100 is not used for the experiment because it is completely sludge and less useful for observing the effects on anti-desertification.

The equations derived in this section are named as Eco-Soil Mixing Model. Eq 4.1

and Eq 4.15 are able to build up the relation among the sludge volumetric content, sludge weight content and volatile solid content (organic matter or organic content). In the following sections, the sludge weight content of Eco-Soil is frequently used for finding relation with other parameters.

4.1.2 Dry Bulk Density

Dry bulk density (BD) shows the density of the eco-soil in natural drying process and is important for calculating porosity, saturated moisture content, volumetric moisture content and numerical and computational simulation.

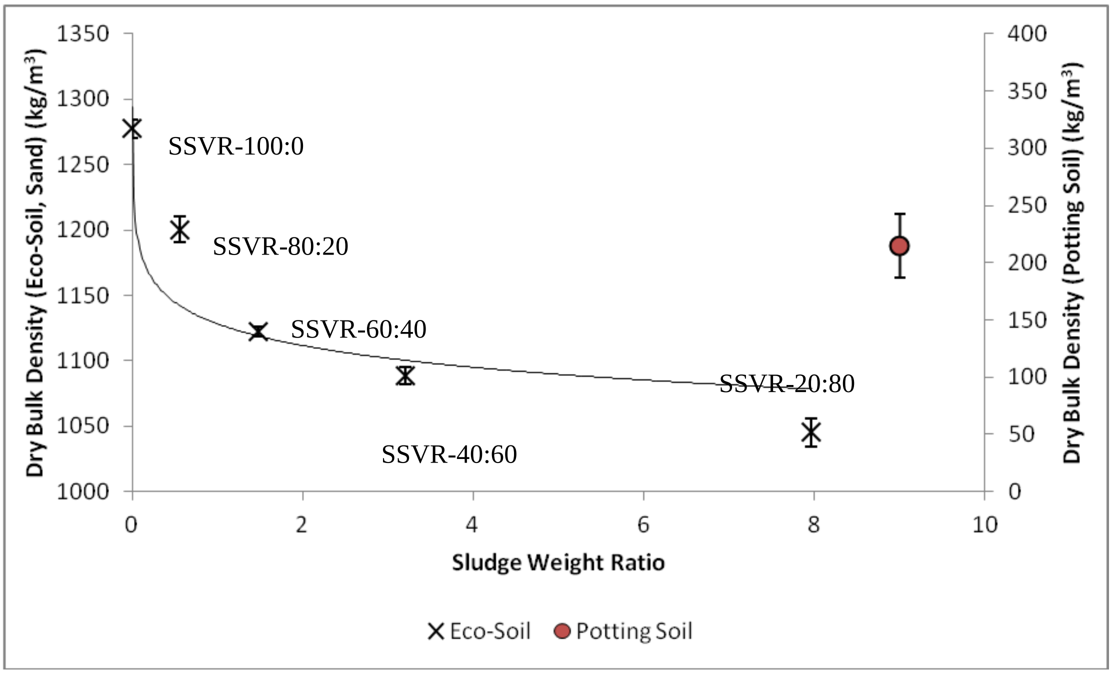

Figure 4. 4 Dry bulk density of arid sand, Eco-Soil and potting soil

As the addition of sludge to the simulated sand, the dry bulk density of the Eco-Soil drops from 1200.39 to 1045.16 kg/m^3 and compared with 1277.47 kg/m^3 of arid sand.

The decreasing trend is shown to be logarithmic distributed with a correlation coefficient of 0.9661. Because the density of sludge is low, the BD of Eco-Soil exhibits a decreasing trend when the sludge volumetric content increases. However, the BD of the sand is large as compared with activated sludge, hence the minimum Eco-Soil BD (SSVR 20:80) still has an average value of 1048.50 kg/m^3. This value is still 4.87 times as that of potting soil, which is tested to be averagely 215.08 kg/m^3. Larger BD density can bring the advantages in the windy and arid area, because the materials with low BD, such as potting soil, are readily blown away under strong winds. In addition, the BD value affects site productivity and is an indicator of soil compaction and porosity (Suuster *et al*., 2011). Together with the Particle Density (PD), the BD is also used for calculating the porosity of the Eco-Soil.

4.1.3 Particle Density

The particle density (PD) of soil represents one of the soil's basic physical properties and depends on the compositions of both the mineral and the organic soil components (Rühlmann *et al*., 2006). The PD is also an important parameter to evaluate the soil porosity together with the BD. The PD analysis results are shown in Figure 4.5.

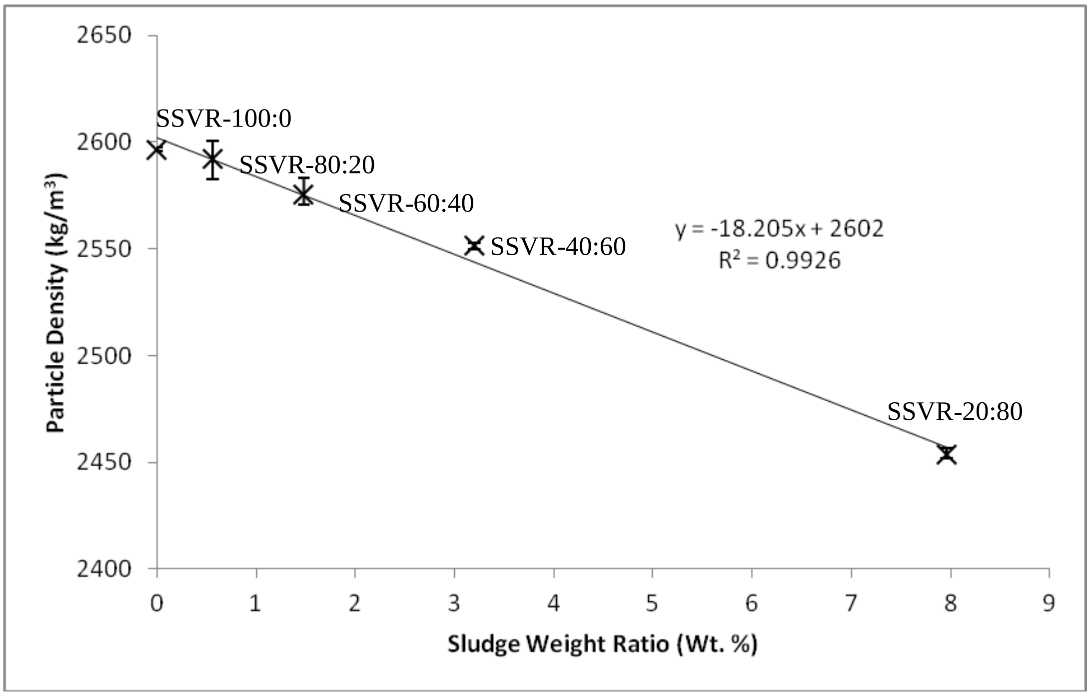

Figure 4. 5 Particle density of Eco-Soil with various sludge contents.

Figure 4.5 shows that the particle densities of Eco-Soil decreas from 2596.57±0.78 kg/m^3 to 2453.76±2.43 kg/m^3 while the sludge weight contents ($[SLC_{wt,\%}]$) increase from 0 to 7.96 %. The results reveal that the PDs of Eco-Soil decrease due to the addition of activated sludge. However, the lowest PD of Eco-Soil still exhibits a high value of 2453.76 kg/m^3 when the sludge weight content reaches 7.96 wt. %, which is corresponding to a SSVR of 20:80. It is because the arid sand serves major contents of the mass in the mixtures. Large PD of Eco-Soil also offers advantages for reducing the mobility of the growing medium in windy condition. The potting soil in this study gives no PD result because the substrate appeared to be floating on the water surface when filling water into the pyknometers. Therefore, the PD of this potting soil can not be estimated by the BS-1377 1990 methods.

4.1.4 Porosity

Porosity is one of the important primary soil properties for evaluating the soil water retention ability and plant available water amount. The total porosity for each Eco-Soil sample is determined by calculation from the particle density and dry bulk density and is shown in Table 4.2.

Table 4. 2 Particle density, dry bulk density and average total porosity under various SSVR ratios

SSVR	Particle Density (kg/m^3)	Dry Bulk Density (kg/m^3)	Average Total Porosity (%)
100:0	2596.57±0.78	1277.47±7.32	50.80
80:20	2591.91±9.06	1200.39±10.00	53.69
60:40	2575.72±6.60	1122.20±3.55	56.43
40:60	2551.51±1.40	1088.31±6.42	57.35
20:80	2453.76±2.43	1045.16±10.54	57.41

The average total porosity exhibits an increasing trend from 50.80 % to 57.41 % when the SSVRs reduce from 100:0 to 20:80. The results of the porosities agree with that the porosity of soil typically decreases as particle size increases because the fine particle offers more porosities than the large one. However, there pores are fine pores. Table 4.3 lists typical porosity values for some materials such as fine sand and clay. Before amendment by activated sludge the arid sand (SSVR 100:0) is found to have an average total porosity value of 50.80 % which was within the upper bound of that in the find sand range (25~53%). After the introduction of activated sludge the

Eco-Soils exhibit porosities higher than 53% and comparable to the upper bound of the range of clay.

Table 4. 3 Representative Porosity Values (Adapted from McWorter and Sunada, 1977)

	Total Porosity		Effective Porosity	
Material	Range	Arithmetic Mean	Range	Arithmetic Mean
Sedimentary material				
Sandstone (fine)	-	-	0.02 - 0.40	0.21
Sandstone (medium)	0.14 - 0.49	0.34	0.12 - 0.41	0.27
Siltstone	0.21 - 0.41	0.35	0.01 - 0.33	0.12
Sand (fine)	0.25 - 0.53	0.43	0.01 - 0.46	0.33
Sand (medium)	-	-	0.16 - 0.46	0.32
Sand (coarse)	0.31 - 0.46	0.39	0.18 - 0.43	0.30
Gravel (fine)	0.25 - 0.38	0.34	0.13 - 0.40	0.28
Gravel (medium)	-	-	0.17 - 0.44	0.24
Gravel (coarse)	0.24 - 0.36	0.28	0.13 - 0.25	0.21
Silt	0.34 - 0.51	0.45	0.01 - 0.39	0.20
Clay	0.34 - 0.57	0.42	0.01 - 0.18	0.06
Limestone	0.07 - 0.56	0.30	~0 - 0.36	0.14
Wind-laid material				
Loess	-	-	0.14 - 0.22	0.18
Eolian sand	-	-	0.32 - 0.47	0.38
Tuff	-	-	0.02 - 0.47	0.21
Igneous rock				
Weathered granite	0.34 - 0.57	0.45	-	-
Weathered gabbro	0.42 - 0.45	0.43	-	-
Basalt	0.03 - 0.35	0.17	-	-
Metamorphic rock				
Schist	0.04 - 0.49	0.38	0.22 - 0.33	0.26

High porosity offers appropriate drainage and air ventilation for the growing medium. The surface tillage layer usually has porosity larger than 50% (Yi, 2009). From this point of view, the Eco-Soils offer promising growing abilities for vegetation due to higher porosity. In addition, porosity is also related to the hydraulic conductivity, the medium with higher porosity normally exhibits higher hydraulic conductivity.

However, there are many complications for this relation therefore it is not a linear proportional distribution.

4.1.5 Particle Size Distribution

Another important primary soil property is particle size distribution (PSD) which has significance in understanding the physical and chemical characteristics. The PSD also affects the strength and load-bearing properties of rocks and soils. This section aims to analyze the water infiltration and retention for the Eco-Soil, therefore the PSD is significantly important. The PSD of the arid sand, Eco-Soil and potting soil are shown in Figure 4.6.

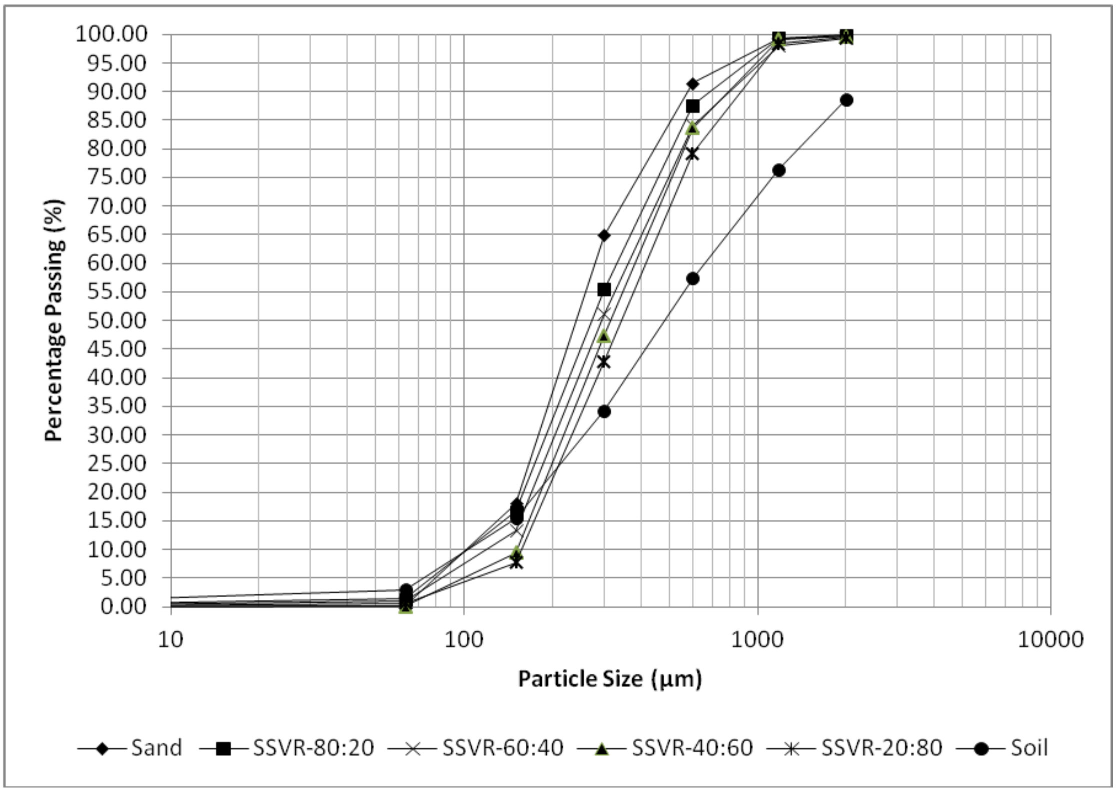

Figure 4. 6 Particle size distribution profile of arid sand, Eco-Soils and potting soil

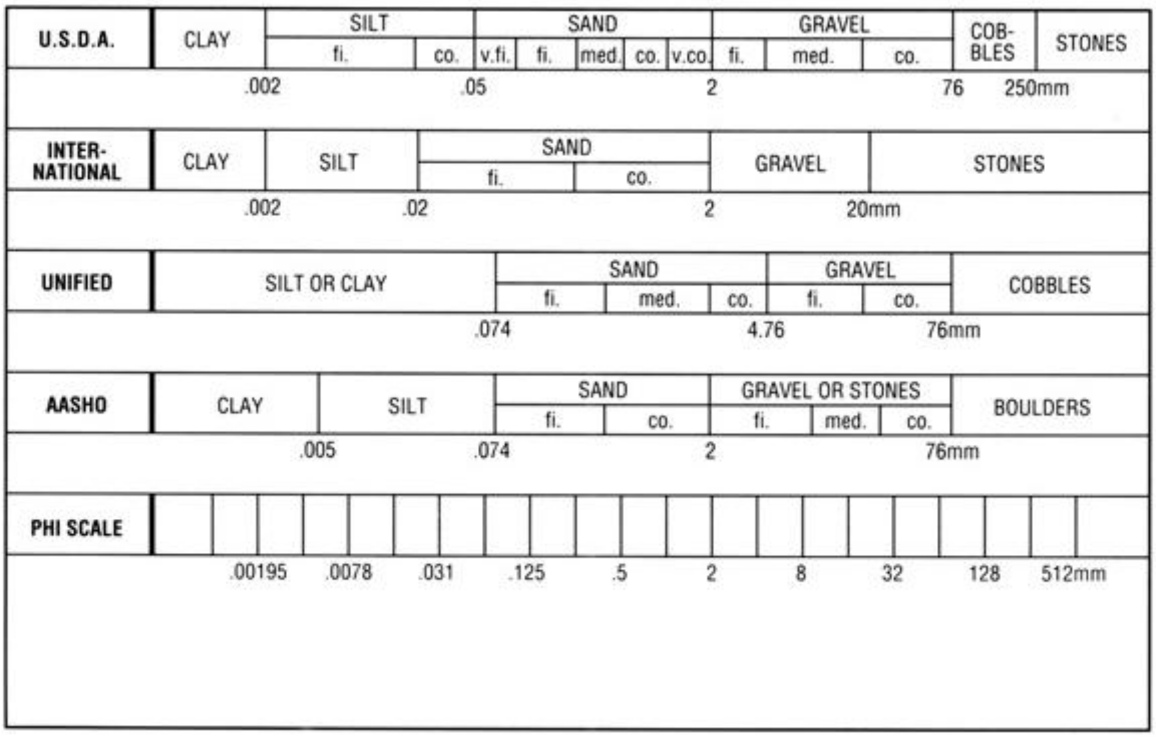

Figure 4. 7 Particle size classification in five different standards

Figure 4.7 shows that different standards or organizations have different definitions of the categories of the materials. According to the United Stated Department of Agriculture, the sand material is classified as very coarse, coarse, medium, fine and very fine categories.

Table 4. 4 Particle size distribution analysis results

SSVR		100:0	80:20	60:40	40:60	20:80	Soil
D5 (mm)		0.08	0.08	0.08	0.10	0.11	0.07
D16 (mm)		0.14	0.15	0.16	0.17	0.18	0.16
D25 (mm)		0.17	0.18	0.19	0.20	0.21	0.21
D50 (mm)		0.24	0.27	0.30	0.32	0.35	0.58
D75 (mm)		0.39	0.46	0.49	0.51	0.55	1.20
D84 (mm)		0.49	0.56	0.63	0.64	0.70	1.70
D95 (mm)		0.80	0.90	1.00	1.05	1.10	2.00
Median (φ)		2.059	1.889	1.761	1.644	1.515	0.786
Median (mm)		0.240	0.270	0.295	0.320	0.350	0.580
Mean (φ)		0.020	0.018	0.017	0.016	0.015	0.009
Mean (mm)		0.986	0.987	0.988	0.989	0.990	0.994
Sorting		-0.010	-0.010	-0.010	-0.010	-0.010	-0.016
Skewness		0.093	0.049	0.044	0.028	0.008	-0.179
Kurtosis		1.153	1.063	1.077	1.029	0.980	0.786
Sand	Very Coase (wt.%)	2.5	4.5	5.0	5.0	6.0	27.5
	Coase (wt.%)	12.5	15.5	21.0	20.0	24.0	21.0
	Medium (wt.%)	32.0	35.0	34.0	39.0	38.0	22.0
	Fine (wt.%)	43.5	35.5	34.5	28.5	27.0	25.0
	Very Fine (wt.%)	8.3	9.4	4.6	6.7	4.5	1.7
Silt (wt.%)		1.2	1.2	0.1	0.9	0.8	0.5

Table 4.4 lists the analysis results of the PSD curves for arid sand, Eco-soil and potting soil samples. The median sizes are read from the PSD curves for 50% retention of the particles and are expressed in phi sizes. The phi particle size is able to be transferred to mm by taking the minus value and exponential on the base of 2 (Eq 3.16). Table 4.4 shows that the median sizes of the Eco-Soil increase from 0.240 to 0.350 mm, reflecting the increasing division particle size. The cumulative weights of the particles under and above the median size are equal. For the arid sand (SSVR 100:0), the cumulative weight of particles small than 0.240 mm is equal to that above this size. As the introduction of activated sludge, the weight fraction of sand is reduced. The activated sludge is small in particle size and exhibits low particle density. The cumulative weights of fine particles for the Eco-Soils reduce then the division sizes for equal weight percentile increase by 0.350 mm.

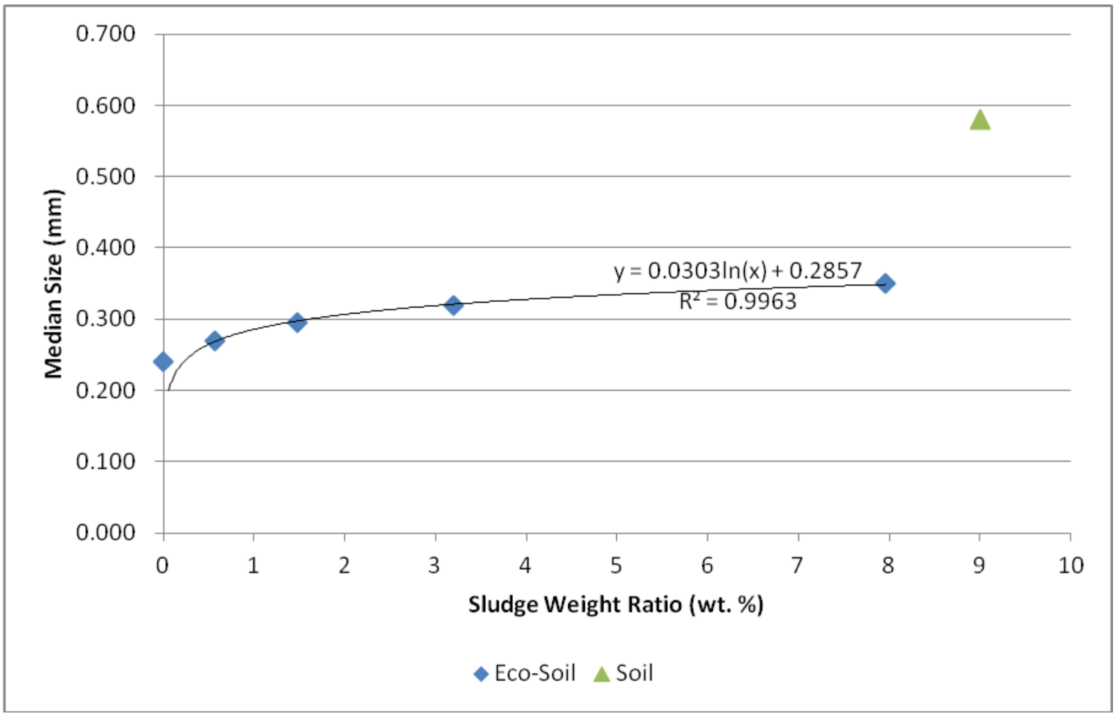

Figure 4. 8 Median sizes of arid sand, Eco-Soil and commercial soil

If the median sizes of Eco-Soil are plotted against sludge weight content, the curve is shown to follow logarithmic distribution. The relation between these two factors are expressed as:

$$[d_{median}] = 0.0303\ln[SLC_{wt.\%}] + 0.2857 \qquad \text{(Eq 4. 16)}$$

The correlated coefficient for fitting the experimental data is shown to be 0.9963. By used of the equation, the median size of the Eco-Soil can be predicted within the range of SSVR 100:0 ~ 20:80. Table 4.3 and Figure 4.5 also show the median size of commercial soil reaches 0.580 mm. This is higher than arid sand and Eco-Soil, because the potting soil is composed by plant tissues, peat and wood pieces, which are light in weight, high in porous and large in size. The fine particles of soil have lower density compared to arid sand and Eco-Soil. As a result, the median size of soil exhibits a higher value.

The mean size indicates the average particle size and is calculated according to Folk (1968) in phi size then transferred to mm.

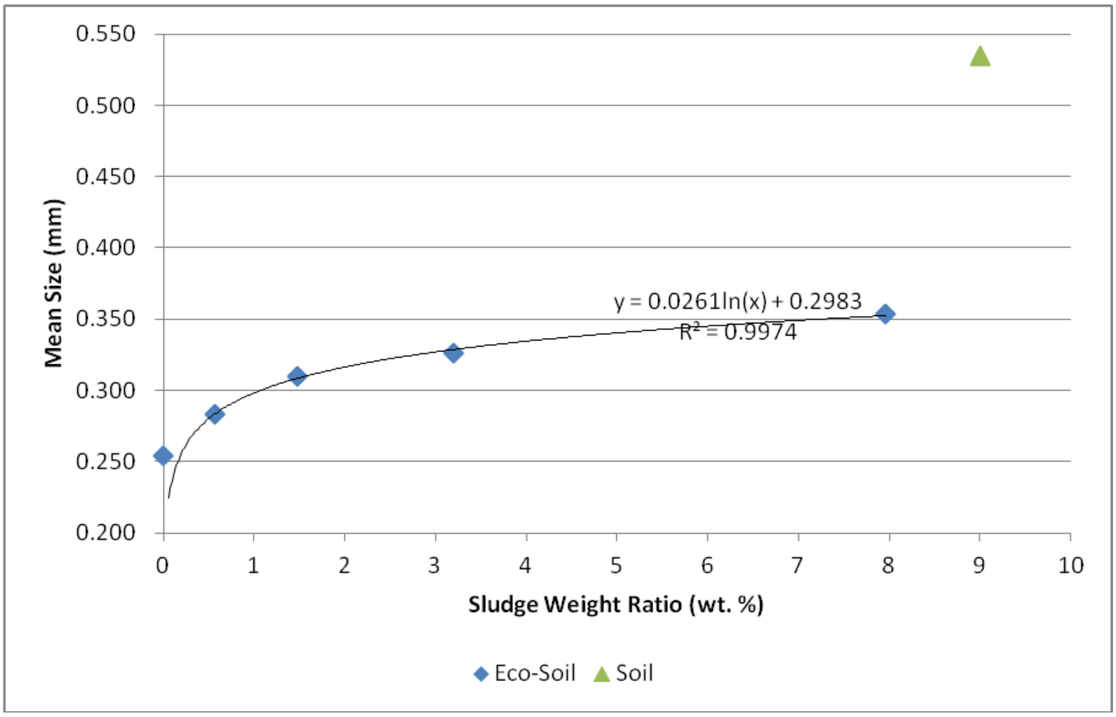

Figure 4. 9 Mean sizes of arid sand, Eco-Soil and potting soil.

Table 4.4 and Figure 4.9 show the mean sizes of arid sand, Eco-Soil and commercial soil. As the same trend of median size results, the mean sizes of Eco-Soil increase and follow logarithmic distribution and can be expressed by equation:

$$[d_{mean}] = 0.0261\ln[SLC_{wt.\%}] + 0.2983 \qquad \text{(Eq 4. 17)}$$

The mean size is calculated by the algebraic average of d_{16}, d_{50} and d_{84}, which stands for the particle size for 16, 50 and 84 % passing by weight. The mean sizes of the samples are affected by the fraction of activated sludge and increase from 0.254 to 0.353 mm. The influence from the activated sludge is large and the increment is about 39.0% from arid sand sample. Compared to commercial potting soil, the mean size is 0.535 mm, which is much larger than the arid sand and Eco-Soil (approximately 2 times), because the particles in the commercial soil are large in volume but low in weight. The results for mean sizes analysis is similar to median sizes, but the mean sizes is better to describe the average particle size for the samples.

From Table 4.4, the D_{50}, which represents the division particle diameter for 50:50 by weight of the cumulative curve, for the substrate samples increased from 0.24 to 0.4 mm for Eco-soil SSVR 100:0 to 20:80. The higher D_{50} value means more weight fraction of the diameter under the D_{50}. In other words, the introduction of activated sludge increased the fine particles in the substrates and also the porosities.

Skewness indicates the degrees of symmetry for the particle size distribution of a substrate. A symmetrical curve has a skewness of 0.00 while the positive skewness number implies the particles skews to the fine sizes, vice versa. From Table 4.3, the skewness of the arid sand and Eco-Soil reduce from 0.093 to 0.008. The results show that the arid sand skews to fine particles. With the increasing fraction of activated sludge in the Eco-Soil, the PSD appears to be more symmetrical and skews to the coarse fraction. The activated sludge particle size is finer than sand particles when the sludge is wet. However, when the activated sludge is dried, the sludge trends to associate the particles, especially the fine particles in the arid sand, to form larger particles. Even though the dried Eco-Soil samples are smashed by grinder, most of the fine particles (<0.150mm) are still adhered by the dried sludge (Figure 4.10). This phenomenon also means the adhesive effects due to activated sludge are strong to hold the shape against a certain shear stress.

Figure 4. 10 Fine particles adhered by activated sludge to form large particles

This effect benefits the substrates in the desert. As a general consideration, the fine particles are readily blown up or away by winds. By the adhesive effects from activated sludge, the fine particles in Eco-Soil become higher in density to withstand the strong wind.

Soil skews to the coarse fraction and exhibits a skewness number of -0.179. The reason is because the commercial potting soil in this study is composed by plant tissues, peat and porous materials. The PSD profile of potting soil is therefore shown to be coarse-skewed.

Kurtosis results for the substrates range from 1.153 to 0.980. According to Folk's (1968) formula, the curves with normal Gaussian distribution result in kurtosis equal to 1.00 while leptokurtic curves are larger than 1.00 and platykurtic curves are small than 1.00. The arid sand exhibits a kurtosis of 1.153 in this study and the particle sizes concentrate between 0.150 to 0.600 mm. With the introduction of activated sludge, the sludge reduces the weight fraction of the fine particles in the cumulative curve. In addition, the activated sludge also combines fine particles to form large ones then increase weight fraction of large particles in the curves. The kurtosis results of the PSD profiles for Eco-Soils therefore reduce from 1.063 to 0.980, in other word, the curve for individual particle size distribution changes from leptokurtic to platykurtic.

The bottom of PSD data for the samples in Table 4.4 also shows the weight percentage of various particle sizes according to USDA's classification. Referred to soil texture diagram (Figure 3.65), the arid sand and Eco-Soil are classified as sand due to very low silt content. Along with the increasing introduction of activated sludge, the silt content shows a decreasing trend. The reason is the adhesive effect from the sludge. The fine particles are associated by the sludge and are hardly broken under strong shear stress.

4.1.6 Field Capacity

Field capacity quantifies the amount of water retained in growing media when the excessive water drains away by gravity after irrigation. The porosity and saturate water content of the growing media indicate the maximum abilities for water storage while the field capacity represents the available water retained in the medium.

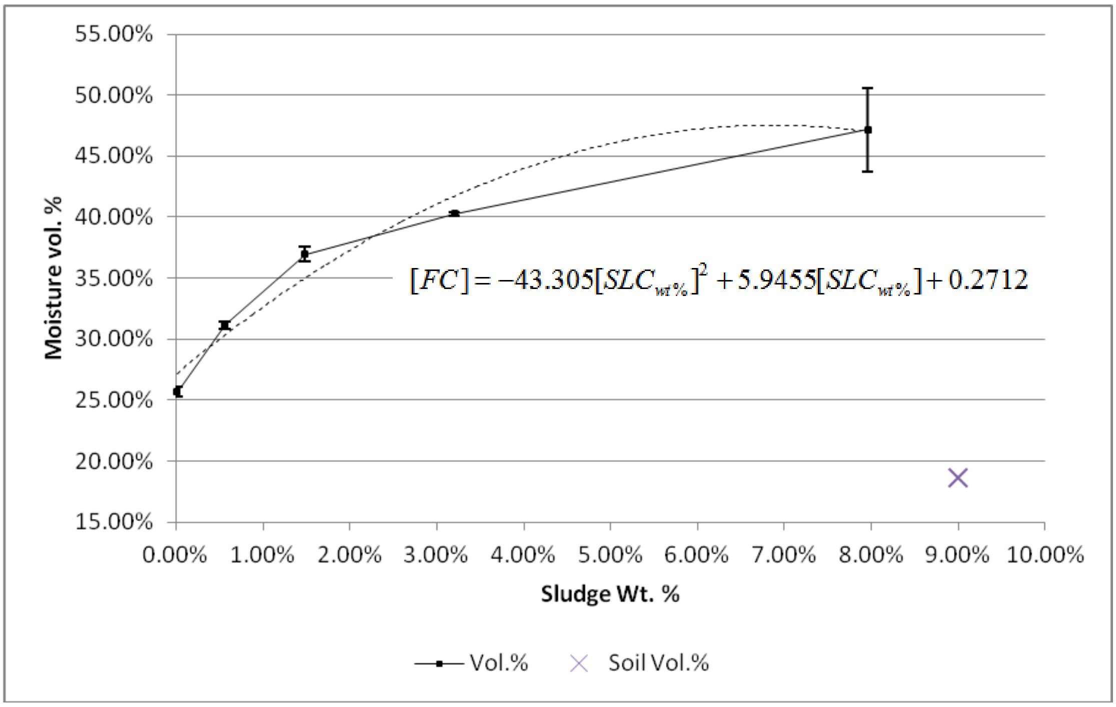

Figure 4. 11 Field capacity for arid sand, Eco-Soil and potting soil

Figure 4.11 shows the field capacity for arid sand, Eco-Soil and commercial potting soil, respectively. Due to higher porosity of the Eco-Soil, the FC appears higher than the commercial potting soil in this study. As the introduction of activated sludge to the arid sand, their Field Capacity (FC) increase from 25.68% to 47.18 vol. %. The activated sludge provides great amount of fine pores to hold the water after drainage of transient water. This phenomenon is revealed by the FC on the curve for the sludge weight content from 0.56% to 1.48% (equivalent to SSVR 80:20 and 60:40, respectively). The FC increases rapidly from 25.68% to 36.96% when the SSVR changes from 100:0 to 60:40. However, the increasing effect reduces when the SSVR reaches 60:40 and 80:20.

The relation between the SSWR and FC is found to be as follow:

$$[FC] = -43.305[SLC_{wt\%}]^2 + 5.9455[SLC_{wt\%}] + 0.2712 \quad \text{(Eq 4. 18)}$$

where [FC] is field capacity with unit m^3/m^3 and [$SLC_{wt\%}$] stands for sludge weight content with unit g sludge /g Eco-Soil. The linear regression is found to be 0.967, which shows a good correlation for the equation and the experimental data.

Table 4. 5 Field Capacity and Permanent wilting points for common soil textural classes (Adapted from Rowell, 1994)

Soil Texture	Field Capacity
Sand	0.12
Loamy Sand	0.14
Sandy Loam	0.23
Loam	0.26
Silt Loam	0.3
Silt	0.32
Sandy Clay Loam	0.33
Silty Clay Loam	0.34
SiltyClay	0.36
Clay	0.36

In view of Table 4.5 (Rowell, 1994), the FCs of the Eco-Soil samples increase from sandy loam to clay level and even higher when the activated is applied to the arid sand. The FC results indicate the water holding capability is greatly improved by the addition of the activated sludge. Because the water is the essential element for plant growth, the capability to hold the water is significantly important in arid and semi-arid area.

4.1.7 Hydraulic Conductivity

Hydraulic conductivity affects the soil infiltration in tillage water management. High water infiltration rate and low evaporation rate result in strong water retention. In arid and semiarid environment, the water storage capability of the growing medium is important. The loss of water content in the growing medium induces degradation of the organisms then brings down the productivity. To enlarge the water storage in the growing medium, studies made efforts to increase the infiltration rate by modify soil surface characteristics, roughness and structure (Lampurlanes and Cantero-Martinez, 2001).

By introduction of the activated sludge, the water retention abilities for Eco-Soil are greatly increased and indicated by the Field Capacity. However, the hydraulic conductivities are brought down due to the clogging of water path ways by the fine sludge particles.

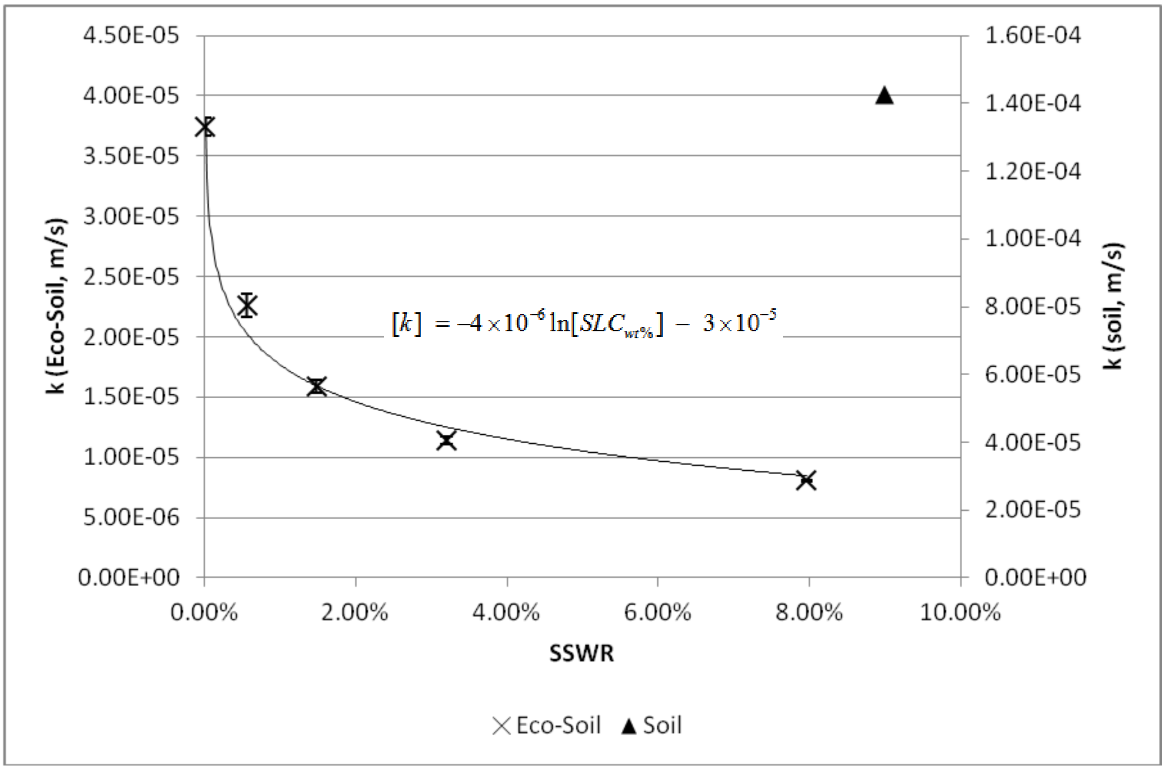

Figure 4. 12 Hydraulic conductivities for arid sand, Eco-Soil and potting soil

Figure 4.12 shows the hydraulic conductivities for arid sand, Eco-Soil and commercial potting soil.

The Eco-Soil aims to enlarge the water storage, which is revealed by the increasing FC content. However, the introduction of activated sludge also brings lower hydraulic conductivity, resulting in lower water infiltration and slower ground water movement.

Figure 4.12 shows the hydraulic conductivities for the Eco-Soil under various sludge weight fractions and comparison with commercial potting soil. Along with the increasing fraction of activated sludge, the hydraulic conductivities quickly reduce from 3.74×10^{-5} m/s to 1.59×10^{-5} m/s (SSWR 1.48% or SSVR 40:60) and further reached 8.06×10^{-6} m/s (SSWR 7.96% or SSVR 20:80). The distribution of hydraulic conductivity against SSWR is found to be logarithmic and described by the following equation:

$$[k] = -4\times10^{-6}\ln[SLC_{wt\%}] - 3\times10^{-5} \qquad \text{(Eq 4. 19)}$$

where the [k] is hydraulic conductivity in m/s and $[SLC_{wt\%}]$ is sludge weight content in g sludge /g Eco-Soil.

The correlation coefficient is found to be 0.954 and indicates a high correlative relation.

According to Table 4.6, the hydraulic conductivities of Eco-Soil with SSVR 80:20, 60:40 and 40:60 (SSWR 0.56%, 1.48% and 3.20%, respectively) are comparable with that of silty sand. However, the hydraulic conductivity of Eco-Soil with SSVR 20:80 (SSWR 7.96%) is comparable to silt or loess level and indicates a low value. A substrate with low hydraulic impedes water infiltrate into the 10~15 cm depth (Pikul and Aase, 2003). Low hydraulic conductivity results in low infiltration in rain event or irrigation. The water becomes surface runoff other than infiltrate into subsoil. This upsets the water retention and the substrates are readily washed out by surface runoff. On the other hand, high hydraulic conductivity results in water infiltrate into deep soil quickly so that little water is retained tillage layer. In addition, high conductivity also exhibit large evaporation due to large fraction of macro pores.

Table 4. 6 Range of values of hydraulic conductivity and permeability (Adapted from Freeze *et al*., 1979)

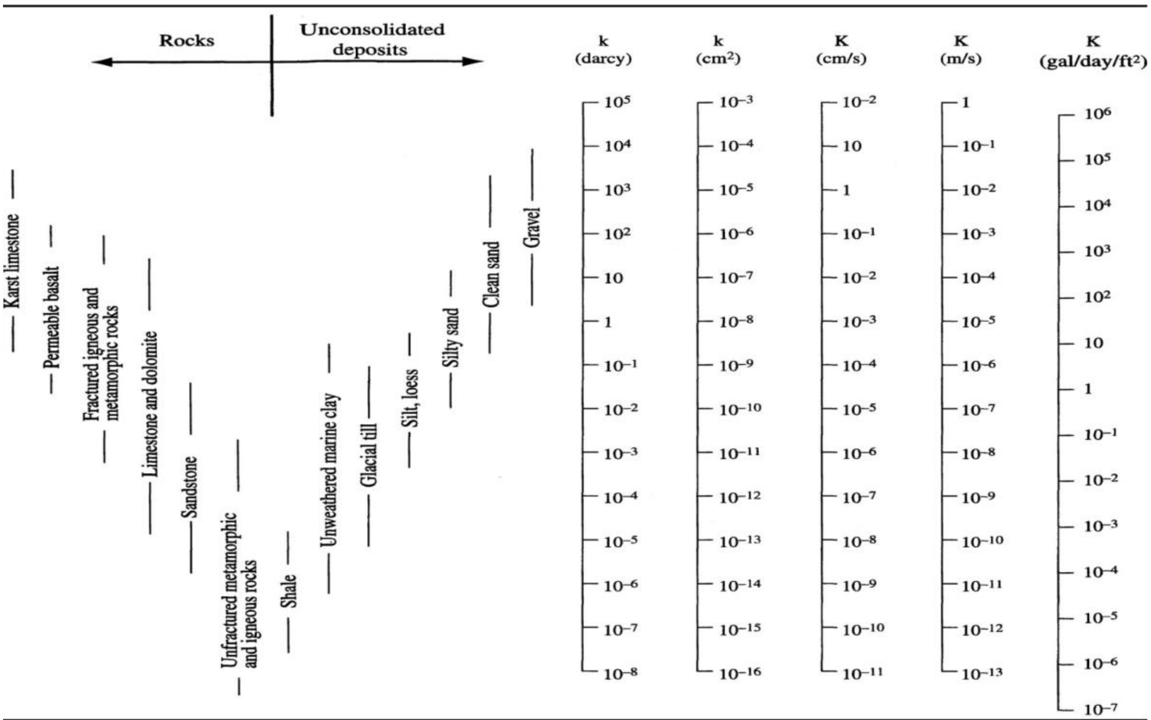

Source: Freeze, Alan R.; Cherry, John A., Groundwater, 1st Edition, © 1979, p. 178, Reprinted by permission of Pearson Education, Inc., Upper Saddle River, NJ.

4.1.8 Seed Germination Index

Previous section discussed the physical properties for the Eco-Soil regarding water management. However, studies found that sewage sludge from various sources are able to inhibit plant growth and development (Oleszczuk, 2008; Ramirez *et al*., 2008) due to the organic and inorganic pollutants in the sludge (Oleszczuk and Hollert, 2011). The reverse effect of sewage sludge towards plant growth is concluded as phyto-toxicity. Seed Germination Index (SGI) is a bioassay test to evaluate the phyto-toxicity for a growing medium, especially in sludge amended soil (Ramirez *et al*., 2008).

35 isolated tomato seeds were soaked in the extracts from arid sand (SSVR 100:0), Eco-Soil, commercial soil and distilled water (Control) for studying the phyto-toxicity for the growing medium. The seed germination percentage (SGP), seed germination index and root length ratio were shown in Figure 4.13.

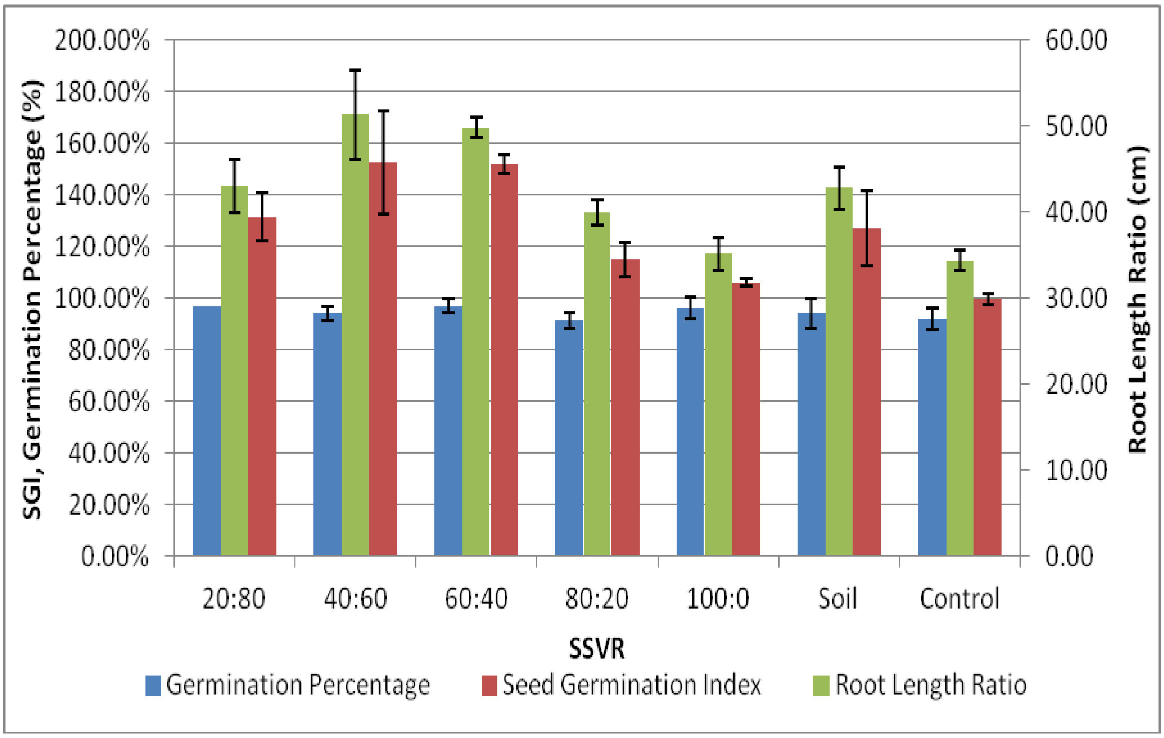

Figure 4. 13 Germination percentage, seed germination index and root length ratio for arid sand, Eco-Soils, commercial soil and control plates

The blue columns show that the average seed germination percentages (SGP) for the six samples are larger than 90%. The SGP for SSVR 80:20 exhibits the lowest result 91.43% compared to 97.14% for SSVR 20:80 and 60:40. However, the variation of the data shows that the significance are low from each other ($P>0.05$, for $n=3$). The SGP results indicate that the six samples had very little reverse effects on seed germination.

Though the SGP for the samples are similar and exhibit values above 90%, the root lengths of the germinated seeds are different from plate to plate. The Root Length Ratio (RLR) is calculated by the cumulative root length of the germinated seeds divided by numbers of germinated seeds. This result indicates how well does the plant grow in the leachates from various samples. The green column in Figure 4.13 shows the RLRs for each sample. Among the arid sand and Eco-Soils, high average RLRs appear on SSVR 40:60 and 60:40 with 51.36 and 49.88 cm/ seed, respectively. Compared to the commercial potting soil sample (RLR 42.84 cm/seed), the RLR for SSVR 40:60 and 60:40 indicate Eco-Soil exhibited more affinitive effects for plant growth.

The red columns show the SGIs for arid sand, Eco-Soils and commercial soil. The trends for the SGIs and RLRs are found to be similar due to the SGRs are similar for each sample. Oleszczuk and Hollert (2011) indicated that for an appropriate growing medium, the SGI should be large than 100%. As read from Figure 4.10, all of the SGIs for arid sand, Eco-Soils and commercials soil are beyond 100% and indicate non-phyto-toxic effects. The SGI for control containing distilled water is 100% for reference. For SSVR 100:0, the GIs are closed to control sample because no nutrient is able to be used for seed germination. As the introduction of activated sludge, the phyto-enhancing substances release from activated sludge and sustain the growth of roots. However, not only the phyto-enhancing but also phyto-toxic substances release at the same time and the SGIs reduce for Eco-Soil with high sludge content such as SSVR 20:80. The highest SGIs appear at SSVR 40:60 and 60:40 with value of 152.63% and 152.36%, respectively. The SGIs for these two SSVRs are higher than commercial potting soil (127.29%) and indicate higher phyto-enhancing effects. Nevertheless, the SGI for SSVR 60:40 is found to be more stable compared to SSVR 40:60 and considered to be optimal SSVR for growing plants.

4.1.9 Summary

This section studies the hydraulic properties of the Eco-Soil under Sand-Sludge Volumetric Ratio (SSVR) of 100:0, 80:20, 60:40, 40:60 and 80:20, and the comparison with commercial potting soil to find out the outcomes by applying activated sludge. The sludge mixing model is derived to build up the relation among SSVR, SSWR and organic content for further studies. The DBD, PD and hydraulic conductivity are found to be decreasing while FC and porosity are increasing due to the introduction of activated sludge. The Eco-Soil properties were compared with that of the commercial potting soil and agricultural references to indicate a suitable SSVR value of 60:40. Thereafter, the seed germination index analysis indicates all the Eco-Soil extracts exhibit phyto-enhancing effects. However, SSVR 60:40 and 40:60 provide better results in SGI studies. Based on the comprehensive analysis and consideration of enlarging the effects of sludge application, the Eco-Soil of SSVR 60:40 is suggested to be suitable mixing ratio for anti-desertification.

4.2 Soil-Water Characteristics Curve for Eco-Soils

4.2.1 SWCC by Sand Funnel method

The SWCC draw by sand funnel method covers the range of substrate pressure -100 ~ -5 kpa absolute (Yi, 2008). This range is narrow, but it reflects dehydration curve for most of the substrates. The SWCCs of the Eco-Soil from SSVR 100:0 to 20:80 and commercial potting soil are shown in Figure 4.14.

The SWCCs of Eco-Soils are shown to be shifted from low to high in the range -600 ~ -100 cmH_2O due to the retention capability increased by the activated sludge. Without introduction of activated sludge, the VWC of arid sand (SSVR 100:0) drops quickly from 6.98% to 0.98%. The fine structure and the moisture retention abilities of activated sludge increase the moisture content under various suction pressures. The effects can be revealed by the increasing moisture content under a certain suction pressure. As an example, at the suction pressure of -407 cm H_2O, the average VWCs of Eco-Soils increase from 2.91% to 21.59% and are proportional to the increasing sludge content. In practical application, more moisture retention is better for growing vegetations. For one thing, the moisture keeps longer within the substrate at dry environment, so that the water availability for vegetation uptake is higher. Secondly, high moisture content is maintained at high suction pressure. This benefits root water uptake for vegetations with lower root suction pressure and increases the water accessibility in arid area. High moisture retention offers opportunities for anti-desertification by maintaining water for vegetation growth, because the water is the essential substance for biochemical reaction for plants.

From the SWCC for Eco-Soil of SSVR 60:40 showed in Figure 4.14, it is approaching to and comparable to that of commercial potting soil. The phenomenon reveals that Eco-Soil of SSVR 60:40 is able to achieve a moisture retention capability comparable to commercial potting soil. In addition, when the SSVR of Eco-Soil reaches 60:40, the SWCC is also found to be comparable to the that of loamy soil (Fu *et al.*, 2011), In addition, the soil water retention for Eco-Soils of higher sludge contents such as SSVR 40:60, 20:80 perform comparable to the clay material (Fu *et al.*, 2011). Loam and clay usually offer good moisture retention effect in the soil physics. Under the consideration for treating more arid area by the maximum usage of activated sludge, the mixing ratio SSVR 60:40 is a considerable selection.

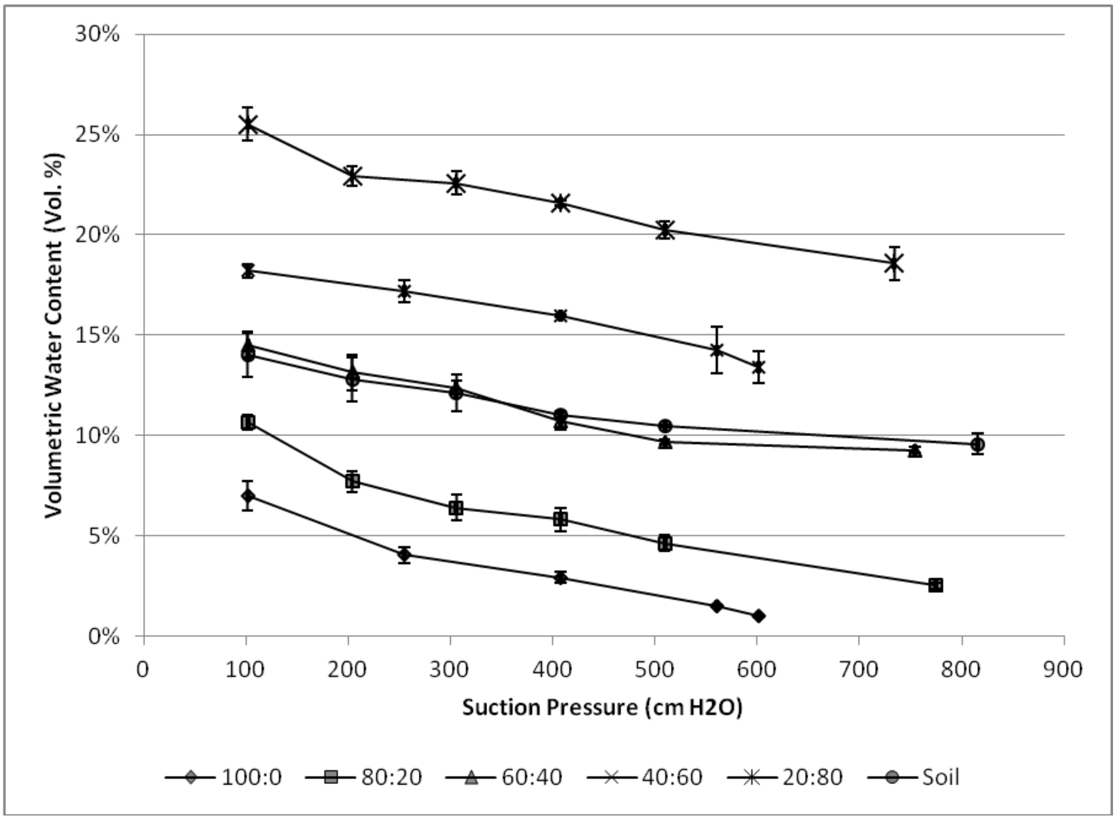

Figure 4. 14 SWCC for Eco-Soils and commercial potting soil by sand funnel method

4.2.2 SWCC by Chemical Solution method

Chemical solution method is able to be use for plotting SWCC for the suction pressure lower than -3000 kpa (equivalent to -3.06×10^4 cmH_2O) (Yi, 2008), which is unable to be obtained by mechanical methods. The relative humidities formed by special chemical salt saturation solutions are referred to certain suction pressure in the substrates. To obtain the moisture retention for this range aids to determine the completed SWCC and fit to numerical models.

Figure 4.15 shows the results of SWCC by chemical solution method. The trend of the SWCC in the range of -2.98×10^6 to -1.10×10^5 cmH_2O for Eco-Soils appears a same trend as that by sand funnel method. The curves are shown to be shifted from SSVR 100:0 to SSVR 20:80. The SWCC for arid sand (SSVR 100:0) shows that the average moisture contents reduce from 0.47% to 0.10% in this suction head range. In other words, very little moisture exists in the high suction head situation for arid sand. The phenomenon reveals that the moisture retention ability for arid sand is weak at low RH conditions such as arid area. Therefore, the vegetations are not able to grow under the dried substrate. With the introduction of activated sludge, the moisture content increased from 0.45% to 8.73% at -1.10×10^5 cmH_2O suction head condition. Even though at high suction pressure condition, such as -2.98×10^6 cmH_2O, the Eco-Soil SSVR 40:60 and 20:80 also retain moisture contents higher than 1.00%. As a substrate focusing on the water retention, the SSVR 40:60 is shown to be a better mixture ratio due to low activated sludge consumption but comparable performance as commercial potting soil.

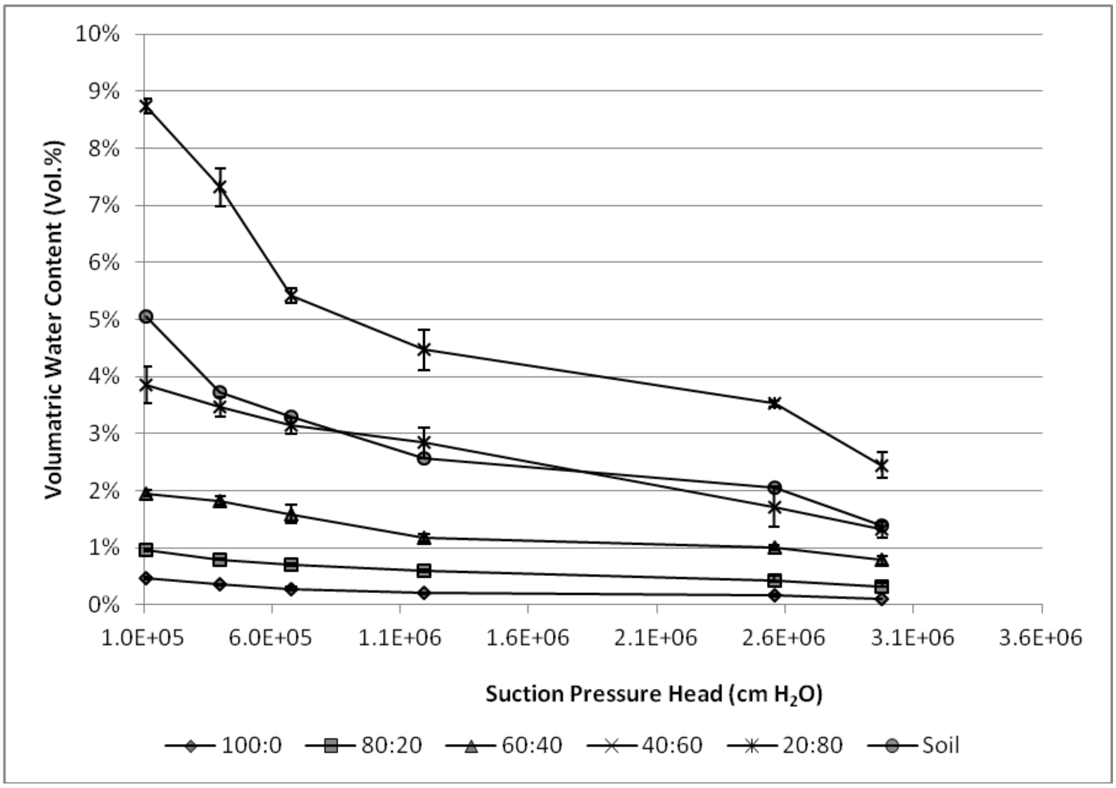

Figure 4. 15 SWCC for Eco-Soils and commercial potting soil by chemical solution method

4.2.4 SWCC Fitted by van Genuchten Model

This study uses the RETC program to simulate the SWCC for the Eco-Soils and potting soil using van Genuchten-Mulean model (van Genuchten, 1980). The data for hydraulic conductivity, saturated moisture content, residual moisture content are input from the experiment results. The fitting factors including α and n were fitted by try and error methods. Figure 4.16~4.21 show the fitting results for the six substrates.

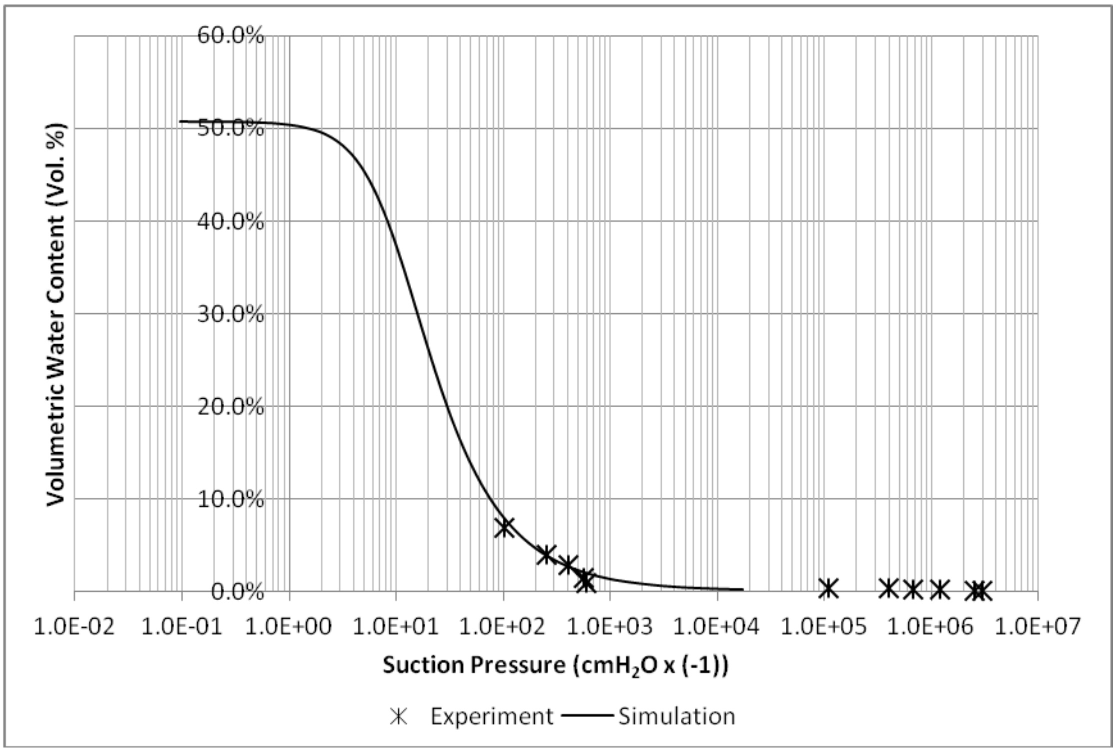

Figure 4. 16 Numerical simulation of SWCC by RETC program for arid sand (SSVR 100:0)

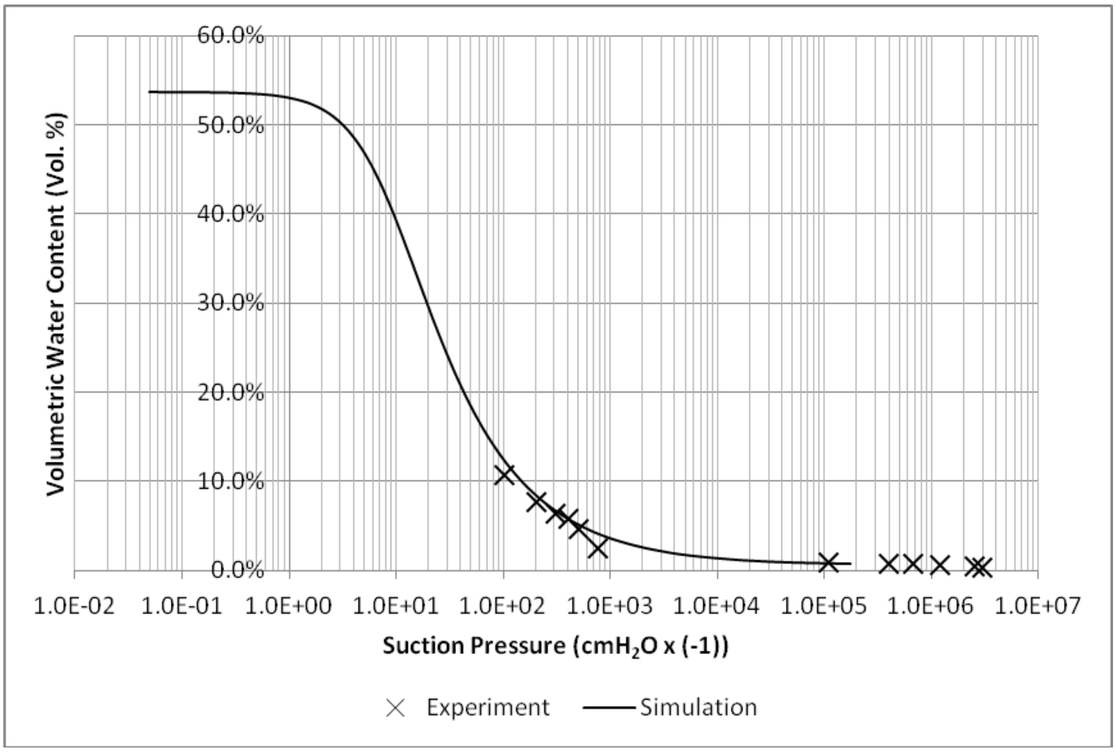

Figure 4. 17 Numerical simulation of SWCC by RETC program for Eco-Soil (SSVR 80:20)

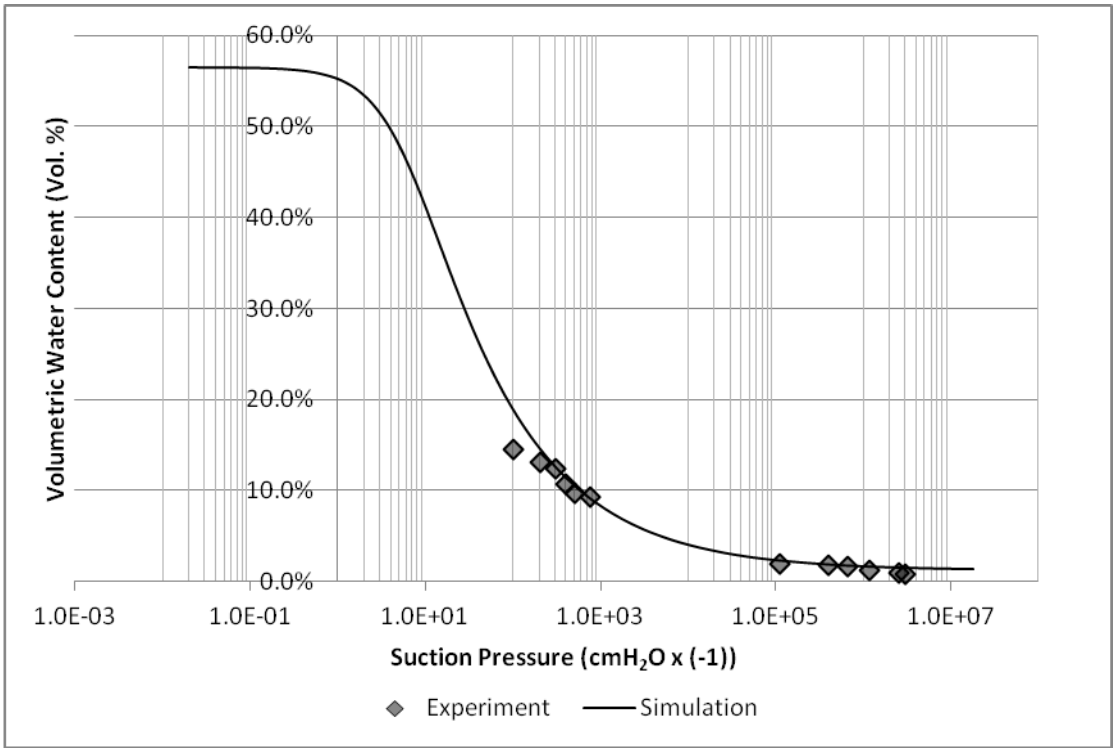

Figure 4. 18 Numerical simulation of SWCC by RETC program for Eco-Soil (SSVR 60:40)

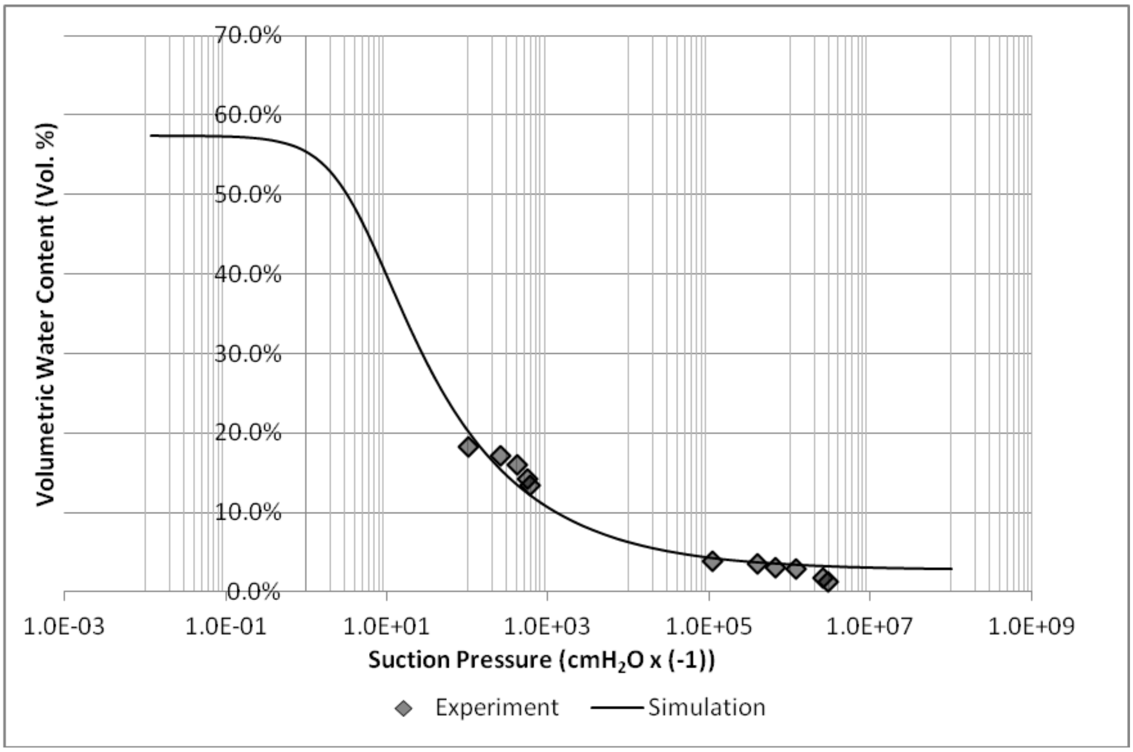

Figure 4. 19 Numerical simulation of SWCC by RETC program for Eco-Soil (SSVR 40:60)

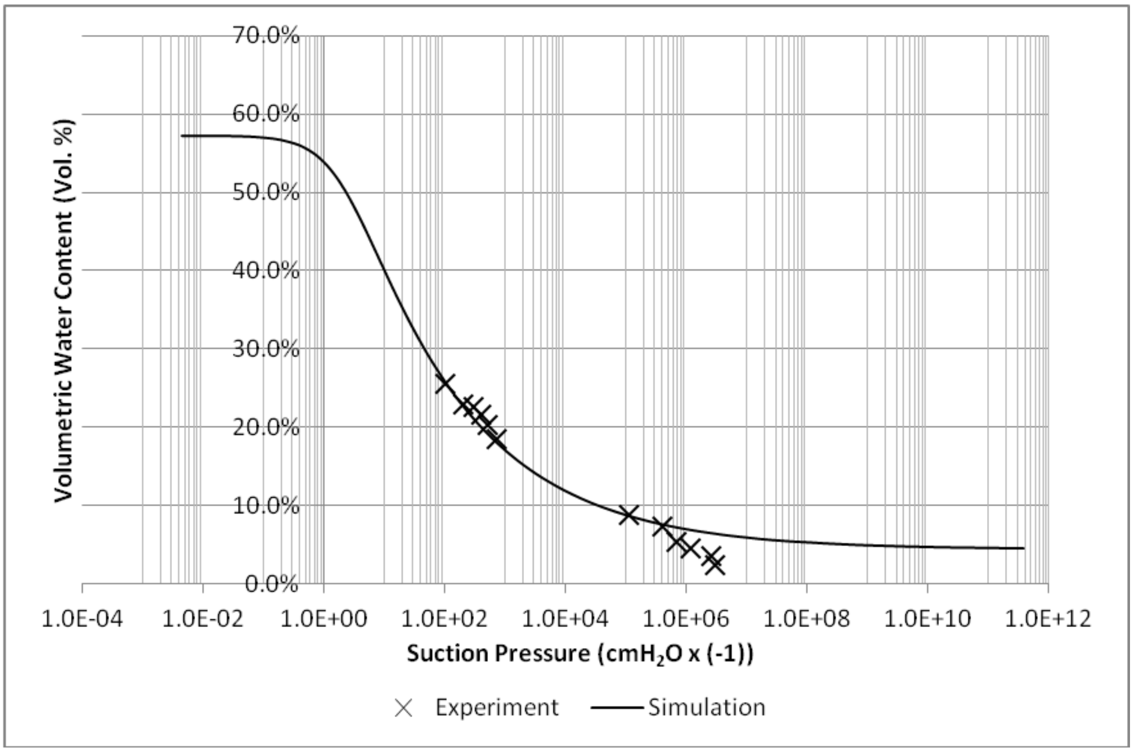

Figure 4. 20 Numerical simulation of SWCC by RETC program for Eco-Soil (SSVR 20:80)

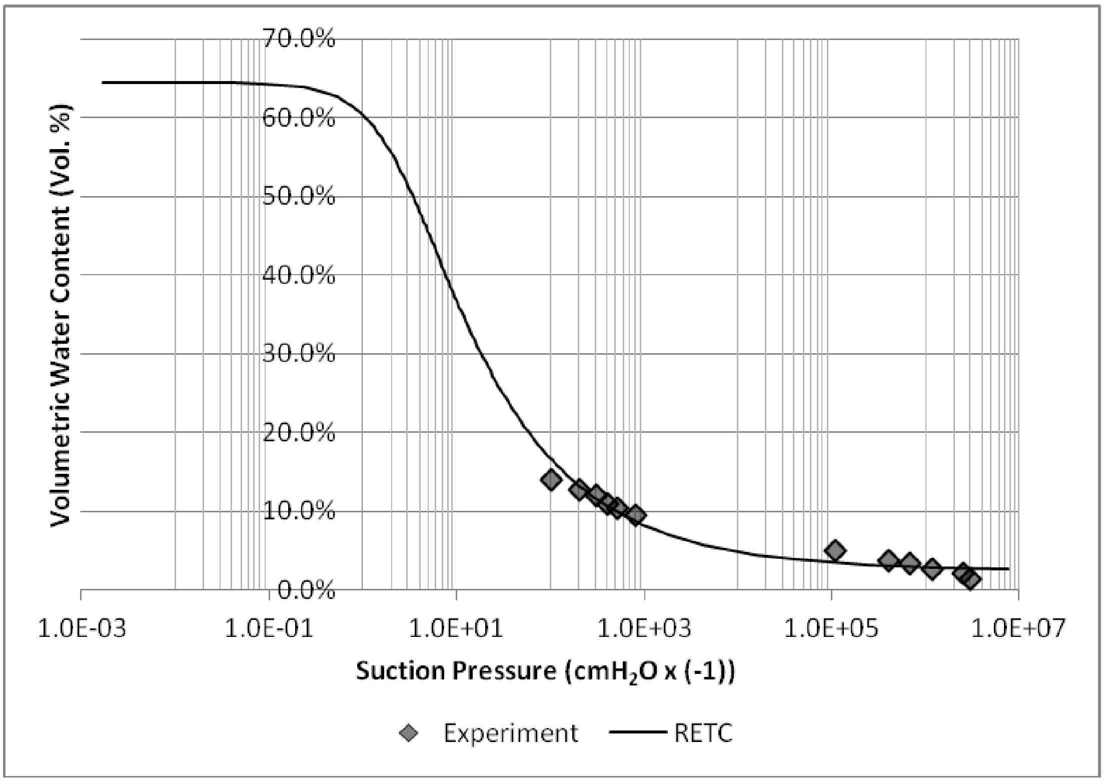

Figure 4. 21 Numerical simulation of SWCC by RETC program for commercial potting soil

Figure 4.16 ~ 4.21 shows the numerical simulation of SWCC for Eco-Soil samples from SSVR 100:0 to 20:80. The van Genuchten-Mualen model with m=1-1/n is chosen for the simulaiton. The Nerual Network Predition function is able to estimate approximate values for hydraulic conductivity, residual and saturated moisture contents for the substrates by inputing particle size distribution, bulk density, water content at 33 and 1500 kPa (Minasny *et al.*, 2004). However, the predition results deviate from the experimental findings for Eco-Soils. The deviation is considerd to be caused by the introduciton of novel substrate fraction, activated sludge.

After series of try and error for finding the α and n, the simulation results for the 6 substrates are shown. The simulation results fit well for Eco-Soil with lower activated sludge content, saying SSVR 100:0 to 60:40, but deviate for large suction pressure range (smaller than -1.19×10^6 cmH_2O). The phenomena are also considered to be brought by the introduction of activated sludge. However, all the curves fit well for the range of suction larger than -1.19×10^6 cmH_2O. The findings show that the van Genuchten model is able to predict the SWCC for suction pressure higher than -1.19×10^6 cmH_2O.

4.2.5 Introduction of Eco-Soil Mixing Model to VG Model

The van Genuchten are shown to be applicable for the suction pressure higher than -1.19×10^6 cmH_2O. The two important fitting factors, α and n, are plotted against the SSWR and shown in Figure 4.22.

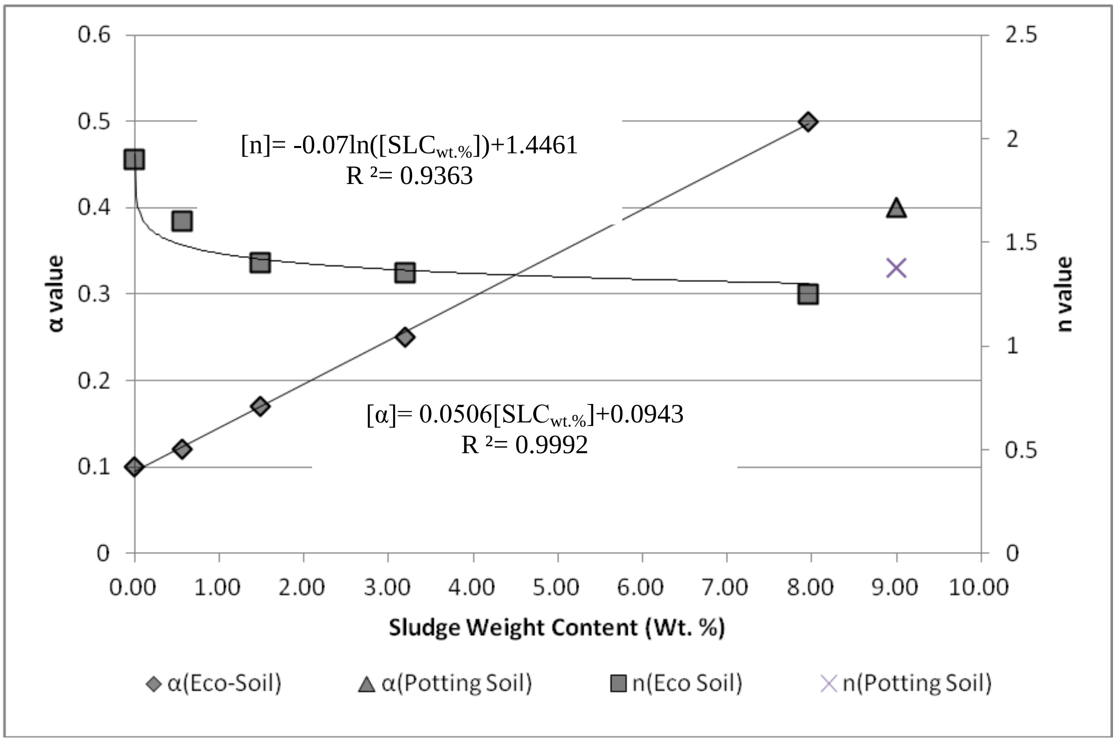

Figure 4. 22 α and n values under various sludge weight contents

Figure 4.22 shows that the α values for Eco-Soils distribute linearly with respect to the sludge weight content ($[SLC_{wt.\%}]$). The relation is found to be

$$[\alpha] = 0.0506[SLC_{wt.\%}] + 0.0943 \qquad \text{(Eq 4. 20)}$$

where the α is fitting factor for VG model; $[SLC_{wt.\%}]$ is sludge weight ratio in the Eco-Soil. The corelaiton coefficient was shown to be 0.9992 and suggested a good fitting.

The n value is found to follow logarithmic distribution with sludge weight content ($[SLC_{wt.\%}]$). The relation is expressed as

$$[n] = -0.07\ln([SLC_{wt.\%}]) + 1.4461 \qquad \text{(Eq 4. 21)}$$

where n is the fitting factor for VG model. The corelation coefficient also exhibited a high value of 0.9363, which reveals strong corelated relation between the simulation and experimental value.

By using m=1-1/n and substituting the α and n equations into van Genuchten model, the model is modified as

$$S_e = \frac{\theta - \theta_r}{\theta_s - \theta_r} = \left[\frac{1}{1 + \left[(0.0506\left[\mathrm{SLC_{wt.\%}}\right] + 0.0943)h \right]^{-0.07\ln\left(\left[\mathrm{SLC_{wt.\%}}\right]\right)+1.4461}} \right]^{1-\frac{1}{-0.07\ln\left(\left[\mathrm{SLC_{wt.\%}}\right]\right)+1.4461}}$$

(Eq 4. 22)

where the θ is VWC, θ_s and θ_r is saturated and residual VWC, respectively.

This combined model is applicable for Eco-Soil from 100:0 to 20:80, in the suciton head range from 0 to -1.19×10^6 cmH_2O.

The relations among SSWR, SSVR or organic content of the Eco-Soil are described in the Eco-Soil Mixing Model. Therefore, once the connection between VG model and sludge mixing model is found, the SWCC is able to be determined by SSWR, SSVR or organic content of the Eco-Soil. The modification of the VG model for Eco-Soils offers a numerical prediction for the SWCC under various Eco-Soil combinations. The finding not only elucidates the numerical relation between SWCC models but also establishes a connection between the novel Eco-Soil and the conventional soil substrate models (Leong and Rahardjo, 1997; van Genuchten, 1980), such as infiltration, evaporation, moisture development models (Simunek, 2004).

4.2.6 Summary

This section describes sand funnel and chemical methods for the Eco-Soils to plot the SWCC in the two important ranges of -600 ~ -100 cmH_2O and -2.98$\times$10^6 to~1.10$\times$10^5 cmH_2O to investigate the soil water characteristics. The results show that the SWCC for both ranges appear to be shifted as the increasing content of activated sludge. The phenomenon reveals the soil water retention capability of arid sand is strengthened by the contribution of activated sludge. As a comparison, the Eco-Soil with sludge content as high as SSVR 60:40 exhibits comparable retention ability than the commercial potting soil for the suction pressure range of -600 ~ -100 cmH_2O. In addition, when the SSVR reached 40:60, the water retention effects of Eco-Soil are shown to be better than potting soil. The experimental SWCCs illustrate the great improvement brought by introducing activated sludge. This serves as a theoretical support for application of Eco-Soil in anti-desertification. The experimental SWCC is also fitted by numerical models such as van Genuchten (VG) model. The results show the VG model is applicable to the range of 0~-1.19$\times$10^6 cmH_2O. The two essential fitting factors of VG model, includingα and n, are able to be expressed numerically and suggested by high correlation coefficients. The finding offers a way to introduce the Eco-Soil Mixing Model into VG model to develop numerical SWCC equation for Eco-Soil. Therefore, the SWCC is able to be predicted by SSWR, SSVR or organic content of the Eco-Soil. The finding elucidates the numerical relation between SWCC models but also built a bridge between the novel Eco-Soil and the conventional substrate models, such as infiltration, evaporation, moisture development models.

4.3 Growth of Okra in Eco-Soils

4.3.1 Plant Growth Pattern

The low productivity of arid sand is caused by the lack of nutrients, such as potassium, nitrogen and phosphorus. The activated sludge obtained from wastewater treatment plant offers rich macro and micro nutrients, which compensate the defects of arid sand for vegetation growth. This study used *Abelmoschus esculentus* (Okra) as sample vegetation to evaluate the growing capability of arid sand, Eco-soil and potting soil. The okra is one of the popular economic crops in lots of arid and semi-arid area in Africa. Okra also have relative short growing period (from seeding to harvesting) and a complete fruiting cycle. These makes okra to be a preferred vegetation for this study.

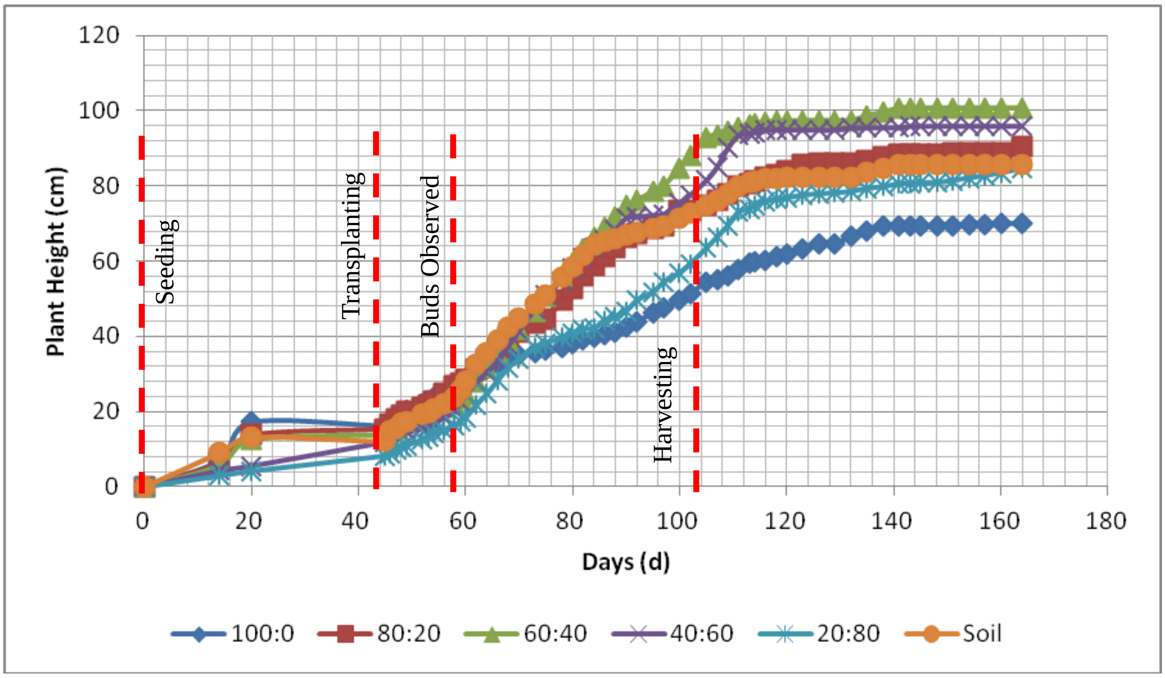

Figure 4. 23 Plant height development for Okra growing in arid, Eco-Soils and Potting Soil

Figure 4.23 shows the average plant height development pattern for okra growing in arid sand, Eco-Soil and potting soil. Plant grew for the first 20 days in the dark environment for germination. The nutrients for primary growth are mainly from the cotyledon in the seeds because okra is dicotyledon plant. The growing height for arid sand, Eco-Soils (SSVR 80:20 and 60:40) and potting soil in germination phase are similar and ranged from 12.5 to 17.75 cm. However, the seed germination rates are observed to be low in SSVR 40:60 and 20:80 when the seeds are buried in the substrates. The seed are observed to be germinated when they are placed upon the surface or cover with shallow substrates. However, the lixivium from Eco-Soil of various SSVR are found to be phyto-enhancing for the okra seeds germination. The low germination rate in fully buried samples is considered to be due to the low air entry value for the fresh mixture of Eco-Soil and low evaporation rate in the room temperature. The fully buried seeds in SSVR 80:20 and 60:40 are observed to be able to germinate and grow well as compared to potting soil due to appropriate nutrient and pore spaces.

The plant heights reduce after transplanting because the plants are buried in the centre of growing pots and the burying depths are deeper than the seeding tray. The slopes of the height growing curves reflect the height development speeds. All of the plant samples show steep slopes between 45th and 116th days. The fast growing period is found in the summer season for the experiment site. The strong solar radiation excites the photosynthesis and therefore increases the plant growth quickly.

After the 116th day, the growth speed slows down and the plants reach their maximum height. The maximum heights of the okra growing in Eco-Soil are found to be proportional to the fraction of activated sludge applied. The vertical growth was closely related to the nitrogen contents offered by the substrates (Lincon and Eduardo, 2010). The nutrients in the potting soils were richer than the Eco-Soils. However, due to the high hydraulic conductivity and large portion of macro pores (Godwin, 1990; Lampurlanés and Cantero-Martínez, 2006), the nutrients are readily washed away through the drainage. The macro pores also accelerates the evaporation of the moisture and do not benefit the nutrients migration.

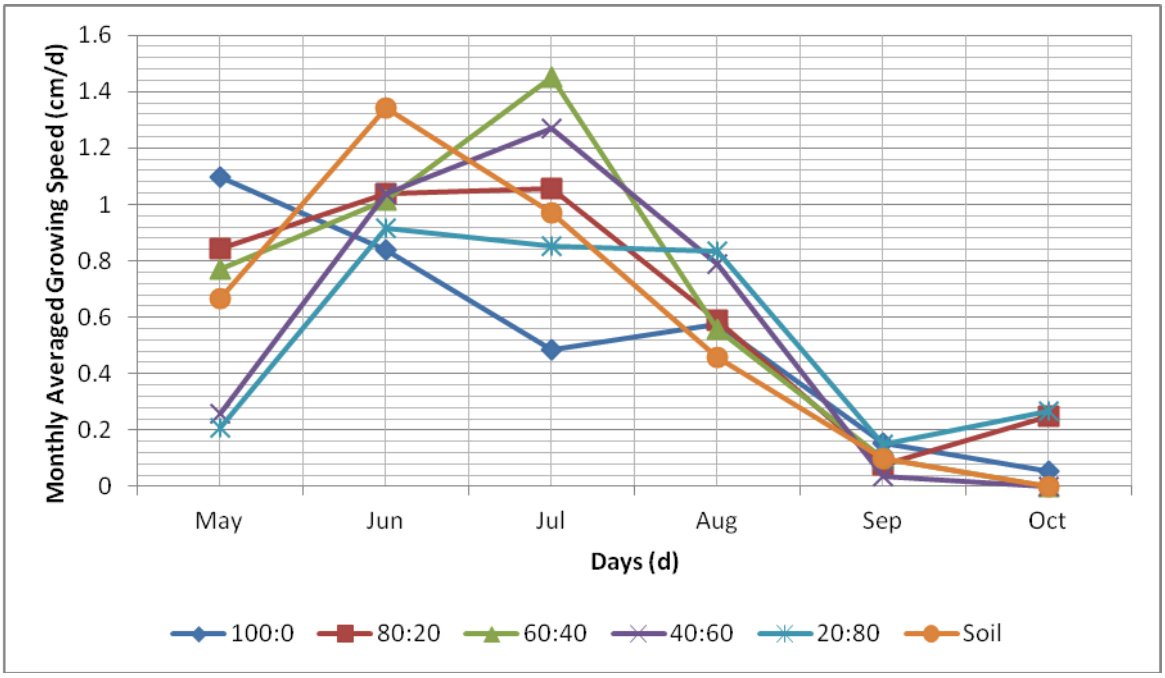

Figure 4. 24 Plant growing speed for Okra growing in arid, Eco-Soil and Potting Soil

Figure 4.24 shows the monthly averaged growth speeds of the plant heights for arid sand, Eco-Soil and potting soil. The results reveal that the growth speeds are low after transplanting in May and indicate the adaptive phase for the plants. The major nutrient utilization is for root development other than plant height development. The critical point appears at about 40^{th} day. The plants growth rate started to increase and even attained a very high value after the 60^{th} day. When the growing period reached the September, the grow rates are found to be low and almost zero. From the 110^{th} day, the first batch of mature pods is observed and the harvesting period begins. The nutrients are used for buds and pods formation other than the plant growth.

4.3.2 Growth of Organs

The growth of various organs of plants reflects the nutrient consumption and transportation. The organs above the ground mainly consist of shoot and leaves while the underground is root (Akanbi, et al., 2012; Harris, 1992).

4.3.2.1 Shoot Dried Weights

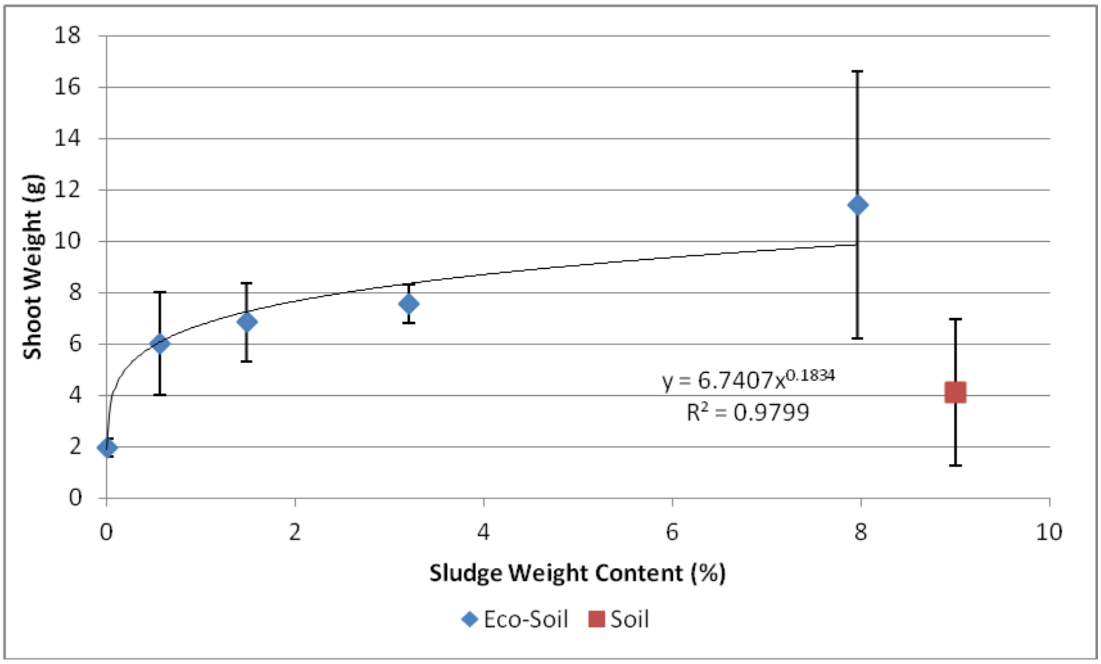

Figure 4. 25 The dry weights of shoots for okra growing in arid sand, Eco-Soils and potting soil

Figure 4.25 shows the shoot dry weights (SDW) of the okra growing in arid sand, Eco-Soils and potting soil. The arid sand provides very little nutrient for plant growth.

Therefore, the plant height and shoot dried weight are found to be the lowest value. The average shoot weight of okra growth in arid sand suggests growing plants in the arid area is not suitable. Even though in this experiment, water was provided evenly for each growing sample, but the deficiency of nutrients resulted in low growing abilities for plants. The results show that external nutrients should be introduced in the arid area to rebuild the productivities.

As observed from the shoot weights using Eco-Soil, the average dried weights are found to be proportional to the amount of activated sludge added. The average SDW increases from 5.98 to 11.47 g/plant for okra growing in Eco-Soil of SSVR 80:20 to 20:80. The shoot dried weight for SSVR 60:40, 40:60 and 20:80 are found to be comparable with the ones by using chemical fertilizer, 400 kg NPK /ha (Akpan-Idioka et al., 2012). The activated sludge provided macro nutrients including nitrogen, phosphorus and potassium for the growth of shoot for okra. The SSWRs are plotted as x-axis in Figure 4.25 and the relation between shoot dried weights and SSWRs is found to be exponential, which is expressed as:

$$\left[\mathrm{wt.}_{\mathrm{Shoot}}\right] = 6.7407\left[\mathrm{SLC}_{\mathrm{wt.\%}}\right]^{0.1834} \qquad \text{(Eq 4. 23)}$$

where the [Wt.Shoot] is shoot dried weight and [$SLC_{wt.\%}$] is sludge weight content in wt. %.

The linear regression coefficient is found to be 0.9799 and indicates a good correlation between the predicted and experimental values.

As a comparison, the average shoot dried weight for the okra growing in potting soils is found to be only 4.08 g/plant. However, the average plant height is comparable to the one growing in SSVR 80:20 Eco-Soil sample. The reason is that the shoot diameter of okra growing in potting soil is smaller than that in Eco-Soil. The potting soil samples have macro pores, which increase the hydraulic conductivity and evaporation (Godwin, 1990). Therefore, the moisture decreases rapidly in growing space and resulted in low transportation of nutrients. In irrigation, high hydraulic conductivity also increases the wastage rate of the nutrients to the bottom runoff. In real application, this may cause penetration of nutrient into deeper layers. Though the initial nutrients for potting soil are found to be rich, these advantages only offer a fast growing speed in the initial and middle stage. The plant height and shoot dried weight are found to be lower than the plants growing in the Eco-Soil.

4.3.2.2 Leaves Dried Weights

Leaf is important organ for plants to absorb oxygen to perform many biochemical reactions. Carbon dioxide and solar radiation are also absorbed through the stomata on the leaves for conducting photosynthesis (Lincon and Eduardo, 2010). The number and size of leaves are directly related to the growing speed of a plant. The growth of leaves of a plant also reflects the nutrient consumption. The deficiencies of certain nutrients, including nitrogen, phosphorus and potassium, can be observed from the symptom on the leaves (Lincon and Eduardo, 2010).

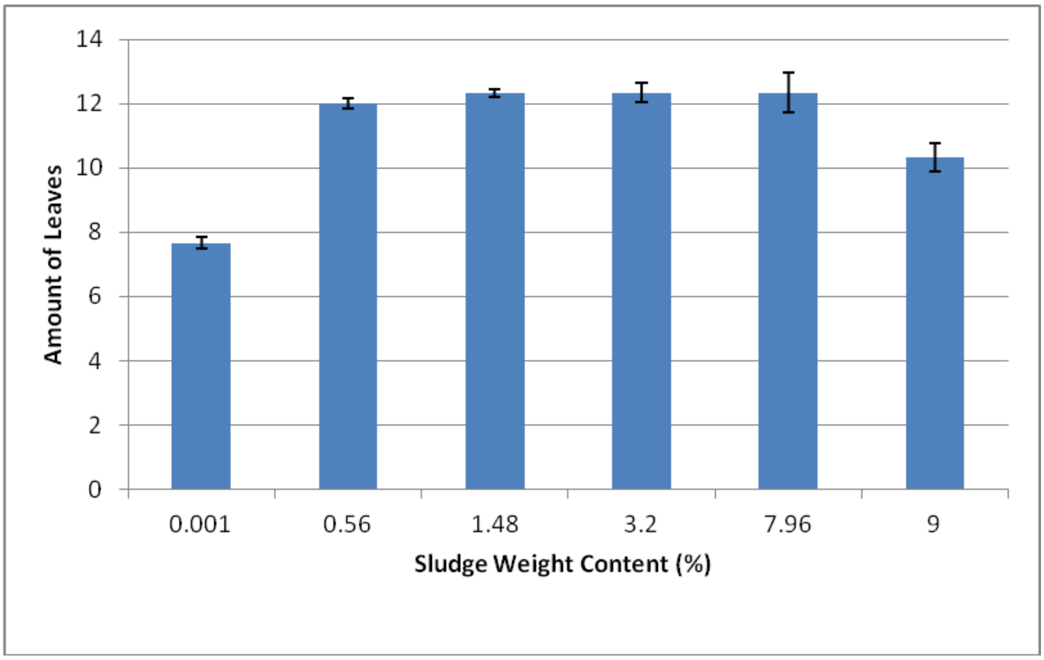

Figure 4. 26 Amount of leaves for the okra growing in arid sand, Eco-Soil and potting soil

Figure 4.26 shows the amount of leaves for the okra growing in arid sand, Eco-Soil and potting soil at the end of growing period. The number of leaves is found to be proportional to the palnt height. Proportional to the introduciton of activated sludge to the arid sand, the average number of leaves increases from 7.67 to 12.33 leaves/pot for Eco-Soil from SSVR 100:0 to 20:80. The number of leaves for okra growing in Eco-Soil are found to be highly comparable to the one in general agricultural condition (Kamaluldeen *et al.*, 2014). The nutrients in the activated sludge provide the growth substances for okra and increase the amount of leaves. As a comparison, number of leaves for the okra growing in potting soil is found to be 10.33 leaves/pot. However, the number of leaves is not enough to compare the capability for the growth of leaves. The dried weighted are requred to describe the total trend of leaves development.

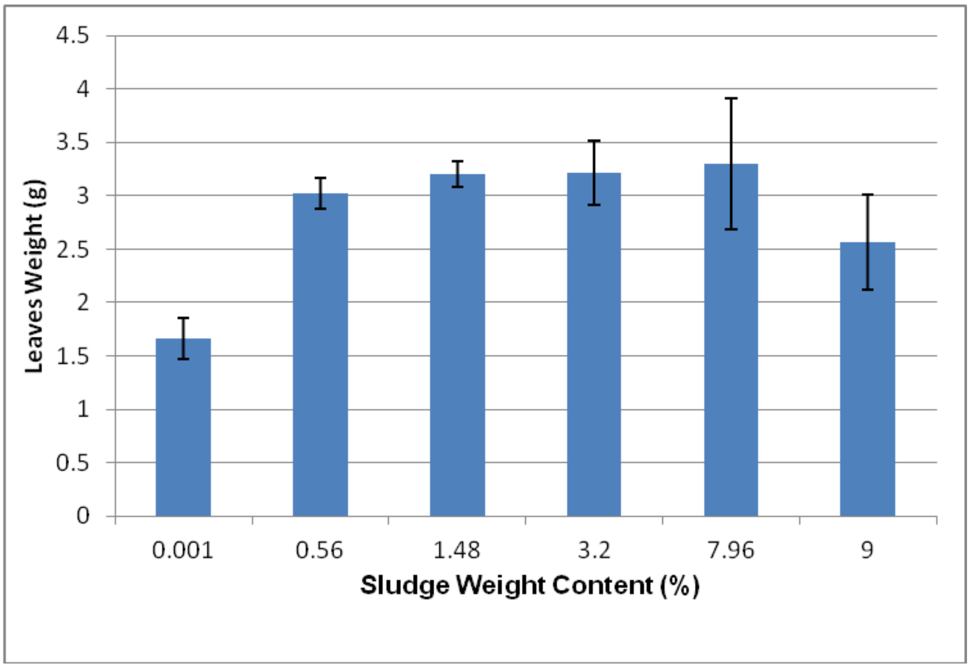

Figure 4. 27 Overall leaves dried weight for the okra growing in arid sand, Eco-Soils and potting soil

The overall Leave Dried Weights (LDW) are shown to be increasing along with the increasing fraction of activated sludge in the Eco-Soils. The LDWs increase from 1.66 to 3.30 g/pot. The overall LDW of okra growing in Eco-Soil of SSVR 20:80 is twice of that in arid sand (SSVR 100:0). This result reveals the significant improvement of the LDW due to the introduction of activated sludge. The LDW in the SSVR 20:80 is found to be fluctuated due to low LDW in two of pots and reduces the average LDW. This reflects the rich nutrients and carbon source in the Eco-Soil of SSVR 20:80 perform unstable development of vegetation for nutrient uptake due to low conductivities. As observed from the SSVR 40:60 and 60:40 samples, the average LDWs are 3.02 and 3.20 g/pot respectively. These values indicate the high efficiencies of nutrient uptake by okra due to appropriate hydraulic conductivities and nutrient pressure (Olomilua et al., 2007; Akpan-Idioka et al., 2012). The average LDW for the okra growing in potting soil is found to be 2.57 g/pot and served as reference value. Based on the consideration of efficiency of nutrient uptake and activated sludge application, the SSVR 40:60 is found to be an optimal selection for leaves growth.

4.3.2.3 Root Development and Dried Weight

The development of roof of a plant is important to reveal the water and nutrient availability of the growing environment. The root systems appear to be different in nutrient deficient substrate compared to sufficient environment.

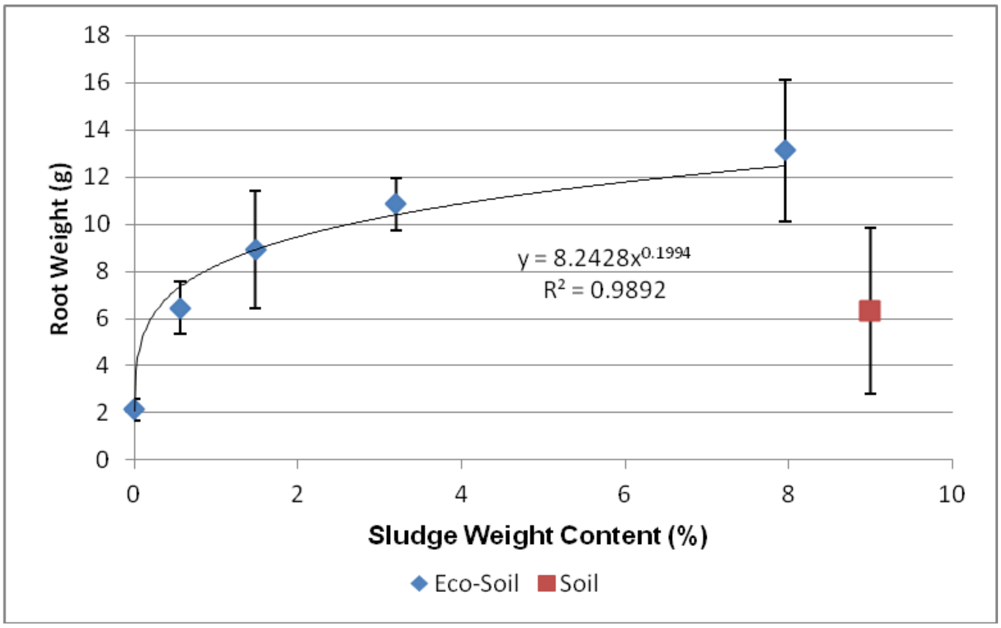

Figure 4. 28 Root Dried Weights for the okra growing in arid sand, Eco-Soil and potting soil

Figure 4.28 shows the overall root dried weights (RDW) for the okra growing in arid sand, Eco-Soils and potting soil. The RDW is found to be increased from 2.15 to 13.12 g/pot due to the increasing nutrient concentration and water retention brought by activated sludge. The distribution is found to be exponential and able to be expressed by

$$[\mathrm{RDW}] = 8.2428[\mathrm{SLC}_{\mathrm{wt.\%}}]^{0.1994} \quad \text{(Eq 4. 24)}$$

where the [RDW] is Rood Dried Weight and $[\mathrm{SLC}_{\mathrm{wt.\%}}]$ is SSWR for Eco-Soil.

The regression coefficient is found to be 0.9892, which indicates a good match with the experimental results.

The RDWs are found to be proportional to the activated sludge fraction in the Eco-Soils. In other words, the nitrogen, phosphorus and potassium contents in the activated sludge offer essential nutrients for root growth (Akpan-Idioka et al., 2012). The higher RDWs also indicate higher availabilities of moisture and nutrients in the growing medium because the root explores the underground environment through gravitropism, thigmotropism, chemotropism, and hydrotropism (Zuo, *et al.*, 2016). The high developed root system reflects higher water and nutrient requirements, which is due to greater growth rate for the upper ground part of plant.

4.3.2.4 Root/Shoot Ratio

The Root/Shoot Ratio (RSR) describes the weight fraction of a plant's under-ground to upper-ground part. The RSR indicates the concentration of nitrogen and phosphorus in the substrate and the uptake rate for the plant (Harris, 1992).

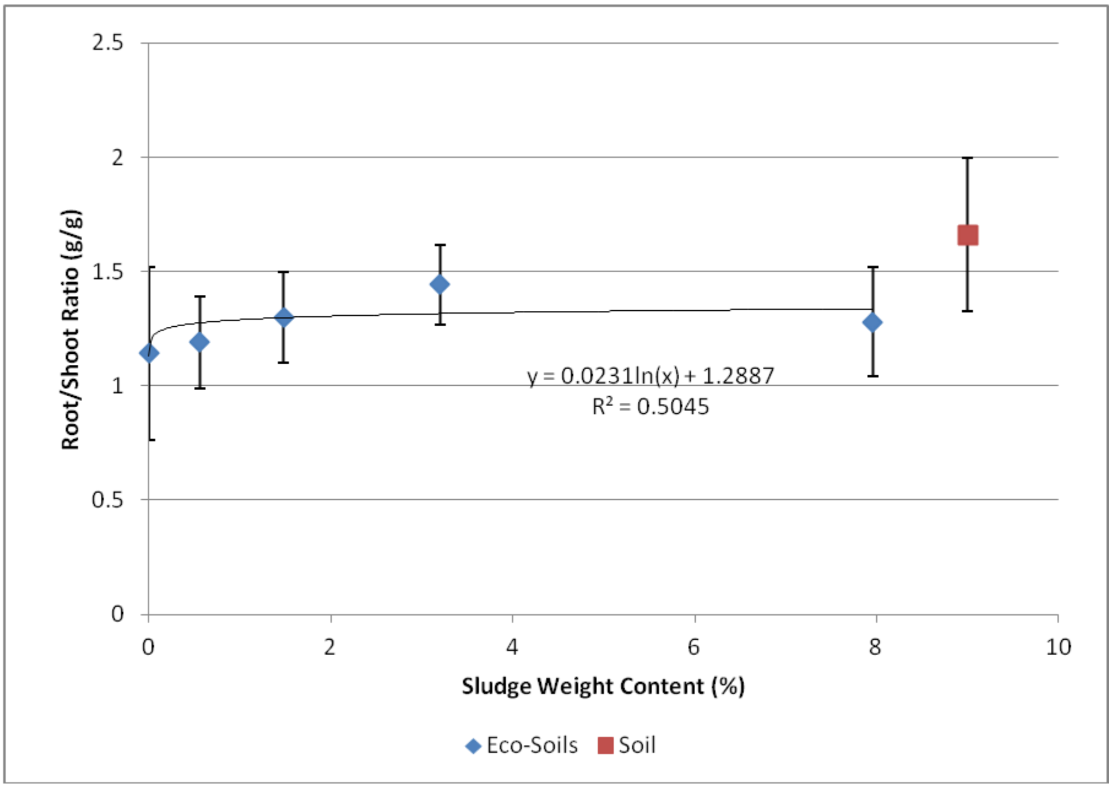

Figure 4. 29 Roof/Shoot ratio of okra growing in arid sand, Eco-Soils and potting soil

Figure 4.29 shows the RSR of okra growing in arid sand, Eco-Soil and potting soil. The RSRs increase from 1.14 to 1.44 g root /g shoot for SSVR 40:60 but reduce to 1.28 g root /g shoot for SSVR 20:80. However, the difference is not so significant for all the plant samples. It has been reported that higher R/S ratio results in stable and healthy performance for a plant (Harris, 1992; Kamaluldeena *et al*., 2014). High RSR indicates that the weight fraction of root is larger than 1.5 times of shoot. This condition usually appears in water or nutrients deficient situation, especially nitrogen. Low RSR reveals improper nutrients uptake, especially phosphorus. From the average values of RSR, the nutrients provided by activated sludge results in fast growing rate for okra (Harris, 1992; Wilsey and Polley, 2006). The nutrients can be obtained from various sources, either the nitrogen fixing bacteria or water. However, the phosphorus is usually provided by the substrates and has low migration abilities (Lincon and Eduardo, 2010). The okra growing in arid sand shows a very low RSR because no phosphorus could be supplied from the sand. With the increasing activated sludge fraction in the Eco-Soil, the RSR increases up to 1.44 g root /g shoot. The okra reflects a lower RSR in the SSVR 20:80 due to the lower mobility of phosphorus due to very low hydraulic conductivity in the substrate. The RSR for okra growing in the potting soil was shown to be 1.66 g root /g shoot and served as a reference. However, the RSR for potting soil also deviates from the optimal value because the higher hydraulic conductivity and macro pores reduce the retention abilities of moisture (Home et al., 2002). From the RSR point of view, the SSVR 40:60 would be a good selection for achieving healthy growth of okra.

4.3.3 Pods Produced from Plant Samples

4.3.3.1 Amount of Pods

The harvesting period for the plant sample started from 105th days from seeding. The number of pods and the weights of pods are important indicators for the nutrient concentration and utilization.

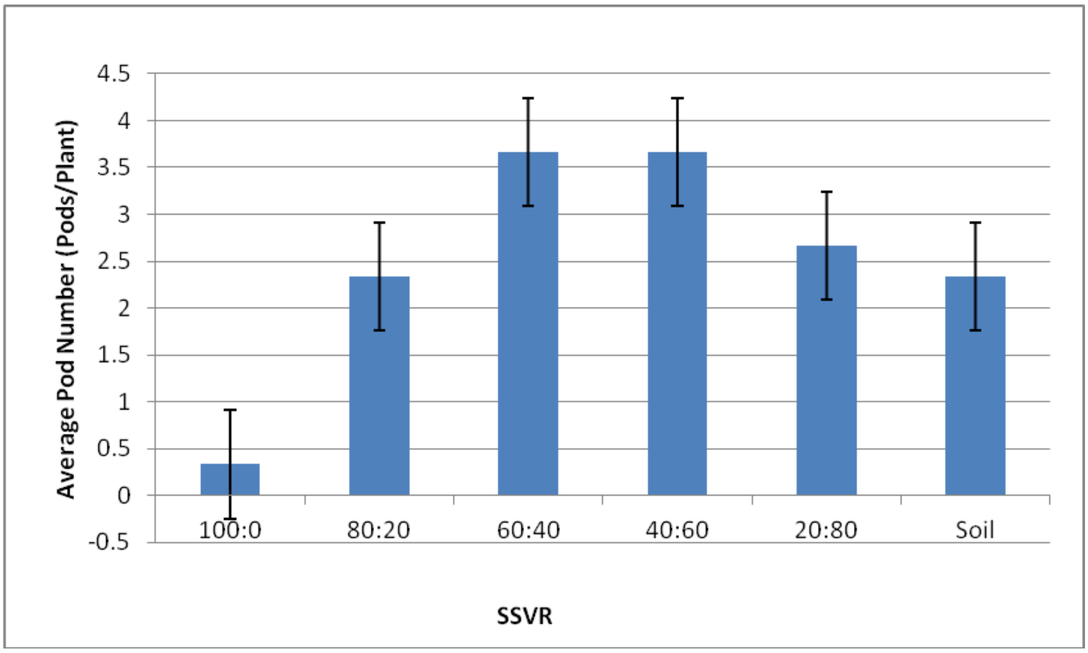

Figure 4. 30 Number of pods produced from okra growing in arid sand, Eco-Soil and potting soil

Figure 4.30 illustrates the number of pods produced from okra growing in arid sand, Eco-Soils and potting soil. The number of pods per plant increase from 0.33 to 3.67 when the volumetric content of activated sludge increase from 0 to 40 vol.%. However, the okra growing in SSVR 20:80 only produces 2.67 pods/plant with high fluctuation. For comparison, the pods produced in potting soil are found to be averagely 2.33 pods/plant. In the observation period, only one pod could be harvested from the okra growing in arid sand and the size and weight of the pod are found to be abnormal as compared to that from other growing mediums (Olomilua et al., 2007; Akpan-Idioka et al., 2012; Kamaluldeena *et al.*, 2014). The macro- and micro-nutrients in the activated sludge stimulate the growth of okra and therefore the pods (Home et al., 2002). From SSVR 80:20 to 20:80, the numbers of harvested pods are larger than that from potting soil. For one thing, sufficient pods production indicates a completed growing cycle could be achieved in Eco-Soils. Secondly, in view of the pods number, the overall performance for Eco-Soil is better than potting soil. This phenomenon indicates the combination of activated sludge and arid sand offers appropriate nutrients concentration and utilization even better than potting soil. The optimized pods number is found from the plants growing in Eco-Soil of SSVR 60:40 and 40:60. The over rich nutrient concentration and low hydraulic conductivity in SSVR 20:80 result in low nutrient utilization rates and a fluctuating performance.

4.3.3.2 Pod Dry Weights

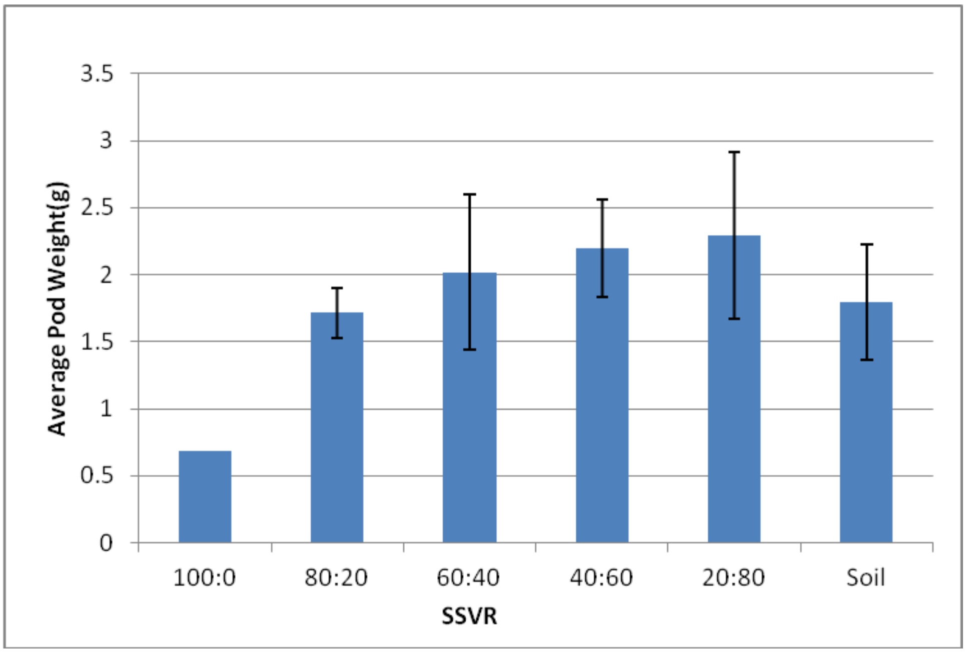

Figure 4. 31 Pod dried weight for okra growing in arid sand, Eco-Soil and potting soil

Figure 4.31 shows the pod dried weight (PDW) for okra growing in arid sand, Eco-Soil and potting soil. The average pot dried weight reflects the nutrient uptate efficiency for the okra in various growing substrates. The okra growing in arid sand

(SSVR 100:0) only produces one pod during the growing period and the pod dried weight is found to be 0.6817 g/pod, which is much lower than other samples. The average PDWs for Eco-Soil range from 1.7151 to 2.3250 g/pod. The overall trend of PDWs is proportional to the introduction of activated sludge, in other words, the nutrient concentration. However, the PDWs for SSVR from 60:40 to 20:80 are not distincted from each other. As a comparison, the average PDW for the pods harvested from the plant samples growing in potting soil is found to be 1.7945 g/pod. In addtion, the PDWs for Eco-Soils perform comparable to the normal growing medium (Akpan-Idioka et al., 2012; Kamaluldeena *et al*., 2014). Within the Eco-Soils samples, the maximum PDW is found in SSVR 20:80 and this revealed the richest nutrient concentration. However, the PDWs for SSVR 60:40 and 40:60 are also larger than the one in potting soil. From the aspect of activated sludge consumption, the SSVR 60:40 would be a better selection.

4.3.4 Seeds Produced from Plant Samples

Seeds analysis reflects the nutrients concentration in the growing substrates and the efficiencies of nutrients utilization. In addition, the seeds analysis also indicates the reproduction abilities of plants.

4.3.4.1 Amount of Seeds

This part focuses on the total amount of seeds produced from each plant. A plant under healthy growing cycle should produce enough amount of seeds for reproduction.

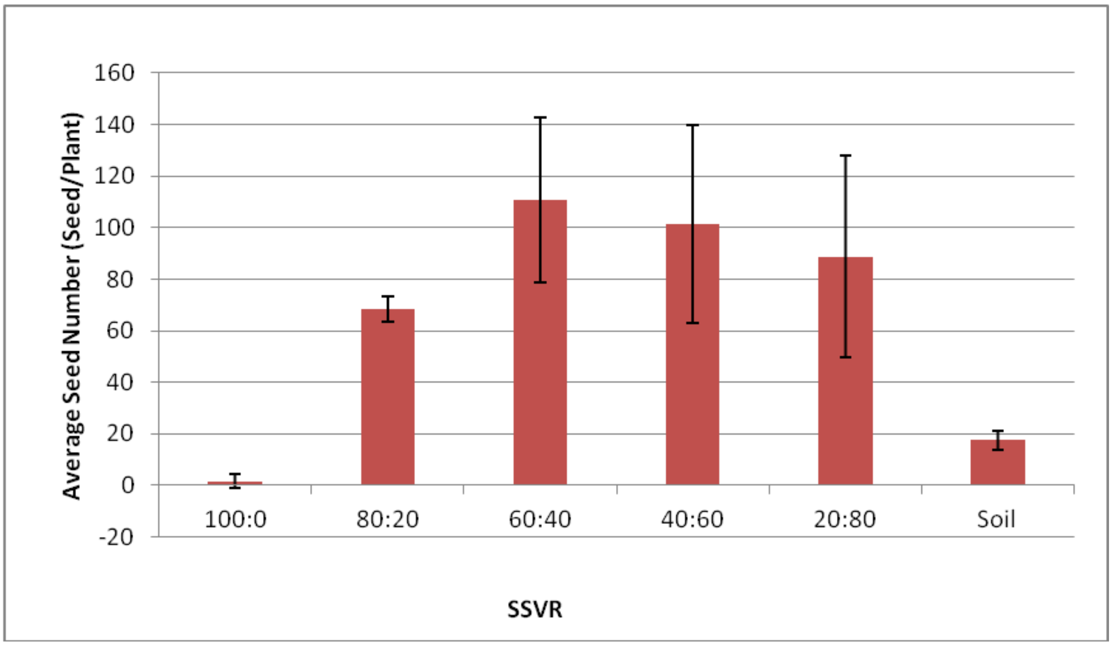

Figure 4. 32 Seed number per pants for okra growing in arid sand, Eco-Soil and potting soil

Figure 4.32 shows the seed number per plant for okra growing in arid sand, Eco-Soil and potting soil. Only one pod can be harvested from the plant in arid sand and 5 matured seeds are found inside the pod. Figure 4.32 shows that 68.33 to 110.67 seeds/plant can be harvested from the okra growing in Eco-Soils samples. The highest seed number is produced from the okra growing in SSVR 60:40 Eco-Soil and indicates the strongest reproduction abilities. The seed harvested from the okra growing in potting soil is found to be 17.50 seeds/plant. The average seed numbers from the okra are found to have little differences among Eco-Soil samples. However, the dramatic change appears when comparing the samples of SSVR 100:0 to 80:20. Thought the nutrients were richest in the potting soil in the initial stage, the high hydraulic conductivities and macro pores exhibit reverse effects in nutrients and moisture content absorption (Home et al., 2002).

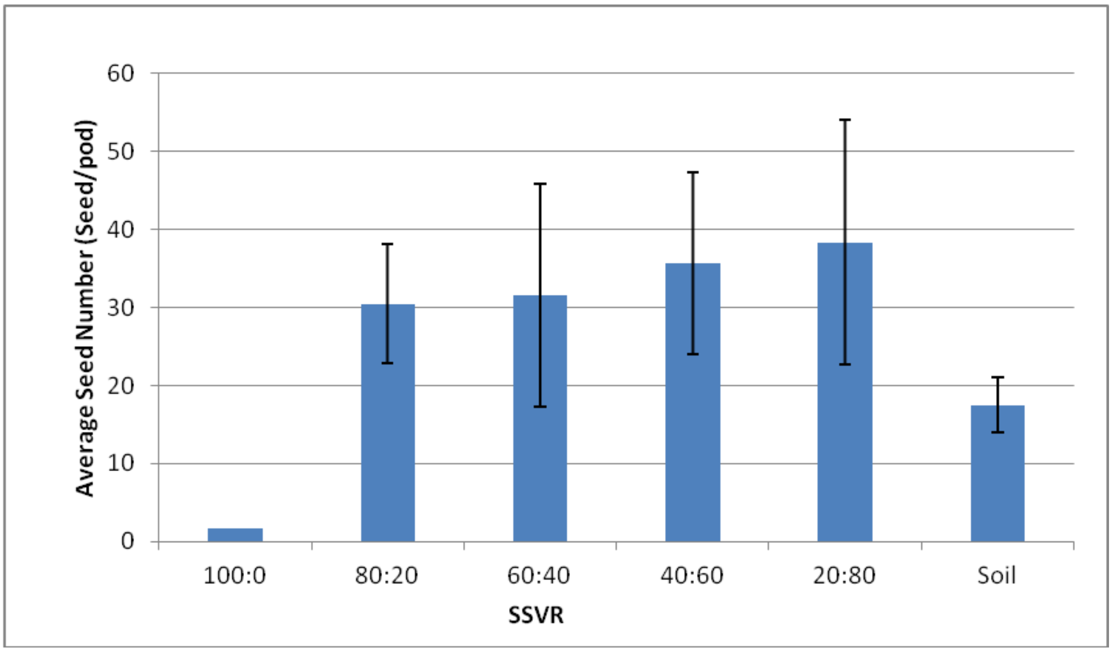

Figure 4. 33 Seed number per pod for okra growing in arid sand, Eco-Soil and potting soil

Figure 4.33 shows seed number per pod for okra growing in arid sand, Eco-Soils and potting soil. Similar with the data for seed number per plant, the arid sand is found to be nutrient and moisture deficient and produces lowest amount of seeds. This is also one of the reasons why the loss of soil productivity results in irreversible change of the environment (Akpan-Idioka et al., 2012). However, with the introduction of activated sludge, the seed numbers increase drastically from 27.16 to 38.33 seeds/pod for okra growing in Eco-Soils. The highest number of seeds in the pods is found from the SSVR 20:80 and indicates better nutrients utilization in producing seeds. The average PDW for the okra growing in SSVR 20:80 is therefore also the highest among the substrates. However, the pods production in SSVR 20:80 is weaker than the 60:40 and 40:60, results in low seed number per plant. Under the same irrigation and environmental conditions, the okra growing in potting soil produces 17.50 seeds per pod. All okras growing in Eco-Soil perform better than that in potting soil. This result reveals the better nutrient uptake efficiency for Eco-Soil.

4.3.4.2 Seed Dried Weight

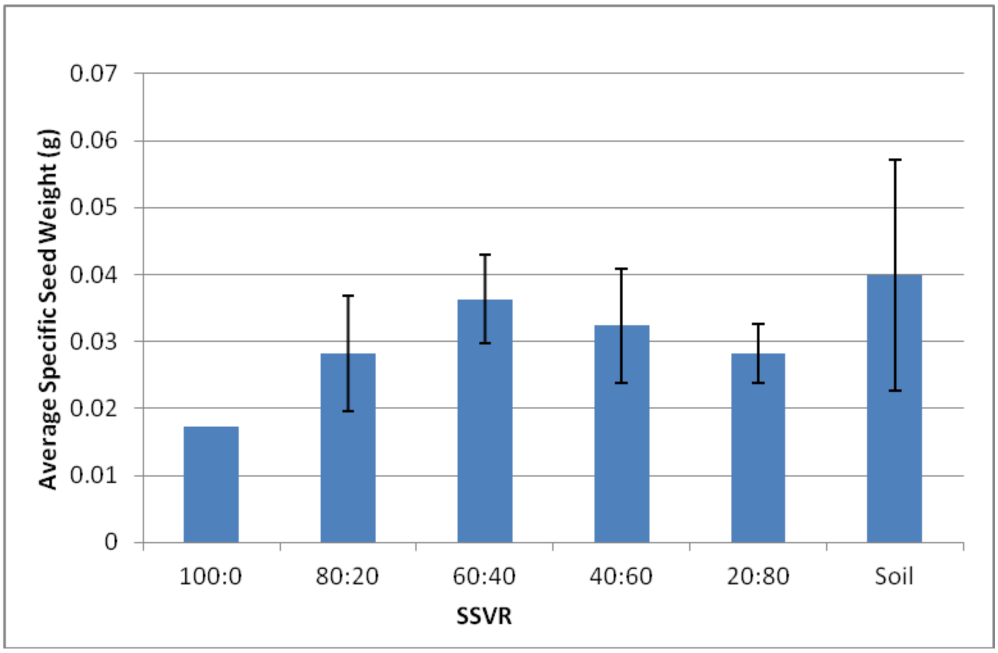

Figure 4. 34 Specific seed dried weight for okra growing in arid sand, Eco-Soil and potting soil

Figure 4.34 shows the specific seed dried weight (SSDW) for okra growing in arid sand, Eco-Soils and potting soil. Because of lack of nutrients, the SSDW of okra growing in arid sand is found to be 0.0173 g/seed which is the lowest value. The weight indicates the maturity of seed. The weight of cotyledon, which provides nutrients for germination of seed, is proportional to the weight of a seed. The seed with lower cotyledon content would be hardly or unable to be germinated. The productivity of the seeds for okra growing in arid sand is found to be weak and results in low reproduction ability. Therefore, the effective way to mitigate and combat desertification should be increasing the productivities in the growing medium in the form of offering nutrients and retaining moisture (Kassas *et al*., 1991). From the data for okra growing in Eco-Soil, the data ranges from 0.0282 to 0.0363 g/seed and the highest SSDW appears for the ones growing in SSVR 60:40 samples. The results for Eco-Soil indicate the high nutrient uptake and utilization in SSVR 60:40. However, the differences between each mixture were not significant. The SSDW from potting soil is found to be 0.0399 g/seed and reveals highest seed availability.

From the performance of the okra to be growing in Eco-Soils, the SSVR 60:40 would be a good selection for achieving sufficient amount of seed and plant availability.

4.3.5 Macro- and Micro-Nutrients

The macro- and micro-nutrients including N, P, K and tracer elements are essential to growth of vegetation. The heavy metal contents are the main factors limiting the application of activated sludge. This section investigates the aforementioned substance concentrations in the Eco-Soil to reveal the reasons behind the growth results of Okra.

4.3.5.1 Macro-Nutrients

Nitrogen, phosphorus and potassium are three macro-nutrients for the growth of vegetation including okra because they are essential elements for plant cells.

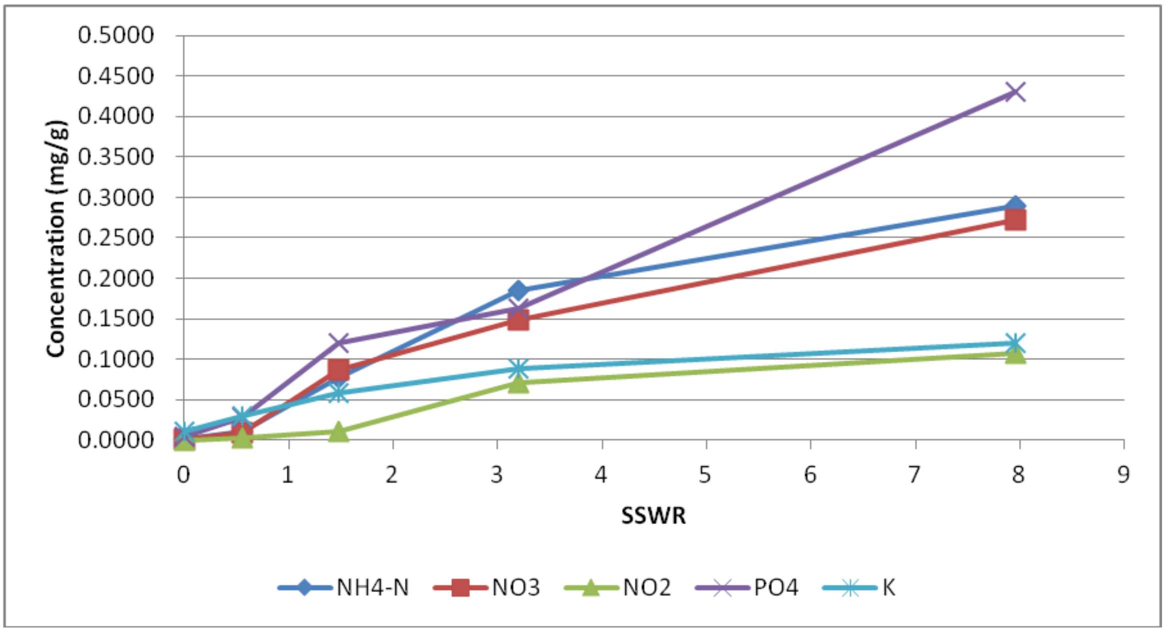

Figure 4. 35 Nutrients for arid sand, Eco-Soil and commercial potting soil samples

Table 4. 7 Nutrients concentration, electric conductivity and pH for arid sand, Eco-Soils and commercial potting soil samples

SSVR	NH_4^+	NO_3^-	NO_2-	PO_4^{3-}	K^+	E-Conductivity	pH
	(mg/g)	(mg/g)	(mg/g)	(mg/g)	(mg/g)	(μ S/cm)	(1:10)
100:0	0.0005	0.0010	0.0004	0.0040	0.0115	6.01	7.01
80:20	0.0103	0.0094	0.0028	0.0282	0.0304	369	6.71
60:40	0.0775	0.0862	0.0103	0.1206	0.0589	610	6.49
40:60	0.1857	0.1486	0.0706	0.1634	0.0890	922.5	6.19
20:80	0.2888	0.2725	0.1079	0.4305	0.1201	1517	6.18
Soil	0.4117	3.6024	0.0062	2.3587	4.8211	1359.5	5.28

Figure 4.35 shows the nutrients, including ammonia, nitrate, nitrite, phosphate and potassium, for arid sand, Eco-Soil and commercial potting soil samples. They represent the macro nutrients for the growth of vegetation. From the curves, the concentration of the nutrients is found to be proportional to the sludge weight content. In addition, the proportionalities are shown to be linear. The nutrients for arid sand are found to be the lowest in the samples. When the nutrients contained in the cotyledon of seed are used up after germination, the low nutrients are not able to sustain the growth of vegetation. Although enough moisture is provided to the plants, the new

cell production and further fruiting is unable to achieve (Lincoln and Eduardo, 2010).

As the introduction of activated sludge, the nutrients including nitrogen, phosphorus and potassium are greatly increased and the concentrations are shown to be linear with the sludge weight contents. The nutrients brought by the activated sludge are found to be comparable to nutrient requirements for plants including Okra (Kouame, 2004). However the ammonia content occupies higher portion in the nitrogen contents for the Eco-Soil as compared with potting soil. The nitrate is the ready uptake nutrient for plants (Lincon and Eduardo, 2010). Therefore, the growth of the plants in Eco-Soil is slower than that in the potting soil for the initial stage of the growing period (Figure 4.23).

However, because the sand provides voids for Eco-Soil to increase the macro pore to allow the ammonia to be oxidized to be nitrite and then nitrate, the ammonia nitrogen content is able to be utilized by vegetation. In addition, compared with potting soil, the lower hydraulic conductivities for Eco-Soil also enhance the effects for retaining the nutrients in the substrates other than drawing out in bottom runoff. Though the commercial potting soil contains rich nutrients in the very beginning (Home *et al.*, 2002), the high hydraulic conductivity makes the nutrients draw out from the growing space when water is irrigated to the substrate. This is why the nutrients dismissed and the sustainable growth of plants is not able to be maintained, unless external nutrients are provided. The loss of nutrients due irrigation results in low fruiting rate for the plant growing in potting soil, because the nutrient retention ability is weaker than that of Eco-Soils.

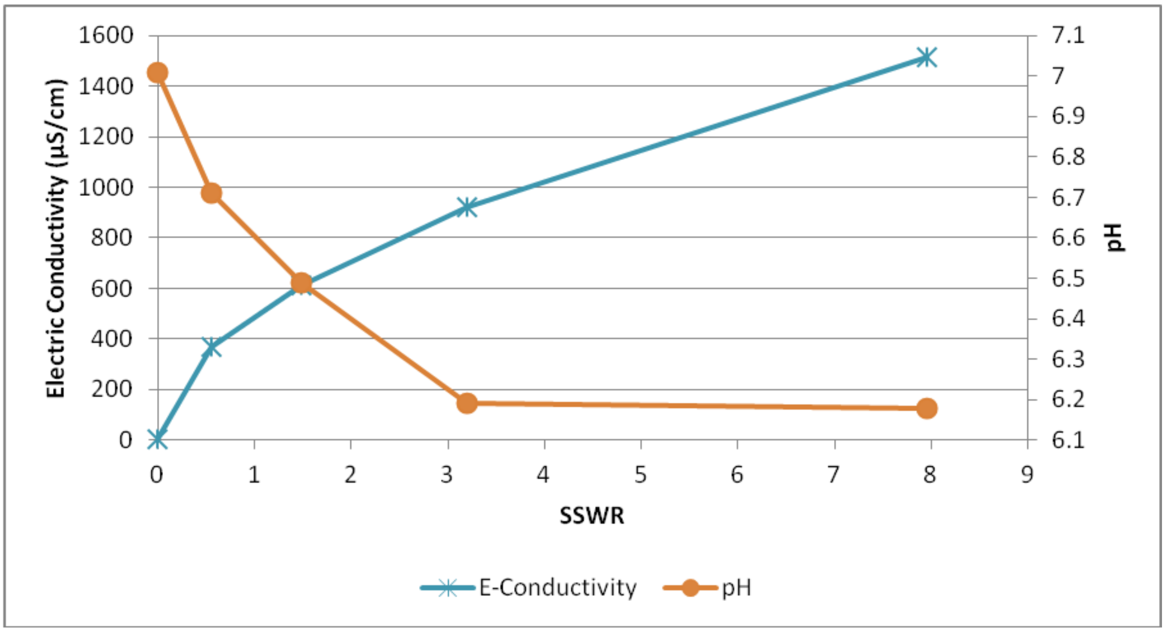

Figure 4. 36 Electric conductivity and pH for arid sand, Eco-Soil samples

The electric conductivity (EC) and pH for arid sand, Eco-Soils samples are shown in Figure 4.36. The EC is found to be proportional to the sludge weight content while the pH is reverse. It has been reported that high EC results in low germination rates in the seed germination assay (Stefanakis et al., 2011; Komilis and Tziouvaras, 2009). This is the reason for declining germination rate for Eco-Soils with higher activated sludge content.

The activated sludge exhibits lower pH, compared with 7, therefore, the pH for Eco-Soils reduces from 7.01 to 6.18. However, the pH for potting soil was around 5.28. The okra shows affinity to pH soil under 6~7 (Akpan-Idiok *et al.*, 2011), therefore the growth of the plants is found to be better for Eco-Soils contain enough nutrients and appropriate pH than potting soils. In addition, most of the vegetations grow well in the substrates with pH between 6~7 (Lincon and Eduardo, 2010).

4.3.5.2 Micro-Nutrients

Heavy metals are also nutrients for the growth of vegetations. However, if the heavy metal contents are too high, the substrates exhibit toxicity towards plant growth.

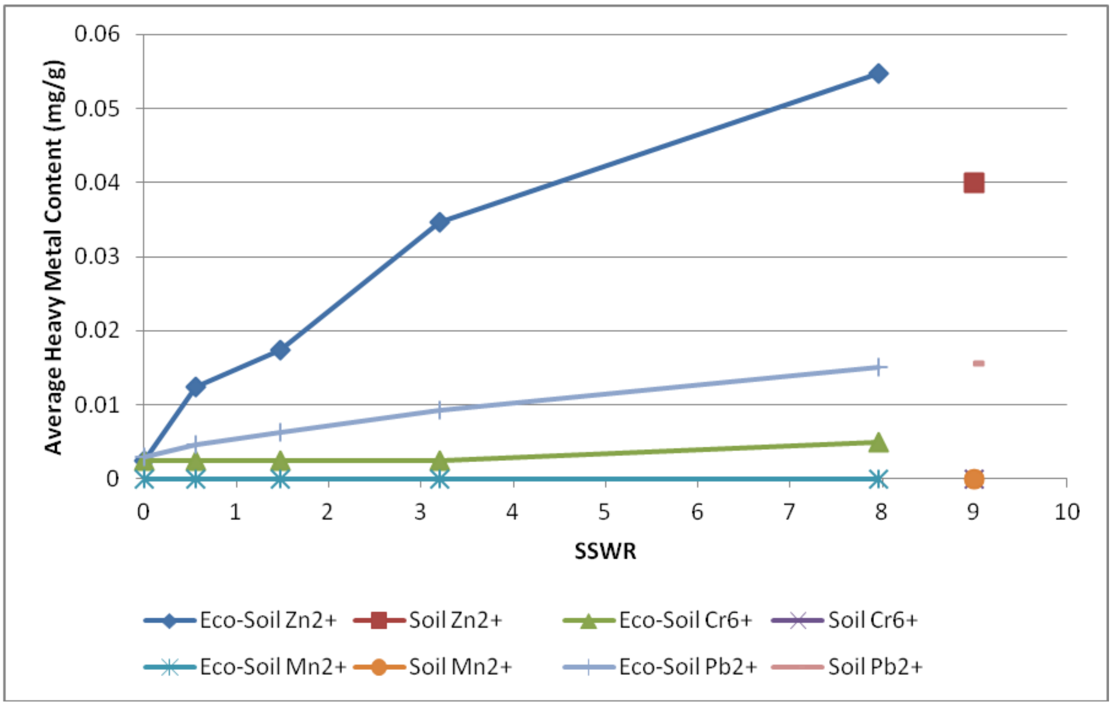

Figure 4. 37 Zn^{2+}, Cr^{6+}, Mn^{2+} and Pb^{2+} concents for arid sand, Eco-Soil and commercial potting soil samples

Zn^{2+}, Cr^{6+}, Mn^{2+} and Pb^{2+} are main heavy metal contents studied in literatures for activated sludge applications (Wang *et al*. 2005; Pathak *et al.*, 2009). Figure 4.37 shows that the Zn^{2+}, Cr^{6+} and Pb^{2+} increase proportionally to the addition of activated sludge weight contents. The Mn^{2+} is found to be below the detection limits and thought to be not presented in the Eco-Soil samples. The average Zn^{2+} content increases from 2.445 ~5.465 $\times 10^{-3}$ mg/g sample while Pb^{2+} and Cr^{6+} from 2.920 ~15.059$\times 10^{-3}$ mg/g and 2.444~4.968 $\times 10^{-3}$ mg/g sample, respectively. Compared to the standards for sludge application, they are all within the application limits.

Table 4.8 Pollutant Limits for the Land Application of Sewage Sludge (Adapted from USEPA, 1994)

Concentration Limits		
Pollutant	**Ceiling Concentrations (Table 1 of 40 *CFR* 503.13) (milligrams per kilogram, dry weight)**	**Pollutant Concentrations (Table 3 of 40 *CFR* 503.13) Monthly Average (milligrams per kilogram, dry weight)**
Arsenic	75	41
Cadmium	85	39
Chromium	3,000	1,200
Copper	4,300	1,500
Lead	840	300
Mercury	57	17
Molybdenum*	75	--
Nickel	420	420
Selenium	100	36
Zinc	7,500	2,800

From Table 4.8, they are all below the required limits for application stated in USEPA standard, which is also used as worldwide reference. The reason is because the activated sludge used in this study comes from the domestic wastewater treatment works in Hong Kong. The sources of wastewater are mainly refuses from citizen and restaurants. In addition, aerobic biological method is used as the core treatment process in the treatments works. Therefore, the heavy metal contents are low in the activated sludge. The remained are used as micronutrients for vegetation growth (Lincoln and Eduardo, 2010). In the real application of Eco-Soil for anti-desertification, the activated sludge from adjacent domestic sewage treatment works is suggested.

The study of macro- and micro- nutrients for growing medium offers in-depth analysis of the phenomenon of plant growing patterns and references for selection of composition of Eco-Soils for anti-desertification.

4.3.6 Summary

This section illustrates the performances of Eco-Soil in growing Okra, compared to arid sand and commercial potting soil. The results showed that the outcomes, including SDW, RDW and LDW, are significantly improved due to introduction of activated sludge. The moisture retention capabilities and nutrients provide essential growth conditions to the growth of vegetation. Within the Eco-Soil samples, the SSVR 60:40 achieves the highest performance, such as pods number, seed numbers and seed weights, and is even better than commercial potting soil. The macro- and micro- nutrients analysis reveals the reasons for the differences of the outcomes. The results indicate the optimal SSVR is 60:40 in the consideration of application efficiency and performance.

4.4 Rainfall-Runoff Analysis for Eco-Soil

In arid area, the water comes from limited precipitation and ground water. The rainfall retention is important for the moisture uptake for vegetation near ground surface and maintaining appropriate humidity. The precipitation falls on the ground and becomes surface runoff after abstraction. However, within the abstraction, the water goes into the deeper layer if the retention capability of the upper soil is low. This limits the ground water uptake for most of the vegetation. By the study of rainfall runoff hydrograph, the retention and detention of the precipitation by Eco-Soils that can be used to mitigate and even combat the desertification.

Hydrograph is important to indicate the rainwater retention and peak detention for growing medium under various precipitation scenarios, and reveal the fraction for distribution of surface and ground water (Gregoire and Clausen, 2011).

The rainfall runoff hydrograph for arid sand (SSVR 100:0), Eco-Soils (SSVR 80:20, 60:40, 40:60 and 20:80) and commercial potting soil under 10, 30, 50, 70 and 100 mm/hr were studied and illustrated in Figure 4.47~4.52.

4.4.1 Control Tank

The intensity of 10, 30, 50, 70 and 100 mm/hr covers the rainfall for 100 year return period occurrence. Therefore the hydrograph produced from these intensities offer valuable reference by applying Eco-Soil in various areas including arid area.

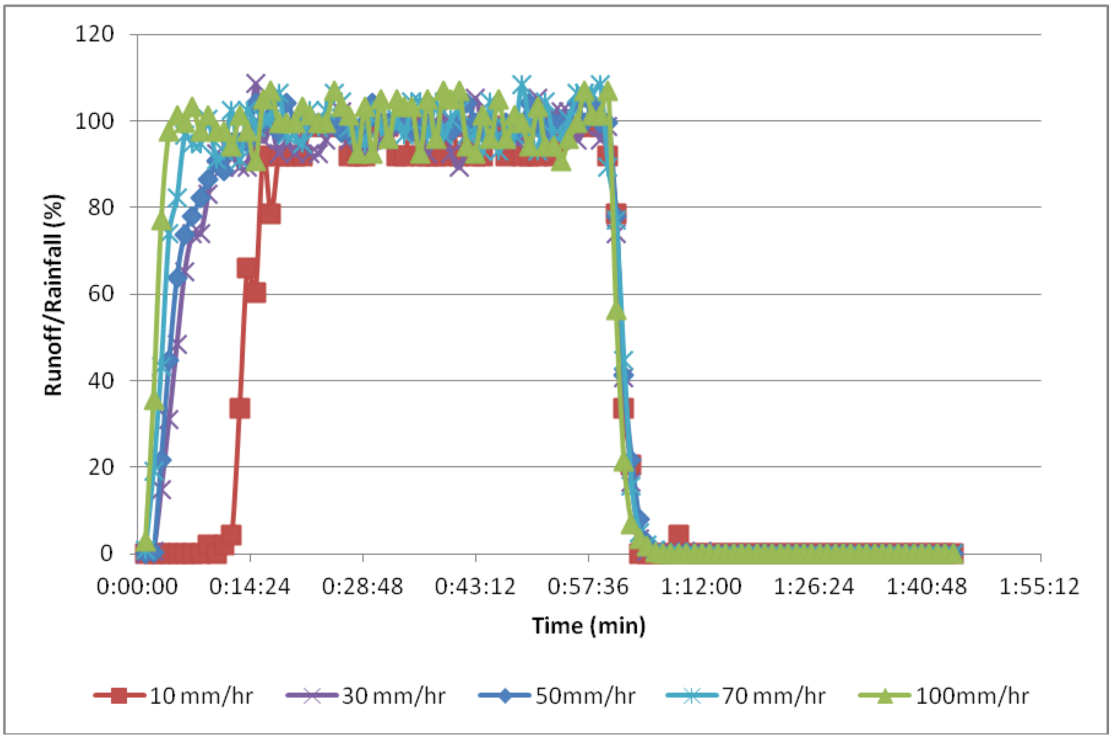

Figure 4. 378 Hydrographs for control tank under various rainfall intensities

Figure 4.38 shows the hydrograph for control tank under rainfall intensities of 10, 30, 50, 70 and 100 mm/hr. The hydrograph indicates that the detention of rainfall is able to be observed in control tank due to the retention of water by filter layer and surface tension of the structual materials, such as grid and supporting blocks. The time for the runoff from far end to the drain is another reason for detention in control tank. The detention effects are obviously reduced as the intensity increase from 10 to 100 mm/hr. However, the detention for the control tank is not contributed by the substrate but the arrangement of the drain port.

4.4.2 Arid Sand

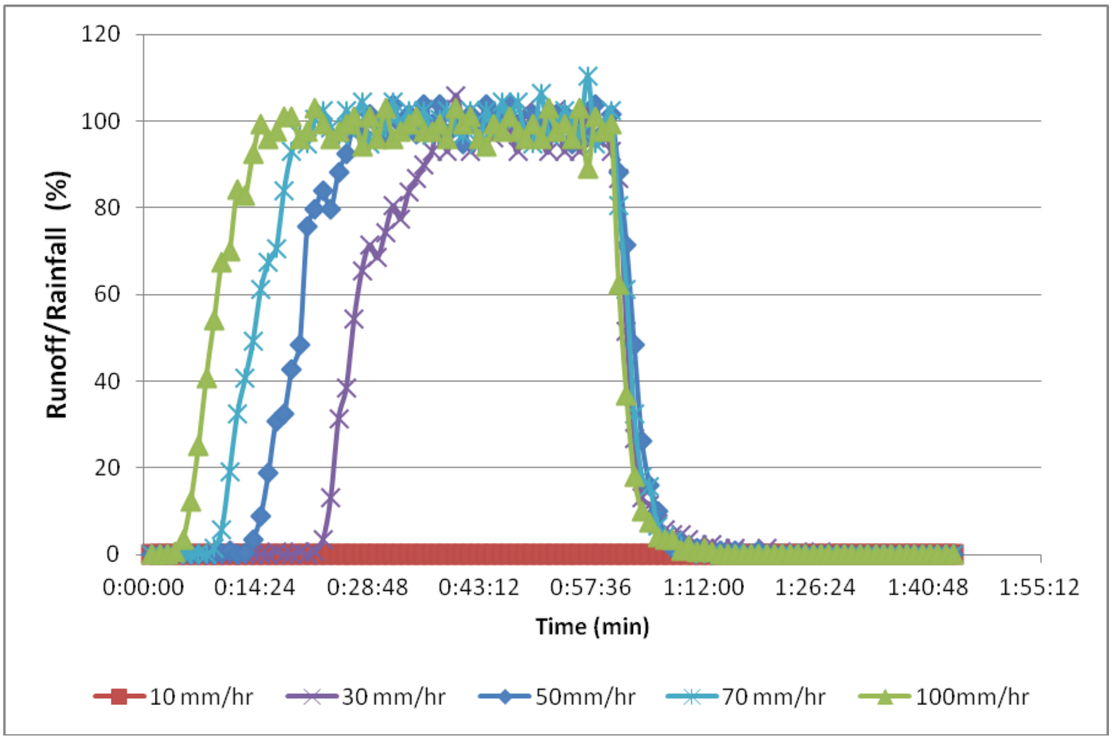

Figure 4. 39 Hydrograph for arid sand (SSVR100:0) tank under various rainfall intensities

The hydrograph for the runoff from arid sand under various rainfall intensities is shown in Figure 4.39. Only four curves are obtained in Figure 4.39 because no runoff is observed from the arid sand sample under 10 mm/hr. In other words, the rainfall of intensity 10 mm/hr is completely retained by arid sand in this experiment. The other four hydrographs is oberved to to have larger differences than those of the control tank.

The hydrograph climbs up and reach plateau for the process when bottom runoff appears and increases to reach the peak runoff. The part of hydrograph, which develop from zero runoff to peak runoff and appears climbing up manner, is defined as the increasing phase by using the Five Phases Analysis method. Slop of this part is closely related to the soil hydraulic conductivity, porosity. To take this part of hydrogh (increasing phase) for study, the data points between 5% to 95% runoff/rainfall are analyzed separately.

The slops for the increasing phase for 30, 50, 70 and 100 mm/hr increase from 8062.7 to 14330 and are shown in Figure 4.40. The slops of the increasing phase were found to be proportional to the ranfall intensities for the same substrate.

The peak detentions of the runoff were defined as the percentage rainfall reached 95% because the peak runoff is found to be fluctuating within 5%.

The peak detention for rainfall intensities of 30, 50, 70 and 100 mm/hr is found to reduce from 38 to 15 min. This is because the maximum retentions capacities for the substrates have been reached and the hydrograph reach plateau (> 95% rainfall rate).

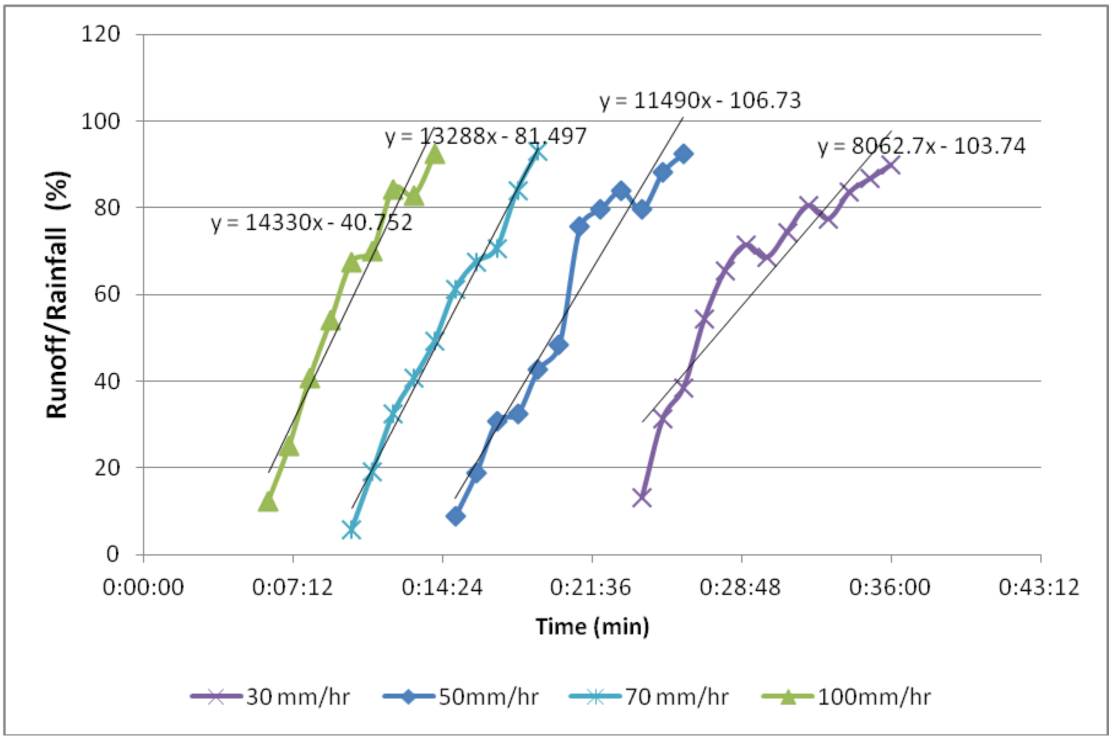

Figure 4. 40 Increasing phases for arid sand (SSVR 100:0) hydrographs under various rainfall intensities

4.4.3 Eco-Soil of SSVR 80:20

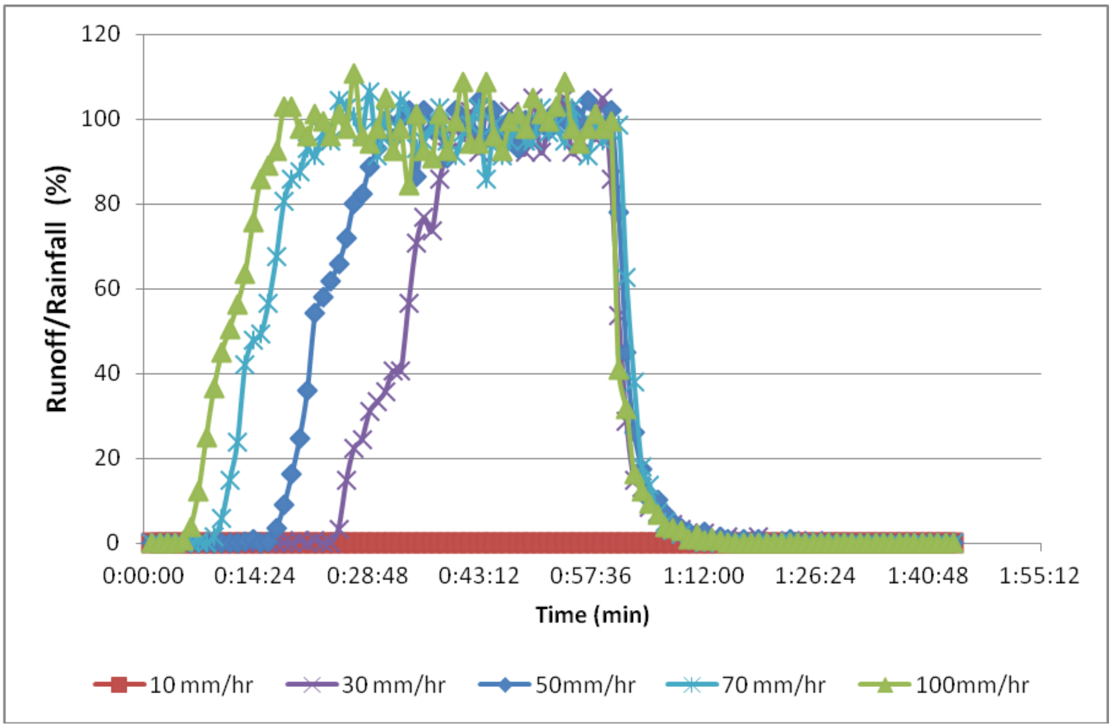

Figure 4. 41 Hydrographs for Eco-Soil of SSVR 80:20 under various rainfall intensities

Figure 4.41 shows the hydrograph for Eco-Soil of SSVR 80:20 tank under various rainfall intensities. The hydrograph for 10 mm/hr rainfall is also found to be invisible because no runoff can be observed from this intensiy. The differences for remaining hydrographs for 30, 50, 70 and 100 mm/hr rainfall are larger than those for arid sand due to lower hydraulic conductivities. These differences are also revealed by the longer peak runoff detentions of the peak runoff. The peak runoff dentention decreases from 40 to 18 min for rainfall intensity increased from 30 to 100 mm/hr.

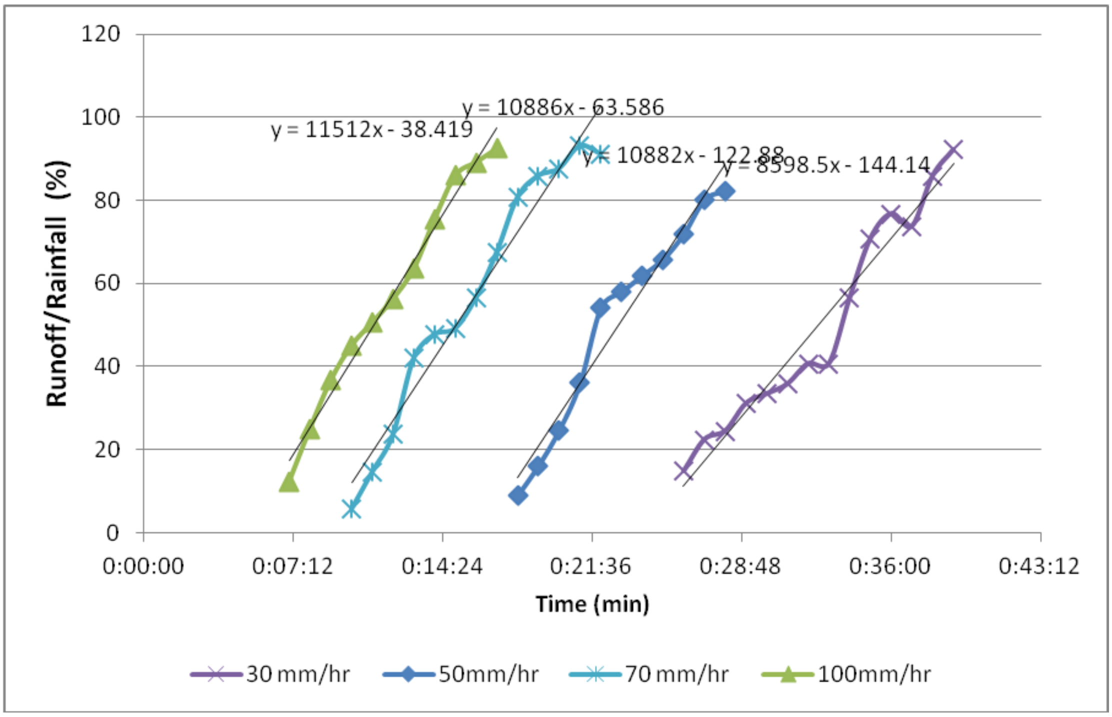

Figure 4. 38 Increasing phases for Eco-Soil of SSVR 80:20 hydrographs under various rainfall intensities

The increasing phases for Eco-Soil of SSVR 80:20 hydrographs under various rainfall intensities are shown in Figure 4.42. The slops of the increasing phase vary from 8598.5 to 11512 according to the enlarging rainfall intensities and are smaller than that for arid sand.

4.4.4 Eco-Soil of SSVR 60:40

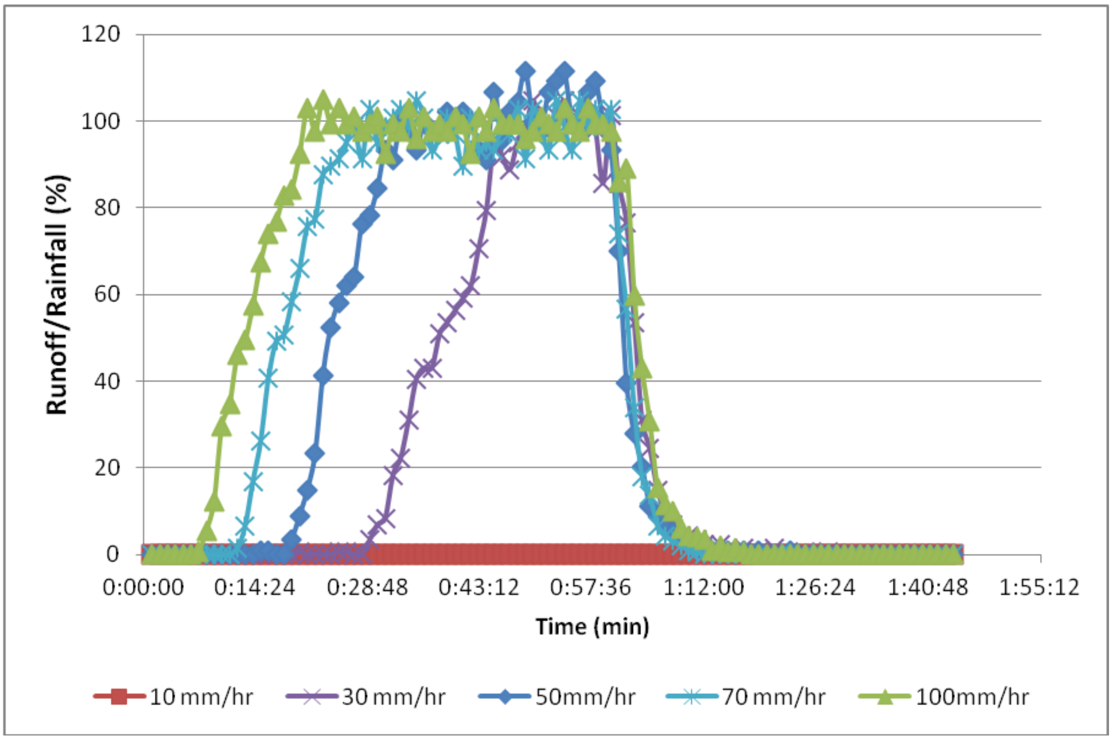

Figure 4. 39 Hydrographs for Eco-Soil of SSVR 60:40 under various rainfall intensities

Figure 4.43 shows the hydrograph for Eco-Soil of SSVR 60:40 tank under various rainfall intensities. As the intensities of rainfall increased from 30 to 100 mm/hr, the hydrograph appears to moved from right to left. The hydrograph for 10 mm/hr is equal to zero due to the rainfall is completely retained by 20 cm of substrate. The detentions for are found to be ranged from 45 to 21 min for 1 hour rainfall under the depth of 30 to 100 mm depth.

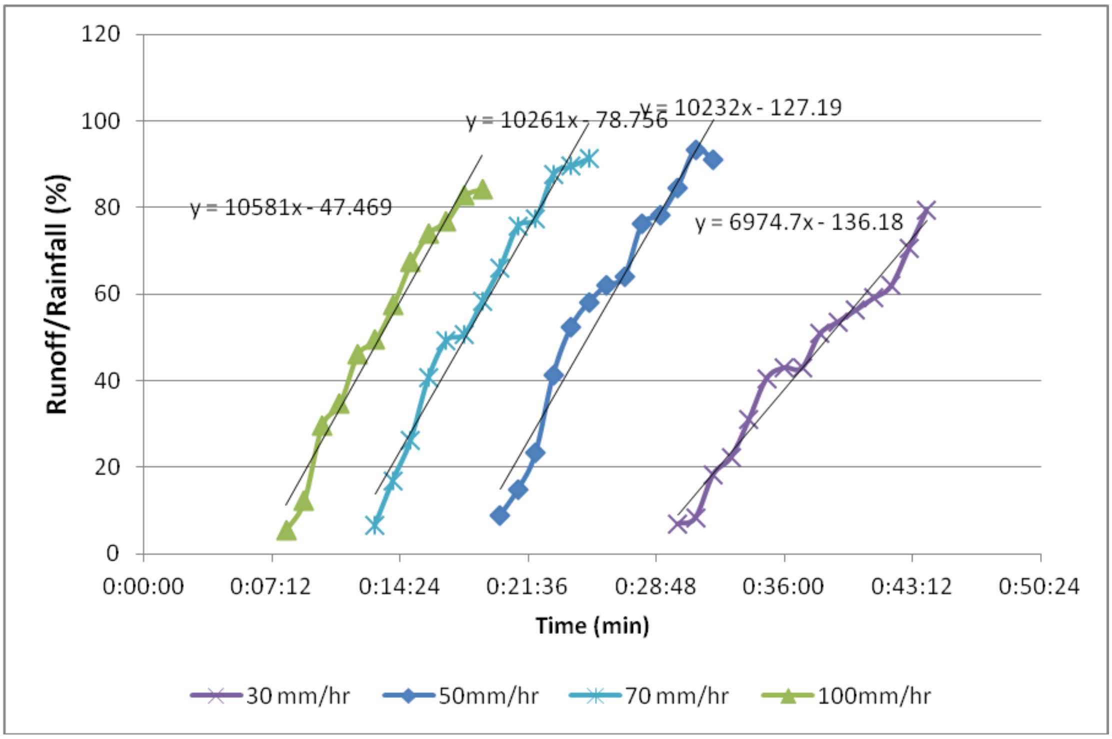

Figure 4. 40 Increasing phases for Eco-Soil of SSVR 60:40 hydrographs under various rainfall intensities

Figure 4.44 shows increasing phases for Eco-Soil of SSVR 80:20 hydrograph under various rainfall intensities. The slops for increase phases ranged from 6974.7 to 10581 for the rainfall intensities of 30 to 100 mm/hr. The slopes are found to be smaller than that of the previous substrate samples (SSVR 80:20).

4.4.5 Eco-Soil of SSVR 40:60

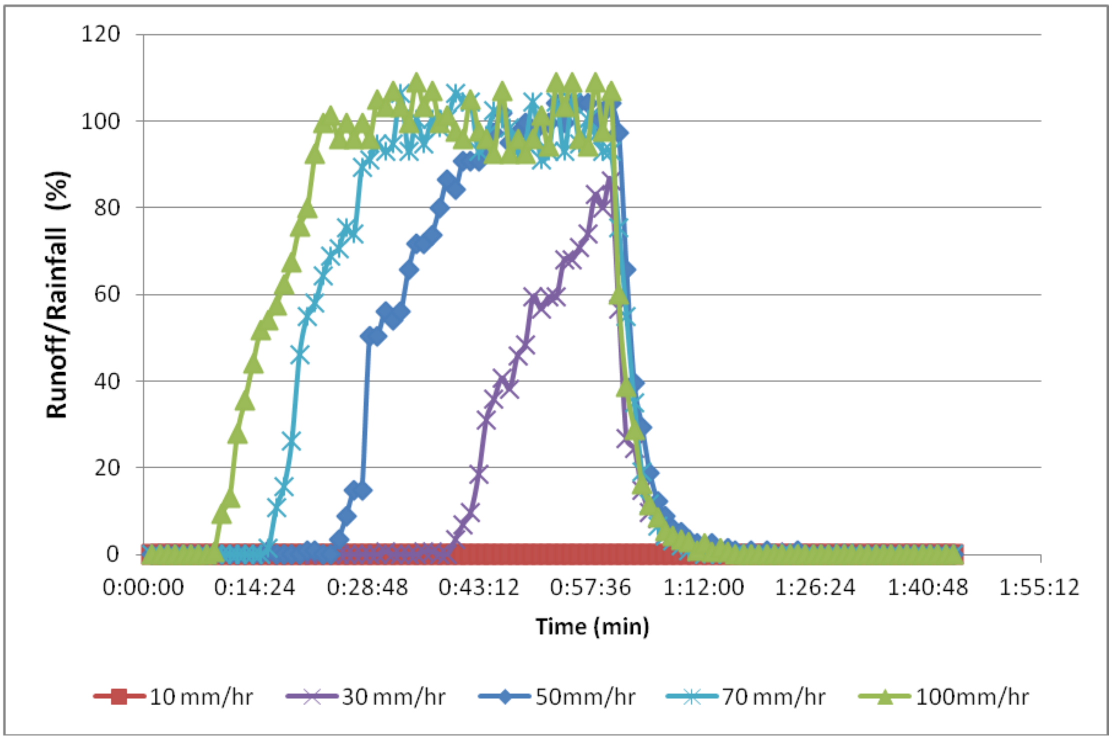

Figure 4. 41 Hydrographs for Eco-Soil of SSVR 40:60 under various rainfall intensities

Figure 4.45 shows the hydrograph for Eco-Soil of SSVR 60:40 tank under various rainfall intensities. The runoff hydrograph for 10 m/hr is not able to be produced under 1-hour duration under the same reasion as the prvious substrates. However, the hydrograph for 30 mm/hr is unable to reach the maximun runoff in 1-hour rainfall. This is because higher retention for the Eco-Soil of SSVR 40:60 due to the increasing content of activated sludge. The peak flow detentions are shown to be ranged from 45 to 23 min for the rainfall increasing from 50 to 100 mm/hr.

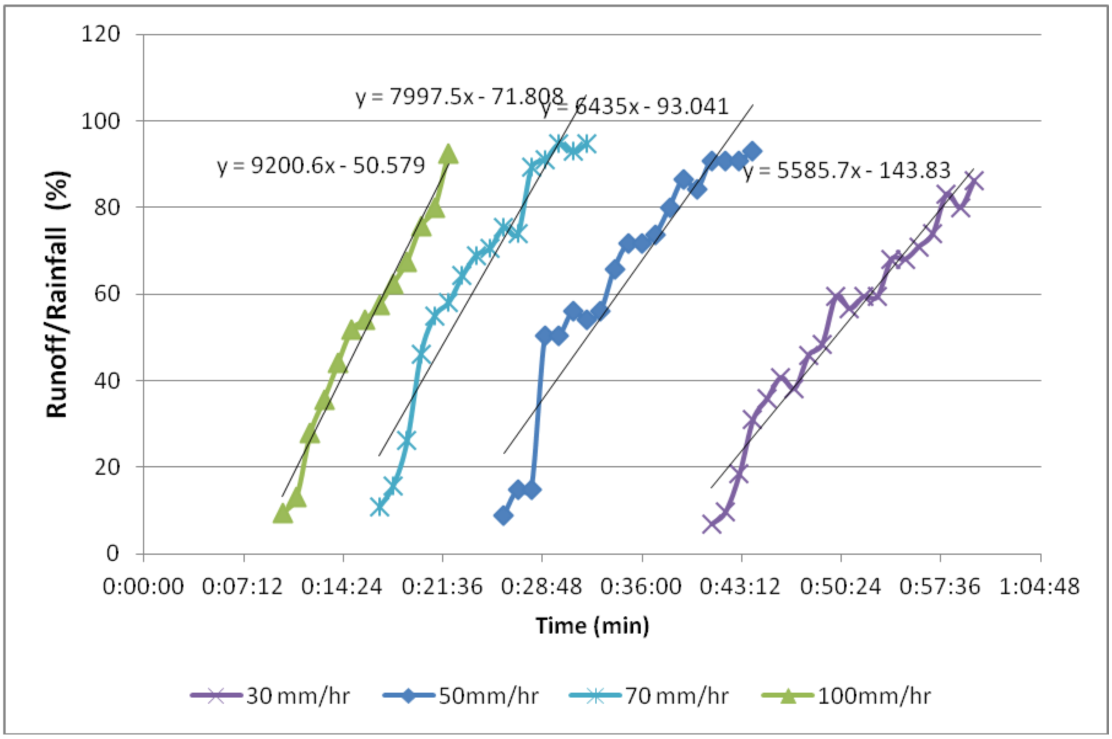

Figure 4. 42 Increasing phases for Eco-Soil of SSVR 40:60 hydrograph under various rainfall intensities

The increasing phases for Eco-Soil of SSVR 40:60 hydrograph under various rainfall intensities are shown in Figure 4.46. The slopes of the increasing phases range from 5585.7 to 9200.6 for rainfall intensities from 30 to 100 mm/hr. The trend of slope for Eco-Soil of SSVR 40:60 is shown to be increasing under the effects of rainfall.

4.4.6 Eco-Soil of SSVR 20:80

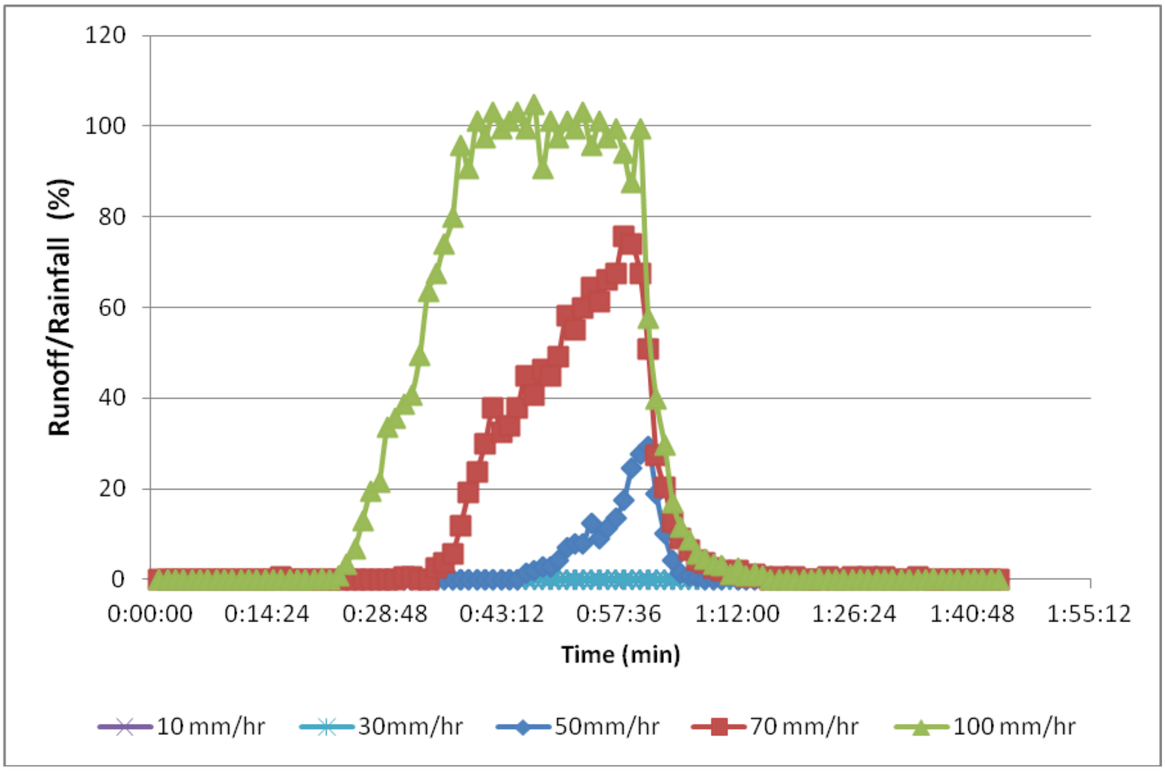

Figure 4. 43 Hydrograph for Eco-Soil of SSVR 20:80 under various rainfall intensities

Figure 4.47 shows hydrograph for Eco-Soil of SSVR 20:80 tank under various rainfall intensities. The hydrographs of 10 and 30 mm/hr are not able to be illustrated due to the retention. In addition, the hydrographs for 50 and 70 mm/hr achieved 29.3 and 75.1 % of rainfall, respectively, but not larger than 95%. The peak detention is only be able to observerd in the hydrograph for 100 mm/hr and it is 39 min.

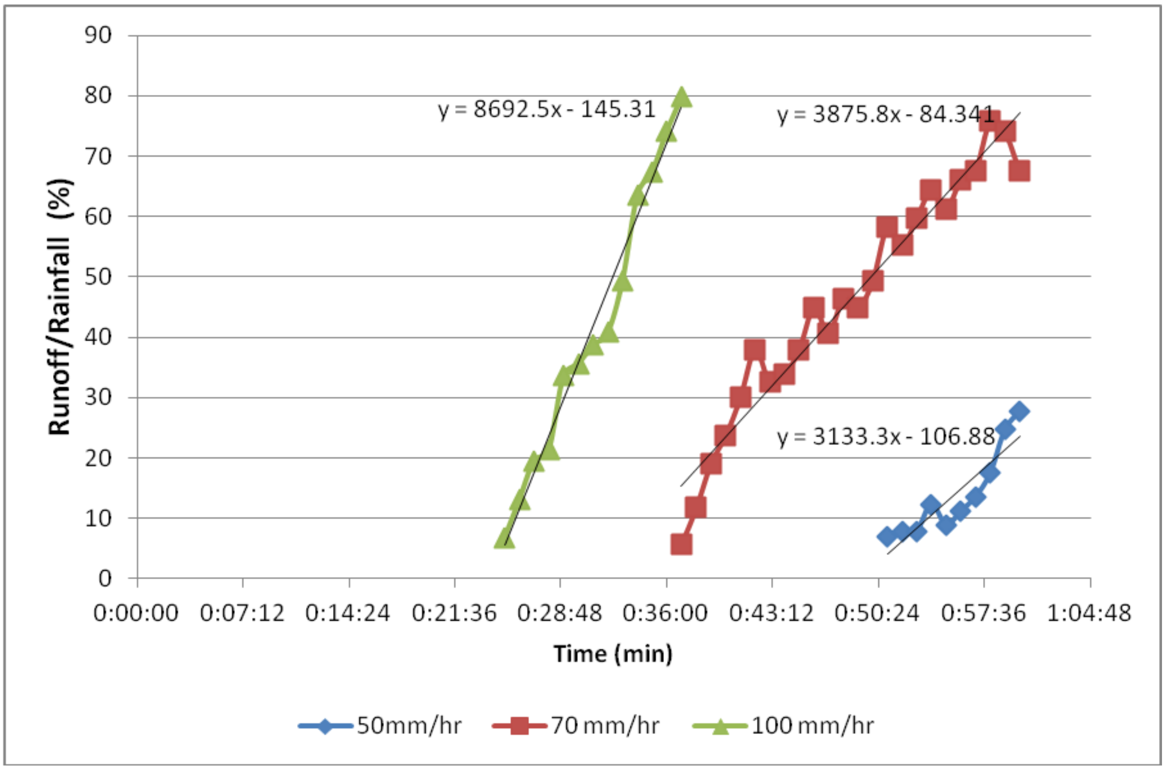

Figure 4. 44 Increasing phases for Eco-Soil of SSVR 20:80 hydrograph under various rainfall intensities

The increasing phases for Eco-Soil of SSVR 20:80 hydrograph under various rainfall intensities is shown in Figure 4.48 The slopes of the increasing phase range from 3133.3 to 8692.5 for the rainfall intensities of 30 to 100 mm/hr. Compared with the slopes for Eco-Soil of SSVR 100:0, 80:20, 60:40 and 40:60, the slopes for the same rainfall event decrease as the sludge content increased. The activated sludge provides fine particle, especially the bacteria, formed more void space for moisture retention. This is revealed by the resultant porosities shown in Table 4.3 for the substrates in this study.

4.4.7 Commercial Potting Soil

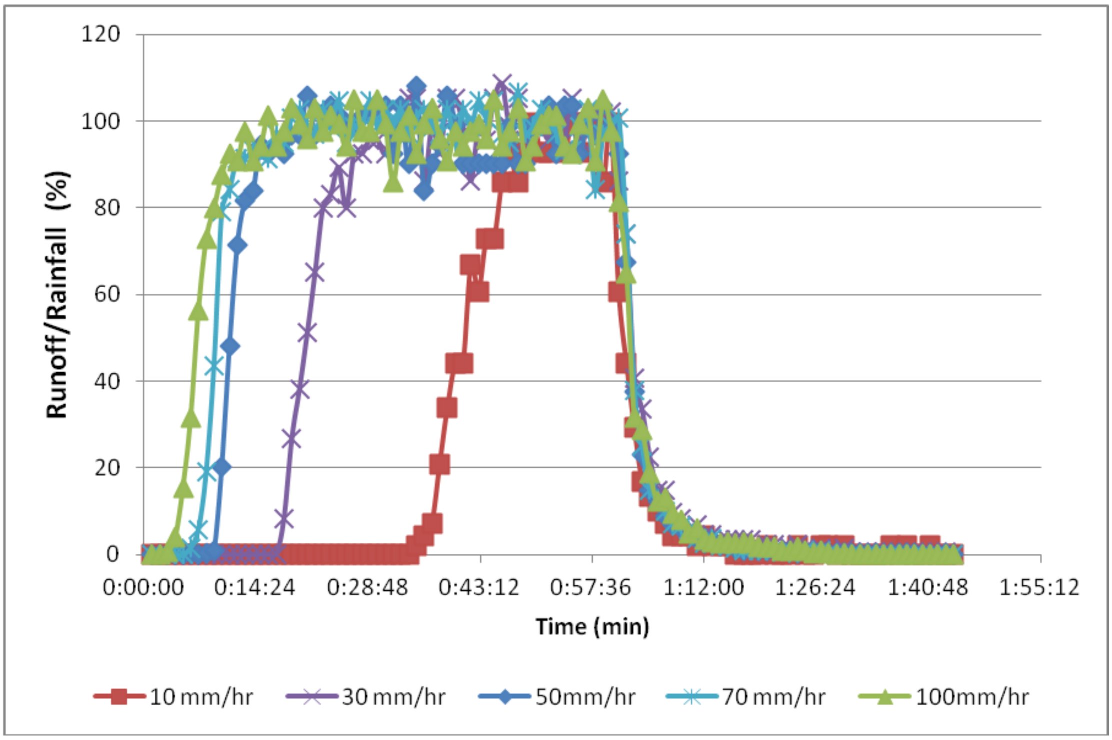

Figure 4. 49 Hydrograph for commercial potting soil under various rainfall intensities

Figure 4.49 shows the hydrograph for commercial potting soil tank under various rainfall intensities. The hydrographs indicate that the commercial potting soil have lower retention and higher conductivity than the Eco-Soil, therefore, totally 5 hydrographs are able to be observed. The detention of the runoff decreases from 50 to 13 min when the rainfall intention increases from 10 to 100 mm/hr.

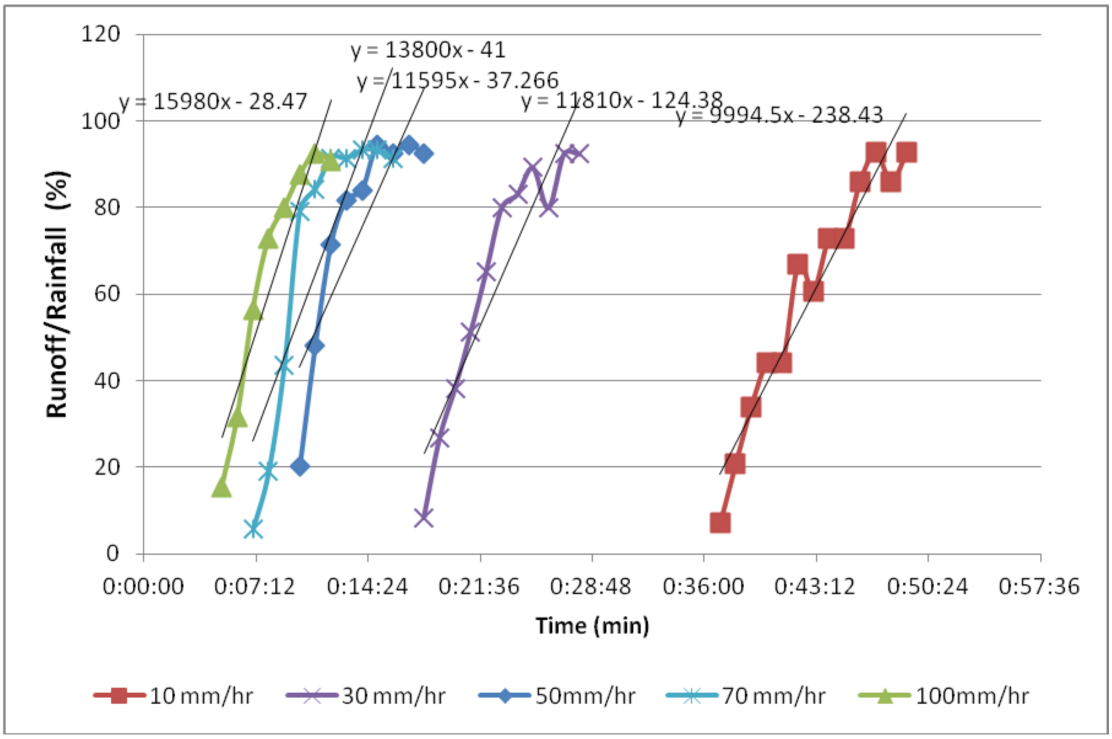

Figure 4. 50 Increasing phases for commercial potting soil hydrograph under various rainfall intensities

Figure 4.50 shows the increasing phases for commercial potting soil hydrograph under various rainfall intensities. The slops range from 9994.5 to 15980 for the rainfall 10 to 100 mm/hr. These increasing speed is larger than the Eco-Soils. The high slopes indicate that, in a precipitaiton event, the runoff readily infiltrate into the deep ground space and leaving lower water contant in the upper layer. This may reduce the accessibilities for the water uptake for vegetation in arid area. Therefore, the commercial potting is not as good as Eco-Soil for anti-desertification.

4.4.8 Overall Comparison

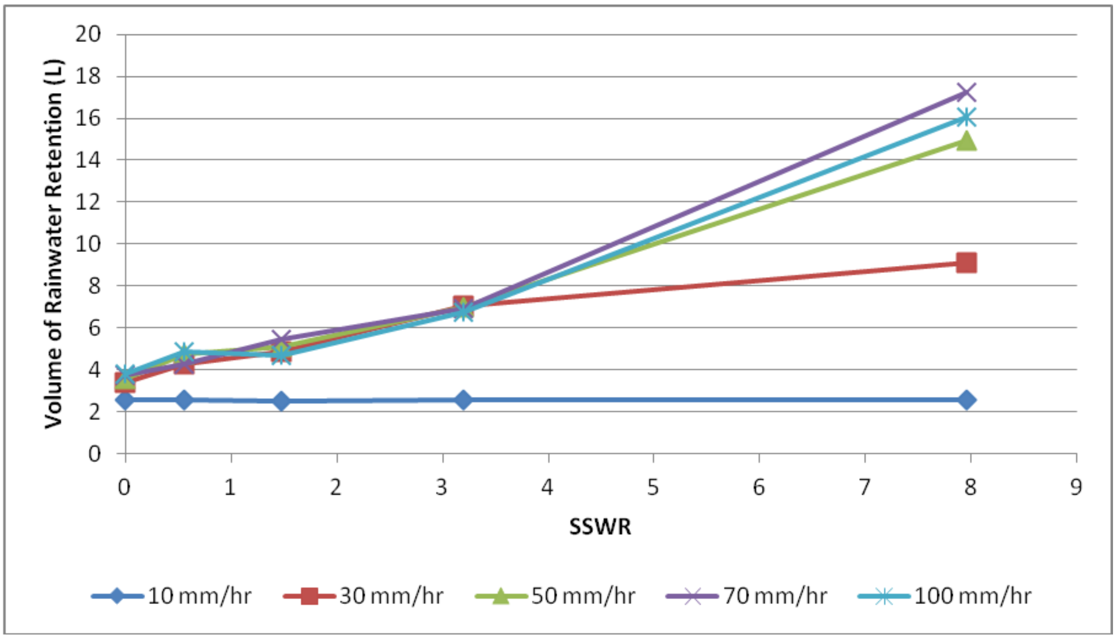

Figure 4. 45 Rainwater retention for arid sand, Eco-Soil and commercial potting soil under various rainfall intensities

Table 4. 9 Rainwater retention for arid sand, Eco-Soil and commercial potting soil under various rainfall intensities

	Rainwater Retention (L) under Rainfall Intensities(mm/hr)					Average Maximum Retention (L)
SSVR	10	30	50	70	100	
100:0	2.58	3.38	3.57	3.72	3.81	3.62
80:20	2.55	4.28	4.74	4.28	4.87	4.54
60:40	2.52	4.88	5.11	5.43	4.68	5.03
40:60	2.58	7.07	6.97	6.92	6.78	6.93
20:80	2.55	9.11	14.94	17.24	16.07	16.08
Soil	1.40	1.82	1.61	1.66	2.00	1.70

Figure 4.51 and Table 4.9 show the rainwater retention for arid sand (SSVR 100:0), Eco-Soils (SSVR 80:20, 60:40, 40:60 and 20:80) and commercial potting soil under various rainfall intensities. The retention curve for 10 mm/hr is shown to be flat and horizontal because the rainfall for this intensity is completely retained by the all of the

substrates, except soil. Other than 10 mm/hr intensity of rainfall, the curve for 30, 50, 70 and 100 mm/hr are increasing. For each rainfall intensity larger than 10 mm/hr, the rainwater retention increased with the increased fraction of activated sludge in the soil-mix. However, the Eco-Soil sample of SSVR 20:80 is unable to reach its maximum retention under 30 mm/hr rainfall. Therefore the point is shown to be lower than the ones for Eco-Soil of SSVR 80:20. 60:40 and 40:60.

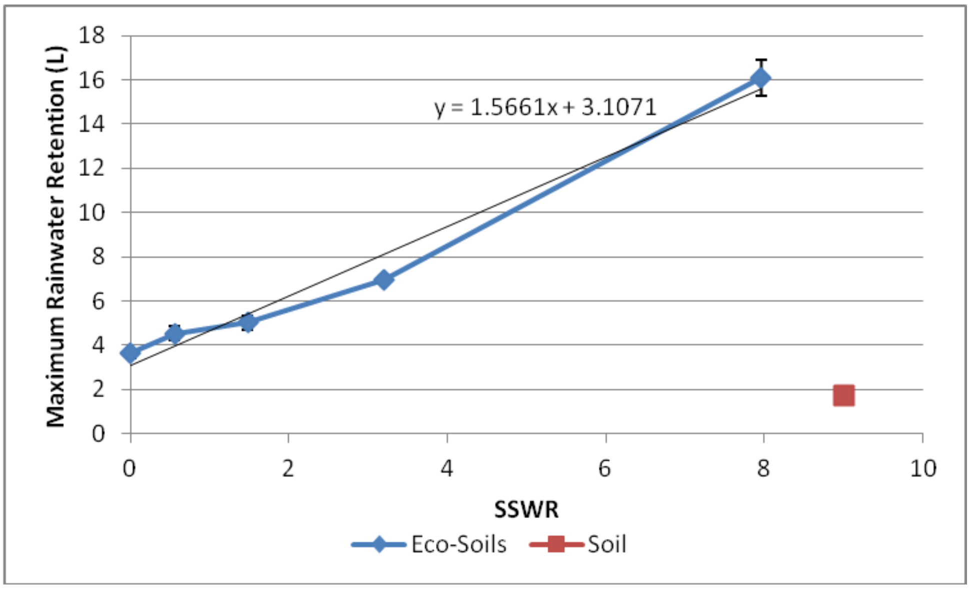

Figure 4. 46 Maximum rainwater retention for arid sand arid sand, Eco-Soils and commercial potting soil

Figure 4.52 shows the maximum rainwater retention for arid sand arid sand (SSVR 100:0), Eco-Soils (SSVR 80:20, 60:40, 40:60 and 20:80) and commercial potting soil. Soil water retention capability is calculated by the volume of water retained in the substrate when peak runoff is observed. Therefore, the average maximum rainwater retention is calculated on the rainfall intensities 30, 50, 70 mm/hr for SSVR 100:0, 80:20, 60:40 and 40:60, respectively and are indicated in Table 4.9. For SSVR 20:80, the maximum retention retention is not reached under the rainfall intensity of 30 mm/hr because there is no runoff produced. The maximum retention is calculated by the data for 50, 70 and 100 mm/hr.

The curve showed in Figure 4.53 illustrates that the maximum rainwater retention increases linearly with the sludge weight content. In other word, the linear releation for the rainwater retention is able to be concluded by the equation:

$$[V_{RT,SAMP,Max}] = 1.5661[SLC_{wt.\%}] + 3.1071 \qquad \text{(Eq 4. 25)}$$

where $[V_{RT,SAMP,Max}]$ is maximum rainwater retention for sample, L;

$[SLC_{wt.\%}]$ is activated sludge content by weight, $_{wt.}\%$;

This equaiton is worked out based on the rainfall intensities rainged 10 to 100 mm/hr and for 20 cm depth of substrates.

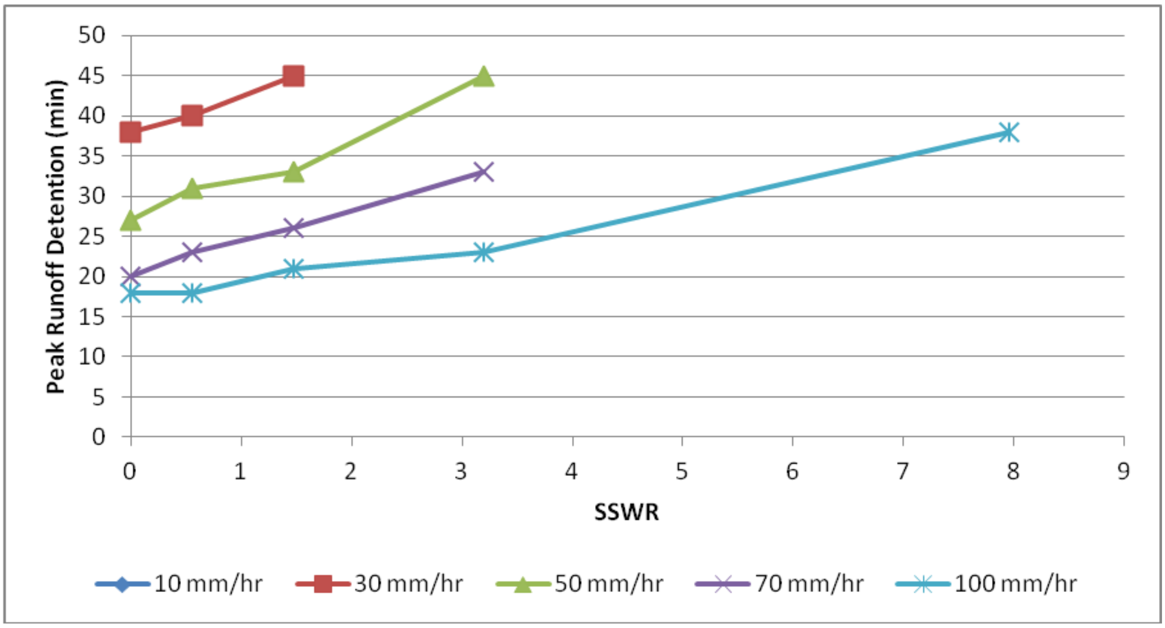

Figure 4. 47 Peak runoff detention for arid sand, Eco-Soils and commercial potting soil under various rainfall intensities

Table 4. 10 Peak runoff detention for arid sand, Eco-Soils and

commercial potting soil under various rainfall intensities

	Peak Runoff Detention (min) under Rainfall Intensities(mm/hr)				
SSVR	10	30	50	70	100
100:0	−	38	27	20	18
80:20	−	40	31	23	18
60:40	−	45	33	26	21
40:60	−	−	45	33	23
20:80	−	−	−	−	38
Soil	50	29	19	17	13

Figure 4.53 and Table 4.10 show the peak runoff detention for arid sand arid sand (SSVR 100:0), Eco-Soils (SSVR 80:20, 60:40, 40:60 and 20:80) and commercial potting soil. Only when the peak runoff is observed, the substrate is saturated under the rainfall events and the peak detention can be counted. For instance, peak runoff dention from 30 mm/hr is able to be observed from the Eco-Soil samples of SSVR 100:0~40:60, but not appears in SSVR 20:80. The curves in Figure 4.54 show that the peak runoff detention in the form of time to peak increases with the sludge weight content. The increasing content of activated sludge offerred high rainwater retention and low hydraulic conductivity to detain the appreance of peak runoff. The trend of the increasing peak runoff detention is found to be linear with respect to the activated sludge content.

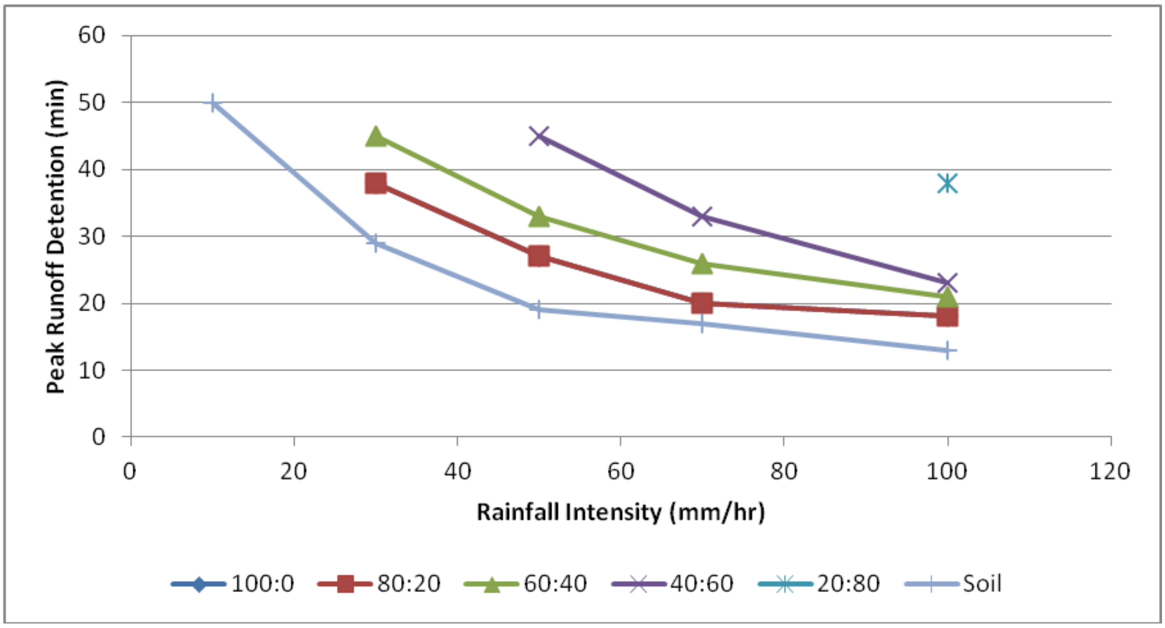

Figure 4. 48 Peak runoff detention for arid sand, Eco-Soils and commercial potting soil under various SSWR

If the peak runoff detention is plotted against rainfall intensities for various types of substrates. The curves were found to be non-linear and the increases of detention effects are reduced under high rainfall intensities situations. There is only one point observed for the SSVR 20:80, because peak runoff is able to be observed for the intensity of 100 mm/hr.

By obtaining the relation of maximum rainwater retention for vaious rainfall intensities, it served a reference accessible water content for top substrate for the vegetation selection for achieving anti-desertification.

4.4.9 Summary

This section investigates the performance of Eco-Soil in stormwater retention and detention. Rainfalls under the intensities of 10, 30, 50, 70 amd 100 mm/hr are simulated by the automatic PRSS to study the runoff pattern from the substrtate samples. The retention capabilities are significantly improve when the arid sand is mixed with activated sludge. The maximum retentions increase protionally to the amount of introduction of activated sludge. The amount of retention for the SSVR 60:40 is found to be 1.39 times as arid sand. The results also show the Eco-Soil provide higher stormwater retention capabilities as commercial potting soil. Therefore, the Eco-Soil is throught to be a more suitable growing medium in anti-desertification.

4.5 Overall Discussions

The Sand Sludge Soil is a type of mixture of arid sand and thickned activated sludge for antidesertification, namely Eco-Soils. The hydraulic properties, the water retention abilities, vegetation growing capabilities and the outcomes are essentially significant for application purposes.

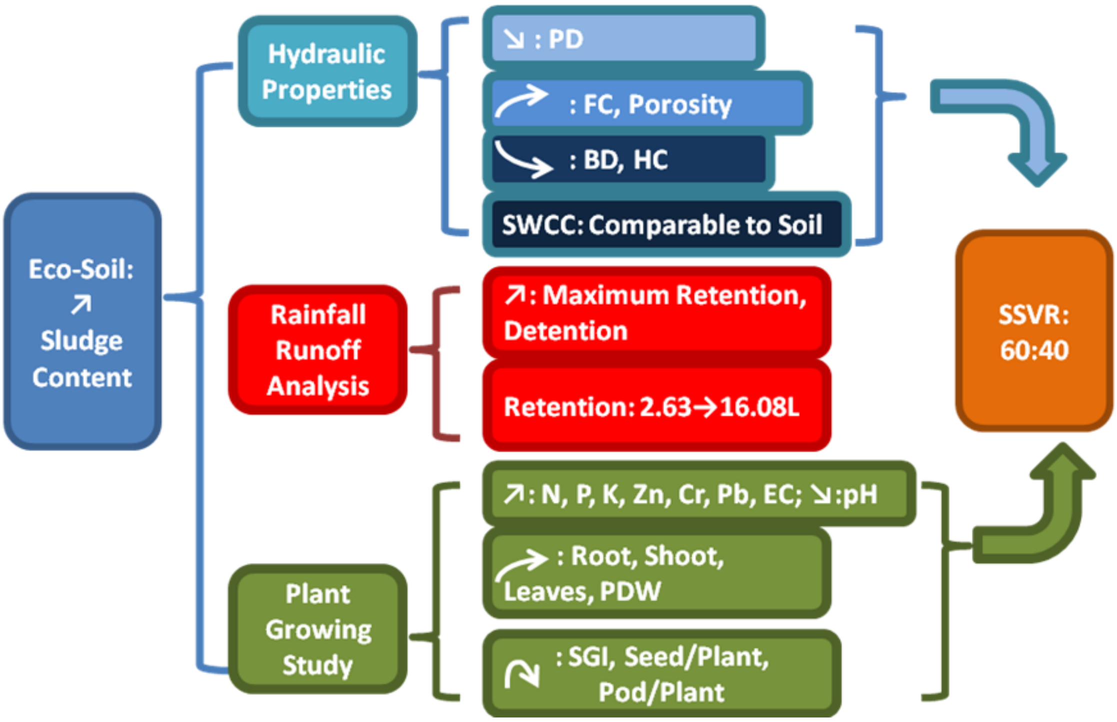

Figure 4. 55 Overall findings for Eco-Soils

Section 4.1 discusses the composition of Eco-Soils and developes equations including Eq 4.1 and Eq 4.8 for corelating the sand sand sludge weight ratio with sludge volumetric ratio and volatile soild content or organic matter. The following parts in seciton 4.1 investigate the hydraulic properties including bulk density, particle density, porosity, particle size distribution, field capacity and hydraulic conductivity, and their relation with respect to the sludge weight ratio. By the equations (Eq 4.17-Eq 4.19), the hydraulic properties are able to be predicted in applying the Eco-Soils for anti-desertification.

Section 4.2 discusses the soil water characteristic curves (SWCC) for arid sand, Eco-Soils and commercial potting soils. The SWCCs of Eco-Soils are found to be shifted as poportional to the increasing fraction of activated sludge. The soil water retention capability is found to be comparable to commercial soil when the SSVR reach 40:60. The results indicate the water retention capability is greatly improved by introduction activated sludge. The van Genuchten (VG) model are fitted by the hydraulics properties found in section 4.1 to simulate the SWCC via the RETC program. The fitting factors including α and n are found to follow instinct relation with sludge weight ratio. This provided numerical relation for predicting the fitting factors in VG model and therefore the Eco-Soil mixing model is able to be introduced to VG model. The finding of Eq 4.22 offers prediction of the SWCCs for Eco-Soils in the applications for anti-desertification and soil water process simulation.

Section 4.3 investigates the micro-ecosystem in the form of plant growing study. In the consideration of growth of vegetation, especially gemination of seeds in the growing medium, the organic matter plays an important indicator. The low OM provides little nutrient content to sustain the vegeration growth while high OM excites the growth of microorganisms which inhibit vegetation growth. From the growing patterns for Okra in the 6 types of substrates (arid sand, Eco-Soils and potting soil) the growing speed is significantly improved by the nutrients contained in activated sludge. The Eco-Soils of SSVR 60:40 and 40:60 provide rich macronutrients including nitrogen, phosphorus and potassium, together with appropriate electric conductivity and pH, for vegetation growth. The outcomes such as pod number, pod weight, seed number and specific seed weight are found to be promissing as compared with commercial potting soil and some other literatures.

Section 4.4 illustrates the bottom runoff patterns for the 6 textures under vairous rainfall intensities, which covers the range of possible intensities in arid and semi arid area, to investigate the rain water retention and detentions. The results show that the maximum retention are proportional to and linear with the sludge wight content. Therefore, the rainwater retention is also to be predicted by the Eq 4.25 to determine the necessary irrigation for vegetion when applying Eco-Soils for anti-desertification purposes.

Under the consideration of the appropriate hydraulic properties for vegetration growth, the optimal outcome of vegetation growth and maximum application of activated sludge, the SSVR 60:40 is found to be the optimal selection for the application of Eco-Soils for anti-desertification.

5. Conclusions

This study investigates the fractional composition, hydraulic properties and phyto-toxicity of a novel growing medium, namely the Eco-Soil, for anti-desertification. The mixing fraction and organic content results are used to develop the numerical models for the relation among SSVR, SSWR and organic content. Essential hydraulic properties, including bulking density, particle density, porosity and particle size distribution, were examined and their relations between Eco-Soil mixing ratios are elucidated by equations. The field capacities and hydraulic conductivities indicate suitable SSVR for water retention and migration physically. Seed germination percentage, root length ratio and seed germination index further reveal the plant affinity for Eco-Soil extracts. Consequently, the optimal SSVR of Eco-Soil for anti-desertification is found to be 60:40 based on hydraulic properties and phyto-toxicity results.

SWCC relates the soil moisture content with soil water potential and serves as an identity for substrates. It plays important role in most of soil water movement relations. Experimental methods for the Eco-Soils are used to determine the SWCC in the two important suction head ranges of -600 ~ -100 cmH_2O and -2.98×10^6 to～ 1.10×10^5 cmH_2O. The results show that the SWCC for both ranges appear to be shifting as sludge content increasing. The phenomena reveal the increasing soil water retention capability because of the introduction of activated sludge. Eco-Soil with sludge content as high as SSVR 60:40 exhibits higher retention effect than the commercial potting soil where the suction head range of -600 ~ -100 cmH_2O. In addition, when the SSVR reaches 40:60, Eco-Soil performs better than potting soil in the aspect of water retention. The experimental SWCC illustrates significant improvements brought by introduction of activated sludge. The experimental SWCC can be also simulated by numerical models including van Genuchten (VG) model. For all of the Eco-Soils, the VG model is applicable in the suction head range of $0\sim-1.19\times10^6$ cmH_2O. The regression relation between the sludge weight content and the two essential fitting factors, α and n, is found to exhibit good correlation. The finding offers a way to introduce the Eco-Soil Mixing Model into VG model to develop numerical SWCC equation for Eco-Soils. Therefore, the SWCC can be determined by SSWR, SSVR or organic content of the Eco-Soils. The findings not only elucidate the numerical relation with SWCC models but also built a bridge between the novel Eco-Soil and the other conventional pedotransfer functions, such as infiltration, evaporation, moisture development models.

The morphological and physiological characteristics of the growth of *Abelmoschus esculentus* (Okra) were investigated in arid sand, Eco-Soils (SSVR 80:20, 60:40, 40:60 and 20:80) and potting soil. The vertical development of plants reveals that the growth is affected by nutrient concentration and consumption, especially nitrogen content in the substrates, and also by the environment parameters, such as the solar radiation. The results show that the okra growing in SSVR 60:40 and 40:60 can be up to a height of around 90 cm. From the analysis of plant organs, the shoot dried weights and root dried weights are shown to have non-linear relation with the SSWR. The root/shoot ratio results show that the okra growing in SSVR 40:60 achieves the suggested value of 1.5 g root/g shoot for a healthy plant. The fruiting data shows that the okra growing in SSVR 60:40 achieves both highest pod number and seed number. This indicates the reproduction abilities are stimulated by this SSVR of Eco-Soil. In the consideration of maximizing the application efficiency of activated sludge and the growth of vegetation, the SSVR 60:40 is considered to be an optimal selection for anti-desertification.

The bottom runoff patterns of the 6 types of substrates under vairous rainfall intensities were studied to investigate the rain water retention and detention characteristics. The results show that the retention is proportional to and linear with the sludge wight contents. Therefore, the rainwater retention can be predicted by Eco-Soil Mixing Model to estimate the necessary irrigation for vegetion when applying Eco-Soils for anti-desertification purposes.

Finally, based on the comprehensive analysis, Eco-Soil of SSVR 60:40 exhibits appropriate hydraulic properties and plant affinity for anti-desertification.

6. Further Study Recommendation

As the Eco-Soil is a novel material for anti-desertification purpose, there will be lots of valuable aspects for further studies including:

- Pilot-scale and large-scale application of activated sludge in the natural conditions
- Antibiotics accumulated in vegetation growing in Eco-Soils
- Transformation of bacteria community in the Eco-Soils in application for anti-desertification
- Economics for application of Eco-Soils for anti-desertification
- Application of Eco-Soils in urban green roof system

References

Adeel, Z., Safriel, U., Niemeijer, D. and White, R.. (2005) Ecosystems and human well-being: desertification synthesis, Millennium Ecosystem Assessment.

Agus S S, Leong G E C, Rahard joH R. (2001) Soil- w ater ch aracteristic curves of singapore residual soils . Geotechnical and Geological Engineering, 19, 285~ 309.

Ahuja, L.R., Naney, J.W., Williams, R.D., (1985) Estimating soil water characteristics from simpler properties or limited data. Soil Science Society of America Journal, 49 (5), 1100–1105.

Akanbi WB, Togun AO, Adeniran JA, Olaniyan AB. Effect of split application of organio mineral fertilizer on okra growth, nutrient uptake and fruit yield. Nigerian Journal of Horticultural Science (2004);9:102–9.

Akpan-Idioka, A.U.,Udob, I.A., Braidec, E.I. (2012) The use of human urine as an organic fertilizer in the production of okra (Abelmoschus esculentus) in South Eastern Nigeria, Resources, Conservation and Recycling 62, 14–20

Alba, K., Ritzoulis, C. Georgiadis, N., Kontogiorgos, V. (2013) Okra extracts as emulsifiers for acidic emulsions, Food Research International, 54, 1730–1737

Ankeny, M.D., (1992) Methods and theory for unconfined infiltration measurements. In: Topp, G.C., Reynolds, W.D., Green, R.E. (Eds.), Advances in Measurement of Soil Physical Properties: Bringing Theory into Practice, SSSA Special Publication No. 30. SSSA, Madison, USA, pp. 123–141.

Ankeny, M.D., Kaspar, T.C., Horton, R., (1990) Characterization of tillage and traffic effects on unconfined infiltration measurements. Soil Science Society of America Journal, 54, 810–837.

Anon., (1989) The sludge dilemma. Operation Forum, 4, 15-16.

Appels, L., Baeyens, J., Degrève, J., Dewil, R., (2008) Principles and potential of the anaerobic digestion of waste-activated sludge. Progress in Energy and Combustion Science 34, 755–781.

Araujo, M.A.V.C., Teixeira, J.C.F., Teixeira, S.F.C.F., (2008) Application of laser anemometry for measuring critical bed shear stress of sediment core samples. Continental Shelf Research 28, 2718–2724.

Arya, L.M., Paris, J.F., (1981) A physicoempirical model to predict the soil moisture characteristics from particle-size distribution and bulk density data. Soil Science Society of America Journal, 45 (6), 1023–1030.

Asadi, H., Ghadiri, H., Rose, C.W., Yu, B., Hussein, J., (2007) An investigation of flow-driven soil erosion processes at low streampowers. Journal of Hydrology 342, 134–142.

Asadi, H., Moussavi, A., Ghadiri, H., Rose, C.W., (2011) Flow-driven soil erosion processes and the size selectivity of sediment. Journal of Hydrology 406, 73–81.

Asiegbu, J.E. (1987) Effects of organic matter substrate sources and time of photosynthatesink removal on flower and pod production in okra Abelmoschus esculentus (L.) Moench, East African Agricultural and Forestry Journal, 54(4):293–7.

Augustyniak, M., Migula, P., Mesjasz-Przyby1owicz, J., Tarnawska, M., Nakonieczny, M., Babczyńska, A., Przyby1owicz, W. and Augustyniak, M.G. (2007) Short-term effects of dimethoate on metabolic responses in Chrysolina pardalina (Chrysomelidae) feeding on Berkheya coddii (Asteraceae), a hyper-accumulator of nickel. Environmental Pollution, 150, 218-224.

Awodun MA, Olafusi RA. (2007) Effect of integrated application of goat manure and urea on soil nutrient content and yield of okra. Nigerian Journal of Soil Science,, 17:126–9.

Ayoub, A.T.. Extent, severity and causative factors of land degradation in the Sudan. Journal of Arid Environments, (1998), 38, 397–409.

Balks, M.R., McLay, C.D.A., Harfoot, C.G., (1997) Determination of the progression in soil microbial response, and changes in soil permeability, following application of meat processing effuent to soil. Applied Soil Ecology, 6, 109-116.

Ball, B.C., Campbell, D.J., Hunter, E.A., (2000) Soil compactibilityin relation to physical and organic properties at 156 sites in UK.Soil & Tillage Research, 57, 83–91.

Bastida, F., Moreno, J.L., Garcia, C., Hernandez, T., (2007). Addition of urban waste to semiarid degraded soil: long-term effect. Pedosphere 17, 557–567.

Baveye, P., Vandevivere, P., Hoyle, B., L, DeLeo, P.C., deLozada, D.S., (1998). Environmental impact and mechanisms of the biological clogging of saturated soils and aquifer materials. Critical Rev. Environ. Sci. Tech. 28, 123-191.

Bayr, S.,Kaparaju, P., Rintala, J. Screening pretreatment methods to enhance thermophilic anaerobic digestion of pulp and paper mill wastewater treatment secondary sludge, Chemical Engineering Journal, (2013), 233, 479-486.

Bear, J. (1972). Dynamics of Fluids in Porous Media. Dover Publications. ISBN 0-486-65675-6.

Beck, A.J., Johnson, D.L. and Jones, K.C.. The form and bioavailability of non-ionic organic chemicals in sewage sludge-amended agricultural soils. The Science of the Total Environment, (1996), 185, 125-149.

Benites, V.M., Machado, P.L.O.A., Fidalgo, E.C.C., Coelho, M.R., Madari, B.E., (2007). Pedotransfer functions for estimating soil bulk density from exiting soil survey reports in Brazil. Geoderma 139, 90–97.

Benson, C. H., Daniel, D. E., and Boutwell, G. P. (1999) Field performance of compacted clay liners, Journal of Geotechnical and Geoenvironmental Engineering Eng., 125, 390-403.

Benson, C. H., Thorstad, P. A., Jo, H.-Y., and Rock, S. A. (2007) Hydraulic performance of geosynthetic clay liners in a landfill final cover, Journal of Geotechnical and Geoenvironmental Engineering Eng., 133, 814-827.

Benson, C., Zhai, H., Wang, X., (1994). Estimating the hydraulic conductivity of compacted clay liners. J. Geotech. Eng. 120, 366– 387.

Benson, C.H., Trast, J.M., (1995). Hydraulic conductivity of thirteen compacted clays. Clays Clay Miner. 43 (6), 669– 681. Benson, C., Zhai, H., Wang, X., (1994). Estimating the hydraulic conductivity of compacted clay liners. J. Geotech. Eng. 120, 366– 387.

Bernoux, M., Arrouays, D., Cerri, C., Volkoff, B., Jolivet, C., (1998). Bulk densities of Brazilian Amazon soils related to other soil properties. Soil Science Society of America Journal, 62, 743–749.

Bhattacharyya, R., Prakash, V., Kundu, S., Gupta, H.S., (2006). Effect of tillage and crop rotations on pore size distribution and soil hydraulic conductivity in sandy clay loam soil of the Indian Himalayas. Soil & Tillage Research, 86, 129–140.

Bohling, B., (2009).Measurements of threshold values for incipientmotion of sediment particles with two different erosion devices. J. Mar. Syst. 75, 330–335.

Bouwer, H., Chaney, R.L., 1974. Land treatment of wastewater. Adv. Agron 26, 133-176.

Breulmann, M., Masyutenko, N. P., Kogut, B.M., Schroll R., Dörfler, U., Buscot, F., Schulz, E., (2014) Short-term bioavailability of carbon in soil organic matter fractions of different particle sizes and densities in grassland ecosystems, Science of the Total Environment 497–498 29–37

Brooks, R.H., Corey, A.T., 1964. Hydraulic properties of porousmedia. Hydrol. Paper, vol. 3.Colorado State Univ, Fort Collins, CO.

Bruce, A.M. and Davis, R.A.. Sewage sludge disposal: current and future options. Water Science Technology, (1989), 21, 1113-1128.

Burkhill HM. The useful plants of West Tropical Africa. Families M–R, vol. 4, 2nd

Cameira, M.R., Fernando, R.M., Pereira, L.S., (2003). Soil macropore dynamics affected by tillage and irrigation for a silty loam alluvial soil in southern Portugal. Soil & Tillage Research, 70, 131–140.

Cameron, K.C., Buchan, G.D., (2006). Porosity and pore size distribution. In: Lal, R. (Ed.), Encyclopedia of Soil Science,ence. CRC Press, Boca Raton, FL, USA, pp. 1350–1353.

Cameron, K.C., Di, H.J., McLaren, R.G., (1997). Is soil an appropriate dumping ground for our wastes. Australian Journal of Soil Research 35, 995-1035.

Cao, Y.Z. and Song, Z.W.. Plant Physiology. China:Lan Zhou University Press, (1998).

Caravaca, F., Lax, A., Albaladejo, J., (2001). Soil aggregate stability and organic matter in clay and fine silt fractions in urban refuse-amended semiarid soils. Soil Science Society of America Journal, 65, 1235–1238.

Caravaca, F., Lax, A., Albaladejo, J., (2004). Aggregate stability and carbon characteristics of particle-size fractions in cultivated and forested soils of semiarid Spain. Soil & Tillage Research 78, 83–90.

Cassaro, F.A.M.,Borkowski, A.K.,Pires, L.F.,Saab, S.D.C., (2011). Characterization of a Brazilian clayey soil submitted to conventional and no-tillage management practices using pore size distribution analysis. Soil & Tillage Research, 111, 175–179.

Cayet, C., Lichtfouse, E., (2001). δ13C of plant-derived n-alkanes in soil particle-size fractions. Organic Geochemistry, 32, 253–258.

Chen, T.F., Wang, X.F., Dong, P., (2010) A simplemethod formeasuring themoisture characteristic curves of sandy soils, Geotechnical Investigation & Survey ing, 2, 33~36

Chin, K.B., Leong, E.C., Rahardjo, H., (2010). A simplified method to estimate the soil–water characteristic curve. Canadian Geotechnical Journal, 47, 1382–1400.

Ching, J., Chen, Y.C., Phoon, K.K., (2009). Reducing uncertainty in undrained shear strength. Geotechnical Risk and SafetyTaylor and Francis Group, London 978-0415-49874-6.

Chiu, C.F., Yan, W.M., Yuen, K.V., (2012). Reliability analysis of soil–water characteristic curve and its application to slope stability analysis. Engineering Geology, 135–136, 83–91.

Chou, C.-W., Seagren, E. A., Aydilek, A. H., and Lai, M. (2011) Biocalcification of sand through ureolysis, Journal of Geotechnical and Geoenvironmental Engineering Eng., 137, 1179-1189.

Christensen, B.T., (1987). Decomposability of organic matter in particle size fractions from field soils with straw incorporation. Soil Biology & Biochemistry, 19, 429–435.

Chu, J., Stabnikov, V., and Ivanov, V. (2012) Microbially induced calcium carbonate precipitation on surface or in the bulk of soil, Geomicrobiol. J., 29, 544-549 .

Cook, F.J., Kelliher, F.M., McMahon, S.D., (1994). Changes in infiltration during wastewater irrigation of a highly permeable soil. J. Environ. Qual. 23, 476-482.

Cuisinier, O., Le Borgne, T., Deneele, D., Masrouri, F. (2011) Quantification of the effects of nitrates, phosphates and chlorides on soil stabilization with lime and cement, Engineering Geology, 117, 229–235

da Costa, P.A., Mota, J.C.A., Romero, R.E., Freire, A.G., Ferreira, T.O., (2014). Changes in soil pore network in response to twenty-three years of irrigation in a tropical semiarid pasture from northeast Brazil. Soil & Tillage Research, 137, 23–32.

Dam, R.F.,Mehdi, B.B., Burgess, M.S.E.,Madramootoo, C.A., Mehuys, G.R., Callum, I.R., (2005). Soil bulk density and crop yield under eleven consecutive years of corn with different tillage and residue practices in a sandy loam soil in central Canada. Soil and Tillage Research 84, 41–53.

Daniel, E. D. and Wu, Y.-K. (1993) Compacted clay liners and covers for arid sites, J. Geotech. Eng., 119, 223-237.

Darkoh, M.B.K.. The nature, cause and consequences of desertification in the drylands of Africa. Land Degradation and Development, (1998), 9, 11–20.

De Vos, B., Meirvenne, M.V., Quataert, P., Deckers, J., Muys, B., (2005). Predictive quality of pedotransfer functions for estimating bulk density of forest soils. Soil Science Society of America Journal, 69, 500–510.

Deurer, M., Grinev, D.,Young, I., Clothier, B.E.,Muller, K., (2009). The impact of soil carbon management on soil macropore structure: a comparison of two apple orchard systems in New Zealand. Eur. Journal of Soil Science,60, 945–955.

Dodane, P.D., Mbéguéré, M., Sow, O., Strande, L., (2012), Capital and Operating Costs of Full-Scale Fecal Sludge Management and Wastewater Treatment Systems in Dakar, Senegal, Environ. Sci. Technol. 46, 3705−3711

Dregne, H., Kassas, M. and Rozanov, B.. A new assessment of the world status of desertification. Desertification Control Bulletin, (1991), 20, 6-18.

Ebina, T., Minja, R. J.A., Nagase, T., Onodera, Y., Chatterjee, A., (2004) Correlation of hydraulic conductivity of clay–sand compacted specimens with clay properties, Applied Clay Science, 26, 3– 12.

Echeverria, J.C., Morena, M.T., Mazkiaran, C., Garrido, J.J., (1999). Characterization of the porous structure of soils: adsorption of nitrogen (77 K) and carbon dioxide (273 K), and mercury porosimetry. Eur. Journal of Soil Science,50, 497–503.

Eckenfelder, W.W. and Santhanam, C.J.. Sludge treatment, New York:Marcel Dekker, (1981).edition Kew, United Kingdom: Royal Botanic Gardens; 1997.

Egloffstein, T. A. (2001) Natural bentonitese influence of the ion exchange and partial desiccation on permeability and self-heating capacity of bentonites used in GCLs, Geotextiles and Geomembranes, 19, 427-444.

Ehlers, W., van der Ploeg, R.R., (1976) Evaporation, drainage and unsaturated hydraulic conductivity of tilled and untilled fallow soil. Z. Pflanzenern. Bodenk. 3, 373–386.

Ellies, A., Hartge, K.H., MacDonald, R., Ramirez, C., (2003).Organische Bodensubstanz und Benetzbarkeit von Bodenproben-eine interpretation. Journal of Plant Nutrition and Soil Science,ence, 166, 120– 123.

Emanuel, K.A.. The dependence of hurricane intensity on climate. Nature, (1987), 326, 483–485.

Environment Protection Agency. (1979) Process design manual sludge treatment and disposal, USA:EPA,

Federal Register. 40 CFR Part 503, (1993) Standards for the disposal of sewage sludge, USA:EPA.

Ferna´ndez, J.M. *, Plaza, C., Garcı´a-Gil, J.C., Polo, A., (2009) Biochemical properties and barley yield in a semiarid Mediterranean soil amended with two kinds of sewage sludge, Applied Soil Ecology, 42, 18–24

Fernández, J.M., Senesi, N., Plaza, C., Brunetti, G., Polo, A., (2009). Effects of composted and thermally dried sewage sludges on soil and soil humic acid properties. Pedosphere 19, 281–291.

Ferreras, L.A., Costa, J.L., Garcia, F.O., Pecorari, C., (2000). Effect of no-tillage on some soil physical properties of a structural degraded Petrocalcic Paleudoll of the southern ‘‘Pampa’’ of Argentina. Soil & Tillage Research, 54, 31–39.

Folk, R. L., 1968, Petrology of Sedimentary Rocks: Austin, University of Texas Publication, 170 p.

Folk, Robert L.; Ward, William C. (1957). "Brazos River bar: a study in the significance of grain-size parameters". Journal of Sedimentary Petrology, 27 (1), 3–26.

Fredlund D C, Rahard jo. C hen Zhongy,i Zh ang Zaim ing, C hen Yu jiong, et a.l . Vers ion. soil m echan ics for un saturated so ils. Beijing: Ch ina A rch itectu re& Bu ild ing Press, (1997), 92 - 95.

Fredlund D C, Rahard J. Chen Z.Y., Zhang Z.M, Chen, Y.J., (1997),Version. soil mechanics for unsaturated soils. Beijing: China Architecture& Building Press, 92 - 95.

Fredlund, D.G., Xing, A., (1994). Equations for the soil–water characteristic curve. Canadian Geotechnical Journal, 31, 521–532.

Frink, C.R. and Hullar, T.L..(1985), Criteria and Recommendations for Land Applications of Sewage Sludge in the North
East. Pennsylvania Agricultural Experiment Station, 851.

Fu, X.L., Shao, M.G., Lu, D.Q., Wang, H.M., (2011) Soil water characteristic curve measurement without bulk density changes and its implications in the estimation of soil hydraulic properties, Geoderma, 167-168, 1–8

Gallage, C.P.K., Uchimura, T., (2010). Effects of dry density and grain size distribution on soil–water characteristic curves of sandy soils. Soils and Foundations, 50 (1), 161–172.

Gallipoli, D.,Wheeler, S.J., Karstunen, M., (2003). Modelling the variation of degree of saturation in a deformable unsaturated soil. Geotechnique 53 (1), 105–112.

Gao, T.Y. and Gu, G.W.. Water pollution control Engineering. China:Higher Education Press, (2004).

Garc ́ıa-Orenes, F., Guerrero, C., Mataix-Solera, J., Navarro-Pedre ̃no, J., Gómez, I., Mataix-Beneyto, J., (2005). Factors controlling the aggregate stability and bulk density in two different degraded soils amended with biosolids. Soil & Tillage Research 82, 65–76.

Gerzabek, M.H., Haberhauer, G., Kandeler, E., Sessitsch, A., Kirchmann, H., (2002). Response of organic matter pools and enzyme activities in particle size fractions to organic amendments in a long-term field experiment. Developments in Soil Science,ence, vol. 28B. Elsevier Science B.V, Amsterdam, pp. 329–344.

Girma, T.. Land degradation: a challenge to Ethiopia. Environmental Management, (2001), 27, 815–824.

Gleason, M. H.,Daniel,D. E., and Eykholt, G. R. (1997) Calciumand sodiumbentonite for hydraulic containment applications, Journal of Geotechnical and Geoenvironmental Engineering, 123, 438-445.

Godwin, R.J., (1990). Agricultural Engineering in Development: Tillage for Crop Production in Areas of Low Rainfall. FAO, Rome, Italy, 124 pp.

Golchin, A., Oades, J.M., Skjemstad, J.O., Clarke, P., (1994). Soilstructure and carbon cycling. Australian Journal of Soil Research 32, 1043– 1068.

Gregoire, B.G., Clausen, J.C., (2011), Effect of a modular extensive green roof on stormwater runoff and water quality, Ecological Engineering 37 963–969

Gregorich, E.G., Monreal, C.M., Schnitzer, M., Schulten, H.-R., (1996). Transformation of plant residues into soil organic matter: chemical characterization of plant tissue,isolated soil fractions, and whole soils. Soil Science,ence,161, 680–693.

Grossman R.B., Reinsch T.G.(2002) Bulk density and linear extensibility. In: Dane JH, Topp C, Co-editors. Method of soil analysis part 4 physical methods, Madison, Wisconsin: Soil Science,ence Society of America Inc.

Gupta, R.P., Swartzendruber, D., (1962) Flow-associated reduction in the hydraulic conductivity of quartz sand. Soil Science,ence Society of America Proceedings, 26, 6-10.

Gupta, S.C., Larson,W.E., (1979) Estimating soil water retention characteristics from particle size distribution, organic matter percent, and bulk density. Water Resources Research, 15 (6), 1633–1635.

Gupta, V.V.S.R., Rogers, S., Naidu, R., (1998). Effects of secondary treated sewage e,uent application on the populations of microfauna in a hardwood plantation soil. Bolivar HIAT trial. Geoderma 84, 249-263.

Hajnos,M.,Lipiec, J.,Świeboda, R.,Sokołowska, Z.,Witkowska-Walczak, B., (2006). Complete characterization of pore size distribution of tilled and orchard soil usingwater retention curve, mercury porosimetry, nitrogen adsorption, and water desorption methods. Geoderma 135, 307–314.

Harris, R.W., (1992) Root-Shoot Ratios, Journal of Arboriculture, 18(1), 39-42

Harrison, A.F., Bocock, K.L., (1981). Estimation of soil bulk-density from loss-on-ignition values. Journal of Applied Ecology, 18 (3), 919–927.

Hassink, J., (1995). Decomposition rate constants of size anddensity fractions of soil organic matter. Soil Science Society of America Journal,, 59, 1631– 1635.

Hassink, J., (1997). The capacity of soils to preserve organic C and N by their association with clay and silt particles. Plant Soil, 191, 77–87.

Heuscher, S.A., Brandt, C.C., Jardine, P.M., (2005). Using soil physical and chemical properties to estimate bulk density. Soil Science Society of America Journal,, 69, 51–56.

Hill, R.L., (1990). Long-term conventional and no-tillage effects on selected soil physical properties. Soil Science Society of America Journal,, 54, 161–176

Home, P.G., Panda, R.K., Kar, S., (2002) Effect of method and scheduling of irrigation on water and nitrogen use efficiencies of Okra (Abelmoschus esculentus), Agriculture Water Management, 55 159-170.

Honk Kong SAR Government Environmental Protection Department. Sludge Treatment and Disposal Strategy Reports. HK:Hong-Kong Govt Printer, (1999), 4–5.

Huang, Y., Bol, R., Harkness, D.D., Ineson, P., Eglinton, G., (1996). Post-glacial variations in distributions, 13C and 14C contents of aliphatic hydrocarbons and bulk organicmatter in three types of British acid upland soils. Organic Geochemistry, 24, 273–287.

Hubbard, R.K., Hargrove, W.L., Lowrance, R.R., Williams, R.G., Mullinix, B.G., (1994). Physical properties of a clayey coastal plain soil as affected by tillage. Journal of Soil and Water Conservation, 49, 276–283.

Huntington, T.G., Johnson, Š.E., Johnson, A.H., Siccama, T.G., Ryan, D.F., (1989). Carbon, organicmatter, and bulk density relationships in a forested spodosol. Soil Science, 148 (5), 380–386.

Iannotti, D.A., Pang, T., Toth, B.L., Elwell, D.L., Keener, H.M., Hoitink, H.A.J., (1993). A quantitative respirometric method for monitoring compost stability. Compost Science and Utilization 1, 52-65.

Ito, A., Umita, T., Aizawa, J., Takachi, T. and Morinaga, K. (2000), Removal of heavy metals from anaerobically digested sewage sludge by a new chemical method using ferric sulfate. Water Research, 34(3), 751–758.

Ivanov, V. and Chu, J. (2008) Applications of microorganisms to geotechnical engineering for bioclogging and biocementation of soil in situ, Reviews in Environmental Science and Biotechnology, 7, 139e153.

Jensen, J. and Jepson, S.E..(2005) The production, use and quality of sewage sludge in Denmark. Waste Management, 25, 239–247.

Johansen, C., Falholt, P., Gram, L., (1997). Enzymatic removal and disinfection of bacterial biofilms. Applied and Environmental Microbiology, 63, 3724- 3728

John, B., Yamashita, T., Ludwig, B., Flessa, B., (2005). Storage of organic carbon in aggregate and density fractions of silty soils under different types of land use.Geoderma, 128, 63–79.

Juang, C.H., Ching, J., Lou, Z., Ku, C.S., (2012). New models for probability of liquefaction using standard penetration tests based on an updated database of case histories. Engineering Geology, 133–134, 85–93.

Kamaluldeena, J., Yunusaa, I.A.M., Zerihunb, A., Bruhla, J.J. Kristiansena, P., (2014) Uptake and distribution of ions reveal contrasting tolerancemechanisms for soil and water salinity in okra (Abelmoschusesculentus) and tomato (Solanum esculentum), Agricultural Water Management, 146, 95–104

Kandeler, E., Stemmer, M., Klimanek, E.-M., (1999). Response of soil microbial biomass, urease and xylanase within particle size fractions to long-term soil management. Soil Biology & Biochemistry, 31, 261–273.

Kassas, M.. (1995), Desertification: a general review, Journal of Arid Environments, 30, 115-128.

Kaur, R., Kumar, S., Gurung, H.P., (2002). A pedo-transfer function (PTF) for estimating soil bulk density from basic soil data and its comparison with existing PTFs. Australian Journal of Soil Research, 40, 847–857.

Keijzer, Th.J.S., Kleingeld, P.J., Loch, J.P.G., (1999). Chemical osmosis in compacted clayey material and the prediction of water transport. Engineering Geology, 53, 151–159.

Khanzode, R.M., Vanapalli, S.K., Fredlund, D.G., (2002), Measurement of soil-water characteristic curves for fine-grained soils using a small-scale centrifuge, Canadian Geotechnical Journal, 39: 1209–1217

Kögel-Knabner, I., (2002). The macromolecular organic composition of plant and microbial residues as inputs to soil organic matter. Soil Biology & Biochemistry, 34, 139–162.

Kolstad, D. C., Benson, C. H., and Edil, T. B. (2004) Hydraulic conductivity and swell of nonprehydrated geosynthetic clay liners permeated with multispecies inorganic solutions, Journal of Geotechnical and Geoenvironmental Engineering Eng., 130, 1236-1249

Komilis D.P., Tziouvaras I.S. , (2009) A statistical analysis to assess the maturity and stability of six composts, Waste Management 29,1504–1513

Kuntze, H., Roeschmann, G., Schwerdtfeger, G., Bodenkunde. U., Stuttgart, J.N., Foster, R.C., Nannipieri, P., (1995). Soil structure and biological activity. Soil Biology & Biochemistry, 9, 128–129.

Lack, A. and Evans, D.. (2005) Plant Biology. UK:Taylor and Francis Group.

Ladd, J.N., Foster, R.C., Nannipieri, P., Oades, J.M., (1996). Soil structure and biological activity. In: Stotzky, G., Bollag, J.-M. (Eds.), Soil Biochemistry, vol. 9. Marcel Decker, New York, pp. 23–78.

Lal, R., (1998). Soil erosion impact on agronomic productivity and environment quality. Crit. Rev. Plant Sci. 4, 319–464.

Lampurlanés, J., Cantero-Martínez, C., (2006) Hydraulic conductivity, residue cover and soil surface roughness under different tillage systems in semiarid conditions, Soil & Tillage Research, 85, 13–26.

Lee, D.J., Spinosa, L. and Liu, J.C. (2002), Towards Sustainable Sludge Management. Water , 22–23.

Leij, F.J., Alves, W.J., van Genuchten, M.Th,Williams, J.R., (1996). The UNSODA Unsaturated Hydraulic Database. USEPA, Cincinnati, Ohio (EPA/600/R-96/095).

Leong, E.C., Rahardjo, H., (1997). Review of soil–water characteristic curve equations. Journal of Geotechnical and Geoenvironmental Engineering 123 (12), 1106–1117.

Leong E C, Tripathy S, Rahardjo H. (2003), Total su ct ion m easurem en t of unsaturated soils w ith a device us ing the ch illed - m irror dew - poin t techn ique . Geotechn ique, 53 (2), 173 ~ 182

Lestariningsih, I. D., Widianto, Hairiah, K., (2013) Assessing Soil Compaction with Two Different Methods of Soil Bulk Density Measurement in Oil Palm Plantation Soil, Procedia Environmental Sciences 17172 – 178

Leuschner, H.H., Aldag, R., Meyer, B., (1981). Dichte-Fraktionierung des Humus in Ap-Horizonten von Sandböden mit unterschiedlicher Kö rnung und Nutzungs-Vorgeschichte. Mitteilungen der Deutschen Bodenkundlichen Gesellschaft, 32, 583– 592.

Li, Z.Q., Li, T., Hu, R.L., Li, X., Li, Z.J., (2007)Methods for Testing and Predicting of Swcc in Unsaturated Soilmechanics, Journal of Engineering Geology, 15(05), 0700-0708

Lichtfouse, E., Bardoux, G., Mariotti, A., Balesdent, J., Ballentine, D.C., Macko, S.A., (1997). Molecular, 13C and 14C evidence for the allochthonous and ancient origin of C16–C18n-alkanes in modern soils. Geochim. Comsochim. Acta 61, 1891–1898.

Lincoln, T., Eduardo, Z., (2010) Plant physiology 5th ed, Sinauer Associates Inc. US

Lipiec, J., Hajnos, M., Świeboda, R., (2012). Estimating effects of compaction on pore size distribution of soil aggregates by mercury porosimeter. Geoderma 179–180, 20–27.

Lipiec, J., Kus, J., Slowinska-Jurkiewicz, A., Nosalewicz, A., (2006). Soil porosity and water infiltration as influenced by tillage methods. Soil & Tillage Research, 89, 210–220.

Liu, Y. and Ci, L.J.(2000) Driving action of population increase on desertification. Journal of Arid Land Resources and Environment, 14, 28–33.

Lo, K.S.L. and Chen, Y.H.(1990) Extracting heavy metals from municipal and industrial sludges. Science of Total Environment, 90, 99–116.

López , M.V., Arrúe, J.L., (1997). Efectos del laboreo de conservación en el estado de agregación y en la infiltración de agua en suelos francos de Aragón. In: García, L., González, P. (Eds.), Proceedings of the Congreso Nacional: Agricultura de conservación y medidas agroambientales, Burgos, Spain, 3–4 December, pp. 189–195.

Lu, S.G., Malik, Z., Chen D.P., Wu, C.F., (2014) Porosity and pore size distribution of Ultisols and correlations to soil iron oxides, Catena, 123, 79–87

Carlsson, M., Lagerkvist, A., Morgan-Sagastume, F. (2012) The effects of substrate pretreatment on anaerobic digestion systems: a review, Waste Manage. 32 1634–1650.

Magesan, G.N., McLay, C.D.A., Lal, V.V., (1998). Nitrate leaching from a free-draining volcanic soil irrigated with municipal sewage e,uent in New Zealand. Agriculture, Ecosystems & Environment, 70, 181-187.

Magesan, G.N., Williamson, J.C., Yeates, G.W., Lloyd-Jones, A.Rh., (2000), Wastewater C:N ratio effects on soil hydraulic conductivity and potential mechanisms for recovery, Bioresource Technology, 71, 21-27.

Magesan, G.N., Williamson, J.C., Sparling, G.P., Schipper, L.A., Lloyd-Jones, A.Rh., (1999). Decreased hydraulic conductivity in soils irrigated with waste water field and laboratorystudies. Australian Journal of Soil Research 37, pp. 391-402.

Magoarou, P.. (2000) Urban wastewater in Europe, what about the sludge? in: Langenkamp., H., Marmo, L. (Eds.), Workshop Problems Around Sludge-Proceedings EUR 19657 EN.

Mahmood, T., Elliott, A., (2006) A review of secondary sludge reduction technologies for the pulp and paper industry, Water Research, 40(11), 2093-112

Manrique LA, Jones CA. Bulk density of soils in relation to soil physical and chemical properties. Soil Science Society of America Journal, (1991);55:476-481

Manrique, L.A., Jones, C.A., (1991). Bulk density of soils in relation to soil physical and chemical properties. Soil Science Society of America Journal, 55, 476–481.

Marchioretto, M.M.. Heavy metals removal from anaerobically digested sludge. Ph.D thesis, Wageningen University, Wageningen, Netherlands, (2003).

Marschner, B., Brodowski, S., Dreves, A., Gleixner, G., Gude, A., Grootes, P.M., Hamer, U., Heim, A., Jandl, G., Ji, R., Kaiser, K., Kalbitz, K., Kramer, C., Leinweber, P., Rethemeyer, J., Schäffer, A., Schmidt, M.W.I., Schwark, L., Wiesenberg, G.L.B., (2008). How relevant is recalcitrance for the stabilization of organic matter in soils? Journal of Plant Nutrition and Soil Science,ence 171, 91–110.

Marseille, F., Disnar, J.R., Guillet, B., Noack, Y., (1999). N-alkanes and free fatty acids in humus and A1 horizons of soils under beech, spruce and grass in the Massif-Central(Mont-Lozère), France. Eur. Journal of Soil Science,50, 433–441.

Marttinen, S.K., Hanninen, K., Rintala, J.A., (2004). Removal of DEHP in composting and aeration of sewage sludge. Chemosphere, 54, 265–272.

Mays, L.W. (2011) Water Resources Engineering, 2nded. New Jersey: John Wiley & Sons, Ltd.

McBratney, A.B., Minasny, B., Cattle, S.R., Vervoort, R.W., (2002). From pedotransfer functions to soil inference systems. Geoderma 109 (1–2), 41–73.

McWhorter, D.B., and Sunada, D.K., (1977) Ground-Water Hydrology and Hydraulics. Water Resources Publications, Colorado.

Mengen, K. and Kirkby, E.A., (2001) Principes of Plant Nutrition-5th Ed. Dordrecht:Kluwer Academic Publishers.

Mesjasz-Przybylowicz, J., Nakonieczny, M., Migula, P., Augustyniak, M., Tarnawska, M., Reimold, W.U., Koeberl, C., Przybylowicz, W. and Glowacka, E., (2004) Uptake of cadmium, lead, nickel and zinc from soil and water solution by the nickel hyperaccumulator Berkheya coddii. Acta Biologica Cracoviensia Series Botanica, 46, 75-85.

Messing, I., Jarvis, N.J., (1993). Temporal variation in the hydraulic conductivity of a tilled clay soil as measured by tension infiltrometers. Journal of Soil Science, 44, 11–24.

Minasny, B., Hopmans, J. W. , Harter, T., Eching, S. O., Tuli, A., (2004), Denton, M. A.Neural Networks Prediction of Soil Hydraulic Functions for Alluvial Soils Using Multistep Outflow Data, Soil Science Society of America Journal,, 68, 417–429

Ministry of Land and Resources, China. Geologic disaster and prevention status (2009), China:Ministry of Land and Resources.

Mitchell, A. C. and Ferris, F. G. (2006) The influence of Bacillus pasteurii on the nucleation and growth of calcium carbonate, Geomicrobiol. J., 23, 213e226 .

Moody, J.A., Smith, J.D., Ragan, B.W., (2005). Critical shear stress for erosion of cohesive soils subjected to temperatures typical ofwildfires. J. Geophys. Res. 110, F01004. http://dx. doi.org/10.1029/(2004)JF000141. Morgan, R.P.C., (2005). Soil Erosion and Conservation. Third ed. Blackwell Publishing, Oxford, UK (303 pp.).

Morin, D., Lips, A., Pinches, A., Huisman, J., Frias, C., Norberg, A. and Forssberg, E.. BioMinE Integrated project for the development of biotechnology for metalbearing materials in Europe, in: 16th International Hydrometallurgical Symposium. (2005), 25–29 Sep, Capetown, South Africa.

Munkholm, L.J., Heck, R.J., Deen, B., (2012). Soil pore characteristics assessed from X-ray micro-CT derived images and correlations to soil friability. Geoderma 181–182, 22–29.

Mwendera, E.J., Feyen, J., (1993). Predicting tillage effects on infiltration. Soil Science,ence,155, 229–235.

Nemati, M. and Voordouw, G. (2003) Modification of porous media permeability, using calcium carbonate produced enzymatically in situ, Enzyme Microb. Technol., 33, 635-642.

Nicolás, C., Hernández, T., García, C.(2012) Organic amendments as strategy to increase organic matter in particle-size fractions of a semi-arid soil, Applied Soil Ecology, 57, 50– 58.

Noellemeyer, E., Frank, F., Alvarez, C., Morazzo, G., Quiroga, A., (2009). Carbon contents and aggregation related to soil physical and biological properties under a land-use sequence in the semiarid region of central Argentina. Soil & Tillage Research 99, 179–190.

O'Connor, G.A., (1996) Organic compounds in sludge-amended soils and their potential for uptake by crop plants, The Science of the Total Environment, 185, 71-81

Ogata, N., Komine, H., Nakashima, H., Nagasawa, T., Ishii, T., (1994). Method of designing bentonite/sand mixture to achieve the target permeability. Nendo Kagaku 34 (2), 95– 101 (in Japanese).

Okwadha, G. D. O. and Li, J. (2010) Optimum conditions for microbial carbonate precipitation, Chemosphere, 81, 1143-1148.

Oleszczuk, P., (2008). Phytotoxicity of municipal sewage sludges compost related to physico-chemical properties, PAHs and heavy metals. Ecotoxicol. Environ. Safe. 69, 496–505.

Oleszczuk, P., Hollert, H., (2011) Comparison of sewage sludge toxicity to plants and invertebrates in three different soils, Chemosphere, 83, 502–509

Oliveira, R., (1997). Understanding adhesion: a means for preventing fouling. Exp. Therm. Fluid Sci. 14, 316–322.

Olomilua AL, Akanbi OSO, Ojeniyi S. (2007)Effects of pig manure on nutrient composition, growth and yield of okra. Nigerian Journal of Soil Science,17:109–12.

Pagliai, M., Vignozzi, N., Pellegrini, S., (2004). Soil structure and the effect of management practices. Soil & Tillage Research, 79, 131–143.

Pathak, A., Dastidar, M.G., Sreekrishnan, T.R., (2009) Bioleaching of heavy metals from sewage sludge: A review, Journal of Environmental Management, 90, 2343–2353

Pelegrin, F., Moreno, F., (1994). Measurement of the water infiltration into a tilled and untilled soil using a rainfall simulator. In: Jensen, H.E., Schjønning, P., Mikkelsen, S.A., Madsen, K.B. (Eds.), Soil Tillage for Crop Production and Protection of the Environment, Proceedings of 13th International Conference, Aalborj, Denmark, July 24–29, pp. 453–458.

Pelegrin, F., Moreno, F., Martin-Aranda, J., Camps, M., (1988). The influence of tillage methods on soil-water conservation in SW Spain. In: Tillage and Traffic in Crop Production, Proceedings of the 11th International Conference of the International Soil Tillage Research Organization, vol. 2. Edinburgh, Scotland, 11–15th July, pp. 803–808.

Pelegrin, F., Moreno, F., Martin-Aranda, J., Camps, M., (1990). The influence of tillage methods on soil physical properties and water balance for a typical crop rotation in SW Spain. Soil & Tillage Research 16, 345–358.

Petit, F., (1990). Evaluation of grain shear stresses required to initiate movement of particles in natural rivers. Earth Surface Processes and Landforms, 15, 135–148.

Petrov, R. J. and Rowe, R. K. (1997) Geosynthetic clay liner (GCL) e chemical compatibility by hydraulic conductivity testing and factors impacting its performance, Canadian Geotechnical Journal, 34, 863-885.

Phoon, K.K., Kulhawy, F.H., (1999)a. Characterization of geotechnical variability. Canadian Geotechnical Journal, 36, 612–624.

Phoon, K.K., Kulhawy, F.H., (1999)b. Evaluation of geotechnical property variability. Canadian Geotechnical Journal, 36, 625–639.

Phoon, K.K., Kulhawy, F.H., (2003). Evaluation of model uncertainties for reliability-based foundation design. Proc. Ninth International Conference on Applications of Statistics and Probability in Civil Engineering, San Francisco, pp. 1351–1356.

Phoon, K.K., Liu, S.L., Chow, Y.K., (2003). Estimation of model uncertainties for reliabilitybased design of cantilever walls in sand. Proc. Int. Workshop on Limit State Design in Geotechnical Engineering Practice (LSD(2003). Massachusetts Institute of Technology, Cambridge (CDROM).

Phoon, K.K., Santoso, A., Quek, S.T., (2010). Probabilistic analysis of soil-water characteristic curves. Journal of Geotechnical and Geoenvironmental Engineering 136 (3), 445–455.

Pikul, J.L., Jr., Aase. J.K., (2003). Water infiltration and storage affected by subsoiling and subsequent tillage. Soil Science Society of America Journal, 67:859-866.

Pires, L.F.,Cassaro, F.A.M., Reichardt, K.,Bacchi, O.O.S., (2008). Soil porous system changes quantified by analyzing soil water retention curve modifications. Soil & Tillage Research, 100, 72–77.

Planquart, P., Bonin, G., Prone, A. and Massiani, C. (1999), Distribution, movement and plant availability of trace metals in soilsamended with sewage sludge composts-application to low metal loadings. The Science of the Total Environment, 241, 161-179.

Puhakka, J.A., Viitasaari, M.A., Latola, P.K., Määttä, R.K., (1988). Effect of temperature on anaerobic digestion of pulp and paper industry wastewater sludges. Water Science and Technology, 20 (1), 193-201.

Quénéa, K., Largeau, C., Derenne, S., Spaccini, R., Bardoux, G., Mariotti, A., (2006). Molecular and isotopic study of lipids in particle size fractions of a sandy cultivatedsoil (Cestas cultivation sequence, Southwest France): sources, degradation, andcomparison with Cestas forest soil. Organic Geochemistry, 37, 20–44.

Radcliffe, D.E., Tollner, E.W., Hargrove,W.L., Clark, R.L., Golabi, M.H., (1988). Effect of tillage practices on infiltration and soil strength of a Typic Hapludult soil after 10 years. Soil Science Society of America Journal, 52, 798–804.

Raei, B., Asadi, H., Moussavi. A., Ghadiri, H. (2015), A study of initial motion of soil aggregates in comparison with sand particles of various sizes, Catena, 127, 279–286.

Ragusa, S.R., deZoysa, D.S., Rengasamy, P., (1994). The effect of microorganisms, salinity and turbidity on hydraulic conductivity of irrigation channel soil. Irrigation Science, 15, 159-166.

Rajkai, K., Kabos, S., Genuchten, V., Jansson, P.E., (1996). Estimation of water-retention characteristics from the bulk density and particle-size distribution of Swedish soils. Soil Science,ence,161 (12), 832–845.

Ramirez, W.A., Domene, X., Ortiz, O., Alcaniz, J.M., (2008). Toxic effects of digested, composted and thermally-dried sewage sludge on three plants. Bioresource Technology, 99, 7168–7175.

Reichert et al., (2009) J.M. Reichert, L.E.A.S. Suzuki, D.J. Reinert, R. Horn, I. Håkansson Reference bulk density and critical degree-of-compactness for no-till crop production in subtropical highly weathered soils Soil & Tillage Research,102 , 242–254

Roca-Pérez, L., Martínez, C., Marcilla, P., Boluda, R., (2009) Composting rice straw with sewage sludge and compost effects on the soil–plant system, Chemosphere, 75, 781–787

Rossi AM, Hirmas DR, Graham RC, Sternberg PD. (2008), Bulk density determination by automated three-dimensional laser scanning. Soil Science Society of America Journal, 72,1591-1593

Rühlmann, J, Körschens, M, Graefe, J.(2006), A new approach to calculate the particle density of soils considering properties of the soil organic matter and the mineral matrix, Geoderma, 130, 272– 283.

Rühlmanna, J., T, Körschensb, M., Graefea, J., (2006) A new approach to calculate the particle density of soils considering properties of the soil organic matter and the mineral matrix, Geoderma 130, 272– 283

Salehi, M., Strom, K., (2012). Measurement of critical shear stress for mud mixtures in the San Jacinto estuary under different wave and current combinations. Continental Shelf Research 47, 78–92

Salt, D.E., Smith, R.D. and Raskin, I. (1998), Phytoremediation. Annual Review on Plant Physiology and Plant Molecular Biology, 49, 643–668.

Sarah, P., (2006). Soil organic matter and land degradation in semi-arid area, Israel. Catena 67, 50–55.

Sasanian, S.,Newson, T.A., (2013). Use ofmercury intrusion porosimetry formicrostructural investigation of reconstituted clays at high water contents. Engineering Geology, 158, 15–22.

Sauerbeck, D. (1987), Effects of agricultural practices on the physical, chemical and biological properties of soils: Part II
- Use of sewage sludge and agricultural wastes. In: H. Barth and P. L'Hermite (Eds.), Scientific Basis for Soil Protection
in the European Community. UK:Elsevier Applied Science, Barking, 181-210.

Saxton, K.E., Rawls,W.J., Romberger, J.S., Papendick, P.I., (1986). Estimating generalized soil water characteristics from texture. Soil Science Society of America Journal, 50, 1031–1036. Sheng, D., Zhou, A.N., (2011). Coupling hydraulic with mechanical models for unsaturated soils. Canadian Geotechnical Journal, 48, 826–840.

Schachtschabel, P., Blume, H.-P., Brümmer, G., Hartge, K.-H., Schwertmann, U., (1992). Lehrbuch der Bodenkunde/Scheffer; Schachtschabel. Ferdinand Enke Verlag, Stuttgart.

Schaetzl RJ, Anderson S. (2005) Soils: genesis and geomorphology. New York: Cambridge University Press.

Schafer, P.L. and Farrrel, J.B. (2000) Performance comparisons for staged and high-temperature anaerotic digestion systems, Proceedings of WEFTEC (2000), Water Enviornment Federation, Alexandria, VA.

Sequeira, C. H., Wills, S. A., Seybold, C. A., West, L. T., (2014) Predicting soil bulk density for incomplete databases, Geoderma 213, 64–73

Shaw, J.C., Bramhill, B., Wardlaw, N.C., Costerton, J.W., (1985). Bacterial fouling in a model core system. Applied and Environmental Microbiology, 49, 693-701.

Shen, Y.C., Zhang, K.B. and Wang, X. , (2001)Desertification, China: Chinese Environmental Science Press.

Sheng, D., Zhou, A.N., (2011). Coupling hydraulic with mechanical models for unsaturated soils. Canadian Geotechnical Journal, 48, 826–840.

Shi, Z.H., Fang, N.F., Wu, F.Z.,Wang, L., Yue, B.J.,Wu, G.L., (2012). Soil erosion processes and sediment sorting associated with transport mechanisms on steep slopes. Journal of Hydrology 454–455, 123–130.

Siemonsma JS, Kouame C. Abelmoschus esculentus (L.) Moench. In: Grubben GJH, Denton OA, (2004) Plant resources of tropical Africa. Wageningen, Netherlands: PROTA Foundation/Backhuys Publishers, 25–9.

Sillers,W.S., Fredlund, D.G., (2001). Statistical assessment of soil–water characteristic curve models for geotechnical engineering. Canadian Geotechnical Journal, 38, 1297–1313.

Simunek, R., Soil Physics with Hydrus, (2010), Taylor and Francis Group:United States

Sivakumar, M.V.K., (2007) Interactions between climate and desertification. Agricultural and Forest Meteorology, 142, 143–155.

Six, J.,Bossuyt, H.,Degryze, S.,Denef, K., (2004). A history of research on the link between (micro)aggregates, soil biota, and soil organic matter dynamics. Soil & Tillage Research, 79, 7–31.

Skopp, J.M., (2000). Physical properties of primary particles. In: Summer, M.E. (Ed.), Handbook of Soil Science,ence. CRC Press, Boca Raton, pp. A3–A17.

Sollins, P., Swanston, C., Kleber, M., Filley, T., Kramer, M., Crow, S., Caldwell, B.A., Lajtha, K., Bowden, R., (2006). Organic C and N stabilization in a forest soil: evidence from sequential density fractionation. Soil Biology & Biochemistry, 38, 3313–3324.

Spinosa, L., Vesilind, P.A., (2001). Sludge into biosolids. In: Processing, Disposal, Utilization. IWA Publishing, London, UK.

State Forestry Administration, China. , (2005) The third national desertification and sandy land monitoring, China:State Forestry Administration.

Stefanakis, A.I., Komilis, D.P., Tsihrintzis, V.A., (2011) Stability and maturity of thickened wastewater sludge treated in pilot-scale sludge treatment wetlands, Water Research, 45 6441-6452

Steinberg, S.L. and Poritz,D., (2005) Measurement of hydraulic characteristics of porous media used to grow plants in microgravity. Soil Science Society of America Journal, 69:301–-310.

Steinberg, S.L., Kluitenberg, G.J., Jones, S.B., Daidzic, N.E., Reddi, L.N., Xiao, M., Tuller, M., Newman, R.M., Or, D., Alexander, J.I.D., (2005) Physical and Hydraulic Properties of Baked Ceramic Aggregates Used for Plant Growth Medium, Journal of the American Society for Horticultural Science, 130(5), 767–-774.

Stemmer, M., Gerzabek, M.H., Kandeler, E., (1998). Organic matter and enzyme activity in particle-size fractions of soils obtained after low-energy sonication. Soil Biology & Biochemistry, 30, 9–17.

Stocks-Fischer, S., Galinat, J. K., and Bang, S. S. (1999) Microbiological precipitation of CaCO3, Soil Biology & Biochemistry,, 31, 1563-1571.

Stoll, U. (1995), Municipal sewage sludge management, Environment Systems Reviews. Bangkong, Thailand:Environment Systems Information Center (ENSIC), 39 .

Strasser, H., Brunner, H. and Schinner, F.. Leaching of iron and toxic heavy metals from anaerobically-digested sewage sludge. Journal of Industrial Microbiology Biotechnology, (1995), 14 (3–4), 281–187.

Strong, D.T., De Wever, H., Merckx, R., Recous, S., (2004). Spatial location of carbon decomposition in the soil pore system. Eur. Journal of Soil Science,55, 739–750.

Sun, S.Y.. (2011), Sludge produciton reached 22 million tons per year, People's Daily.

Suuster, E., Ritz, C., Roostalu, H., Reintam, E., Kõlli, Raimo., Astover, A., (2011), Soil bulk density pedotransfer functions of the humus horizon in arable soils, Geoderma, 163, 74–82

Suwardji, P., Eberbach, P.L., (1998). Seasonal changes of physical properties of an Oxic Paleustalf (Red Kandosol) after 16 years of direct drilling or conventional cultivation. Soil & Tillage Research 49, 65–77.

Tarantino, A., (2009). A water retention model for deformable soils. Geotechnique 59 (9), 751–762.

Tchobanoglous, G., Burton, F., Stensel, H.D., (2004) Wastewater Engeineering 4th Ed, Mc Graw Hill:Singapore

Tebrügge, F., Düring, R.A., (1999). Reducing tillage intensity—a review of results from a long-term study in Germany. Soil & Tillage Research 53, 15–28.

Timm LC, Pires LF, Reichardt K, Roveratti R, Oliveira JCM, Bacchi OOS. (2005) Soil bulk density evaluation by conventional and nuclear methods. Journal of Soil Research, 43(1), 97-103

Tobler, D. J., Cuthbert, M. O., Greswell, R. B., Siley, M. S., Renshaw, J. C., Handley-Sidhu, S., and Phoenix, V. R. (2011) Comparison of rates of ureolysis between Sporosarcina pasteurii and an indigenous groundwater community under conditions required to precipitate large volumes of calcite, Geochim. Cosmochim. Acta, 75, 3290-3301.

Tomasella, J., Hodnett, M.G., (1998). Estimating soil water retention characteristics from limited data in Brazilian Amazonia. Soil Science, 163, 190–202.

Tranter, G., Minasny, B., McBratney, A.B., Murphy, B., McKenzie, N.J., Grundy, M., Brough, D., (2007). Building and testing conceptual and empirical models forpredicting soil bulk density. Soil Use and Management 23 (4), 437–443.

Uko AE, Udo IA, Shiyam JO. (2009) Optimizing poultry manure rates for two okra (Abelmoschus esculentus) varieties in a warm wet climate. Journal of Agricultural Biotechnology and Ecology, 2(3), 273–85.

UNCED. , (1992) Report of the United Natiom Conference on Environment and Development,Vol. I, New York: UN.

United Nations. The most definitive assessment of the severity of desertification on a global scale,

Uwe, H.. , (2008) Implementing the United Nations Convention to Combat Desertification from a parliamentary point of view, Seventh Parliamentarians Forum on the United Nations Convention to Combat Desertification.

Van Genuchten M T. (1980),A closed-form equation for predicting the hydraulic conductivity of unsaturated soils.Soil Science Society of America Journal, 44, 892~898.

Van Genuchten MTh, Wierenga PJ. (1986), Solute dispersion coefficients and retardation factors. In: Klute A. Methods of soil analysis part 1. Physical and mineralogical method (2nd edition), Madison Wisconsin: American Society of Agronomi Inc. and Soil Science,ence Society of America Inc.

Vanapalli, S.K., Fredlund, D.G., Pufahl, D.E., (1999). The influence of soil structure and stress history on the soil–water characteristics of a compacted till. Geotechnique 49 (2), 143–159.

Van-Camp, L., Bujarrabal, B., Gentile, A-R., Jones, R.J.A., Montanarella, L., Olazabal, C., Selvaradjou, S-K., (2004). Reports of the Technical Working Groups Established under the Thematic Strategy for Soil Protection. EUR 21319 EN/3. Office for Official Publications of the European Communities, Luxembourg, pp. 872.

Vinten, A.J.A., Minelgrin, U., Yaron, B., (1983). The effect of suspended solids in wastewater on soil hydraulic conductivity: II. Vertical distribution of suspended solids. Soil Science Society of America Journal, 47, 408-412.

Vlyssides A G, Karlis P K, (2004). Thermal-alkaline solubilization of waste activated sludge as a pre-treatment stage for anaerobic digestion. Bioresource Technology, 91(2): 201–206.

Wai, W. H. O., Lam, K. W.D., Liu, Y.H., (2014), Extensive Green Roofs: first step towards sustainable urban drainage system design in Hong Kong, DSD International Conference (DSDIC (2014).

Wairiu,M.,Lal, R., (2006). Tillage and land use effects on soil microporosity in Ohio, USA and Kolombangara, Solomon Islands. Soil & Tillage Research, 88, 80–84.

Wall, D. K. and Zeiss, C. (1995) Municipal landfill biodegradation and settlement, Journal of Environmental Engineering, 121, 214-224.

Wang, C., Hu, X., Chen, M.L. and Wu, Y.H.. (2005), Total concentration and fractions of Cd, Cr, Pb, Cu, Ni and Zn in sewage sludge from municipal and industrial wastewater treatment plants. Journal of Hazardous Materials, 119 (1–3), 245–249.

Wang, H.L., Wang, C.J., Chen, F., Ma, M.P., Lin, Z.L., Wang, W.W., Xu, Z.T. and Wang, X.D.. (2011), Modification to degradation of hexazinone in forest soilsamended with sewage sludge. Journal of Hazardous Materials. 199-200, 96–104

Wang, L., Shi, Z.H.,Wang, J., Fang, N.F., Wu, G.L., Zhang, H.Y., (2014). Rainfall kinetic energy controlling erosion processes and sediment sorting on steep hillslopes: a case study of clay loam soil from the Loess Plateau, China. Journal of Hydrology 512, 168–176.

Wang, X.M., Chen, F.H., Hasi, E., Li, J.C., Desertification in China: An assessment, Earth-Science Reviews (2008), 88,188-206

Wang, Y., Au, S.K., Cao, Z.J., (2010). Bayesian approach for probabilistic characterization of sand friction angles. Engineering Geology, 114, 354–363.

Wang, Y., Au, S.K., Kulhawy, F.H., (2011). Expanded reliability-based design approach for drilled shafts. Journal of Geotechnical and Geoenvironmental Engineering 137 (2), 140–149.

Water Environment Federation. Manual of practice No. 8. Design of wastewater treatment plants-fourth Edition, (1998), 3, Chaps. 17-24.

Water Environment Federation. Manual of Practice No. FD-9. Wastewater residuals stabilization, USA: WEA, (1995).

Whiffin, V. (2004)Microbial CaCO3 precipitation for the production of biocement. Ph. D. thesis. Murdoch University, Perth, Western Australia.

Wierenga PJ, Van Genuchten MTh. (1989) Solute transport through small and large unsaturated soil columns. Groundwater, 27(1), 35-42

Wiesenberg, G.L.B. , Dorodnikov, M., Kuzyakov, Y., (2010), Source determination of lipids in bulk soil and soil density fractions after four years of wheat cropping, Geoderma 156, 267–277

Wiesenberg, G.L.B., Schwark, L., (2006). Carboxylic acid distribution patterns of temperate C3 and C4 crops. Organic Geochemistry, 37, 1973–1982.

Wiesenberg, G.L.B., Schwarzbauer, J., Schmidt, M.W.I., Schwark, L., (2004)a. Sources and turnover of organic matter in agricultural soils derived from n-alkane/n-carboxylicacid compositions and C-isotope signatures. Organic Geochemistry, 35, 1371–1393.

Wikipedia. Plant. http://en.wikipedia.org/wiki/Plant#cite_note-urlplant.5B2.5D_-_Definition_from_the_Merriam-Webster_Online_Dictionary-2, (2011)

Wilcock, P.R., (1988). Methods for estimating the critical shear stress of individual fractions in mixed-size sediment. Water Resources Research, 24, 1127–1135.

Wild, S.R., (1991) The Fate and Behaviour of PAHs in Sewage Sludge-amended Agricultural Soils and Their Uptake by
Plants. Ph.D. Thesis, Lancaster University, Lancaster, UK.

Wilsey , B.J., Polley H. W., (2006) , Aboveground productivity and root–shoot allocation diVer between native and introduced grass species, Oecologia, 150:300–309

Wilson, G.. Burning and burying – dealing with sludge.Water Waste Treatment, (1998), 36.

Wu, L., Ma, L.Q., Martinez, G.A., (2000). Comparison of methods for evaluating stability and maturity of biosolids compost. Journal of Environmental Quality 29, 424-429.

Yan, W.M., Yuen, K.V., Yoon, G.L., (2009). Bayesian probabilistic approach for the correlations of compression index for marine clays. Journal of Geotechnical and Geoenvironmental Engineering 135 (12), 1932–1940.

Yang, H., Rahardjo, H., Leong, E.C., Fredlund, D.G., (2004). Factors affecting drying and wetting soil–water characteristic curves of sandy soils. Canadian Geotechnical Journal, 41, 908–920.

Yasuhara, H., Neupane, D., Hayashi, K., and Okamura, M. (2012)Experiments and predictions of physical properties of sand cemented enzymatically-induced carbonate precipitation, Soils and Foundations, 52, 539-549.

Yeates, G.W., (1995). Effect of sewage effluent on soil fauna in a Pinus radiata plantation. Australian Journal of Soil Research 33, 555-564.

Yi, R.R.. Domestic activated sludge had became a secondary pollution in China. Sicnence Times, (2010).

Yi, Y.L., (2008), Soil Phisical Research Methods, Peking University Press: China

Young, J.L., Spycher, G., (1979), Water-dispersible soil organicmineral particles: I. Carbon and nitrogen distribution. Soil Science Society of America Journal, 43, 324–328.

Yuen, K.V., (2010). Recent developments of Bayesian model class selection and applications in civil engineering. Structural Safety 32 (5), 338–346.

Yuen, K.V., Kuok, S.C., (2011). Bayesian methods for updating dynamic models. Applied Mechanics Reviews, 64 (1), 010802-1–010802-18.

Yuen, K.V., Mu, H.Q., (2011). Peak ground acceleration estimation by linear and nonlinear models with reduced order Monte Carlo simulation. Computer-Aided Civil and Infrastructure Engineering, 26 (1), 30–47.

Zhai, Q., Rahardjo, H., (2013). Quantification of uncertainties in soil-water characteristic curve associated with fitting parameters. Engineering Geology, 163, 144–152.

Zhang, L.M., Chen, Q., (2005). Predicting bimodal soil–water characteristic curves. Journal of Geotechnical and Geoenvironmental Engineering 131 (5), 666–670.

Zhang, L.M., Tang, W.H., Zhang, L.L., Zheng, J.G., (2004). Reducing uncertainty of prediction from empirical correlations. Journal of Geotechnical and Geoenvironmental Engineering 130 (5), 526–534.

Zhong, D., (1998). Dynamic evolution of sand deserts in China. Gansu Culture Press, Lanzhou, China. 224 pp. (in Chinese).

Zhou, H., Peng, X., Peth, S., Xiao, T.Q., (2012). Effect of vegetation restoration on soil aggregate microstructure quantified with synchrotron-based micro-computed tomography. Soil & Tillage Research, 124, 17–23.

Zhou, H.,Peng, X.H.,Perfect, E.,Xiao, T.Q.,Peng, G.Y., (2013). Effects of organic and inorganic fertilization on soil aggregation in an Ultisol as characterized by synchrotron based X-ray micro-computed tomography. Geoderma 195–196, 23–30.

Zhou, J., Yu, J.L., (2005). Influence affecting the soil–water characteristic curve. J. Zhejiang University (Science) 6A (8), 797–804.

Zhou, W.H., Yuen, K.V., Tan, F., (2014), Estimation of soil–water characteristic curve and relative permeability for granular soils with different initial dry densities, Engineering Geology, 179,1–9

Zhu, Z., Wu, Z., Liu, S., Di, X., (1980). An introduction to Chinese desert. Science Press, Beijing. 107 pp. (in Chinese).

Zu, Y.Q., Li, Y.N., Christian, S., Laurent, L. and Liu, F.. Accumulation of Pb, Cd, Cu and Zn in plants and hyperaccumulator choice in Lanping lead–zinc mine area, China. Environment International, (2004), 30, 567– 576.

Zuo, X.A., Jing Z.G., Lv, P., Zhou X., Li, Y.L., Luo, Y.Y., Luo, Y.Q., Lian J., Yue X.Y., (2016), Plant functional diversity mediates the effects of vegetation and soilproperties on community-level plant nitrogen use in the restorationof semiarid sandy grassland, Ecological Indicators, 64, 272–280